Facultad de Ciencias
Sede Bogotá

UNIVERSIDAD
NACIONAL
DE COLOMBIA

REVISTA COLOMBIANA DE CIENCIAS QUÍMICO-FARMACÉUTICAS

Universidad Nacional de Colombia
Facultad de Ciencias
Departamento de Farmacia

REVISTA COLOMBIANA DE CIENCIAS QUÍMICO-FARMACÉUTICAS
Universidad Nacional de Colombia, Facultad de Ciencias, Departamento de Farmacia.
ISSN 0034-7418, Fax: 3165060, Cra. 30 No. 45-03, Bogotá, D. C., Colombia.
Correo electrónico: *rcciquifa_fcbog@unal.edu.co*
http://www.revistas.unal.edu.co/index.php/rccquifa
http://www.scielo.org.co/scielo.php?script=sci_serial&pid=0034-7418&rep=
https://scholar.google.com/citations?user=TvBT68sAAAAJ&hl=es

MISIÓN

La *Revista Colombiana de Ciencias Químico-Farmacéuticas* es un órgano de difusión en el cual se publican investigaciones científicas, comunicaciones técnicas y revisiones temáticas originales en las áreas de las ciencias farmacéuticas (véanse Normas para publicación). La revista está destinada principalmente a químicos farmacéuticos, químicos, ingenieros químicos, médicos cirujanos, médicos veterinarios, y a otros profesionales de las ciencias físicas y naturales, de la ingeniería y de las profesiones sanitarias relacionadas con el uso de medicamentos.

VISIÓN

En pro de la difusión de las investigaciones, los contenidos de la *Revista Colombiana de Ciencias Químico-Farmacéuticas* son de acceso libre, con ello se espera llegar a un número mayor de lectores, propiciando la consolidación de comunidades académicas. Además, se proyecta que los contenidos publicados contribuyan al desarrollo e innovación de las ciencias farmacéuticas.

ÉTICA

La responsabilidad de lo expresado en cada artículo es exclusiva de los autores y no representa ni compromete posiciones de la revista ni del cuerpo editorial. Los contenidos publicados pueden reproducirse siempre que se cite la fuente respectiva. Esta revista sigue los lineamientos del COPE (Committee on Publication Ethics), que pueden ser consultados en *http://publicationethics.org/*

Contenido

Scientific research article / *http://dx.doi.org/10.15446/rcciquifa.v49n2.88854*

Domestic wastewater treatment plants as sources of macrolide-lincosamide-streptogramin B- and penicillin-resistant *Staphylococcus aureus* in Brazil

Sílvia Letícia Oliveira Toledo[1], Renata Michelle Silveira Silva[1], Isabella Cristina Rodrigues dos Santos[1], William Gustavo Lima[2], Leticia Gonçalves Rodrigues Ferreira[1], Magna Cristina Paiva[1]*

[1]Laboratório de Diagnóstico Laboratorial e Microbiologia Clínica, Universidade Federal de São João del-Rei, Campus Centro-Oeste Dona Lindu, Divinópolis, Minas Gerais, Brasil.

[2]Laboratório de Microbiologia Médica, Universidade Federal de São João del-Rei, Campus Centro-Oeste Dona Lindu, Divinópolis, Minas Gerais, Brasil.

*Corresponding author E-mail address: magnacpaiva@ufsj.edu.br

Received: 21 October 2019

Revised: 14 April 2020

Accepted: 15 April 2020

Summary

Staphylococcus aureus is one of the main bacteria that affect human health. Its reduced susceptibility to beta-lactam antibiotics has driven the clinical use of macrolides and lincosamides. However, the presence of macrolide-lincosamide-streptogramin B (MLS_B)-resistant *S. aureus* strains is increasingly common. Wastewater treatment plants (WWTPs) are the main anthropogenic source of resistance determinants. However, few studies have assessed the importance of this environment on the dissemination of MLS_B-resistant *S. aureus* strains. Thus, we aimed to evaluate the impact of a domestic WWTP on the resistance to MLSB and penicillin in *S. aureus* in southeast Brazil. Of the 35 isolates tested, 40.6% were resistant to penicillin. Resistance to erythromycin (8.6%) and quinolones (2.8%) was less common. Despite the low rate of resistance to clindamycin (2.8%), many isolates showed reduced susceptibility to this antibiotic (57.1%). Regarding the resistance phenotypes of staphylococci isolates, inducible MLS_B resistance (D-test positive) was found in two isolates. In addition, 27 *S. aureus* isolates showed the ability to produce penicillinase. In this article, we report for the first time the importance of WWTPs in the dissemination of MSL_B resistance among *S. aureus* from southeast Brazil.

Key words: Antibiotic resistance, D-test, penicillin zone-edge test, quinolones, *Staphylococcus aureus*, water environment.

Resumen

Plantas de tratamiento de aguas residuales domésticas como fuentes de *Staphylococcus aureus* resistente a macrólidos-lincosamida-estreptogramina B- y penicilina en Brasil

Staphylococcus aureus es una de las principales bacterias que afectan la salud humana. Su susceptibilidad reducida a los antibióticos betalactámicos ha impulsado el uso clínico de macrólidos y lincosamidas. Sin embargo, la presencia de cepas resistentes a macrólido-lincosamida-estreptogramina B (MLS_B) de *S. aureus* es cada vez más común. Las plantas de tratamiento de aguas residuales (PTAR) son la principal fuente antropogénica de determinantes de resistencia. Sin embargo, pocos estudios han evaluado la importancia de este entorno en la diseminación de cepas de *S. aureus* resistentes a MLS_B. Nuestro objetivo fue evaluar el impacto de una PTAR doméstica en MLS_B y la resistencia a la penicilina en *S. aureus* en el sureste de Brasil. De los 35 aislamientos analizados, el 40,6% eran resistentes a la penicilina. La resistencia a la eritromicina (8,6%) y quinolonas (2,8%) fue menos común. A pesar de la baja tasa de resistencia a la clindamicina (2,8%), muchos aislamientos mostraron sensibilidad reducida a este antibiótico (57,1%). Con respecto a los fenotipos de resistencia de los aislamientos de estafilococos, la resistencia inducible a MLS_B (prueba D positiva) se encontró en dos aislamientos. Además, 27 aislamientos de S. aureus mostraron la capacidad de producir penicilinasa. En este artículo informamos, por primera vez, la importancia de las PTAR en la difusión de la resistencia a MSL_B entre *S. aureus* del sureste de Brasil.

Palabras clave: Resistencia a antibióticos, prueba D, prueba de borde de zona de penicilina, quinolonas, *Staphylococcus aureus*, ambiente acuático.

Resumo

Estações de tratamento de águas residuais domésticas como fontes de Staphylococcus aureus resistente a macrolídeo-lincosamida-estreptograma e B- e penicilina no Brasil

O *Staphylococcus aureus* é uma das principais bactérias que afetam a saúde humana. Sua reduzida suscetibilidade aos antibióticos beta-lactâmicos tem impulsionado o uso clínico de macrolídeos e lincosamidas. No entanto, a presença de cepas de *S. aureus* resistentes a macrolídeo-lincosamida-estreptogramina B (MLSB) é cada vez mais comum. As estações de tratamento de esgoto (ETEs) são a principal fonte antropogênica de

determinantes de resistência. No entanto, poucos estudos avaliaram a importância desse ambiente na disseminação de cepas de *S. aureus* resistentes ao MLSB. Assim, nosso objetivo foi avaliar o impacto de uma ETE doméstico na resistência ao MLSB e à penicilina em *S. aureus* no sudeste do Brasil. Dos 35 isolados testados, 40,6% eram resistentes à penicilina. Resistência à eritromicina (8,6%) e quinolonas (2,8%) foi menos comum. Apesar da baixa taxa de resistência à clindamicina (2,8%), muitos isolados apresentaram sensibilidade reduzida a esse antibiótico (57,1%). Em relação aos fenótipos de resistência dos isolados de estafilococos, a resistência induzível ao MLSB (D-teste positivo) foi encontrada em dois isolados. Além disso, 27 isolados de *S. aureus* mostraram a capacidade de produzir penicilinase. Neste artigo relatamos pela primeira vez a importância das ETEs na disseminação da resistência do MSLB entre *S. aureus* do sudeste do Brasil.

Palavras-chave: : Resistência a antibióticos, D-teste, teste da borda da zona da penicilina, quinolonas, *Staphylococcus aureus*, ambiente aquático.

Introduction

Staphylococcus aureus is one of the major bacterial pathogens of medical interest [1]. Although it is estimated that approximately 20% of the general human population are persistently colonized with *S. aureus*, this microorganism can cause a wide variety of clinical complications ranging from self-limited superficial infections to severe bacteremia or pneumonia [2]. Various classes of antimicrobials are used for the treatment of these infections, such as β-lactams, macrolides, lincosamides and quinolones [3]. In addition, with the emergence of penicillin- and oxacillin-resistant strains since the 1960s, the use of vancomycin (glycopeptide) has also become common. Methicillin-resistant *S. aureus* (MRSA) strains, which are resistant to all β-lactams, were initially only detected in hospital settings [4]. However, since 1990, reports of resistant strains within the community have been described [5]. In the United States, the mortality rate from MRSA-associated infections outnumber those caused by HIV/AIDS and tuberculosis combined [6]. The colonization rate in American hospital settings is quite variable, and in some cases may affect up to 85% of patients [7]. In Brazil, 31% of *S. aureus* isolates from hospitalized patients are characterized as MRSA [8].

Macrolides and lincosamides are therapeutic options for the treatment of MRSA infection; however clinical failure of therapy has been reported when the strains harbor the *erm* gene. This gene encodes clindamycin-induced resistance and cross-resistance to erythromycin, conferring the macrolide-lincosamide-streptogramin B (MLS_B) resistance *phenotype* [9]. In general, exposure to subinhibitory antibiotic concentrations is related to MLS_B resistance. In this context, wastewater is an important environment

for the development of bacterial resistance as it harbors a complex bacterial community, receives residues of several antimicrobials and is considered a hotspot for gene exchange, including the exchange of genes that confer antimicrobial resistance (e.g., *erm, bla*$_{ampo}$, *norA, acrABC, tetK, mecA* and *blaZ*) [10, 11].

According to previous studies, the prevalence of *S. aureus* in wastewaters is low compared to clinical environments [12]. However, it should be highlighted that wastewater treatment plants (WWTPs) may be an important reservoir and source of MSL_B-resistant *S. aureus* [13, 14]. Thus, considering the possibility of bacterial exchange between the clinical and environmental settings, investigation of the presence of resistant *S. aureus* strains in WWTPs is of great relevance as it may contribute to containing the spread of these microorganisms [13]. While many studies have investigated the resistance of enterobacteriaceae present in WWTPs, there is limited information on antibiotic-resistant *S. aureus* in this environment, which is of importance in developing countries [14]. Thus, we aimed to investigate the susceptibility of *S. aureus* isolates recovered from of a community WWTP in Brazil to several clinically important antimicrobials. In addition, the presence of clindamycin-induced resistance and penicillinase production was studied in isolates to determine the potential for this environment to act as a reservoir and source of MSL_B- and penicillin-resistant *S. aureus*.

Materials and methods

Sample collection and recovery of *Staphylococcus aureus*

The area selected for this study was the city of Divinópolis (Minas Gerais), located in southeast Brazil (232 945 inhabitants). One liter of both raw sewage (RS) and effluent (EF) were collected from the Rio Pará WWTP (geographical coordinates: 20°08'20"S and 44°53'02"W) on June 8, 2015. The WWTP studded adopts the conventional activated sludge treatment system and receive domestic sewage generated by approximately 10% of the population from Divinópolis, been that their effluent is discharged in the Pará River. All samples were stored in sterilized polypropylene bottles and transported on ice to the laboratory within 2 h of collection. The sample collection was authorized by *Companhia de Saneamento de Minas Gerais* (Copasa), a publicly owned company responsible for the collection and treatment of sewage and water supply in the state of Minas Gerais (Brazil).

For the isolation of *S. aureus*, 100 μL of RS and EF were plated directly *onto mannitol salt agar* (Labm, Brazil) *in duplicate* after being serially diluted (10^{-1} to 10^{-5}) in a sterile saline solution 0.85% (NaCl). The plates were incubated at 37 °C for up to 48 h. After this incubation period, plates that had grown 20 to 200 colonies were selected for determination

of the number of colonies forming units (CFU) per milliliter of RS and EF. Mannitol-fermenting colonies, which are yellow in color, were selected, inoculated in brain heart infusion (BHI) broth (Difco, India) and incubated at 37 °C for 24 h. Subsequently, the isolates were repeatedly streaked onto the same agar to check their purity. We also considered tests for catalase, coagulase and DNase, in addition to Gram staining, to confirm the species identification (*S. aureus* is positive for all these proves) [15]. The colonies isolated and identified as *S. aureus* were stored in nutrient broth containing 25% glycerol at -80 °C until further use.

Determination of antibiotic susceptibility profile

The antimicrobial susceptibility profile was determined by the disc diffusion method according to the recommendations of the Clinical Laboratory Standard Institute [16]. The following antimicrobials (DME Sensidisc, Brazil) were tested: β-lactams (penicillin, PEN), macrolides (erythromycin, ERT), lincosamides (clindamycin, CLN), and quinolones (ciprofloxacin, CIP; ofloxacin, OFX; norfloxacin, NOR). Cefoxitin disk (DME Sensidisc, Brazil) was used to predict the oxacillin susceptibility profile. *Staphylococcus aureus* ATCC 29213 was used as control.

Inducible clindamycin-resistance assay

The D-test was performed according to the CLSI (2017) [16] to phenotypically determine resistance to MSL_B. Briefly, the antimicrobials clindamycin (2 μg) and erythromycin (15 μg) were placed at a distance of 15-26 mm on the surface of Mueller-Hinton agar (Alere, USA) which had been inoculated with each *S. aureus* isolate. The plates were then incubated at 35 ± 2 °C for 16-18 h. Verification of flattening in the erythromycin inhibition halo resembling the letter "D" indicates inducible resistance to clindamycin (figure 1). *Staphylococcus aureus* ATCC25923 and *S. aureus* ATCC29213 were used as controls.

Penicillinase production

Penicillinase production was investigated in all *S. aureus* isolates by the penicillin zone-edge method according to the CLSI (2017) [16]. This test is based on the appearance of the inhibition zone edge surrounding the penicillin G disk (DME Sensidisc, Brazil) after the disc-diffusion assay. The result was defined as negative when the appearance of the edge was fuzzy, resembling a "beach", and as positive when the edge was sharp like a "cliff". *Staphylococcus aureus* ATCC25923 and *S. aureus* ATCC29213 were used as controls.

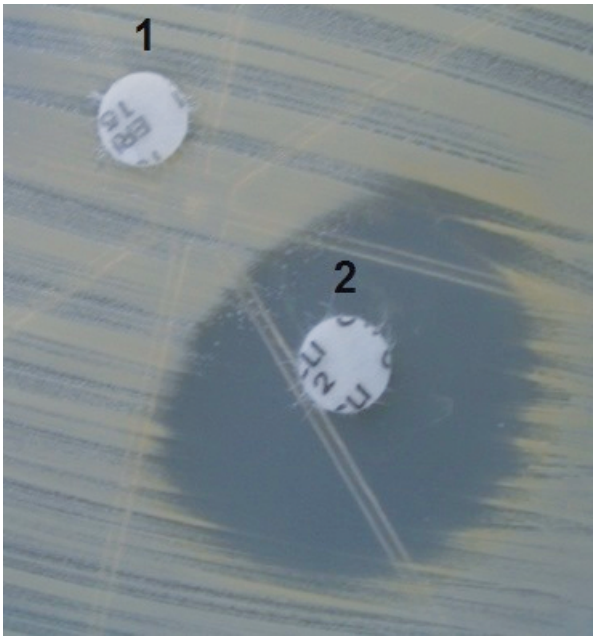

Figure 1. Representation of a positive result in the phenotypic test for inducible MLS_B resistance (D-test) in *S. aureus* isolates. 1 - Erythromycin. 2 - Clindamycin.

Results and discussion

Methicillin-resistant *S. aureus* is one of the most prevalent multidrug-resistant microorganisms that cause infection in both the community and in health-care settings. Macrolides and lincosamides are therapeutic options for the treatment of MRSA-infections; however, resistance to these antibiotics has increased in recent years [17]. This phenomenon in *S. aureus* has rapidly emerged, mainly due to exposure to subinhibitory antibiotic concentrations combined with the acquisition of antibiotic-resistance genes, such as those of the *erm* family [18, 19]. Wastewater treatment plants combine these two factors, as well as having a nutrient-rich environment that favors microbial proliferation [10]. However, despite the importance of WWTPs in the dissemination of antimicrobial resistance, there is little available information concerning the impact of this environment on MSL_B resistance in *S. aureus*. Furthermore, only few studies have evaluated the influence of domestic WWTPs on antimicrobial resistance in developing countries, and the dynamics of this phenomenon remain to be fully elucidated in these regions [10, 14]. Thus, in this study we aimed to evaluate the resistance profile as well as the phenotypic characteristics related to the clindamycin-induced resistance and penicillinase production in *S. aureus* isolated from a full-scale domestic WWTP in Brazil.

Microbiological analyses revealed 260 and 20 CFU/mL of *S. aureus* from RS and EF samples, respectively. In fact, several studies have revealed that, although there is often a high level of microbes present in the initial stages of wastewater treatment, microorganisms are either eliminated or reduced in final stage [12, 20]. Similar to this study, the sewage treatment employed in WWTPs in Spain (88.3%) [21] and Germany (99.9%) [22] also showed high clearance rates for *Staphylococcus*. The drastic reduction in the *S. aureus* population after wastewater treatment can, at least in part, be explained by the retention time of the effluent. According to Li *et al.* (2015) [23], the retention time of effluent has a negative effect on the survival of *S. aureus* because it disrupts important cell surface properties such as the zeta potential, hydrophobicity, and charge density.

A total of 35 different colonies (33 from RS and 2 from EF) were isolated on the mannitol agar, and these were included in the antimicrobial susceptibility tests and for phenotypic identification of resistance. As observed in table 1, in general the isolates showed high sensitivity to the antimicrobials tested except penicillin, which showed a considerable resistance rate (40.6%, 13/32) (figure 2). In accordance with our data, a high percentage of penicillin-resistant *S. aureus* in domestic WWTPs has also been found in Tunisia (100%) [24], Portugal (57.1%) [25] and Spain (40.62%) [21].

Despite previous studies having indicated the presence of MRSA in WWTPs [14, 13, 26-28], our study did not identify any isolates with this phenotype (figure 2). Gram-negative bacteria are the predominant infectious agents in Latin America and the Caribbean, while Gram-positive bacteria are more frequent in the USA, Europe, and countries of the Pacific region [26]. Thus, it is expected that the selective pressure driving the spread of MRSA will be less frequent in Latin countries such as Brazil. Corroborating this hypothesis, MRSA isolates are most common in WWTPs in the USA [13, 14], Australia [27], Taiwan [28] and Spain [21].

One of the most interesting findings from the current study was the low level of resistance to quinolones observed among the isolates. These antibiotics are partially metabolized by humans and animals, remaining active in the aquatic environment, and they are not removed by the treatments normally performed in WWTPs [29]. Thus, quinolone-resistant strains can be easily found in this environment. In this study, of the *S. aureus* isolates tested, none showed resistance to levofloxacin and norfloxacin, and only one isolate from EF was resistant to ofloxacin (3.1%, 1/32). Similarly, most *S. aureus* isolates were sensitive to erythromycin (91.4%, 32/35) (figure 2). In the past decade, the clinical use of erythromycin has been limited and is often substituted with other antibiotics due to their better pharmacokinetic proprieties and fewer side effects [30]. Thus, the low rate of erythromycin resistance reported in this study can be explained by reduced selective pressure related to this antibiotic. In turn, although clindamycin-resistant *S. aureus* was uncommon in the WWTP studied, it should be

Table 1. Summary of resistance profile and identification phenotypic of inducible MSL_B resistance and penicillinase production from *S. aureus* isolated in a full-scale domestic wastewater treatment plants (WWTP).

S. aureus isolated	Antimicrobial resistance profile[a]							Phenotypic tests[b]	
	ERT	CLN	PEN	LEV	NOR	OFX	OXA	D-test	Penicillinase
Raw sewage									
SA1BEB	S	S	S	S	S	S	S	-	+
SA2BEB	S	I	S	S	S	S	S	-	+
SA3BEB	S	I	**R**	S	S	S	S	-	+
SA4BEB	S	S	S	S	S	S	S	-	+
SA5BEB	S	S	**R**	S	S	S	S	-	+
SA6BEB	S	S	S	S	S	S	S	-	+
SA7BEB	S	S	S	S	S	S	S	-	+
SA8BEB	S	S	**R**	S	S	S	S	-	+
SA1CEB	S	S	**R**	S	S	S	S	-	+
SA2CEB	S	S	S	S	S	S	S	-	+
SA3CEB	S	S	S	S	S	S	S	-	+
SA4CEB	S	**R**	**R**	S	S	S	S	-	+
SA5CEB	S	I	S	S	S	S	S	-	+
SA6CEB	S	I	S	S	S	S	S	-	-
SA1DEB	S	I	**R**	S	S	S	S	-	+
SA2DEB	S	I	S	S	S	S	S	-	+
SA5DEB	S	I	S	S	S	S	S	-	+
SA7DEB	S	I	S	S	S	S	S	-	+
SA8DEB	S	I	S	S	S	S	S	-	+
SA1EEB	I	I	**R**	S	S	S	S	-	+
SA2EEB	S	I	**R**	S	S	S	S	-	+
SA5EEB	S	I	S	S	S	S	S	-	+
SA1FEB	S	I	S	S	S	S	S	-	-
SA2FEB	S	S	S	S	S	S	S	-	+
SA5FEB	S	I	**R**	S	S	S	S	-	+

(*Continued*)

Table 1. Summary of resistance profile and identification phenotypic of inducible MSL_B resistance and penicillinase production from *S. aureus* isolated in a full-scale domestic wastewater treatment plants (WWTP).

S. aureus isolated	Antimicrobial resistance profile[a]							Phenotypic tests[b]	
	ERT	CLN	PEN	LEV	NOR	OFX	OXA	D-test	Penicillinase
SA6FEB	**R**	I	S	S	S	S	S	+	-
SA2GEB	**R**	I	NT	NT	NT	NT	S	-	NT
SA3GEB	I	S	NT	NT	NT	NT	S	-	NT
SA4GEB	S	I	**R**	S	S	S	S	-	+
SA7GEB	S	S	S	S	S	S	S	-	-
SA8GEB	I	S	**R**	S	S	S	S	-	-
SA2HEB	**R**	I	NT	NT	NT	NT	S	+	NT
SA3HEB	S	I	S	S	S	S	S	-	+
Effluent									
SA3AEF	S	I	**R**	S	S	S	S	-	+
SA6AEF	S	S	**R**	S	S	R	S	-	+

[a]S: susceptible; R: resistant; I: intermediate. [b]positive test (+); negative test (-). NT: not tested; ERT: erythromycin; CLN: clindamycin; PEN: penicillin; CIP: ciprofloxacin; OFX: ofloxacin; NOR: norfloxacin; OXA: oxacillin.

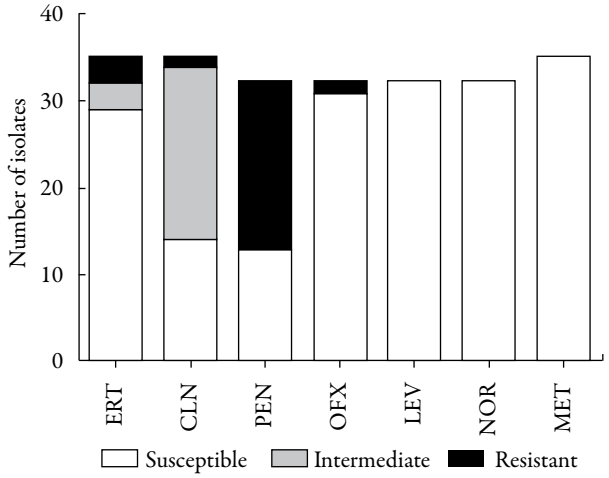

Figure 2. Susceptibility profile of *Staphylococcus aureus* isolated from a full-scale domestic wastewater treatment plants (WWTP). ERT: erythromycin; CLN: clindamycin; PEN: penicillin; OFX: ofloxacin; LEV: levofloxacin; NOR: norfloxacin; MET: methicillin.

noted that 20 isolates (57.1%) showed an intermediate level of susceptibility to this lincosamide, which highlights the possibility of the spread of resistance within this environment (figure 2). Goldstein *et al.* [13] reported that sewage represents an important route of dissemination of MLS_B-resistant *S. aureus*, and the most common resistance gene related to this phenotype was identified to be *ermC*. The family of erythromycin ribosomal methylase (*erm*) genes encodes an adenine-specific N-methyltransferase that methylates the 23S region of rRNA, conferring resistance to all macrolides, lincosamides, and streptogramin B [19].

Erythromycin-induced MSL_B resistance was investigated by D-zone test. Two of 35 isolates tested, both derived from RS, were found to be D-test-positive (5.7%). This finding corroborates a study by Hess & Gallert [22], which reported that inducible MLS_B resistance (D-test-positive) in *S. aureus* from sewage (14-19%) occurs at a lower frequency than constitutive MLS_B resistance (62.2-75.5%). Penicillinase production was also investigated in 32 *S. aureus* isolates by the penicillin zone-edge method. A total of 27 isolates were found to produce penicillinase, although several of these (55.5%) were susceptible to penicillin. According to Kaase *et al.* [31] the penicillin zone-edge test is the most sensitive phenotypic method for penicillinase detection, but some species that not showed genetic determinants to this beta-lactamase, might have positive result in test. Thus, the inconsistencies between the findings in this study highlight the need to confirm, by molecular methods, whether *blaZ* gene is present in the positive isolates.

In summary, MRSA isolates were absent, and we found a reduced rate of resistance to erythromycin in full-scale domestic WWTPs studded. The high frequency of resistance to penicillin, in turn, suggests the indiscriminate use of this antibiotic in the region of station. In addition, the high rate of intermediate sensitivity to clindamycin among the isolates suggests that domestic sewage can contribute to the advancement of MLS_B-resistant *S. aureus*. However, future studies should be performed to better understand the dynamics of this phenomenon, especially in WWTPs from other regions of Brazil.

Acknowledgements

The authors would like to thank the University of São João del-Rei for its support during the research. W.G.L. is grateful to *Coordenação de Aperfeiçoamento de Pessoal do Nível Superior* (CAPES) for a Ph.D. fellowship.

Disclosure statement

No potential conflict of interest was reported by the authors.

References

1. S.Y.C. Tong, J.S. Davis, E. Eichenberger, T.L. Holland, V.G. Fowler, Jr., *Staphylococcus aureus* infections: Epidemiology, pathophysiology, clinical manifestations, and management, *Clin. Microbiol. Rev.*, **28**, 603-661 (2015).

2. J.A. Lindsay, M.T. Holden, *Staphylococcus aureus*: superbug, super genome?, *Trends Microbiol.*, **12**, 378-385 (2004).

3. P. Moreillon, New and emerging treatment of *Staphylococcus aureus* infections in the hospital setting, *Clin. Microbiol. Infect.*, **14**, 32-41 (2008).

4. M. Abbas, M. Paul, A. Huttner, New and improved? A review of novel antibiotics for Gram-positive bacteria, *Clin. Microbiol. Infect*., **23**, 697-703 (2017).

5. M. Bassetti, E.M. Trecarichi, A. Mesini, T. Spanu, D.R. Giacobbe, M. Rossi, E. Shenone, G.D. Pascale, M.P. Molinari, R. Cauda, C. Viscoli, M. Tumbarello, Risk factors and mortality of healthcare-associated and community-acquired *Staphylococcus aureus* bacteraemia, *Clin. Microbiol. Infect.*, **18**, 862-869 (2012).

6. H.W. Boucher, G.R. Corey, Epidemiology of methicillin-resistant *Staphylococcus aureus*, *Clin. Infect. Dis*., **46**, 344-349 (2008).

7. H. Grundmann, M. Aires-de-Sousa, J. Boyce, E. Tiemersma, Emergence and resurgence of meticillin-resistant *Staphylococcus aureus* as a public-health threat, *Lancet*, **368**, 874-885 (2006).

8. A.C. Gales, H.S. Sader, J. Ribeiro, C. Zoccoli, A. Barth, A.C. Pignatari, Antimicrobial susceptibility of gram-positive bacteria isolated in Brazilian hospitals participating in the SENTRY Program (2005-2008), *Braz. J. Infect. Dis.,* **13**, 90-98 (2009).

9. D.M.R. Amorim, O.C. Person, P.J. Amaral, I.I. Tanaka, Inducible resistance to clindamycin among *Staphylococcus aureus* isolates, *O Mundo da Saúde, São Paulo*, **33**, 401-405 (2009).

10. H. Chen, M. Zhang, Occurrence and removal of antibiotic resistance genes in municipal wastewater and rural domestic sewage treatment systems in eastern China, *Environ. Int.*, **55**, 9-14 (2013).

11. C.A. Michael, D. Dominey-Howes, M. Labbate, The antimicrobial resistance crisis: Causes, consequences, and management, *Front. Public. Health*, **145**, 1-8 (2014).

12. K.E. Shannon, D.Y. Lee, J.T. Trevors, L.A. Beaudette, Application of real-time quantitative PCR for the detection of selected bacterial pathogens during municipal wastewater treatment, *Sci. Total Environ.*, **382**, 121-9 (2007).

13. R.E.R. Goldstein, S.A. Micallef, S.G. Gibbs, J.A. Davis, X. He, A. George, L.M. Kleinfelter, N.A. Schreiber, S. Mukherjee, A. Sapkota, S.W. Joseph, A.R. Sapkota, Methicillin-resistant *Staphylococcus aureus* (MRSA) detected at four U.S. wastewater treatment plants, *Environ. Health Perspect.*, **120**, 1551-1558 (2012).

14. A. Naquin, J. Clement, M. Sauce, R. Grabert, M. Sherpa, R. Boopathy, Presence of antibiotic resistant *Staphylococcus aureus* in sewage treatment plant, *J. Water Sustainabil.*, **4**, 227-236 (2014).

15. E.W. Koneman, W.C. Winn-Jr, S.D. Allen, W.M. Janda, G.W. Procop, P.C. Schreckenberger, G.L. Woods, "Koneman, diagnóstico microbiológico: texto e atlas colorido", 6th. ed., Guanabara Koogan, Rio de Janeiro, 2008.

16. Clinical and Laboratory Standards Institute (CLSI), "Performance Standards for Antimicrobial Disk Susceptibility Testing", 28th ed., M02-A2, Wayne, PA, 2017.

17. M. Dadashi, M.J. Nasiri, F. Fallah, P. Owlia, B. Hajikhani, M. Emaneini, M. Mirpour, Methicillin-resistant *Staphylococcus aureus* (MRSA) in Iran: A systematic review and meta-analysis, *J. Glob. Antimicrob. Resist.*, **12**, 96-103 (2017).

18. S. Teeraputon, P. Santanirand, T. Wongchai, W. Songjang, N. Lapsomthob, D. Jaikrasun, S. Toonkaew, P. Tophon, Prevalence of methicillin resistance and macrolide-lincosamide-streptogramin B resistance in *Staphylococcus haemolyticus* among clinical strains at a tertiary-care hospital in Thailand, *New Microbes New Infect.*, **19**, 28-33 (2017).

19. G. Maravić, Macrolide resistance based on the Erm-mediated rRNA methylation, *Curr. Drug Targets Infect. Disord.*, **4**, 193-202 (2004).

20. M.C. Paiva, M.P. Ávila, M.P. Reis, P.S Costa, R.M. Nardi, A.M. Nascimento, The microbiota and abundance of the Class 1 Integron-Integrase gene in tropical sewage treatment plant influent and activated sludge, *PLoS One*, **10**, 1-12 (2015).

21. P. Gómez, C. Lozano, D. Benito, V. Estepa, C. Tenorio, M. Zarazaga, C. Torres, Characterization of staphylococci in urban wastewater treatment plants in Spain, with detection of methicillin resistant *Staphylococcus aureus* ST398, *Environ. Pollut.*, **212**, 71-76 (2016).

22. S. Hess, C. Gallert, Demonstration of staphylococci with inducible macrolide-lincosamide-streptogramin B (MLS_B) resistance in sewage and river water and of the capacity of anhydroerythromycin to induce MLS_B, *FEMS Microbiol. Ecol.*, **88**, 48-59 (2014).

23. J. Li, X. Zhao, X. Tian, J. Li, J. Sjollema, A. Wang, Retention in treated wastewater affects survival and deposition of *Staphylococcus aureus* and *Escherichia coli* in sand columns, *Appl. Environ. Microbiol*., **81**, 2199-2205 (2015).

24. S.M. Ben, M.S. Abbassi, P. Gómez, L. Ruiz-Ripa, S. Sghaier, C. Ibrahim, C. Torres, A. Hassen, *Staphylococcus aureus* isolated from wastewater treatment plants in Tunisia: occurrence of human and animal associated lineages, *J. Water Health*, **15**, 638-643 (2017).

25. C. Faria, I. Vaz-Moreira, E. Serapicos, O.C. Nunes, C.M. Manaia, Antibiotic resistance in coagulase negative staphylococci isolated from wastewater and drinking water, *Sci. Total Environ*., **407**, 3876-3882 (2009).

26. C.M. Luna, E. Rodriguez-Noriega, L. Bavestrello, M. Guzmán-Blanco, Gram-negative infections in adult intensive care units of Latin America and the Caribbean, *Crit. Care Res. Pract.*, **2014**, 480463 (2014).

27. J.M. Thompson, A. Gündoğdu, H.M. Stratton, M. Katouli, Antibiotic resistant *Staphylococcus aureus* in hospital wastewaters and sewage treatment plants with special reference to methicillin-resistant *Staphylococcus aureus* (MRSA), *J. Appl. Microbiol.*, **114**, 44-54 (2013).

28. M.T. Wan, C.C. Chou, Class 1 integrons and the antiseptic resistance gene (qacEΔ1) in municipal and swine slaughterhouse wastewater treatment plants and wastewater-associated methicillin-resistant *Staphylococcus aureus*, *Int. J. Environ. Res. Public Health*, **12**, 6249-6260 (2015).

29. N. Dorival-García, A. Zafra-Gómez, F.J. Camino-Sánchez, A. Navalón, J.L. Vílchez, Analysis of quinolone antibiotic derivatives in sewage sludge samples by liquid chromatography-tandem mass spectrometry: comparison of the efficiency of three extraction techniques, *Talanta*, **106**, 104-118 (2013).

30. D. Jelić, R. Antolović, From erythromycin to azithromycin and new potential ribosome-binding antimicrobials, *Antibiotics (Basel)*, **5**, 1-29 (2016).

31. M. Kaase, S. Lenga, S. Friedrich, F. Szabados, T. Sakinc, B. Kleine, S.G. Gatermann, Comparison of phenotypic methods for penicillinase detection in *Staphylococcus aureus*, *Clin. Microbiol. Infect.*, **14**, 614-616 (2008).

How to cite this article

S.L. Oliveira-Toledo, R.M. Silveira-Silva, I.C. Rodrigues dos Santos, W.G. Lima, L. Gonçalves-Rodrigues-Ferreira, M.C. Paiva, Domestic wastewater treatment plants as sources of macrolide-lincosamide-streptogramin B- and penicillin-resistant *Staphylococcus aureus* in Brazil, *Rev. Colomb. Cienc. Quím. Farm.*, **49**(2), 267-279 (2020).

Artículo de investigación tecnológica / *http://dx.doi.org/10.15446/rcciquifa.v49n2.88917*

Determinación de la estabilidad e irritabilidad del hidrolizado de sericina

Hector Correa-Rivero*, Elaine Díaz-Casañas, Osmel Bernal Veitía, Yolanda Malvarez Fernández

Dirección de Producción, Centro Nacional de Sanidad Agropecuaria (CENSA), San José de las Lajas, Mayabeque, Cuba.

*Correo electrónico: hcorrea@censa.edu.cu

Recibido: 8 de enero de 2020

Revisado: 16 de abril de 2020

Aceptado: 17 de abril 2020

Resumen

La sericina es una proteína globular que se obtiene a partir de los capullos del gusano de seda *Bombyx mori* y tiene aplicaciones en la industria farmacéutica, alimentaria y cosmética. El objetivo de este trabajo fue determinar la estabilidad e irritabilidad dérmica y oftálmica del hidrolizado de sericina (líquido). 3 lotes producidos a escala piloto se almacenaron en frascos de polietileno de alta densidad en diferentes condiciones de temperatura: 40±2 ºC por 6 meses y temperatura hasta los 30 ºC durante 18 meses. Se hizo una evaluación fisicoquímica y microbiológica a tiempo inicial y 1, 2, 3, 6 meses (acelerada) y 3, 6, 9, 12, 18 meses (anaquel). Se llevaron a cabo los estudios toxicológicos correspondientes a productos con fines cosméticos. Se constató que las características organolépticas, densidad, el pH, la concentración de proteínas y la identidad de los lotes en las dos condiciones de temperaturas y no hubo variación significativa en el tiempo del estudio. Se definió el tiempo de vida útil del producto en 18 meses. Se concluyó que el hidrolizado de sericina en frascos de polietileno de alta densidad es estable a temperaturas hasta 30 ºC durante 18 meses y no clasificó como irritante dérmico, ni oftálmico.

Palabras clave: Sericina, estabilidad, irritabilidad.

Summary

Determination of the stability and irritability of the sericin hydrolyzate

Sericin is a globular protein that is obtained from the cocoons of the *Bombyx mori* silkworm and has applications in the pharmaceutical, food and cosmetic industries. The objective of this work was to determine the stability and dermal and ophthalmic irritability of the sericine hydrolyzate (liquid). 3 batches produced on a pilot scale were stored in high density polyethylene bottles under different temperature conditions: 40 ± 2 °C for 6 months and temperature up to 30 °C for 18 months. A physical-chemical and microbiological evaluation was performed at initial time and 1, 2, 3, 6 months (accelerated) and 3, 6, 9, 12, 18 months (shelf). Toxicological studies corresponding to products for cosmetic purposes were performed. It was found that the organoleptic characteristics, density, pH, protein concentration and the identity of the lots in the two temperature conditions, there was no significant variation in the study time. The shelf life of the product was defined in 18 months. It was concluded that the sericin hydrolyzate in high density polyethylene bottles is stable at temperatures up to 30 °C for 18 months and this product did not classify as dermal or ophthalmic irritant.

Keywords: Sericin, stability, irritability.

Introducción

La proteína sericina es un polímero natural producido por el gusano de seda *Bombyx mori* [1]. Esta glicoproteína es soluble en agua y es 25%-30% del peso del capullo; además actúa como un adhesivo que une dos filamentos de fibroína para formar el hilo de seda [1, 2]. La molécula es hidrófila con un peso molecular que varía de 20 a 400 kDa y consta de 18 aminoácidos (incluidos los esenciales). Los grupos polares (grupos carboxilo, hidroxilo y amino) de las cadenas laterales de aminoácidos y su composición orgánica, solubilidad y la organización estructural permite la reticulación, las copolimerizaciones y las combinaciones con otros polímeros, que en conjunto transmiten propiedades únicas a la sericina, que hacen de esta un producto antioxidante, hidratante, cicatrizante, antibacteriano, con protección antimicrobiana, que también protege de la radiación ultravioleta y es antitumoral [3-5].

Con el desarrollo de la sericultura en Cuba, la producción de derivados del gusano de seda está en auge, entre ellos el hidrolizado de sericina, materia prima de la industria

cosmética [6]. El Centro Nacional de Sanidad Agropecuaria con la Entidad de Ciencia, Tecnología e Innovación "Sierra Maestra" diseñaron, desarrollaron, registraron y comercializan el hidrolizado de sericina (líquido), que se obtiene a través de un proceso de extracción y purificación de esta proteína presente en el capullo del gusano de seda.

La seguridad y la eficacia de los productos están influenciadas no solo por sus propiedades intrínsecas sino por su estabilidad en el tiempo, por lo cual fue necesario, determinar el tiempo de vida útil e irritabilidad dérmica y oftálmica de este producto para fines cosméticos, lo que constituyó el objetivo de este trabajo.

Materiales y métodos

Los 3 lotes producidos a escala piloto se identificaron como HS01, HS02 y HS03 y fueron envasados en frascos de 100 mL de polietileno de alta densidad, con tapón de goma y retapa de aluminio, una de las presentaciones en las que se propone para circular en el mercado.

Se tomaron cantidades suficientes de producto de cada lote para evaluar sus características fisicoquímicas y microbiológicas en el tiempo inicial y a los 1, 3 y 6 meses para la estabilidad acelerada en condiciones de temperatura controlada en 40±2 °C. Para la estabilidad en anaquel la condición de almacenamiento fue a temperatura ambiente que en Cuba tiene una media anual de 25 °C. Según las regulaciones vigentes [7] en los productos que no requieren refrigeración, la condición de almacenamiento en anaquel en la zona climática donde se encuentra Cuba es hasta 30 °C. El estudio se realizó durante 18 meses y las evaluaciones fueron en tiempo inicial y a los 1, 3, 6, 9, 12, 18 meses.

Características organolépticas

Se evaluó la apariencia física en cuanto a olor y color, mediante la utilización de los órganos sensoriales [8,9].

Concentración de proteínas

El análisis de la concentración de proteínas se determinó por el método de Lowry [10], que es de tipo colorimétrico. Se utilizó dodecilsulfato de sodio (SDS) al 1% para diluir las muestras y se empleó albúmina de suero bovino (BSA) como patrón [11].

Identidad por electroforesis en geles de acrilamida con dodecilsulfato de sodio (SDS PAGE)

Se determinó la identidad por electroforesis en geles de acrilamida con SDS. El principio del método se basa en que la carga eléctrica que poseen las moléculas de proteínas,

las cuales migran a diferentes velocidades cuando se le aplica un campo eléctrico al sistema, a un pH previamente establecido, así se logró la resolución de una mezcla de proteínas [12].

pH

El pH se determinó con un pH-metro marca Mettler-Toledo y se consideró como límite de aceptación entre 4 y 6, según las características propias de la formulación.

Límite microbiano

Se procedió según lo establecido por la *The United States Pharmacopeia*, *USP 41* [13] para determinar el total de microorganismos viables aerobios e identificar las especies de microorganismos aislados [9] por el método de placa vertida o número más probable (NMP).

Irritabilidad

Los estudios de irritabilidad se desarrollaron de acuerdo con las guías generales para los ensayos de sustancias químicas de la *Organization for Economic Cooperation and Development* (OECD), en los principios de *Buenas prácticas de laboratorio* (BPL), según las leyes aplicadas al bienestar y cuidado humanitario de animales de laboratorio [14, 15], así como los lineamientos éticos trazados por la Organización Mundial de la Salud [16]. Los procedimientos se refinaron para minimizar la incomodidad, angustia o dolor de los animales.

Oftálmica. Se usaron 3 conejos albinos de Nueva Zelandia, adultos jóvenes de 1,8 a 2 kg de peso. El producto se aplicó con una jeringuilla de 1 mL (0,1 mL, sin aguja), directamente en el borde superior del limbo corneal, se separó el párpado inferior para evitar el derrame del producto, así este quedó en el saco conjuntival. Una vez administrado el compuesto el ojo tratado debió permanecer cerrado por espacio de 15 segundos, para ello se ejerció una ligera presión con los dedos índice y pulgar sobre los párpados. El otro ojo se tomó como control y no recibió tratamiento alguno. Se empleó en el examen de los ojos una solución de fluoresceína de sodio al 2 % para visualizar una eventual degradación de la córnea y un iluminador manual.

Dérmica. Se emplearon 3 conejos albinos de Nueva Zelandia, adultos jóvenes de 1,8 a 2 kg de peso. El producto se aplicó en una de las dos áreas depiladas de cada animal (6 cm^2), la cual se cubrió con un parche de gasa estéril. El área de la piel sin tratar de cada animal se utilizó como control. La sustancia en estudio se mantuvo expuesta en el sitio de la piel cubierto con el parche de gasa estéril durante 4 h.

Al retirarse cada parche se lavó la zona de aplicación con solución de cloruro de sodio 0,9 % estéril. Inmediatamente después de retirar el parche, se examinó a los conejos para detectar signos de eritema o edema, luego a los 60 minutos y a las 24, 48 y 72 h, luego, se registraron las reacciones dérmicas observadas [17]. El periodo de observación se mantuvo durante 14 días después de la administración de la sustancia en estudio.

Análisis estadístico

Se empleó el paquete estadístico Statgraphics Plus versión 5.1 (Statistical Graphics Corp., EUA) para verificar si existían diferencias entre los lotes con respecto a las variables pH y concentración de proteínas.

Resultados

Los resultados de la evaluación inicial realizada a los 3 lotes mostraron una buena reproducibilidad tecnológica. En cuanto a sus características organolépticas no se observaron cambios perceptibles, ni se detectaron signos visuales de inestabilidad física. Todos los lotes tanto en el estudio de estabilidad acelerada como en anaquel mantuvieron las especificaciones de calidad establecidas con una apariencia líquido claro de color amarillo pálido y también se mantuvo su olor característico.

En la figura 1 se puede apreciar que la concentración de proteínas tanto en el estudio de estabilidad acelerada como en el anaquel se mantiene en el intervalo 4-8 mg/mL durante el estudio de estabilidad de los lotes.

En la figura 2 se observa la presencia de la sericina, el hidrolizado de esta proteína obtenido en los 3 lotes evaluados (tanto en anaquel como en estabilidad acelerada) mostró una talla de 40-66 kDa. Donde L1 A: lote 1 estabilidad anaquel y L1 Ac: lote 1 estabilidad acelerada y así sucesivamente con los 3 lotes estudiados.

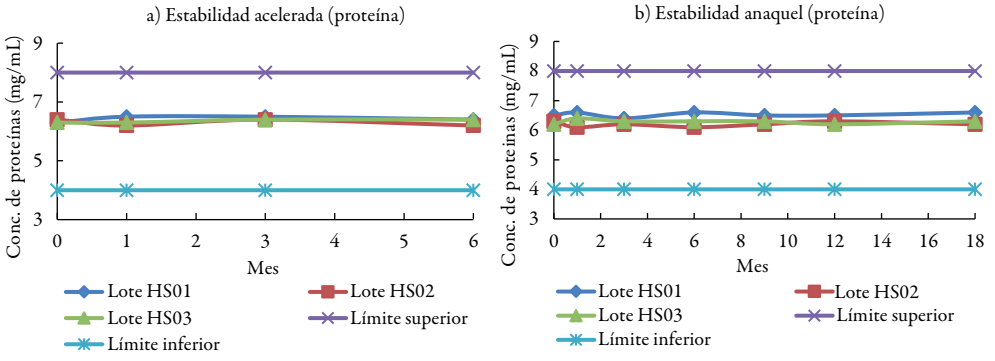

Figura 1. Resultados del contenido de proteínas: a) acelerada; b) anaquel.

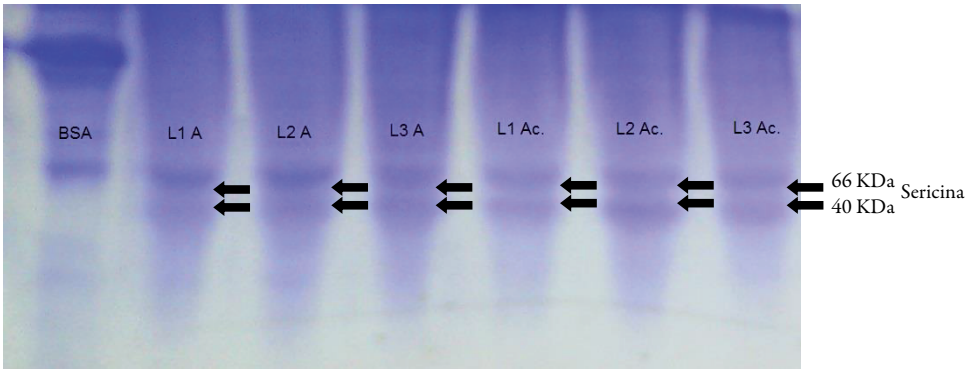

Figura 2. Patrón electroforético (SDS-PAGE) del hidrolizado de sericina.

El producto se diseñó con un pH en el intervalo de 4 a 5. En este sentido, tanto en el estudio de estabilidad acelerada y en anaquel, el pH de todos los lotes fue estable y no se manifestaron diferencias significativas entre los lotes durante los diferentes tiempos, lo que se puede apreciar en la figura 3.

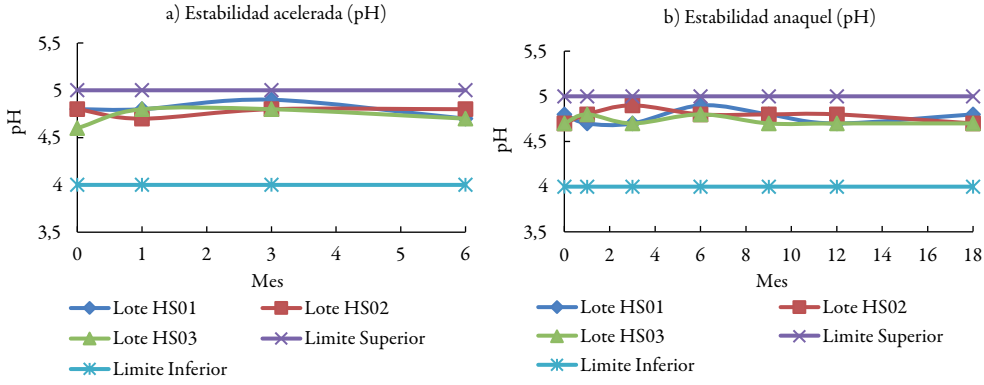

Figura 3. Resultados del pH en el tiempo: a) acelerada; b) anaquel.

Todos los lotes cumplieron con las especificaciones de límite microbiano establecidas, donde el conteo total de bacterias aerobias estuvo por debajo de 10^3 UFC/mL y el conteo total de hongos no fue superior a 20 UFC/mL, además no hubo presencia de los microrganismos patógenos: *Escherichia coli*, *Staphylococcus aureus*, *Pseudomona aeruginosa*, *Salmonella typhi* ni de otras enterobacterias [9, 13].

En los ensayos de toxicidad la aplicación dérmica y oftálmica del hidrolizado de sericina hechos en animales de experimentación no provocaron alteraciones dérmicas ni oftálmicas. En ambos ensayos un valor de índice de irritación primario y ocular igual a cero. Como se puede apreciar en las tablas 1 y 2 respectivamente.

En ambos ensayos no se observaron otros signos clínicos en los animales. No fue necesaria la toma de muestras de piel para el estudio histopatológico. El producto en estudio se clasifica como no irritante dérmico y ni ocular por los resultados en las condiciones experimentales evaluadas.

Tabla 1. Resultados del ensayo de irritación dérmica del producto en conejos.

Reacciones dérmicas observadas	Tiempo de observación (después de retirado el parche)					Índice de irritación primaria (IIP)
	0 h	1 h	24 h	48 h	72 h	
Eritema y formación de escaras	0	0	0	0	0	0
Formación de edema	0	0	0	0	0	0

Tabla 2. Resultados del ensayo de irritación oftálmica del producto en conejos.

Tiempo de observación (horas)	Lesiones oculares observadas		
	Córnea	Iris	Conjuntiva
1	0	0	0
24	0	0	0
42	0	0	0
72	0	0	0
Total (máximo valor 110)	0	0	0
Índice de irritación ocular (IIO)	0		

Discusión

La estabilidad de los productos farmacéuticos depende de factores ambientales como temperatura, humedad, luz, y de factores relacionados con el producto entre los que sobresalen las propiedades físicoquímicas del principio activo y de los excipientes, la forma farmacéutica y su composición, los procesos de fabricación, la naturaleza y propiedades del envase utilizado. Es por ello que el estudio de estabilidad es la principal herramienta para evaluar la fecha de caducidad y las condiciones de almacenamiento para los productos [18].

En este caso el producto no es un medicamento, pero si una materia prima registrado para elaboración de productos cosméticos. Según los resultados antes expuestos, el producto mantiene sus propiedades fisicoquímicas y sus características en las condiciones y periodo de almacenamiento evaluadas, lo que concuerda con lo que establecen las regulaciones para este tipo de producto, así se definió su periodo de validez [18].

La concentración del ingrediente activo es fundamental porque de esta depende la actividad biológica, con la concentración de proteína de seda (sericina) que posee el producto se pueden fabricar productos cosméticos y farmacéuticos. La sericina de esta formulación se corresponde con la fracción de mayor solubilidad en agua, atendiendo al proceso (altas temperaturas) mediante el cual se obtuvo. Según Kunz *et al.* [19], los diversos métodos de extracción de sericina, su origen y la variedad de capullo, proporcionan diferentes características y peso molecular, lo que puede reflejarse además en propiedades biológicas.

Como se ha mencionado anteriormente, el peso molecular de la sericina se ve afectado por factores como la temperatura, el pH y el tiempo del proceso de extracción que se utilice, en este caso se obtuvieron dos bandas de aproximadamente de 40 y 60 kDa, respectivamente, esto es similar a lo reportado por Çapar y Aygün [20], quienes determinaron el peso molecular por métodos cromatográficos. Otros autores [21, 22] han obtenido sericina con fracciones de peso molecular entre 12 y 66 kDa; 50 y 150 kDa; 100 y 200 kDa.

La determinación del pH es necesaria para detectar cualquier alteración de este indicador durante el almacenamiento, lo que asegura que el valor de pH del hidrolizado de sericina es compatible con los componentes de la formulación. El pH en todos los lotes fue estable y no se manifestaron diferencias durante el periodo de almacenamiento en los diferentes tiempos evaluados, sin que excediera los límites establecidos para este producto. En este caso el pH se estableció sobre lo ácido y lo más cercano posible al de la piel, ya que uno de los componentes de la formulación es efectivo solo en condiciones ácidas [23].

En ambos estudios de estabilidad, tanto en acelerada como en anaquel, los 3 lotes cumplieron con el límite microbiano, que permiten controlar la carga microbiana en procesos como la purificación, la formulación y el envase. Estos resultados demostraron que la selección del envase final contribuyó a que el producto se mantuviera dentro de las especificaciones establecidas por la USP 41 [13], aunque todas las funciones del acondicionamiento son importantes, puede afirmarse que la protección es el factor crítico ya que incide sobre la estabilidad del producto [24, 25].

En los ensayos de toxicidad, la aplicación dérmica y oftálmica del hidrolizado de sericina, realizados en animales de experimentación no provocaron alteraciones dérmicas ni oftálmicas, por lo que no mostraron signos clínicos que evidenciaran un proceso tóxico.

De forma general, los 3 lotes mantuvieron las especificaciones evaluadas dentro de los límites establecidos, lo que indica que fue certera la selección de los excipientes de la formulación, así como del envase, aspecto fundamental para garantizar la estabilidad del medicamento [24, 25]. Se concluyó que el hidrolizado de sericina en frascos de polietileno de alta densidad es estable a temperaturas hasta 30 °C durante 18 meses y no es irritante.

Agradecimientos

Los autores desean agradecer a la dirección del Proyecto Nacional de Sericultura de Cuba, especialmente a la ECTI Sierra Maestra por su contribución al financiamiento de esta investigación.

Conflicto de intereses

Los autores declaran que no existe conflicto de intereses.

Referencias

1. R.I. Kunz, R.M. Costa, L.F. Chasko, M.R. Marçal, Silkworm Sericin: Properties and biomedical applications, *Biomed. Res. Int.*, **2016**, 8175701 (2016).

2. M. Mondal, K. Trivedy, S.N. Kumar, The silk proteins, sericin and fibroin in silkworm, *Bombyx mori Linn*, a review, *Caspian J. Environ. Sci.*, **5**(2), 63-76 (2007).

3. P. Aramwit, S. Kanokpanont, W. De-Eknamkul, T. Srichana, Monitoring of inflammatory mediators induced by silk sericina, *J. Biosci. Bioeng.*, **107**(5), 556-561 (2009).

4. T. Wei, M.Z. Li, R.J. Xie, Preparation and structure of porous silk sericin materials, *Macromol. Mater. Eng.*, **290**(1), 188-194 (2005).

5. J.H. Wu, Z. Wang, S.Y. Xu, Preparation and characterization of sericin powder extracted from silk industry wastewater, *Food Chem.*, **103**(4), 1255-1262 (2007).

6. M.C. Pérez-Hernández, *Sericultura: bases científicas para su desarrollo sostenible en Cuba*, tesis doctoral, Instituto Nacional de Ciencia Agrícolas (INCA), 2017.

7. Regulación 24, *Requerimientos de los estudios de estabilidad para el registro de nuevos ingredientes farmacéuticos activos*, CECMED, La Habana, 2000.

8. NC-26-131, *Medicamentos veterinarios. Líquidos de administración oral o de uso externo, especificaciones generales de calidad*, CECMED, La Habana, 1985.

9. Regulación N.° 37, *Buenas prácticas de laboratorio para el control de medicamentos*, CECMED, La Habana, 2012.

10. O.H. Lowry, N.J. Rosebrough, A.L. Farr, R.J. Randall, Protein measurement with the folin-phenol reagent, *J. Biol. Chem.*, **132**, 265-275 (1951).

11. J.A. Whitsett, B.L. Ohning, G. Rose, J. Meuth, T. Weaver, Hydrophobic surfactant-associated protein in whole lung surfactant and its importance for biophysical activity in lung surfactant used for replacement therapy, *Pediatr. Res.*, **20**, 460 (1986).

12. A.H. Gordon, Electrophoresis of proteins in polyacrilamide and starch gels, en: *Laboratory techniques, biochemistry and molecular biology*, T.S. Work, E. Work, editors, Academic Press-Elsevier, New York, 1973.

13. *Farmacopea USP 41*, The United States Pharmacopeial Convention, Inc., Washington, D. C., 2018, p. 176, 253.

14. OECD, *Guideline for testing of chemicals*, OECD 405, Acute Eye Irrtitation/ Corrotion, 2012.

15. Regulación N.° 97-2012, Buenas prácticas de laboratorio para el control de medicamentos CECMED, La Habana, 2012.

16. WHO, *Draft regional guidelines on stability testing of active substances and pharmaceutical products*, URL: http://www.emro.who.int/emp/media/pdf/EMRC5312En.pdf

17. OECD, *Guideline for testing of chemicals*, OECD 404, Acute Dermal Irrtitation/ Corrotion, 2015.

18. Regulación N.° 23-2000, *Requerimientos de los estudios de estabilidad para el registro de productos farmacéuticos nuevos y conocidos*, CECMED, La Habana, 2000.

19. R.I. Kunz, R.M. Brancalhão, L.F. Ribeiro, M.R. Natali, Silkworm sericin: Properties and biomedical applications, *BioMed Res. Int.*, **2016**, 8175701 (2016).

20. G. Çapar, S.S. Aygün, Characterization of sericin protein recovered from silk wastewaters, *Turk. Hij. Den. Biyol. Derg.*, **72**(3), 219-234 (2015).

21. R. Sothornvit, R. Chollakup, P. Suwanruji, Extracted sericin from silk waste for film formation, *Songklanakarin J. Sci. Technol.*, **32**, 17-22 (2010).

22. P. Aramwit, O. Keongamaroon, T. Siritientong, N. Bang, O. Supasyndh, Sericin cream reduces pruritus in hemodialysis patients: a randomized, double-blind, placebo-controlled experimental study, *BMC Nephrol.*, **13**, 119 (2012).

23. R. Kirk, R. Sawyer, H. Egan, "Composición y análisis de alimentos de Pearson", Compañía Editorial Continental. México, 2004.

24. V. Ratna, Stability of drugs: Packaging and stability, 2005, URL: http://www.pharmainfo.net/free-books/stability-drugs?page=4961.

25. G.A. Shabir, Review of pharmaceutical product stability, packaging and the ICH Guidelines, *Am. Pharm. Rev.*, **11**(1), 139-141 (2008).

Cómo citar este artículo

H. Correa-Rivero, E. Díaz-Casañas, O. Bernal-Veitía, Y. Malvarez-Fernández, Determinación de la estabilidad e irritabilidad del hidrolizado de sericina, *Rev. Colomb. Cienc. Quím. Farm.*, **49**(2), 280-290 (2020).

Scientific research article / *http://dx.doi.org/10.15446/rcciquifa.v49n2.88988*

Safety assessment of complex benzoic acid using *in vitro* permeation assays with pig skin in Franz cells

Laura A. Martínez, Lina M. Sanabria, Yolima Baena*

Universidad Nacional de Colombia, Sede Bogotá, Facultad de Ciencias, Departamento de Farmacia, Grupo de investigación Sistemas para la liberación controlada de moléculas biológicamente activas (Silicomoba), A. A. 14490, Carrera 30 # 45-03, Bogotá D.C., Colombia.

*Corresponding author E-mail address: ybaenaa@unal.edu.co

Received: 25 September 2019

Revised: 17 April 2020

Accepted: 18 April 2020

Summary

Franz cells are one of the main tools to evaluate the transepithelial permeation of compounds through the performance of *in vitro* tests, these allows inferring the safety behavior of a compound in the skin. The objective of this research was to determine the permeation behavior of benzoic acid from complexes with polyelectrolytes $\left(EuB_{75}Cl_{25}, EuB_{100}\right)$, compared to benzoic acid without complexing, to infer its safety behavior. In a first phase, skin storage conditions were established comparatively evaluating the diffusion parameters (flow and permeation constant) and transepithelial water loss, using ears skin of freshly slaughtered pigs, stored in 1M NaCl at -2 °C for 3 days; it was worked under infinite doses conditions. Subsequently, the permeation test of two complexes between Eudragit E and benzoic acid, in comparison with benzoic acid, was carried out under finite dose conditions. The benzoic acid quantification was performed with an analytical method validated by HPLC-DAD. The results showed no significant differences showing that biological samples can be stored for 72 h under the conditions described. The permeation behavior of the complexed benzoic acid with respect to the free benzoic acid showed a better safety profile, since there was a lower permeation for the first case. These results show that complexation of benzoic acid could decrease the sensitivity reactions that it normally presents, based on the decrease in its permeation.

Key words: Franz cells, preservatives, benzoic acid, complexes, skin, security.

Resumen

Evaluación de seguridad del ácido benzoico complejado empleando ensayos de permeación *in vitro* con piel de cerdo en celdas de Franz

Las celdas de Franz son una de las herramientas para evaluar la permeación transepitelial de compuestos mediante la realización de ensayos *in vitro*, estos permiten inferir el comportamiento de seguridad de un compuesto en la piel. El objetivo de esta investigación fue determinar el comportamiento de permeación del ácido benzoico a partir de complejos con polielectrolitos $\left(EuB_{75}Cl_{25}, EuB_{100}\right)$ en comparación con el ácido benzoico sin complejar, para inferir su comportamiento de seguridad. En una primera fase, se establecieron las condiciones de almacenamiento de la piel comparando los parámetros de difusión (flujo y constante de permeación) y pérdida de agua transepitelial, empleando piel de orejas de cerdos recién sacrificados, almacenadas en NaCl 1M a -2°C por 3 días; se trabajó bajo condiciones de dosis infinitas. Posteriormente, se realizó el ensayo de permeación de dos complejos entre ácido benzoico y Eudragit E, en comparación con el ácido benzoico, bajo condiciones de dosis finitas. La cuantificación del ácido benzoico fue realizada con un método analítico validado por HPLC-DAD. Los resultados evidenciaron que las muestras biológicas pueden almacenarse durante 72 h en las condiciones descritas. El comportamiento de permeación del ácido benzoico complejado respecto al ácido benzoico libre demostró tener un mejor perfil de seguridad, puesto que hubo una menor permeación para el primer caso. Estos resultados demuestran que la complejación del ácido benzoico podría disminuir las reacciones de sensibilidad que normalmente este presenta, basándose en la disminución de su permeación.

Palabras clave: Celdas de Franz, preservantes, ácido benzoico, complejos, piel, seguridad.

Introduction

Preservatives are widely used and necessary in all products with risk of deterioration because by inhibiting the growth of bacteria and fungi they prevent microbiological contamination of the product, protecting the consumer from possible infection [1]. Although there are many molecules for this purpose, it has been reported that the majority generates allergic reactions and sensitization by contact, being necessary the search for stable antimicrobials, broad spectrum and pH range, non-toxic or irritating [2].

One of the preservatives commonly used in cosmetics, food and medicine is benzoic acid (figure 1). Despite being considered a harmless substance, its topical application can generate hives, erythema, and stinging, probably by induction in the skin of large amounts of prostaglandin D2 [3]. In this sense, possible strategies that reduce the allergic reactions normally presented by this preservative have been evaluated, and the formation of complexes with polyelectrolytes is an important alternative because they modify its physicochemical properties, functionality and could even improve its safety [4].

Because the skin represents a significant route for the non-invasive administration of compounds, the evaluation of the toxicity and activity of molecules such as preservatives must be assessed [5]. *In vitro* tests conducted in Franz cells are considered as one of the main tools to evaluate transepithelial permeation, which consist of two compartments, one donor and another recipient where it is sampled periodically to evaluate the amount of compound that has penetrated through tissue over time [6]. These compartments are separated by a synthetic or natural membrane [7, 8].

Consequently, permeation tests were performed with benzoic acid and with the complexes $EuB_{75}Cl_{25}$ and EuB_{100} (figure 2) generated by the ionic interactions of the molecules involved, where Eu corresponds to the Eudragit E100 polyelectrolyte (figure 3), B to the benzoate ion and Cl to the chloride ion that act as counterions, the subscripts indicate the percentage at which each counterion is neutralizing the polymer; these complexes have shown in previous studies carried out within the research group, that their antimicrobial activity is maintained [4, 6]. This work is intended to assess whether there is a difference in the permeation behavior of complexes containing benzoic acid against the uncomplexed compound, from which it could be inferred if there is a difference in their biological safety.

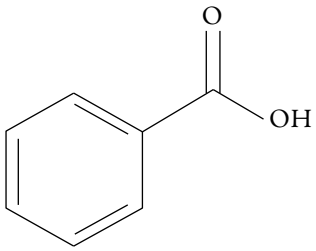

Figure 1. Molecular structure of benzoic acid [3].

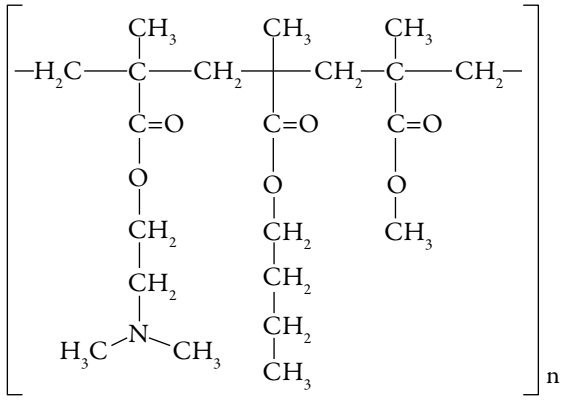

Figure 2. Approximate structure of the complexes formed between Eudragit® E100 and benzoic acid.

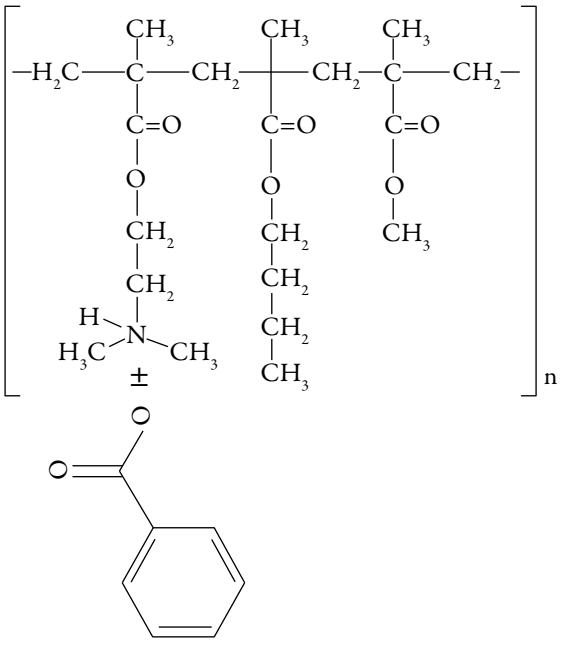

Figure 3: Chemical structure of the Eudragit® E100 PE [4].

Materials and methods

Materials

Benzoic acid (99%) Sigma Aldrich (U.S., lot: 09128 DCV); HPLC Tedia grade acetonitrile (U.S., lot: 905154); phosphoric acid (85%) Carlo Erba (E.U, lot: 8C109098E);

sodium chloride J.T Baker (U.S., lot: t10c54); 2.39M hydrochloric acid; Eudragit® E100 (Germany, lot: B140101519); complexes $EuB_{75}Cl_{25}$ and EuB_{100} HPLC grade water.

Biological material

For the development of the permeation tests, ear skin obtained from freshly slaughtered pigs weighing between 80-100 kg and with an average age of 4-6 months was used, these were removed and stored immediately in 1 M NaCl solution [9] under cooling conditions (4-8 °C). Once transported, it was verified that the skin did not present any type of lesion, spot, or tattoo making cuts of skin of 600 µm thickness to the samples with appropriate acceptance criteria. The integrity of the skin was determined through the measurement of transepithelial water loss (TEWL), using the Cutometer® dual MPA 580 with a Courage + Khazaka® model TM 300 tewameter, selecting pig skins with values below 35 g/h/m^2 [10].

Operating conditions of the Franz cell system for transdermal permeation studies

Permeation assays were performed using Franz cells (PermeGear® brand) under two different conditions: infinite doses and finite doses. The first condition was used to establish the physicochemical parameters of permeation [11], which allowed to define the storage conditions of pig skin so that it would not be required to test immediately after the animal was slaughtered. Finite dose tests were performed simulating the conditions of use [11] in which benzoic acid would be used as a preservative, with the purpose of evaluating the safety profile of complexed benzoic acid $(EuB_{75}Cl_{25}, EuB_{100})$, and free. The development of this work was endorsed by *Comité de Ética de la Facultad de Ciencias de la Universidad Nacional de Colombia* (*Acta Nº 07 de 2015*). Below are the details of each methodology used.

Infinite doses

Through the infinite dose tests, an enough benzoic acid (>100 µg/cm^2) was applied to reach the maximum flow per unit area [11], corresponding to 2.3 mg/mL solution's benzoic acid. Permeation tests were carried out in three Franz cells at 32 °C, 400 rpm stirring, 0.9% NaCl receptor medium adjusted to pH 7.4 [12], using pig skin cuts obtained from different pigs with 600 µm thickness (using the dermatome Aesculap-B.Braun model ACCULAN® 3Ti) [13] and diffusion area 1.75 ± 0.20 cm^2. Before starting the test, the skin could equilibrate in the assembly for 15 minutes at 32 °C, with an environmental relative humidity of 60% and the TEWL was measured (to establish that the skin was suitable for study). The application of 500 µL of the benzoic acid solution (>100 µg/cm^2) was carried out in the donor compartment, which remained occluded. The exposure time was 6 h, taking 500 µL aliquots of the receiving compartment at 0.5; 1; 1.5; 2; 3; 4 and 6 h, immediately replenishing with the

receiving medium. Quantification of benzoic acid was performed by HPLC-DAD (Shimadzu® Prominence series) as soon as the aliquots were obtained in each sampling. The analytical methodology was previously validated using as phosphoric acid (1%)/acetonitrile (70:30) mobile phase, flow of 1 mL/min, isocratic temperature of 35 °C and injection volume of 10 µL. This procedure was followed with samples of the skin of ears of freshly slaughtered pigs and after stored for 72 h in 1 M NaCl at -2 °C.

From these tests the diffusion parameters were obtained: permeation flow (equation 1) and permeability coefficient (equation 2), as well as the transepithelial water loss (TEWL) values of the two types of swine skin samples, establishing through the statistical analysis of the Kolmogorov Smirnov, Fisher and t Student tests (95% confidence level) if there was a significant difference between the diffusion and TEWL parameters of the pig samples at 0 and 72 h after slaughter.

$$Jss = \frac{dQr}{A\ dt} \qquad \text{(Equation 1)}$$

Where, dQr is the amount of drug transported through the membrane inside the receptor compartment (µg), A is the active diffusion area (cm^2) and dt is the exposure time (h).

$$Kp = \frac{Jss}{Cd} \qquad \text{(Equation 2)}$$

Where, Jss is the flow calculated at steady state ($mg/cm^2/h$) and Cd is the concentration of drug in the donor compartment (mg/cm^3).

Finite doses

Solutions of 2.0 mg/mL benzoic acid (pH 5) were prepared in triplicate by adding the amount of equivalent complex to obtain the desired concentration. Permeation tests were performed in triplicate in Franz cells at 32 °C, 400 rpm agitation, 0.9% NaCl receptor medium adjusted to pH 7.4 [12], using pig skin cuts obtained from different pigs, 600 µm thick [13] and diffusion area 1.75 ± 0.20 cm^2; the skin was used under the conditions previously mentioned (TEWL less than 35 $g/h/m^2$). A volume of 17.6 µL of the solution (10 $\mu g/cm^2$) was applied in the donor compartment without occlusion to simulate the conditions of use. The exposure time was 6 h, taking 500 µL aliquots of the receiving compartment at 0.5; 1; 1.5; 2; 3; 4 and 6 h, immediately replenishing with the receiving medium. The quantification of benzoic acid was performed by HPLC-DAD as soon as the aliquots were obtained in each sampling. The results were statistically analyzed, establishing whether there was a significant difference in the maximum permeated concentrations, using the Kolmogorov Smirnov, Fisher, and t Student tests assuming a 95% confidence level.

Results

Infinite doses

The diffusion and TEWL parameters were established in pig samples from freshly slaughtered pigs and after stored for 72 h in 1 M NaCl at -2 °C. Regarding the maximum flow of benzoic acid in the steady state, values of 125 μg/cm^2/h and 106 μg/cm^2/h were obtained in pig samples at 0 h and 72 h respectively. From the permeation flows obtained, the permeation coefficient of benzoic acid (Kp) was calculated, which was 0.0544 cm/h at 0 h and 0.0461 cm/h at 72 h. According to the Kolmogorov Smirnov and Fisher tests, it was determined that the data of the permeation flows and coefficients at 0 and 72 h follow a normal distribution, as well as homoscedasticity between the variances of the samples (table 1). Through the Student t test, it was obtained that the experimental statistic (t exp) is -2.01 for the flow and permeation coefficient, with a critical value of 2.78 (t tab) and probability of presenting a t experimental < t theoretical (P (T ≤ t) of 0.114 (>0.05), so there is no statistically significant difference in permeation parameters between samples of freshly slaughtered pig skins and those stored for 72 h in 1 M NaCl at -2 °C.

Simultaneously with the permeation test, the loss of transepithelial water (TEWL) was determined. For skins of freshly slaughtered pigs the loss of transepithelial water is 33.3 g/h/m^2 and 31.7 g/h/m^2 for pig samples stored for 72 h (table 2). However, after performing the statistical analysis, the Kolmogorov Smirnov, Fisher and t Student tests showed that there is no significant difference in the loss of transepithelial water, obtaining an experimental t of -0.315, a critical value of 2.78 and a probability of presenting an experimental t < theoretical t (P (T ≤ t) of 0.768 (>0.05). In turn, the transepithelial water loss (TEWL) values in pig samples at 0 and 72 h, present a normal distribution and equality of variances (table 2)

Finite dose

The maximum concentrations of benzoic acid in the $EuB_{75}Cl_{25}$, EuB_{100} and free were determined. For the complexes $EuB_{75}Cl_{25}$ and EuB_{100} the maximum concentrations of benzoic acid were 2.88 μg/mL and 2.99 μg/mL respectively, with a maximum value of 3.43 μg/mL in uncomplexed benzoic acid (table 3). The results obtained show normality in the distribution of the samples of the three compounds, an experimental value (D exp) of 0.267 and a critical value (D tab) of 0.708 for the averages of the maximum concentrations of benzoic acid in the complexes $EuB_{75}Cl_{25}$, EuB_{100} and free benzoic acid.

Table 1. Kolmogorov Smirnov, Fisher and t Student tests applied to the kinetic parameters (flow and permeation coefficient) of freshly slaughtered and stored swine skin for 72 h.

	Benzoic acid 0 h		**Benzoic acid 72 h**	
Parameter	**Flow (μg/cm²/h)**	**Kp (cm/h)**	**Flow (μg/cm²/h)**	**Kp(cm/h)**
Average	125.0	0.0544	106	0.0461
Variance	14.3	2.71E-06	249	4.71E-05
Statistical test				
Kolmogorov Smirnov (Dexp)	0.267	0.267	0.467	0.467
Kolmogorov Smirnov (Dtab)	0.708	0.708	0.708	0.708
Ho	The analyzed data follow a normal distribution			
	Flow		**Kp**	
Type of test	**Statistical t student**	**Test F**	**Statistical t student**	**Test F**
Experimental statistic	-2.01	17.3	-2.01	17.4
P(T ≤ t), P(F ≤ f)	0.114	0.0544	0.114	0.0544
Critical value	2.78	19	2.78	19
Ho	$\mu 1 = \mu 2$	$S_1^2 = S_2^2$	$\mu 1 = \mu 2$	$S_1^2 = S_2^2$

Table 2. Kolmogorov Smirnov, Fisher, and t Student tests applied to the loss of transepithelial water (TEWL) of freshly slaughtered and stored swine skin for 72 h.

Parameter	**TEWL (g/h/m²) 0 h**	**TEWL (g/h/m²) 72 h**
Average	33.3	31.7
Variance	5.15	7.28
Test Kolmogorov Smirnov		
Kolmogorov Smirnov (D exp)	0.267	0.477
Kolmogorov Smirnov (D tab)	0.708	0.708
Ho	The analyzed data follow a normal distribution	
Test Fisher		
Experimental statistic F (F exp)	1.99	
P(F ≤ f)	0.334	
Critical value F (F tab)	19	
Ho		
Test t Student		
Experimental statistic t (t exp)	-0.315	
P(T ≤ t)	0.768	
Critical value t (t tab)	2.78	
Ho	$\mu 1 = \mu 2$	

Table 3. Kolmogorov Smirnov test applied to the maximum concentrations of benzoic acid, $EuB_{75}Cl_{25}$, EuB_{100} complexes.

Compound	Benzoic acid	Benzoic acid from the $EuB_{75}Cl_{25}$ complex	Benzoic acid from the EuB_{100} complex
Average maximum concentration	3.43 μg/mL	2.88 μg/mL	2.99 μg/mL
Variance	0.0786	0.0256	0.0541
Kolmogorov Smirnov (Dexp)	0.267	0.267	0.267
Kolmogorov Smirnov (D tab)	0.708	0.708	0.708
Ho	The analyzed data follow a normal distribution		

In relation to the Fisher test (table 4), it is observed that for the $EuB_{75}Cl_{25}$, EuB_{100} complex the experimental F is 3.07, and 26.9 in the EuB_{100}, with a critical value of 19 for both compounds, presenting homecedasticity only for the complex $EuB_{75}Cl_{25}$.

Table 4. Fisher test applied to the maximum concentrations of the complexes $EuB_{75}Cl_{25}$, EuB_{100} comparing equality of variances with benzoic acid.

Compound	Benzoic acid from the $EuB_{75}Cl_{25}$ complex	Benzoic acid from the EuB_{100} complex
Average maximum concentration	2.88 μg/mL	2.99 μg/mL
Variance	0.0256	0.00292
F	3.07	26.9
P(F ≤ f)	0.246	0.0359
Critical value F	19	19
Ho	$S_1^2 = S_2^2$	$S_1^2 = S_2^2$

The Student t test of equal variances was applied for $EuB_{75}Cl_{25}$, and of unequal variances for the EuB_{100} complex. Table 5 shows the data calculated in the Student t test; for the $EuB_{75}Cl_{25}$ complex there is a statistically significant difference between the maximum concentration of the benzoic acid of the $EuB_{75}Cl_{25}$ complex and that of the uncomplexed benzoic acid, the experimental t is 2.91, with a critical value of 2.78 and the probability of presenting an experimental t < theoretical t (P (T ≤ t) is 0.0435 (< 0.05).

In the complex EuB_{100}, the t statistic is 2.65, the critical value is 2.92 and the probability of presenting an experimental t < theoretical t (P (T ≤ t) is 0.0888 (>0.05). Therefore, there is no significant difference between the averages of concentrations of free and complexed benzoic acid in EuB_{100}.

Table 5. Student t test applied to the maximum concentrations of the complexes $EuB_{75}Cl_{25}$ and EuB_{100} comparing equality of means with benzoic acid.

Compound	Benzoic acid from the $EuB_{75}Cl_{25}$ complex	Benzoic acid from the EuB_{100} complex
Average maximum concentration (μg/mL)	2.88	2.99
Variance	0.0256	0.00292
Statistical t	2.91	2.65
P(T ≤ t)	0.0435	0.0588
Critical value t	2.78	2.92
Ho	$\mu_1^2 = \mu_2^2$	$\mu_1^2 = \mu_2^2$

Discussion

Infinite doses

In the tests carried out at infinite doses, an amount of benzoic acid was applied with which the maximum flow per unit area was reached and maintained. Under these conditions, it was possible to determine the diffusion parameters such as the permeability coefficient (Kp) and the maximum flow in the steady state [11]. In figure 4, the cumulative amount of benzoic acid (permeated amount) is observed as a function of time, whose slope represents the maximum permeation flow, from which the permeation coefficient (Kp) [14, 15] is calculated.

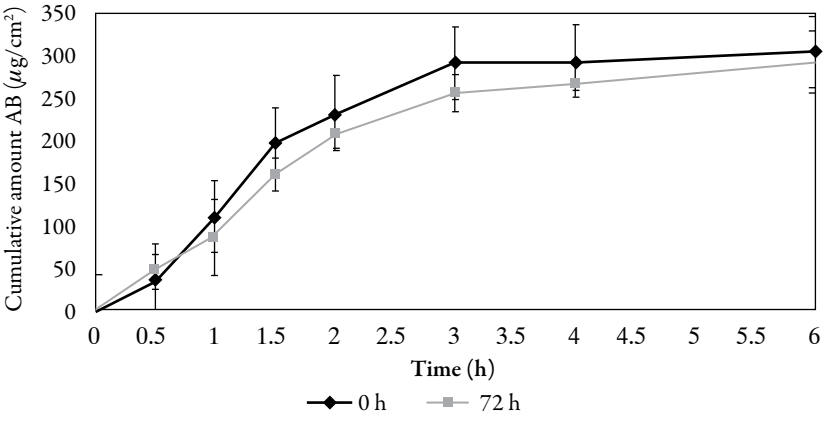

Figure 4. Permeation profile of benzoic acid (AB) using pig skin at 0 h and 72 h after the animal is slaughtered.

Simultaneously, the measurement of transepithelial water loss (TEWL) was performed, this evaluates the integrity of the skin assuming an increase in water loss when the skin is affected [10], therefore, it is necessary to guarantee optimal skin conditions in the performance of the tests avoiding excessive prediction in the permeation of the compounds. According to the values reported by the equipment manufacturers, the TEWL for healthy human skin is 10 to 25 g/h/m^2; however, in the literature, values of 30.21 ± 1.27 g/h/m^2 are reported for pig skin [10], data close to the TEWL of the samples used. Even so, there is a discrepancy in the values reported in other groups (2-10 g/h/m^2) which may be a consequence of differences in equipment calibration methods, values reported by manufacturers and conditions of use, for these reasons, the standardization of TEWL measurement methods is required to obtain reproducible data that can be compared.

As mentioned previously, diffusion parameters and transepithelial water loss (TEWL) were used as comparison criteria to assess whether there was a significant difference in their values after performing permeation tests with ear samples obtained from freshly slaughtered pigs and with samples stored for 72 h in 1M NaCl at -2 °C. With this in mind, the statistical analysis carried with the Student t test required that the values of the samples have a normal or Gaussian distribution (Kolmogorov Smirnov test), as well as a prior determination of the homoscedasticity between the groups to be compared (Fisher test) to establish the type of test to be applied (Student t test for equal or unequal variances) [16, 17]. After performing the statistical analysis, it was evidenced that there is no significant difference in the diffusion parameters in the TEWL measurements between the pig samples of freshly slaughtered pigs and samples stored for 72 h in 1 M NaCl at -2 °C. Therefore, storage ensures proper maintenance of biological samples for permeation studies.

The storage method used is the cooling and use of a saline medium to preserve the samples. Skin cooling is a simple, cost-effective and easily available method for short-term storage as is the interest of the study, reduces the metabolic rate of cells and nutritional demands [18], inhibits bacterial proliferation and together with a medium such as NaCl allows the viability of the samples for a certain time. The use of an ion exchange preservation medium (1 M NaCl solution, -2 °C for a maximum of three days) was carried out based on previous studies of the research group, where it was shown that it has several advantages over other means of preservation (MEM, Williams, RPMI and PBS buffer), since in addition to maintaining the skin with an adequate level of integrity, it facilitates the separation of the epidermis, it has a simpler composition than other media whose components could interfere with the analytical determination [9] and in turn is cost effective.

Consequently, the tests can be carried out without the need for pigs to be slaughtered immediately, which facilitates the operational conditions for carrying out the studies and, in turn, through proper storage the structural and functional integrity of the skin is guaranteed to obtain reliable results [18].

Finite doses

Because the concentrations of benzoic acid as a preservative are used from 0.1 to 0.2% in topical formulations [19], 2 mg/mL benzoic acid solutions were used to simulate the conditions of use. In figure 5, the maximum concentrations reached by benzoic acid (free and $EuB_{75}Cl_{25}$ and EuB_{100} complexes) are observed in permeation tests carried out over a period of 6 h.

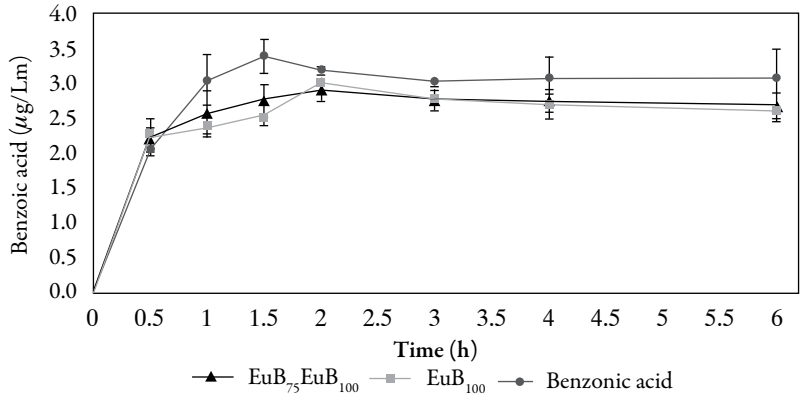

Figure 5. Permeation tests of complexes $(EuB_{75}Cl_{25}, EuB_{100})$ and benzoic acid.

According to the statistical analysis performed, it was obtained that the maximum permeate concentration of benzoic acid in the $EuB_{75}Cl_{25}$ complex is significantly different from that of free benzoic acid. This allows us to conclude that the $EuB_{75}Cl_{25}$ complex has a greater safety index since the permeate concentration of benzoic acid from the complex is lower than that of free benzoic acid (figure 5). For the EuB_{100} complex the concentration is not significantly different from that of the uncomplexed benzoic acid, despite not presenting a statistically significant difference, it is observed in figure 5, that its safety profile could be better than that of benzoic acid without complexing, since the maximum concentration permeated in the EuB_{100} is lower, being necessary to carry out additional tests that allow to conclude respect to the permeation of the same.

This difference in permeation behavior of free benzoic acid with respect to complexing can be explained by the strong electrostatic interaction between the positive charges of Eudragit® E100 and the negative charges of benzoic acid that are present in the

complexes, as a consequence of the acid base reaction that is given between them for their training. This interaction hinders the diffusive process of benzoic acid, which as part of the complex is included in a macrostructure with high molecular weight, which does not easily pass through the skin, but only to the extent that benzoic acid is released from the complex in its free form, which generates a decrease in the permeation rate, compared to uncomplexed benzoic acid [20].

Conclusions

Benzoic acid is partially absorbed dermally (between 22 and 89%) and at low doses irritation symptoms may appear [3], in this sense the use of complexes with polyelectrolytes and benzoic acid could be an alternative to the current preservative (without complexing), since it would improve its safety profile by decreasing the percentage that this compound can permeate the skin, without losing its antimicrobial activity.

Acknowledgments

The authors thank Colciencias for the funding granted to the research project that supported this research work (contrato 037-2016).

Disclosure statement

No potential conflict of interest was reported by the authors.

References

1. T. Sandle, *Pharmaceutical microbiology: essentials for quality assurance and quality control*, Cambridge: Elsevier Ltd Eds, London, 2015, Vol. 1, p. 171.
2. D. Sasseville, Hypersensitivity to preservatives, *Dermatol. Ther.*, **17**(3), 251-263 (2004).
3. A. Olmo, J. Calzada, M. Nuñez, Benzoic acid and its derivatives as naturally occurring compounds in foods and as additives: Uses, exposure and controversy, *Crit. Rev. Food Sci. Nutr.*, **57**(14), 3084-3103 (2015).
4. D. Le Cerf, A.S. Pepin, P.M. Niang, M. Cristea, D.C. Karakasyan, L. Picton, *et al.*, Formation of polyelectrolyte complexes with diethylaminoethyl dextran: Charge ratio and molar mass effect, *Carbohydr. Polym.*, **113**, 217-224 (2014).

5. M. Brown, G.P. Martin, S. Jones, F. Akomeah, Dermal and transdermal drug delivery systems: Current and future prospects, *Drug Deliv*., **13**(3), 175-187 (2006).

6. Y. Baena, L.J. Dallos, R.H. Manzo, L.F. Ponce D'León, Estandarización de celdas de Franz para la realización de ensayos de liberación de fármacos a partir de complejos con polielectrolitos, *Rev. Colomb. Cienc. Quím. Farm*., **40**(2), 174-188 (2011).

7. A. Simon, M. Amarob, A. Healy, L. Cabral, V. Sousa, Comparative evaluation of rivastigmine permeation from a transdermal system in the Franz cell using synthetic membranes and pig ear skin with *in vivo-in vitro* correlation, *Int. J. Pharm.*, **512**(1), 234-241 (2016).

8. V.P. Shah, H.I. Maibach, J. Jenner, *Topical drug bioavailability, bioequivalence, and penetration*, Springer Eds, New York, 2014, Vol. 2, p. 23.

9. N. Solarte, *Estudio de las condiciones para la evaluación de permeación transdérmica de un ingrediente funcional cosmético in vitro empleando piel de cerdo en celdas de Franz*, Unpublished bachelor thesis, Universidad Nacional de Colombia, Bogotá, 2013, p. 7-19.

10. F. Netzlaff, K.H. Kostka, C.M. Lehr, U.F. Schaefer, TEWL measurements as a routine method for evaluating the integrity of epidermis sheets in static Franz type diffusion cells *in vitro*. Limitations shown by transport data testing, *Eur. J. Pharm. Biopharm*., **63**(1), 44-50 (2006).

11. R. Gutiérrez- Fernández de Molina, *Estudios de difusión a través de piel de formulaciones liposómicas de acyclovir*, Ph. D. thesis, Universidad Complutense de Madrid, 2011. URL: http://eprints.ucm.es/13458/, accessed November 2017.

12. L. Aponte, *Estudios de permeación transdérmica in vitro: estado del arte y perspectivas*, Unpublished bachelor thesis, Universidad Nacional de Colombia, Bogotá, 2015, p. 15.

13. C. Ehrhardt, K. Kim, *Drug absorption studies in situ, in vitro and in silico models*, Springer Eds, New York, 2008, Vol. 1, p. 14.

14. V. de Caro, G. Giandalia, M.G Siragusa, C. Paderni, G. Campisi, L.I Giannola, Evaluation of galantamine transbuccal absorption by reconstituted human oral epithelium and porcine tissue as buccal mucosa models: Part I, *Eur. J. Pharm. Biopharm.*, **70**(3), 869-873 (2008).

15. A. Gimeno, A.C Calpena, R. Sanz, M. Mallandrich, C. Peraire, B. Clares, Transbuccal delivery of doxepin: Studies on permeation and histological investigation, *Int. J. Pharm.*, **477**(1-2), 650-654 (2014).

16. R.A. Sánchez-Turcios, t-Student. Usos y abusos, *Rev. Mex. Cardiol.*, **26**(1), 59-61 (2015).

17. R. Serrano, *Introducción al análisis de datos experimentales: tratamiento de datos en Bioensayos*, Universitat Jaume Eds, España, 2003, Vol. 1, p. 61.

18. M. Geerligs, *Skin layer mechanics*, PhD thesis, Technische Universiteit Eindhoven, 2010, p 26.

19. R.C. Rowe, P..heskey, S.C. Owen, *Handbook of Pharmaceutical Excipients*, American Pharmaceutical Association and Pharmaceutical Press Eds, London, 2000, Vol. 1, p. 61.

20. L. Bartosova, J. Bajgar, Transdermal drug delivery in vitro using diffusion cells, *Curr. Med. Chem.*, **19**(27), 4671-4677 (2012).

How to cite this article

L.A. Martínez, L.M. Sanabria, Y. Baena, Safety assessment of complex benzoic acid using *in vitro* permeation assays with pig skin in Franz cells, *Rev. Colomb. Cienc. Quím. Farm.*, **49**(2), 291-305 (2020).

Artículo de investigación tecnológica / *http://dx.doi.org/10.15446/rcciquifa.v49n2.89484*

Desarrollo y validación de un método de cromatografía gaseosa para la determinación de mentol, salicilato de metilo, timol y ácido benzoico en solución antiséptica

Antonio Fonseca Gola[1], Juan Manuel Cordoví Velázquez[2], Niurka Benítez Guerra[1], Mirna Fernández Cervera[3]*

[1]Laboratorio Farmacéutico Líquidos Orales de Bayamo, Medilip, Carretera Central Vía Santiago de Cuba km 845, Bayamo, Granma, Cuba. Correos electrónicos: AFG: antoniofg@medilip.biocubafarma.cu, NBG: niurka@medilip.biocubafarma.cu

[2]Joven Club de Computación. 9na e/ Ave. Granma y 3ra, Bayamo, Granma, Cuba. Correo electrónico: jmcordv@nauta.cu

[3]Instituto de Farmacia y Alimentos (IFAL), Departamento de Farmacia, Universidad de La Habana, Calle 222 # 2317 e/ 23 y 31, La Lisa, La Habana, Cuba.

*Correos electrónicos: mirnafc@ifal.uh.cu, mirnafc@gmail.com

Recibido: 27 de enero de 2020

Revisado: 19 de abril de 2020

Aceptado: 20 de abril 2020

Resumen

Se desarrolló y validó un método por cromatografía gaseosa para la cuantificación simultánea de mentol (MT), salicilato de metilo (SM), timol (TM) y ácido benzoico (AB) en una solución antiséptica bucal. Se utilizó una columna DB-WAX y dietilenglicol como estándar interno. Se determinó la linealidad en un intervalo de concentraciones de 64,00 a 96,00 µg/mL (MT), 80,00 a 120,00 µg/mL (SM), 96,00 a 144,00 µg/mL (TM) y 48,00 a 72,00 µg/mL (AB), obteniendo coeficientes de correlación superiores a 0,999, y coeficientes de variación de los factores de respuestas de 1,18, 1,95, 3,52 y 1,48%, respectivamente. Se establecieron límites de detección de 0,51; 1,14; 3,34 y 1,402 ng/mL para el MT, SM, TM y AB, respectivamente, mientras los límites de cuantificación fueron de 1,45, 3, 43, 9, 73 y 4, 36 ng/mL en cada caso. Los porcentajes de recuperación fueron de 100,03, 99, 31, 99, 92 y 100,12; con coeficientes de variación de 0,42, 0,79, 0,66 y 0,76% para cada caso. El método fue lineal, exacto, preciso y selectivo para la determinación de los analitos en el control de calidad.

Palabras clave: Ácido benzoico, cromatografía gaseosa, mentol, salicilato de metilo, timol, validación de métodos analíticos.

Summary

Development and validation of a gas chromatographic method for the determination of menthol, methyl salicylate, thymol, and benzoic acid in antiseptic solution

A method was developed and validated by gas chromatography for the simultaneous quantification of menthol (MT), methyl salicylate (SM), thymol (TM) and benzoic acid (AB) in an oral antiseptic solution. A DB-WAX column and diethylene glycol was used as internal standard. Linearity was determined in a concentration range of 64.00 to 96.00 µg/mL (MT), 80.00 to 120.00 µg/mL (SM), 96.00 to 144.00 µg/mL (TM) and 48.00 to 72.00 µg/mL (AB) achieving correlation coefficients greater than 0.999, and coefficients of variation of the response factors of 1.18, 1.95, 3.52 and 1.48%, respectively. Detection limits were established: 0.51, 1.14, 3.34 and 1.402 ng/mL for MT, SM, TM, and AB, respectively, while the quantification limits were 1.45, 3.43, 9.73 and 4.36 ng/mL in each case. Recovery percentages were 100.03, 99.31, 99.92 and 100.12; with coefficients of variation of 0.42, 0.79, 0.66 and 0.76% for each case. The method was linear, accurate, precise, and selective for the determination of analytes in quality control.

Keywords: Benzoic acid, gas chromatography, menthol, methyl salicylate, thymol, validation of analytical methods.

Introducción

Diversos tratamientos y terapias con medicamentos combinados se han desarrollado con productos que se utilizaron originalmente como terapias independientes para controlar más rápidamente y de mejor forma las enfermedades. Para el químico analítico, esto presenta un gran desafío. Muchas veces los componentes de estos medicamentos combinados tienen diferencias significativas en sus propiedades físicas (solubilidad, punto de fusión, etc.) y químicas (pKa, máximo de absorción UV, estabilidad en los disolventes etc.) [1]. Por tanto, esto requerirá el desarrollo de métodos analíticos que permitan el análisis de las formulaciones multicomponentes.

La validación es un requisito indispensable para la utilización de los métodos de ensayo en la industria farmacéutica, esta solo será exhaustiva para aquellos métodos no normalizados, los diseñados o utilizados en el laboratorio y los métodos modificados o utilizados fuera de su alcance [2-4].

La validación de los métodos demuestra que los procedimientos analíticos son convenientes para su uso intencional. Es un requisito básico para asegurar la calidad y fiabilidad de los resultados de todas las aplicaciones analíticas. Las normas que se refieren a los procedimientos de validación de las técnicas analíticas incluyen lo relacionado con el establecimiento de los límites de detección y cuantificación, la precisión, exactitud, especificidad, rango y robustez [2-5].

Variedad de métodos analíticos han sido desarrollados para la determinación individual o en combinación de mentol [6-16], timol [17-19], ácido benzoico [20-27] y salicilato de metilo [7, 8, 12, 13,16, 28, 29] con el empleo de diferentes formas de preparación de las muestras de acuerdo con el tipo de matriz en donde se encuentren los compuestos de interés.

Las técnicas que más comúnmente se han empleado son la cromatografía líquida de alta resolución y los de cromatografía gaseosa (CG), esta última es uno de los métodos más reportados para la determinación de estos analitos de forma individual o combinada, debido a su alta sensibilidad y versatilidad. La volatilidad de estos compuestos ha hecho que la CG sea una opción para su determinación en materia prima o producto final. Sin embargo, hasta el presente, no existe una metodología específica para determinar estos cuatro compuestos simultáneamente.

El hecho de que la solución antiséptica bucal no aparece en ninguna *Farmacopea* justifica la necesidad de desarrollar y validar los métodos analíticos empleados en la evaluación de su calidad.

Teniendo en cuenta las interferencias en la cuantificación simultánea de los cuatro analitos fue necesario el desarrollo de un método por CG sencillo y fácil de aplicar; con disolventes orgánicos disponibles y que no fueran agresivos con el material de relleno de las columnas cromatográficas de uso cotidiano. El presente estudio tuvo como objetivo desarrollar y validar un método de cromatografía gaseosa para el análisis simultáneo de mentol, ácido benzoico, salicilato de metilo y ácido benzoico en una solución antiséptica bucal.

Materiales y métodos

Reactivos químicos

Los reactivos usados fueron timol, material de referencia químico (MRQ) (F0D391, EE.UU.); mentol MRQ (R00640, EE.UU.); ácido benzoico MRQ (H0L534, EE.UU.); salicilato de metilo MRQ (G1L203, EE.UU.) y dietilenglicol MRQ (G0J412, EE.UU.).

Optimización del sistema cromatográfico

Para establecer el sistema cromatográfico a emplear en la determinación simultánea del mentol (MT), salicilato de metilo (SM), timol (TM) y ácido benzoico (AB) se aplicó un diseño multifactorial general de dos bloques, con 72 experimentos completamente aleatorizados. Para el inyector y detector se establecieron dos niveles de temperatura (220 y 250 °C); mientras que para el flujo se propusieron tres velocidades entre 50 y 70 cm/s. Posteriormente, se establecieron tres programas de temperatura (PT):

PT-1: temperatura inicial (Ti) a 60 °C mantenida por 5 min incrementándose hasta 220 °C a razón de 12 °C/min. La temperatura final (Tf) 220 °C fue mantenida por 5 min.

PT-2: Ti de 60 °C que se incrementó hasta 220 °C a razón de 8 °C/min. La Tf a 220 °C fue mantenida por 5 min.

PT-3: Ti de 80 °C incrementándose hasta 220 °C a razón de 8 °C/min. La Tf a 220 °C fue mantenida por 5 min.

El diseño propuesto se analizó a través del *software* profesional Design Expert, versión 8.0.6 del 2011, Stat, Ease, Inc. (EE.UU.). Como variables de respuesta se utilizaron: resolución Rs ≥2, factor de cola o asimetría As <2, platos teóricos N >2000, temperatura del inyector y detector, velocidad de flujo y programa de temperatura. Para cada variable se analizaron los niveles de ajuste a través de los coeficientes de determinación ($r^2 \geq 0,98$), los coeficientes de determinación ajustados (r^2 ajustado ≥ 0,98), los coeficientes de determinación predictivos (r^2 predictivo ≥ $\pm$0,02 respecto a r^2 ajustado) y la precisión adecuada (≥ 4). Se obtuvieron varias propuestas de condiciones cromatográficas seleccionando la de mayor valor de deseabilidad, estadígrafo inferencial de los sistemas multifactoriales mostrado a través de los gráficos de rampas.

El análisis se hizo en un equipo Shimadzu modelo 2010 (Kyoto, Japón) con detector de ionización por llama de hidrógeno. La columna empleada fue DB-WAX de 30 m x 0,32 mm, película 0,25 μm (Agilent, EE.UU.).

Primero, se realizaron dos extracciones con 10 y 5 mL de cloroformo (Merck, Alemania). La muestra fue acidulada con 1 mL de HCl 0,1 mol/L para el aislamiento de los analitos del medio acuoso. El dietilenglicol (Panreac, España) 80 μg/mL fue empleado como estándar interno. Se pesaron con exactitud patrones de mentol, salicilato de metilo, timol y ácido benzoico, las cantidades fueron 40, 50, 60 y 30 mg, respectivamente. Se trasvasaron con ayuda de 60 mL de etanol 96% hacia un matraz de 100 mL. Luego se transfirieron 5 mL hacia un embudo separador de 100 mL y se procedió igual que en la preparación de las muestras.

Posteriormente, alrededor de 100 mg de dietilenglicol se pesaron con exactitud y se trasvasaron hacia un matraz aforado de 50 mL con ayuda de 30 mL de metanol. Se completó volumen con el mismo disolvente y se homogenizó.

Finalmente, 5 mL de la muestra se trasvasaron hacia un embudo separador de 100 mL. Se añadió 1 mL de ácido clorhídrico 0,1 mol/L; se extrajo durante 1 min con 10 mL de cloroformo, se dejó en reposo hasta separación de fases. Luego se trasvasó la fase clorofórmica (abajo) hacia un matraz de 25 mL que contenía 1 mL del estándar interno, a través de un embudo y papel de filtro rápido que contenía 2 g de sulfato de sodio anhidro previamente humedecido con 4 mL de cloroformo. Se realizó una segunda extracción con 5 mL del mismo solvente realizando la misma operación anterior. Por último, se lavó el filtro con 8 mL de cloroformo y se incorporaron al matraz. Se completó volumen con cloroformo y se homogenizó.

Validación del método analítico

De acuerdo con las metodologías descritas [2-5] se desarrollaron los ensayos de especificidad, robustez, estabilidad de las muestras, linealidad, exactitud y precisión (repetibilidad y precisión intermedia) para determinar las tolerancias del método para cada analito de interés. En este estudio fue empleado el lote 6003 de solución antiséptica.

Selectividad. Se comprobó si existía interferencia del placebo analizando los resultados de la muestra, el placebo y el estándar interno con el placebo, al aplicar el procedimiento analítico optimizado. No deben obtenerse señales del placebo en la zona de elusión de los analitos estudiados.

Estabilidad de las muestras. Se realizó la determinación cuantitativa de los analitos al inicio y a 2, 3, 8, 16, 23, 38 y 72 h. Se realizaron análisis durante 3 días, conservando las muestras en frascos ámbar, inyectando la misma disolución y comprobando la ausencia de productos de degradación. Luego se calculó el coeficiente de variación el cual debía ser inferior al 2%, en cuanto al valor de las concentraciones relativas de las inyecciones, como criterio de estabilidad.

Robustez. Para este ensayo se consideraron las posibles variaciones aleatorias de los parámetros como temperatura del inyector y el detector (-5 °C, para ambos), programa de temperatura: tiempo de inicio (+2 °C), tiempo final (-2 °C), velocidad del flujo (2 cm/s) y las columnas DB-WAX y Rext-WAX (Agilent, EE.UU.).

Linealidad. Se utilizó el método de patrones de referencia. Se realizaron las determinaciones correspondientes al 80, 90, 100, 110 y 120%, por quintuplicado. Se calculó, en cada caso, la relación entre la concentración y la respuesta. Luego se hizo un análisis de regresión simple por el método de los mínimos cuadrados, utilizando como variable independiente las concentraciones para cada nivel estudiado y como

dependiente las áreas bajo la curva de los picos cromatográficos. Se determinaron los estadígrafos de linealidad (ecuación de la recta, coeficientes de regresión, de determinación, y del factor de respuesta (CVfr%). Se ejecutó la prueba de significación estadística de la desviación estándar de la pendiente y la prueba de proporcionalidad o desviación estándar del intercepto. En ambos casos se analizaron los intervalos de confianza (IC) y la prueba t de Student. Para el primer caso el IC debe incluir el cero y mostrar diferencias estadísticas significativas en el estadígrafo inferencia, mientras que la segunda prueba el IC debe incluir la unidad y la dócima de Student no debe mostrar diferencias significativas. Además, se analizó la autocorrelación de los residuales para la pendiente con el estadígrafo Durbin-Watson.

Exactitud. Se determinaron los porcentajes de recuperación ($\%_{Rec}$), las desviaciones estándar (DS) y el coeficiente de variación (CV), en cada nivel (80, 100 y 120%) y el CV_{global} para cada uno de los analitos. Se aplicó la prueba de *Cochran* para comprobar si la variación de la concentración producía diferencias significativas en la respuesta del método en los diferentes niveles de concentración y la prueba de Student en comparación del porcentaje de recuperación,100%.

Precisión. Para desarrollar este estudio se realizaron las precisiones en condiciones de repetibilidad y precisión intermedia.

Repetibilidad. Se hicieron 10 determinaciones sobre el mismo material de muestra, analizando tres niveles de concentración (80, 100 y 120%). Se calculó el CV y se comparó con el criterio establecido (≤2,0%). Las determinaciones las realizó el mismo analista en las mismas condiciones de trabajo.

Precisión intermedia. Dos analistas evaluaron las concentraciones de 80, 100 y 120% por quintuplicado, en 3 días diferentes. Para cada caso se evaluó la media, DE y el CV. Para el procedimiento se realizaron análisis multifactoriales de las varianzas para las concentraciones de los analitos; se compararon las posibles diferencias entre los días y los analistas y se llevaron a cabo pruebas de contrastes múltiples de rangos y gráficos de medias para determinar si alguno de los factores tenía efectos estadísticamente significativos para cada caso de estudio. También se analizaron las interacciones significativas entre los factores. El método utilizado para discernir entre las medias fue el procedimiento de las menores diferencias significativas de Fisher. Se comprobó, mediante pruebas de análisis de varianzas múltiples (Manova), si había diferencias estadísticas significativas entre los analistas que emplearon igual método, y también, los dos días en que se realizaron los análisis, para obtener resultados con un nivel de confianza del 95%.

Límites de detección (LD) y cuantificación (LC). Estos se determinaron por el procedimiento de la desviación estándar de la respuesta y la pendiente de la recta de

calibrado para métodos instrumentales que no corrigen la señal frente a un blanco y el método de extrapolación de la curva de calibración a concentración cero. Las señales a concentración cero se obtuvieron a partir de los interceptos de las curvas de linealidad para cada analito. Se prepararon muestras a concentraciones entre 1,0 y 5,0% respecto a las concentraciones nominales. Cada nivel de concentración se corrió por triplicado, se determinaron los promedios de las áreas y las desviaciones estándar de las respuestas de los blancos (Sbl). Con estos resultados se expresaron las ecuaciones de las rectas de las respuestas del blanco (Ybl) y de las Sbl, para cada uno de los analitos. A partir de los valores de las Ybl y de las Sbl se calcularon los LD y LC teóricos.

Incertidumbre del método de análisis. Las incertidumbres específicas, combinadas y expandidas fueron determinadas a partir de los resultados de las pruebas que miden los errores aleatorios y sistemáticos, estos a su vez determinaron las variabilidades en los resultados para las cuantificaciones de los analitos de interés [30].

Aplicación del método de análisis

El método fue aplicado para las cuantificaciones de los analitos en lotes pilotos de la solución antiséptica recién elaborados. Las determinaciones se realizaron por quintuplicado estimando la media y el coeficiente de variación. Los criterios de aceptación para cada uno de los analitos fueron: mentol: 40,0 ± 4,0 mg/100 mL; salicilato de metilo: 50,0 ± 5,0 mg/100 mL; timol: 60,0 ± 6,0 mg/100 mL y ácido benzoico: 30,0 ± 3,0 mg/100 mL.

Resultados y discusión

El diseño de un método capaz de cuantificar simultáneamente el mentol, salicilato de metilo, timol y ácido benzoico fue indispensable. Estos se encontraban presentes en la solución antiséptica y se optó por un método por CG sencillo y fácil de aplicar; con el uso de disolventes orgánicos disponibles y no agresivos con el material de relleno de las columnas cromatográficas de uso cotidiano. También se consideró la propiedad química que poseen los analitos de ser compuestos orgánicos hidrocarbonados fácilmente ionizados por un detector de ionización por llama.

El diseño experimental multifactorial facilitó determinar condiciones óptimas a partir de la realización de un número definido de observaciones. El establecimiento de las variables de respuestas permitió la determinación de modelos matemáticos adecuados. Los estadígrafos inferenciales, derivados de la evaluación del diseño experimental, permitieron caracterizar con un 95,0% de confianza si los modelos matemáticos eran adecuados para la predicción de los resultados. Los estadígrafos inferenciales del diseño experimental multifactorial se muestran en la tabla 1.

Tabla 1. Estadígrafos inferenciales del diseño factorial para la determinación de las condiciones cromatográficas.

Variable respuesta	r^2	r^2 ajustado	r^2 predictivo	Precisión adecuada
Rs_MT	0,999980	0,999961	0,999917	781,436954
Rs_SM	0,999640	0,999280	0,998476	199,288232
Rs_TM	0,999974	0,999948	0,999890	559,501130
Rs_AB	0,999777	0,999554	0,999056	177,302064
As_MT	0,995050	0,990099	0,979051	39,960180
As_SM	0,997401	0,994802	0,989002	64,435524
As_TM	0,994560	0,989119	0,976978	48,805209
As_AB	0,995137	0,990274	0,979420	43,768948
N_MT	0,999870	0,999740	0,999451	398,433020
N_SM	0,999697	0,999394	0,998718	211,246983
N_TM	0,998772	0,997545	0,994805	104,245498
N_AB	0,999498	0,998995	0,997874	155,370950
Ttc	1		N/A	1,001E-307

Rs: resolución, As: asimetría, N: platos teóricos, MT: mentol, SM: salicilato de metilo, TM: timol, AB: ácido benzoico.

Los r^2 estuvieron en razonable acuerdo con los r^2 ajustados, ambos con valores superiores a 0,98 justificando menos del 2,0% de las variabilidades debidas a los errores sistemáticos y aleatorios. Los resultados de las precisiones predictivas no arrojaron resultados que difieran a los ajustados con diferencias mayores a 0,02 unidades. La precisión adecuada midió la relación señal/ruido. Al obtenerse valores superiores a 4 (según criterio de DX8) se consideraron todos los modelos matemáticos adecuados, por lo que dichos modelos pudieron ser utilizados para el estudio estadístico de los resultados del diseño multifactorial propuesto. En el caso del tiempo total de corrida de los cromatogramas con equilibrio del coeficiente de determinación igual a uno (mayor grado de ajuste), el estadístico r^2 predictivo no está definido por tener un ajuste perfecto, con variación despreciable o nula de los valores residuales en la ecuación de ajuste por mínimos cuadrados y la precisión adecuada deja de presentar valor de criterio por las mismas razones. La coincidencia, en cuanto a ajustes de las relaciones de residuales teóricos y reales, indicó la capacidad de los modelos matemáticos propuestos para explicar sus comportamientos con un grado de probabilidad superior al 0,05. Esto demuestra el alto nivel de confianza del método estadístico por ello fue empleado como predictivo

del mejor comportamiento en la toma de decisiones respecto a las condiciones cromatográficas. En la figura 1 se muestran los gráficos de rampas de las condiciones de los tratamientos seleccionados como los más deseables; los valores de los parámetros cromatográficos más probables a obtener y el valor de deseabilidad.

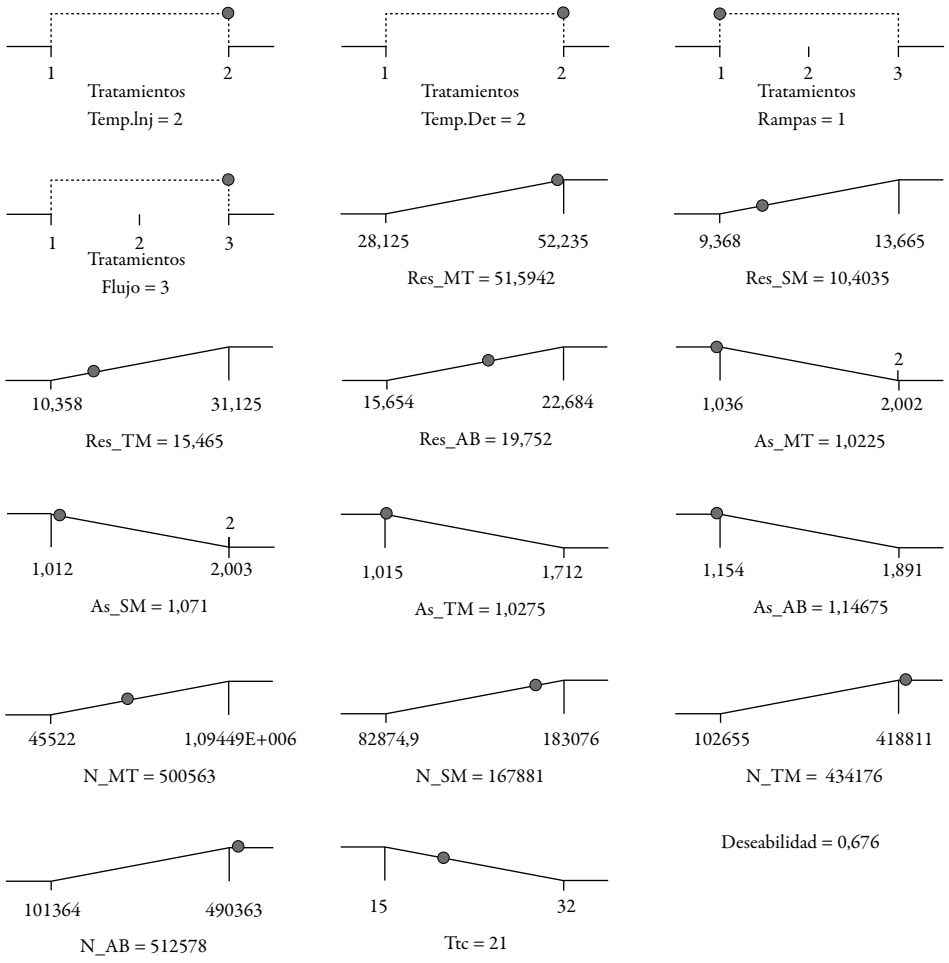

Figura 1. Gráficos de rampa del diseño multifactorial para la predicción de las condiciones cromatográficas. Rs: resolución, As: asimetría, N: platos teóricos, Tr: tiempo de retención, MT: mentol, SM: salicilato de metilo, TM: timol, AB: ácido benzoico.

Como resultado de todo lo anterior el programa sugirió 18 posibles soluciones, de las cuales la primera resultó ser la de mejor deseabilidad con un 67,6% de probabilidad de ejecutarse satisfactoriamente. La corrida propuesta coincidió con la número 10, estándar 53, del diseño experimental factorial propuesto. Los valores predichos difieren

muy poco de los valores reales obtenidos. La comparación de los resultados se puede verificar en la tabla 2, que se incluye el porcentaje de coincidencia obtenido por la relación de los valores. Los valores más altos se obtuvieron en aquellas medidas en que el valor numérico fue más pequeño, por lo que se esperaban resultados superiores. Sin embargo, no superan el 3% de variabilidad, por lo que las predicciones se consideran acertadas.

Tabla 2. Comparación de resultados entre las condiciones reales y predictivas del sistema cromatográfico propuesto.

	Rs/ MT	**Rs/ SM**	**Rs/ TM**	**Rs/ AB**	**As/ MT**	**As/ SM**	**As/ TM**	**As/ AB**	**N/ MT**	**N/ SM**	**N/ TM**	**N/ AB**
Valor real	50,62	10,48	15,31	20,21	1,12	1,18	1,09	1,22	110008	167357	418811	490363
Valor predicho	50,62	10,47	15,35	20,24	1,15	1,18	1,07	1,26	110008	167357	418811	490363
Porcentaje de coincidencia	100,00	99,95	100,22	100,17	102,67	100,16	98,16	102,85	99,99	99,99	100,00	99,99

Rs: resolución, As: asimetría, N: platos teóricos, MT: mentol, SM: salicilato de metilo, TM: timol, AB: ácido benzoico.

Los parámetros cromatográficos como tiempo de retención (Tr), asimetría (As), resolución (Rs) y platos teóricos (N) se muestran en la tabla 3. La resolución se refiere a la medida de separación entre los picos de interés respecto a la línea base. Los platos teóricos es una función de la eficiencia de la columna y es específicamente para asegurar que los compuestos que eluyan estén resueltos uno del otro, para establecer el poder separativo del sistema. Un pico es considerado resuelto cuando el valor de R es mayor que 2,0 [5]; mientras que una columna es eficiente cuando N es mayor que 2000 (se entiende por eficiencia de una columna cuando más interactúan los componentes de una muestra en análisis con la fase estacionaria lográndose una mayor retención y resolución de los analitos). La asimetría indica la aproximación de la curva a la campana gaussiana, debido a efectos intra y extracolumnares en el proceso separativo; la unidad para picos simétricamente perfectos y su valor varía a medida que el *fronting* o el *tailing* del pico se hacen más pronunciadas. Un pico se considera simétrico cuando su valor está por debajo de 2,0 y cercano a 1,0 [5].

A partir del análisis de los resultados del diseño experimental se fijaron las siguientes condiciones de trabajo: columna DB-WAX de 30 m de longitud, 0,32 mm DI y 0,25 μm; flujo: 70 cm/s; gas transportador: hidrógeno; temperatura inyector: 250 °C; temperatura detector de ionización de llama: 250 °C; programa de temperatura: temperatura

Tabla 3. Parámetros cromatográficos obtenidos con el sistema seleccionado.

Parámetro cromatográfico	Mentol	Salicilato de metilo	Timol	Ácido benzoico
Tr (min)	9,54	11,973	17,867	21,065
As	1,098	1,043	1,018	1,113
Rs	54,876	39,912	51,762	42,658
N	1 676 447,45	2 333 620,51	2 545 695,58	3 025 563,27

Rs: resolución, As: asimetría, N: platos teóricos, Tr: tiempo de retención.

inicial de 60 °C por 5 min, incrementándose hasta 220 °C a razón de 12 °C/min y temperatura final de 220 °C mantenida por 3 min; tiempo de corrida: 25 min; modo de división de la muestra (Split): 1:5, flujo detector H2 y aire 50 m/L y 480 m/L, respectivamente, y volumen de inyección: 1 µL.

Validación del método seleccionado

En la figura 2 se muestran los cromatogramas de la muestra, el placebo y el estándar interno con el placebo obtenidos durante la comprobación del parámetro de la especificidad del método. Al observar los cromatogramas se evidenció que no existen interferencias por parte de los analitos ni de los excipientes presentes en la formulación, por tanto, se considera que el método es específico y aplicable al control de calidad del producto terminado.

En los laboratorios de control de calidad que analizan grandes volúmenes de producción es necesario incluir varias muestras de lotes de un mismo producto para hacer los ensayos de cuantificación, lo que algunas veces prolonga el tiempo de análisis. Después de diluidas se evaluó la estabilidad para comprobar el periodo de tiempo durante el cual las muestras mantenían su concentración sin variación.

La tabla 4 muestra los resultados del estudio de estabilidad de las muestras en el cual se comprobó que las mismas fueron estables durante 3 días después de su preparación. El coeficiente de variación mayor, obtenido para el MT, no excedió del 0,26%. En todos los casos los resultados estuvieron por debajo del criterio de aceptación y cumplieron para los cuatro analitos con valores de CV < 2,0%. Se puede considerar que las muestras fueron estables durante ese periodo.

En la tabla 5 se resumen los resultados del ensayo de robustez. Los resultados estadísticos mostraron que la variación de los parámetros cromatográficos fue muy pequeña, siendo menores que el valor asignado como criterio de aceptación. Esto confirma que

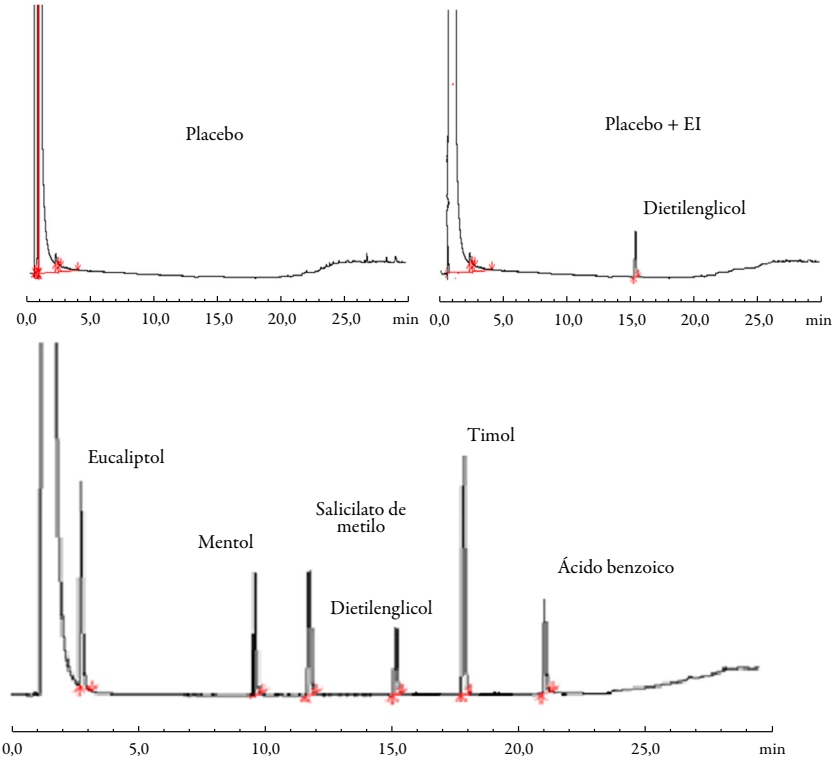

Figura 2. Selectividad del método. EI: estándar interno.

Tabla 4. Concentración de los cuatro analitos en el estudio de estabilidad de las muestras.

Tiempo (h)	Concentración (mg/mL)			
	Mentol	**Salicilato de metilo**	**Timol**	**Ácido benzoico**
0	41,215	50,650	59,091	31,345
2	41,163	50,564	58,789	31,369
3	41,011	50,542	58,991	31,402
8	41,055	50,551	58,987	31,389
16	40,996	50,563	58,878	31,423
23	41,014	50,490	59,003	31,431
38	41,016	50,548	59,025	31,509
72	40,871	50,456	59,012	31,374
Media (mg/mL)	41,043	50,546	58,972	31,405
DS	0,1059	0,0570	0,0944	0,0506
CV (%)	0,2580	0,1127	0,1602	0,1612

los resultados obtenidos se mantuvieron dentro de los valores permisibles y que las variaciones en el método cromatográfico no influyeron en la calidad de los resultados, por lo que el método propuesto se consideró robusto.

Tabla 5. Robustez del método.

Analito	Parámetro								Srob
MT	***s***	***t***	***u***	***v***	***w***	***x***	***y***	***z***	0,871
	98,55	97,95	98,19	97,60	98,30	99,21	99,21	97,98	
	VA	VB	VC	VD	VE	VF	VG	$V \leq S_R\sqrt{2}$	
	0,603	0,260	0,380	0,096	0,216	0,531	0,536	1,231	
SM	*s*	*t*	*u*	*v*	*w*	*x*	*y*	*z*	1,486
	97,50	98,08	97,28	98,59	98,45	98,72	98,69	99,02	
	VA	VB	VC	VD	VE	VF	VG	$V \leq S_R\sqrt{2}$	
	0,857	0,208	0,624	0,058	0,323	0,197	0,169	2,101	
TM	*s*	*t*	*u*	*v*	*w*	*x*	*y*	*z*	1,075
	108,54	108,27	107,84	107,03	107,85	108,43	108,24	109,32	
	VA	VB	VC	VD	VE	VF	VG	$V \leq S_R\sqrt{2}$	
	0.537	0,164	0,146	0,804	0,687	0,008	0,256	1,520	
AB	*s*	*t*	*u*	*v*	*w*	*x*	*y*	*z*	1,071
	99,27	98,44	98,86	99,62	99,03	98,29	98,12	98,47	
	VA	VB	VC	VD	VE	VF	VG	$V \leq S_R\sqrt{2}$	
	0,571	0,012	0,113	0,374	0,076	0,675	0,127	1,514	

s, *t*, *u*, *v*, *w*, *x*, *y*, *z*: concentraciones (%); VA, VB...VG: variabilidades calculadas, según procedimiento. MT: mentol; SM: salicilato de metilo; TM: timol; AB: ácido benzoico; S: desviación típica.

En la tabla 6 se observan los resultados estadísticos de la prueba de linealidad del método. Existieron fuertes relaciones seriadas entre las variables dependientes (Y, área bajo la curva) y las independientes (X, concentración) dado que los coeficientes de correlación presentaron valores superiores al 99,0% y los coeficientes de determinación mayores del 98,0%. El grado de ajuste o sensibilidad se demostró, además, por los valores de los coeficientes de los factores de respuestas (CVfr), que para todos los analitos fueron menores del 5,0% y la existencia de relaciones seriadas avaladas por el análisis de las varianzas de las regresiones con valores de probabilidades inferiores al 0,05. Los valores de probabilidades superiores al 0,05 de los estadígrafos de Durvin-Watson no mostraron indicios de una autocorrelación serial en los residuos, con un nivel de

confianza del 95,0%. Al aplicar la prueba t de Student se demostró la existencia de una relación estadísticamente significativa, lo que indica que la probabilidad de que b≠0 fue muy elevada, superior al 99,9%. En el análisis estadístico de los interceptos, con las dócimas t de Student, se demostró que no existieron diferencias entre las medias de los residuales a cada nivel, para cada uno de los analitos estudiados. Además, los intervalos de confianza incluyen al cero, lo que indica que la probabilidad de que a=0 es muy elevada. En la figura 3 se observan las curvas de linealidad por el método de ajuste de los mínimos cuadrados. Todos los puntos a los distintos niveles se encuentran dentro de los límites de confianza y predicción, demostrando que en los cuatros casos el método de cuantificación se ajusta al modelo propuesto.

Tabla 6. Resultados estadísticos de la prueba de linealidad del método analítico.

Parámetro	Resultado				Límite
	MT	SM	TM	AB	
Ecuación de la recta	25,352X+ 0,00	17,602X-0,00	35,722X-0,00	11,788X+0,00	Y= bx+a
r	0,997	0,991	0,999	0,995	≥ 0,990
r^2	0,993	0,981	0,997	0,989	≥ 0,980
CVfr (%)	1,186	1,958	3,529	1,486	≤ 5,0%
Significación estadística de la pendiente					
Residuo Durwin Watson (DW)	DW =1,681 p = 0,15	DW =2,185 p =0,60	DW =3,18 p =0,99	DW =2,04 p =0,45	p > 0,05
t tab (t n-2, p-valor=0,05) = 2,160	t exp = 57,46	t exp = 34,84	t exp = 91,83	t exp = 45,96	t exp > t tab
Ensayo de proporcionalidad					
t tab (t n-2, p-valor=0,05) = 2,160	t exp = 0,000	t exp = -0,006	t exp = -0,017	t exp = 0,013	t exp < t tab
Intervalo de confianza de la pendiente IC=a ± t·Sa	-0,074 a 0,07	-0,106 a 0,11	0,034 a 0,56	-0,053 a 0,05	Debe incluir el cero

Coeficientes de correlación (r); coeficientes de determinación (r^2); coeficiente de variación del factor de respuesta (CVfr).

t (t n-2, p-valor=0,05)= 2,160.

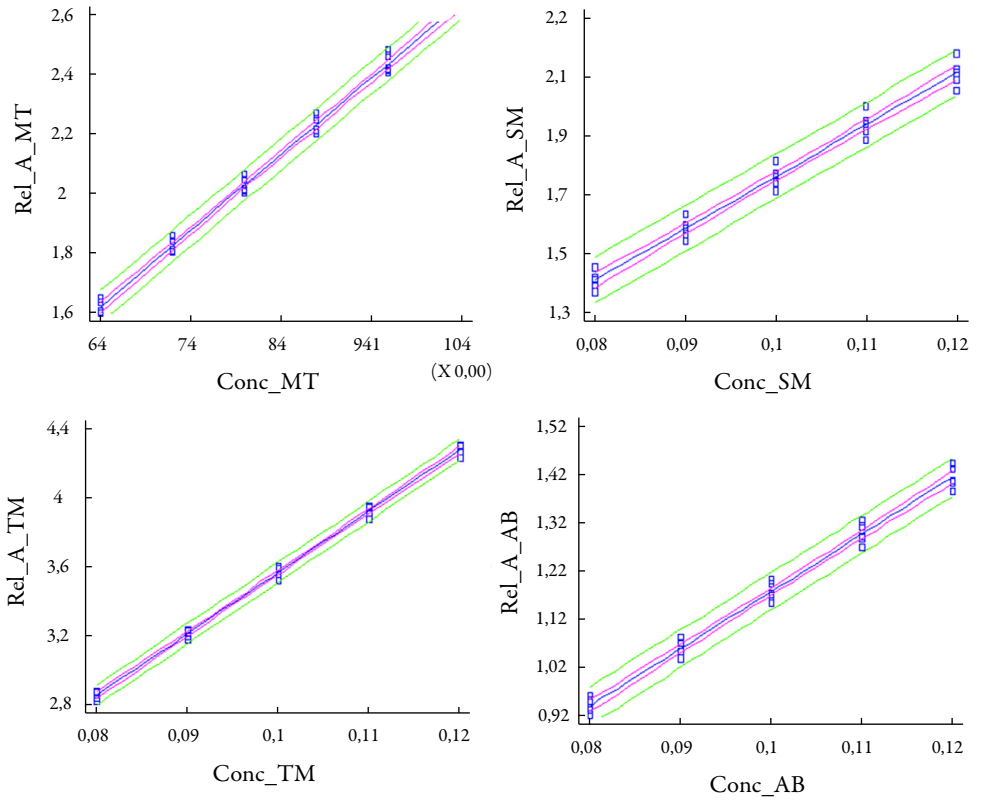

Figura 3. Curva de calibración de la linealidad. MT: mentol, SM: salicilato de metilo, TM: timol, AB: ácido benzoico.

Para el rango seleccionado en el estudio los porcentajes de recobro estuvieron dentro de los límites establecidos para los métodos cromatográficos (98,0-102,0%) y el valor del coeficiente de variación, fue menor que el 2,0% (tabla 7). En la influencia del factor concentración sobre la variabilidad de los resultados de la exactitud, al aplicar la prueba de Cochran, se obtuvieron valores de C calculada menores que la C tabulada para una probabilidad de 0,05, p=3 y n=5; por tanto, las varianzas de las concentraciones empleadas fueron equivalentes, indicando que la concentración no influyó en la variabilidad de los resultados, en el rango estudiado. Al realizar la prueba de significación entre la recuperación, las medias y el 100% de recuperación, se obtuvieron valores de t de Student menores que el valor tabulado, confirmando la elevada exactitud del método ya que el recobrado medio no difiere significativamente del 100%. Teniendo en cuenta estos resultados puede afirmarse que los errores sistemáticos tuvieron muy bajo impacto en la calidad de los resultados y que

al cumplir con los indicadores establecidos para un método cromatográfico, el mismo puede ser utilizado para el fin propuesto. Estos resultados demuestran que el método permite determinar con exactitud los analitos, en el intervalo de 80 a 120% en las condiciones de trabajo estudiadas.

Tabla 7. Exactitud del método analítico.

Parámetro	**Nivel (%)**	**MT**	**SM**	**TM**	**AB**
R (%)	80	99,99	99,98	99,99	99,99
	100	100,00	100,00	99,99	99,97
	120	99,999	99,99	99,99	99,99
S	80	0,741	1,034	0,818	0,613
	100	0,739	1,04	0,821	0,602
	120	0,752	1,048	0,832	0,597
S^2	80	0,549	1,068	0,669	0,375
	100	0,546	1,082	0,674	0,363
	120	0,566	1,099	0,692	0,356
CV (%)	80	0,741	1,034	0,818	0,613
	100	0,739	1,04	0,821	0,603
	120	0,712	1,037	0,819	0,597
Ccal Ctab (0,05;5;3) = 0,746		0,351	0,34	0,335	0,349
tcal ttab (0,05;14) = 2,145		0,036	0,021	0,018	0,02
R (%)		99,99	99,99	99,99	99,98
SGlobal		0,689	0,963	0,763	0,559

MT: mentol; SM: salicilato de metilo; TM: timol; AB: ácido benzoico; R: recobrado; CV: coeficiente de variación.

Se obtuvieron coeficientes de variación menores al 1,0% al evaluar la precisión en condiciones de repetitibidad (tabla 8), en los tres niveles de concentración, para los cuatros analitos. Este valor concuerda con lo expresado como criterio de aceptación (< 2,0%). El análisis de varianza mostró un valor del test de Levene's igual a 0,403 que corresponde a un valor de probabilidad igual a 0,755; indicando que no existen diferencias estadísticas significativas entre las varianzas para los tres niveles de concentración evaluados por lo que se puede considerar que existe homocedasticidad.

Tabla 8. Precisión del método.

Analito	Nivel (%)	Concentración (µg/mL)	CV (%)	Valor de p
MT	80	32,158	0,725	$p_{analista}$ = 0,9980 $p_{día}$ = 1,0000
	100	40,204	0,733	
	120	48,259	0,745	
SM	80	40,235	1,052	$p_{analista}$ = 0,9988 $p_{día}$ = 1,0000
	100	50,294	1,041	
	120	60,373	1,055	
TM	80	48,377	0,830	$p_{analista}$ = 0,9988 $p_{día}$ = 1,0000
	100	60,469	0,825	
	120	72,581	0,831	
AB	80	24,441	0,566	$p_{analista}$ = 0,9997 $p_{día}$ = 1,0000
	100	30,554	0,596	
	120	36,666	0,597	
Levene's = 0,403 p = 0,7549				

MT: mentol; SM: salicilato de metilo; TM: timol; AB: ácido benzoico; valor de p: valor de probabilidad.

La figura 4 muestra los gráficos de medias para la precisión intermedia del método. Los gráficos de bigote indican la homogeneidad de las varianzas entre las distintas mediciones comparadas en los factores analizados evidenciando, la similitud de los resultados entre los analistas y en diferentes días. En la tabla 8 se resumen los valores de probabilidades obtenidos por los dos analistas y los tres días estudiados, evidenciando que no existen diferencias estadísticas significativas para un 95,0% de probabilidad. Estos coeficientes indican baja variabilidad por lo que el proceso de cuantificación, los analistas involucrados en el estudio fueron lo suficientemente precisos y las condiciones de trabajos bien controladas. Por lo que se considera que el método fue preciso asegurando que los errores aleatorios no causaron impacto significativo sobre los resultados en las condiciones antes mencionadas.

Los resultados de la determinación de los límites de detección y cuantificación para el MT, SM, TM y AB se observan en la tabla 9. Las curvas de calibración para la determinación de las respuestas y desviación estándar de los blancos mostraron ajustes adecuados con coeficientes de determinación que justificaron más del 98,0% de las variabilidades de los resultados. Con estos resultados se calcularon los valores de Ybl y Sbl para la determinación de los LD y LC. Estos valores fueron comprobados experimentalmente obteniendo buenos resultados.

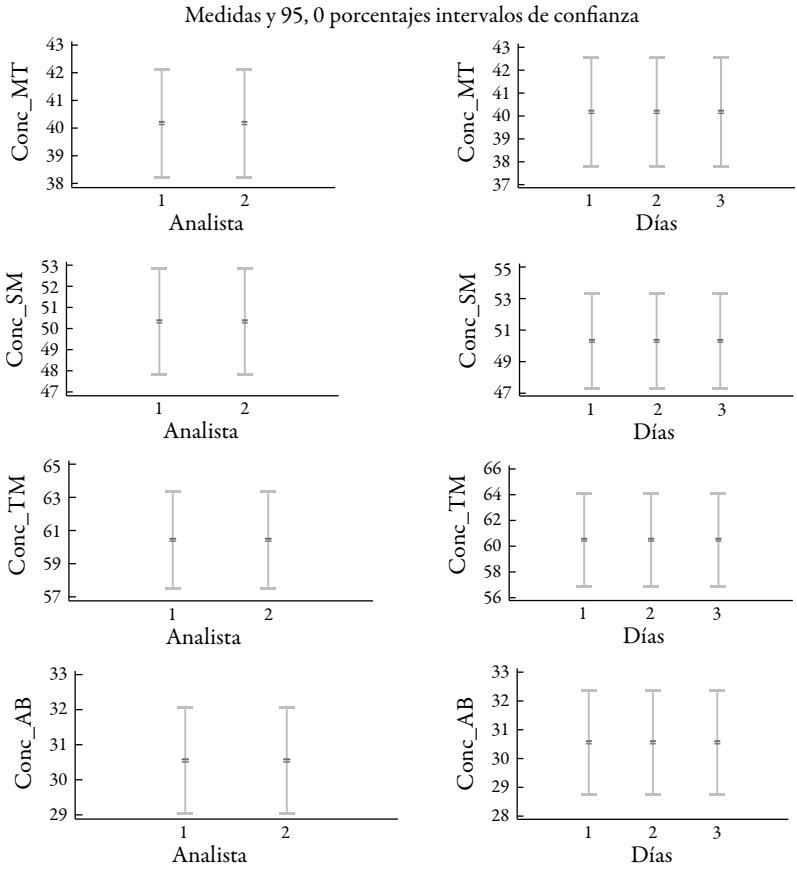

Figura 4. Gráficos de medias para la precisión intermedia del método, según la influencia de los analistas y días. MT: mentol; SM: salicilato de metilo; TM: timol; AB: ácido benzoico.

Tabla 9. Límites de detección y cuantificación del método.

Parámetro cromatográfico	MT	SM	TM	AB
Ecuación de la recta (Y blanco)	26,12 X-0,00	18,18 X-0,00	30,02 X+0,00	59,84 X-0,00
Ecuación de la recta (S blanco)	0,53 X-0,00	0,04 X+0,00	0,53 X+0,00	0,03 X+0,00
r^2 (%)	99,90	100,00	99,99	100,00
Límite de detección (ng/mL)	0,513	1,184	3,348	1,402
Límite de cuantificación (ng/mL)	1,459	3,438	9,734	4,363

MT: mentol; SM: salicilato de metilo; TM: timol; AB: ácido benzoico.

El conjunto de los resultados mostrados permite afirmar que el método por cromatografía gaseosa para la determinación de salicilato de metilo, timol, mentol y ácido

benzoico es lineal, preciso, exacto, selectivo y robusto en el intervalo de 80 a 120% de concentración, por lo que podría ser empleado para el control de calidad de la solución antiséptica.

La tabla 10 resume los valores determinados de las incertidumbres específicas para cada uno de los analitos en cuestión. Los valores demuestran la poca influencia de los errores aleatorios y sistemáticos sobre los resultados en el proceso de cuantificación. Por tanto, hay aproximadamente un 95,0% de probabilidad de que las concentraciones verdaderas de MT, SM, TM y AB, en muestras de rutina, estén contenidas dentro del intervalo proporcionado por la concentración obtenida al analizar la muestra y su incertidumbre asociada.

Tabla 10. Incertidumbres del método cromatográfico desarrollado.

Parámetro	MT	SM	TM	AB
Incertidumbre específica del ensayo de exactitud	± 0,689	± 0,963	± 0,763	± 0,559
Incertidumbre específica del ensayo de precisión intermedia	± 0,101	± 0,180	± 0,167	± 0,064
Incertidumbre combinada (gl= 43)	0,034	0,041	0,037	0,031
Incertidumbre expandida t(0,05, g.l.)= 2,017	± 0,069	± 0,082	± 0,074	± 0,062

MT: mentol; SM: salicilato de metilo; TM: timol; AB: ácido benzoico; gl: grados de libertad.

Los resultados de la cuantificación de las concentraciones de los analitos de interés en lotes pilotos, recién elaborados, de la solución antiséptica se resumen en la tabla 11. Estos pueden considerarse adecuados al obtenerse una repetibilidad dentro de los valores aceptados con coeficientes de variación inferiores al 2,0%.

Tabla 11. Cuantificación de los analitos de interés en la solución antiséptica con el método cromatográfico propuesto.

Lote	Parámetro	MT	SM	TM	AB
6001	Media (mg/100 mL)	40,20	50,29	60,47	30,55
	CV (%)	0,74	1,04	0,82	0,60
6002	Media (mg/100 mL)	40,21	50,52	60,15	30,16
	CV (%)	0,75	1,27	1,08	1,29
6003	Media (mg/100 mL)	40,42	50,03	60,19	30,45
	CV (%)	1,27	1,44	1,12	0,75

MT: mentol; SM: salicilato de metilo; TM: timol; AB: ácido benzoico; CV: coeficiente de variación.

Conclusiones

Un método de cromatografía gaseosa con detector de ionización de llama fue desarrollado y validado para la cuantificación simultánea de mentol, salicilato de metilo, timol y ácido benzoico. El método demostró ser confiable en cada criterio analítico evaluado, por lo que puede ser empleado para el control de calidad del producto terminado. El procedimiento y el sistema empleado en el estudio permitieron la determinación simultánea de los cuatro analitos en un tiempo de 25 min. Finalmente, la aplicación del método fue demostrada satisfactoriamente al analizar lotes pilotos de la solución antiséptica.

Conflicto de intereses

Los autores declaran no tener conflictos de intereses.

Referencias

1. H. Phatak, V. Vaidya, A rapid gas chromatography-mass spectroscopy method for simultaneous quantification of ornidazole and miconazolefrom cream formulations: development, validation and application, *Int. J. Pharm. Sci. Res.,* **7**(7), 2976-2983 (2016).

2. Anexo I: Buenas Prácticas para Laboratorio de Control de Medicamentos, en: *Validación de Métodos Analíticos, Centro para el Control Estatal de Medicamentos, Equipos y Dispositivos Médicos* (CECMED), Ministerio de Salud Pública, La Habana, Cuba, 2013, p. 4-25.

3. Regulación 41-2013, *Validación de métodos analíticos*, Centro para el Control Estatal de Medicamentos, Equipos y Dispositivos Médicos (CECMED), Ministerio de Salud Pública, La Habana, Cuba, 2013, p. 4.

4. Regulación No. 40, *Buenas prácticas de laboratorio para el control de medicamentos*, Centro para el Control Estatal de Medicamentos, Equipos y Dispositivos Médicos (CECMED), Ministerio de Salud Pública, La Habana, Cuba, 2014, p. 3-25.

5. *USP 38*, The United States Pharmacopeia, Official Monographs, Baltimore, Maryland, USA, 2015, p. 6236-6237.

6. Lj. Karuza, K. Folivarski, Validation of the assay method for camphor and menthol in a herbal drug preparation, *J. Pharm. Biomed. Anal.*, **15**, 419-422 (1996).

7. J.S. Valdez, D.K. Martin, M. Mayersohn, Sensitive and selective gas chromatographic methods for the quantitation of camphor, menthol and methyl salicylate from human plasma, *J. Chromatogr. B*, *Biomed. Sci. Appl*., **729**(1-2), 163-171 (1999).

8. E. González-Peñas, M. López-Alvarez, F. Martínez de Narvajas, A. Ursúa, Simultaneous GC determination of turpentine, camphor, menthol and methyl salicylate in a topical analgesic formulation (Dologex®), *Chromatographia*, **52**(3-4), 245-248 (2000).

9. J. Krzek, J.S. Czekaj, W. Rzeszutko, Validation of a method for simultaneous determination of menthol and methyl salicylate in pharmaceuticals by capillary gas chromatography with cool on-column injection, *Acta Pol. Pharm*., **60**(5), 343-349 (2003).

10. J. Fiori, M. Naldi, R. Gotti, HS-SPME-GC-MS for the quantitation and chiral characterization of camphor and menthol in creams, *Chromatographia*, **72**, 941-947 (2010).

11. L.I. Yan-chao, L.I. Yi-xian, Y.A.O. Ling-wen, L.I. Zhen-guo, GC simultaneous determination of camphor, menthol and synthetic borneol in Tongluo Qutong plaster, *Chin. J. Pharm. Anal.,* **32**(4), 672-675 (2012).

12. R.S. Swati, Antidermatophytic activity and gas chromatography of essential oils, *Am. J. Phytomed. Clin. Therap.*, **2**(3), 430-441 (2014).

13. J.S. Rucha, A.I .Patel, K.V. Vikani, N.L. Patel, Analytical method development and validation of pain relief herbal formulations, *Indo Am. J. Pharm. Res.*, **6**(4), 5112-5117 (2016).

14. R. Kalgutkar, K. Ramakrishna, V. Srinivasarao, Method development and validation of menthol in cough syrup by gas chromatography, *Anal. Chem.: An Indian J.*, **16**(1), 001-006 (2016). ISSN: 0974-7419

15. N.A.M. Adib, U.K. Mandal, F. Mohamed, B. Chatterjee, Fast and simple gas chromatographic method for simultaneous estimation of camphor, menthol and ethyl salicylate in analgesic ointment: application in stability study, *J. Pharm. Invest.*, **47**(3), 275-285 (2017).

16. M.N. Abualhasan, A.N. Zaid, N. Jaradat, A. Mousa, GC Method validation for the analysis of menthol in suppository pharmaceutical dosage form, *Int. J. Anal. Chem.*, **2017**, Article ID 1728414, 1-5 (2017).

17. M. Hatipi-Ibrahimi, V. Papajani, S. Ćavar, V. Matevski, GC/MS analysis of the essential oil of *Thymus Longicaulis* Presl. from Kosovo, *Bulletin of the Chemists and Technologists of Bosnia and Herzegovina*, **41**, 6-10 (2013).

18. N. Saini, G.K. Singh, Gas chromatographic validated method for quantification of ayurvedic polyherbal formulation, *Asian J. Pharm.*, **9**, 200-205 (2015).

19. B.O. Louchard, L.C. Costa, A.R.A. Silva, L.K.A.M. Leal, Validation of a high performance liquid chromatography method to quantify thymol in nanocapsules of bioactive essential oil from *Lippia sidoides*, *Int. J. Complement. Alt. Med.*, **10**(2), 00330 (2017).

20. M. Heinänen, C. Barbas, Validation of an HPLC method for the quantification of ambroxol hydrochloride and benzoic acid in syrup as pharmaceutical form stress test for stability evaluation, *J. Pharm. Biomed. Anal.*, **24**(5-6), 1005-1010 (2001).

21. D. Satínský, J. Huclová, R.L. Ferreira, M.C. Montenegro, P. Solich, Determination of ambroxol hydrochloride, methylparaben and benzoic acid in pharmaceutical preparations based on sequential injection technique coupled with monolithic column, *J. Pharm. Biomed. Anal.*, **40**, 287-293 (2006).

22. M. Haider, Development and validation of a stability indicating HPLC method for the estimation of butamirate citrate and benzoic acid in pharmaceutical products, *J. Chromatogr. Separ. Tech.*, **2**(2), 1000111 (2010).

23. L.A. Melikyan, S.S. Martirosyan, R.S. Grigoryan, H.V. Topchyan, T.K. Davtyan, Development and validation of HPLC method for the determination of metronidazole benzoate and related impurites in bulk and pharmaceutical formulations, *Int. J. Pharm. Sci. Res.*, 4(7), 2594-2599 (2013).

24. H. Rouhollah, M. Masoumeh, Simultaneous determination of saccharine, caffeine, salicylic acid and benzoic acid in different matrixes by salt and air-assisted homogeneous liquid-liquid extraction and high-performance liquid chromatography, *J. Chil. Chem. Soc.,* **61**(3), 3090-3094 (2016).

25. D.R. Sahoo, S. Jain, A rapid and validated RP-HPLC method for the simultaneous quantification of benzoic acid, metronidazole and miconazole nitrate in vaginal formulations, *J. Chromatogr. Sci*., **54**(9), 1613-1618 (2016).

26. S. Kumaravel, P. Shanmugapandiyan, New validated stability indicating gradient RP-HPLC method for the assay & related substances of miconazole nitrate and assay of benzoic acid in miconazole nitrate 2.0% w/w gel, *Int. J. Pharma-Bio Sci.*, **8**(2), 308-312 (2017).

27. L.A. Martínez, J.A. Martínez, Y. Baena, Validación de una metodología analítica por HPLC-DAD para la cuantificación de ácido benzoico complejado, en un ensayo de permeación transdérmica *in vitro* empleando piel de cerdo, *Rev. Colomb. Cienc. Quím. Farm.,* **47**(3), 424-440 (2018).

28. J. Pauwels, W. D'Autry, L. Van den Bossche, C. Dewever, M. Forier, S. Vandenwaeyenberg, *et al.*, Optimization and validation of liquid chromatography and headspace-gas chromatography based methods for the quantitative determination of capsaicinoids salicylic acid, glycol monosalicylate, methyl salicylate, ethyl salicylate, camphor and l-menthol in a topical ointment, *J. Pharm. Biomed. Anal.*, **60**, 51-58 (2012).

29. H. Zhi-hong, W. Zhi-li, S. Bao-lin, W. Dong, C. Jian-xin, W. Su-li, G. Bao-jia, Simultaneous determination of salicylic acid, jasmonic acid, methyl salicylate, and methyl Jasmonate from *Ulmus pumila* leaves by GC-MS, *Int. J. Anal. Chem.*, **2015**, 698630 (2015).

30. S. Bell, *A Beginner's Guide to Uncertainty of Measurement*, National Physical Laboratory, Teddington, UK, 1999.

Cómo citar este artículo

A. Fonseca-Gola, J.M. Cordoví-Velázquez, N. Benítez-Guerra, M. Fernández-Cervera, Desarrollo y validación de un método de cromatografía gaseosa para la determinación de mentol, salicilato de metilo, timol y ácido benzoico en solución antiséptica, *Rev. Colomb. Cienc. Quím. Farm.*, **49**(2), 306-328 (2020).

Technological research article / *http://dx.doi.org/10.15446/rcciquifa.v49n2.89486*

Evaluation of physicochemical properties and dissolution studies on quality control of low water solubility drugs (raw materials and pharmaceutical formulations)

Matheus da Silva Ferreira[1], Gilmar Antônio de Carvalho Teles Júnior[2], Carlos Magno Ramos Carvalho Júnior[2], Fernanda de Souza Dias[2], Wilson Saback Dias dos Santos Júnior[2], Marluce Oliveira da Guarda Souza[1], Aníbal de Freitas Santos Júnior[1,2,*]

[1]Department of Exact and Earth Sciences (DCET), State University of Bahia (UNEB), Campus I, 2555 Silveira Martins Street, Cabula, 41150-000, Salvador, Bahia, Brazil.

[2]Department of Life Sciences (DCV), State University of Bahia (UNEB), Campus I, 2555 Silveira Martins Street, Cabula, 41150-000, Salvador, Bahia, Brazil. Tel: +5571 31175313.

*Corresponding author: E-mail address: afjunior@uneb.br (A.F. Santos Júnior).

Received: 23 February 2020

Revised: 25 April 2020

Accepted: 26 April 2020

Summary

The purpose of this study was to evaluate physicochemical properties and dissolution studies of furosemide (FUR), hydrochlorothiazide (HCTZ) and nifedipine (NIF), low water solubility drugs, in raw materials and pharmaceutical formulations. Surface and physicochemical characterization techniques -scanning electronic microscopy (SEM), thermogravimetry (TG), X-ray diffraction (XRD) and infrared (IR) spectrometry- as well as physical and physicochemical tests on tablets and capsules were applied as supporting information on drug quality control. Simple, rapid, and efficient UV-Vis methods were developed and validated for the determination of FUR, HCTZ and NIF samples. SEM exhibited considerable differences in the crystal morphological structures. Among the drugs studied, except for furosemide, more than one polymorph was present in the samples. Drug release profiles were satisfactory for all products. FUR and HCTZ tablets exhibited similar dissolution profiles, with very rapid release to the pharmaceutical specialties (reference, similar and generic). For HCTZ tablets, the similar drug (f2= 48.74) is not equivalent to the reference drug. NIF capsules (reference and compounded) showed a release ≥80% of stated on product labels, in 10 minutes. The results obtained in this study suggest that the quality parameters and drug dissolution profiles may have been influenced by the morphology and size of the crystals, excipients, and technological processes.

Key words: Drugs, low water solubility, physicochemical characterization, dissolution, quality control.

Resumen

Evaluación de propiedades fisicoquímicas y estudios de disolución sobre el control de calidad de fármacos de baja solubilidad en agua (materias primas y formulaciones farmacéuticas)

El propósito de este estudio fue evaluar las propiedades fisicoquímicas y los estudios de disolución de furosemida (FUR), hidroclorotiazida (HCTZ) y nifedipina (NIF), medicamentos de baja solubilidad en agua, en materias primas y formulaciones farmacéuticas. Técnicas de caracterización fisicoquímica y de superficie: microscopía electrónica de barrido (SEM), termogravimetría (TG), difracción de rayos X (XRD) y espectrometría infrarroja (IR), así como pruebas físicas y fisicoquímicas en tabletas y cápsulas que se aplicaron como información de apoyo sobre el control de calidad. Se desarrollaron y validaron métodos simples, rápidos y eficientes de UV-Vis para la determinación de muestras de FUR, HCTZ y NIF. SEM exhibió diferencias considerables en las estructuras morfológicas de cristal. Entre las drogas estudiadas, a excepción de la furosemida, más de un polimorfo estaba presente en las muestras. Los perfiles de liberación de fármacos fueron satisfactorios para todos los productos. Las tabletas FUR y HCTZ exhibieron perfiles de disolución similares, con una liberación muy rápida a las especialidades farmacéuticas (referencia, similares y genéricas). Para las tabletas de HCTZ, el medicamento similar (f2= 48,74) no es equivalente al medicamento de referencia. Las cápsulas NIF (de referencia y compuestas) mostraron una liberación ≥80% de la indicada en las etiquetas del producto, en 10 minutos. Los resultados obtenidos en este estudio sugieren que los parámetros de calidad y los perfiles de disolución del fármaco pueden haber sido influenciados por la morfología y el tamaño de los cristales, excipientes y procesos tecnológicos.

Palabras clave: Drogas, baja solubilidad en agua, caracterización fisicoquímica, disolución, control de calidad.

Introduction

Pharmaceutical development requires knowledge of the physicochemical properties of drugs, pharmaceutical products, and excipients to meet quality control requirements [1]. In addition to the specifications of content, identity, purity, efficacy, and safety, it is also important that the drug be adequately released to meet the therapeutic objective. Thus, biopharmacotechnical aspects are fundamental for pre-formulation studies, especially those related to physicochemical properties, drug dissolution (factors related to the drug, the reaction medium, the excipients and the manufacturing technique used), intestinal permeability and drug absorption [2-4].

Furthermore, on tests and dissolution profiles, other techniques have been highlighted in the pharmaceutical sciences, in order to know the factors related to drugs and excipients, which directly interfere with the finished product and its therapeutic effects [5]. These tests aim to characterize the samples analyzed for the presence of polymorphisms, drug and formulation thermal stability, morphology, particle size, among others. Thus, the techniques of thermal analysis, such as thermogravimetry (TG) and differential thermal analysis (DTA) [6-9] stand out, as well as spectroscopic techniques, such as X-ray diffraction (XRD) [10, 11], infrared spectrometry (IR) [12] and molecular absorption spectrophotometry in the ultraviolet and visible light region (UV-Vis) [13, 14], besides scanning electron microscopy (SEM) [15,16].

Another relevant tool used mainly in prefabrication studies, is the biopharmaceutical classification system (BCS), which groups drugs by biological membranes according to aqueous solubility and permeability [17, 18]. Low solubility drugs (class II and IV) may present release problems of the pharmaceutical form and bioavailability and therefore need to be meticulously characterized from a physicochemical point of view [19]. BCS, along with dissolution studies, has been beneficial to the pharmaceutical industry and regulatory agencies in many countries, as a scientific approach that allows bioavailability testing for bioequivalence and bioavailability testing of solid oral immediate release pharmaceutical forms. Thus, there is a great impact on cost reduction in the development and testing of new drugs [20, 21].

Low solubility drugs include furosemide (FUR), hydrochlorothiazide (HCT) and nifedipine (NIF), used worldwide in antihypertensive therapy. In Brazil, they are included in the National list of essential medicines (RENAME) and the industry makes numerous pharmaceutical alternatives available to consumers and health professionals, such as generic and similar drugs, as well as those manipulated with presentations in individualized dosages, making it necessary to monitor the quality of these drugs marketed in the country [22-25].

Despite being poorly soluble drugs, some studies in Brazil have shown very rapid dissolution (over 85% of the drug within 15 minutes) for medicines containing furosemide (40 mg), hydrochlorothiazide (25 mg) and nifedipine (10 mg) [26, 27]. Hence, the objectives of this study were to evaluate the physicochemical properties of low solubility drugs (furosemide, hydrochlorothiazide and nifedipine) by TG, DTA, XRD, IR, UV-Vis and SEM techniques, and to evaluate the dissolution of oral solid pharmaceutical forms (tablets and capsules) containing FUR, HCTZ and NIF marketed in Salvador, Bahia, Brazil.

Materials and methods

Standards and samples

Reference standards of FUR from the United States Pharmacopeia (USP) (denominated FURP1) were acquired from Sigma Aldrich (St Louis, MO, USA) and those from the Brazilian Pharmacopeia (denominated FURP2) were acquired from the National Institute for Quality Control in Health-INCQS (Fiocruz, Rio de Janeiro, Brazil), respectively. Reference standards of HCT (HCTZP) and NIF (NIFP) from the Brazilian Pharmacopeia were acquired from the National Institute for Quality Control in Health-INCQS (Fiocruz, Rio de Janeiro, Brazil), respectively. Secondary standards (named as FURA; HCTZA and NIFA), were donated by Pharmacia Bioethica® from Salvador, Bahia, Brazil for physicochemical characterization analyses.

Medicine samples,furosemide (40 mg) and hydrochlorothiazide (25 mg) tablets-reference (R), similar (S) and generic (G) and Nifedipine (10 mg) capsules-reference (R) and compounded (C) were purchased from drugstores in Salvador, Bahia, Brazil.

Chemicals

All reagents were of analytical grade. Doubly distilled water was obtained from a Q341 Quimis distiller (São Paulo, SP, Brazil) and used throughout the experiments. Hydrochloric acid (HCl), sodium chloride, monobasic dihydrogen phosphate and dibasic monohydrogen phosphate were purchased from Quimex (Merck, São Paulo, SP, Brazil) and used as the dissolution media for the dissolution tests. Lactose, microcrystalline cellulose, hydroxypropyl cellulose, polyvinylpyrrolidone (PVP), magnesium stearate was donated by Pharmacia Bioethica® (Bahia, Brazil).

Equipments

Thermal analyses (TG and DTA) were investigated using differential thermal analysis (DTG-60, Shimadzu®, Japan), with alumina crucible (approximately 8 mg of sample) at a heating rate of 10 °C min^{-1}, under a nitrogen flow rate of 50 mL min^{-1} and thermal range of 25-900 °C. XRD analyses were performed in a diffractometer (XRD 6000 Shimadzu®, Japan) using a Cu-Kα radiation tube (40 kV, 30 mA). The samples were analyzed at scanning angles of 10 - 80° (2θ) in a step of 2.0° (2θ) min^{-1}. Fourier transform infrared spectroscopy (FTIR) by the ATR method was used, with an FTIR 100S Spectrometer (PerkinElmer®, Waltham, MA, USA), operating between 4000 and 400 cm^{-1}, with a resolution of 4 cm^{-1}, using the KBr pellet method (approximately 5 mg of sample). SEM images were obtained at magnifications of 200 and 500x, using a JEOL JSM-6390-LV microscope (JEOL, Ltd., Akishima, Tokyo, Japan) with an acceleration of tension at

5 kV, using carbon tape to fix materials in the carrier. The sample was vacuum metallized with gold deposition on them to improve microscope viewing. For all tests, the results were analyzed, and graphs were plotted by the OriginPro 8® software.

The evaluation of physical (weight uniformity, friability, and disintegration) and physicochemical (dissolution) tests was performed in accordance with the Brazilian and the United States Pharmacopoeia general methods [25, 28]. Weight variation was obtained on an electronic balance (Mark, M164-AI, Piracicaba, SP, Brazil). The friability tester was an HX 300-2 Ethik (Vargem Grande Paulista, SP, Brazil). The disintegration analyses were carried out on a 301/AC 01 Nova Ética system (Vargem Grande Paulista, SP, Brazil). The dissolution analysis was carried out on a multi-bath (n= 6) dissolution test apparatus 299 Ethik (Vargem Grande Paulista, SP, Brazil). All spectrophotometric measurements were carried out using a 1240 Shimadzu (Kyoto, Japan) UV-Vis spectrophotometer (190-1100 nm) equipped with a diode array detector. The absorbances of sample solutions were read in 1-cm quartz cells. The detector was set at 271, 272 and 340 nm for FUR, HCT and NIF, respectively.

Preparation of reference solutions and dissolution studies

Stock standard solutions of furosemide, hydrochlorothiazide and nifedipine (500 μg mL^{-1}) were prepared in phosphate buffer (pH 5.8), 0.1 mol L^{-1} HCl and simulated gastric fluid without pepsin (pH= 1.0), respectively. Calibration standards with concentrations ranging (in μg mL^{-1}) from 5.0 to 50 (furosemide); 5.0 to 30 (hydrochlorothiazide) and 2.0 to 16 (nifedipine) were prepared daily from the stock standard solution by appropriate dilution and analyzed in triplicate by UV-vis spectrophotometry. Curve equations for each drug were obtained for regression analysis by the least-squares method to calculate the calibration model and the correlation coefficient (r) value.

Dissolution studies were conducted using the Brazilian Pharmacopoeia [25] and the United States Pharmacopoeia [28] general methods (table 1), with six replicates at 37±0.5 °C and 900 mL of dissolution medium.

Table 1. Optimal parameters for dissolution studies of furosemide, hydrochlorothiazide and nifedipine.

Drug	Dosage/ pharmaceutical Form	Dissolution medium	Apparatus	Rotation (rpm)
Furosemide	40-mg/tablets	phosphate buffer (pH 5.8)	2 (paddle)	50
Hydrochlorothiazide	25-mg/tablets	0.1 mol L^{-1} HCl	1 (basket)	100
Nifedipine	10 mg/ capsules	simulated gastric fluid without pepsin (pH= 1.0)	1 (basket)	50

In all experiments, aliquots of 10 mL were withdrawn at predetermined time intervals (1, 3, 5, 10, 15, 20, 25, 30, 45, and 60 minutes) and replaced with an equal volume of fresh medium to maintain a constant total volume in each vessel, following filtration of dissolution samples using 0.45-μm membrane filters; the concentrations of propranolol were determined by the proposed UV spectrophotometric method. The absorbances were converted to concentrations obtained from the equation on the standard curve. Calculations were performed considering the amount of drug removed in each aliquot. The results were expressed as drug release (%) as a function of time.

Dissolution efficiency (DE) was used to evaluate the product dissolution performance under test conditions. This parameter was obtained from the area under the drug dissolution curve up to 60 minutes (AUC0-t), in relation to 100% of the product label value (AUCTR). DE was expressed as a percentage and can be set by the following equation: AUC0-t/AUCTR × 100, where t is time (min) and TR is the product label value [29]. DE values were statistically analyzed using Student's t-test with a significance level of $p \leq 0.05$. The DE results of the tested products were subjected to analysis of variance (Anova) using the Statistical Package for the Social Sciences (SPSS) software (version 22.0, IBM).

Validation of the analytical method

The dissolution test was validated to demonstrate suitability. In Brazil, compendial analytical methods must have their suitability demonstrated for their intended use under laboratory operating conditions by presenting a partial validation study [30]. In this case, partial validation must assess at least the parameters of accuracy, precision, and selectivity. To extend the validation studies, International Conference on Harmonization (ICH) recommendations were used [31]. Thus, analysis of selectivity, linearity, precision (repeatability and intermediate precision), accuracy, limit of detection (LOD) and quantification (LOQ) were performed. Possible interferences were evaluated by testing the components of the formulations and comparing them to a placebo.

Results and discussion

Physicochemical characterization

Thermogravimetry is useful for evaluation of stability tests [32], polymorphism [9], and quality control of drugs [1, 33]. Figure 1 shows the results for thermal analysis (TG and DTA/DTG) of FURP1 (figure 1A), FURP2 (figure 1B) and FURA (figure 1C). The decomposition profiles are observed to be similar. All DTG curves showed two initial events for all analyses with very similar loss mass values. The first event

(between 204.8 and 232.0 °C; Tpeak at 222.5, 222.6 and 218.9 °C (FURP1, FURP2 and FURA, respectively) exhibits a small mass loss (< 3 %), due to evaporation of volatile compounds. In the second (starting at 233 °C; Tpeak= 277 °C), a mass loss (approximately 69 %) was observed without a definite constant mass event in the TG curves, suggesting other sample degradation events, not determined by the DTG, until the end of the test; 2.58 mg (~30%) residue remaining in the crucible suggest that the total decomposition of furosemide occurs at temperatures above 900 °C in an inert atmosphere (N_2).

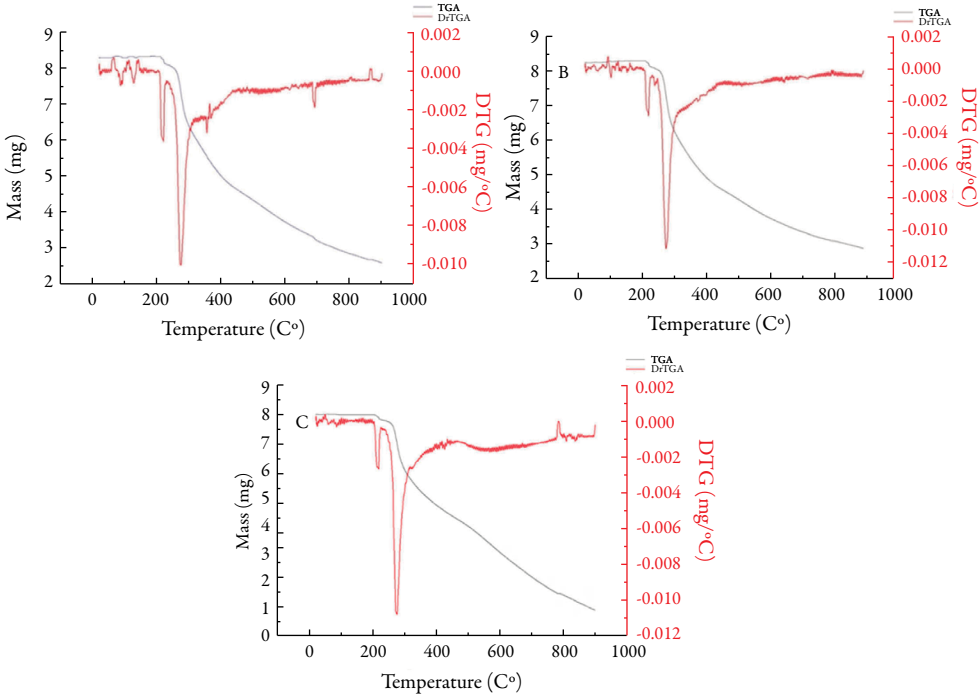

Figure 1. TG/DTG curves for Furosemide: FURP1 (A), FURP2 (B) and FURA (C).

The first decomposition event agrees with Silva *et al*. in 2013, who determined the first decomposition event, with furosemide water loss occurring between 208 and 240 °C, with a mass loss of 2.8% [7]. However, the authors reported two other events in the temperature range between 240 and 407 °C: the second event, between 240 and 290 °C, with a mass loss of 21.6%, related to the majority loss of 2-methyl-furanyl and furanyl. In addition, a third event (between 294 and 407 °C) with SO_2 and CO_2 release was observed. Differences between sample decomposition and the literature may be associated with structural and morphological properties, among others.

In DTA analysis of furosemide (figure 2), there was a discrete endothermic event occurring at approximately 133 °C. The fusion event of furosemide was only clearly observed in FURP1, evidenced by an endothermic peak at 216.8 °C. For FURP1 and FURA, the fusion occurred together with the first decomposition event (212 °C) and peaked at approximately 222.5 °C. Silva *et al*. concluded that, in the first decomposition event, with loss of water, there is a condensation reaction of the furosemide molecules, forming dimers, which may be a carboxylic acid anhydride or an amide [7]. Factors such as the presence of polymorphism, mass used in the test, degree of material compaction and particle size may have directly affected the differences observed between FURP1, FURP2 and FURA for thermal analysis.

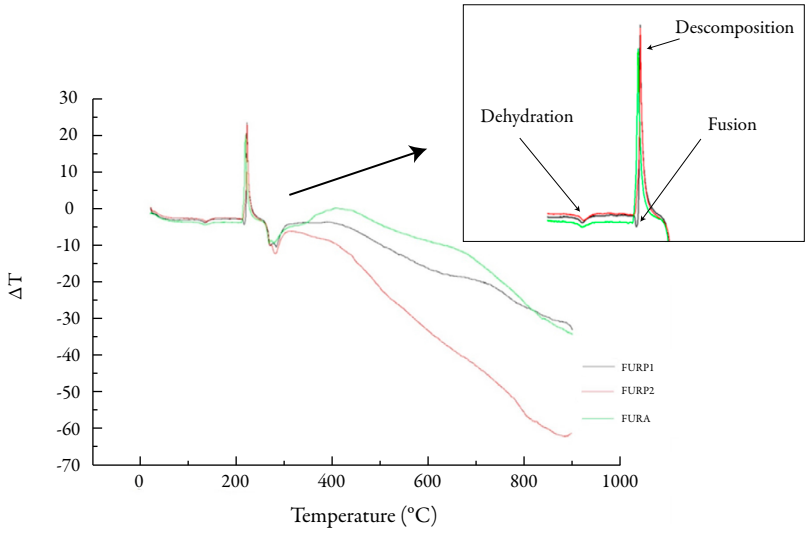

Figure 2. DTA curves for Furosemide for FURP1, FURP2 and FURA.

Thermogravimetric curves (TG/DTG and DTA) for HCTZP (figure 3) showed only a well-delimited degradation event of this drug (between 286.90 and 391.45 °C; T_{peak}= 332.30 °C). The mass loss resulting from this event was approximately 46.5% in relation to the initial mass. For HCTZA, there was also a single mass loss event well defined by DTG (between 286.82 and 394.30 °C; T_{peak}= 321.11 °C) and mass loss (around 48 %). Souza *et al*. in 2018 reported three events for HCTZ degradation [34]. The first (between 309.7 and 381.6 °C); the second (381.6 and 531.0 °C) and the third (531.0 and 727.6 °C), with mass losses of 38.1; 26.9 and 34.8%, respectively. Macêdo *et al*. [35] observed the initiation of drug decomposition at approximately 313.6 °C. DTA curves for Hydrochlorothiazide exhibited two events: the first, defined by an endothermic peak at 270.0 and 270.3 °C; and the second at temperatures of 314.2 and 314.0 °C for HCTZP and HCTZA, respectively.

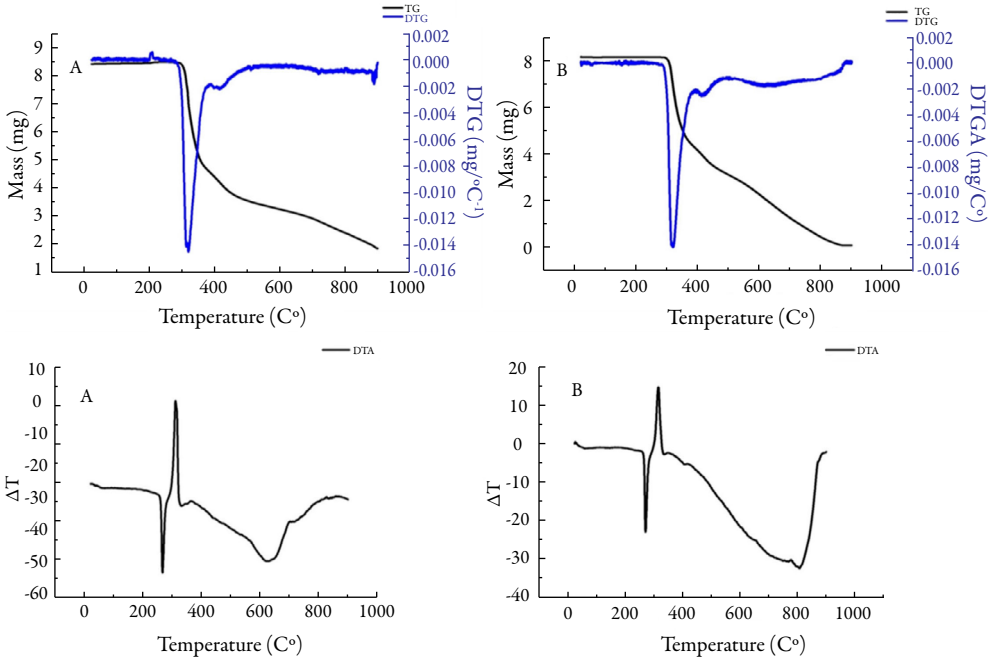

Figure 3. TG/DTG and DTA curves for Hydrochlorothiazide: HCTZP (A) and HCTZA (B).

Figure 4 shows TG/DTG and DTA curves for Nifedipine. For NIFP, an event was observed at approximately 160.0 °C with a mass loss of 0.26%, related to moisture. A second event (between 209.24 and 338.0 °C; T_{peak}= 294.0 °C) was observed, with a mass loss around 89 %, related to the first decomposition step of nifedipine. A last event (between 512.0 and 773.0 °C), with a mass loss of 11.5% was determined. For NIFA, the dehydration event occurred at 178 °C, with a mass loss of 0.72%. The first decomposition step occurred between 212.2 and 346.8 °C (T_{peak}= 290.4 °C), with a mass variation of 94.0%; the second stage began at 577 °C, ending near 900 °C, with a mass loss of 1.35%. At the end of this analysis, 3.9% of the decomposition residue in the crucible was observed.

Both steps of nifedipine decomposition have been reported in other studies. Leite *et al*. [6] observed the first stage of nifedipine decomposition (between 209.2 and 313.8 °C), with a mass loss of 90.1%, and the second stage (between 533.24 and 677.58 °C), with a mass loss of 4.42%, in an inert atmosphere (N_2). Filho *et al*. [36] detected both steps, but only described the first (between 210.0 and 390.0 °C), with 85.2% mass loss in synthetic air. Thus, the results found for thermogravimetric analysis in this study agree with the literature. DTA curves for NIFP and NIFA showed an endothermic peak at 173 °C relative to drug fusion, which is in the range of 171 to 175 °C [6, 25]. No

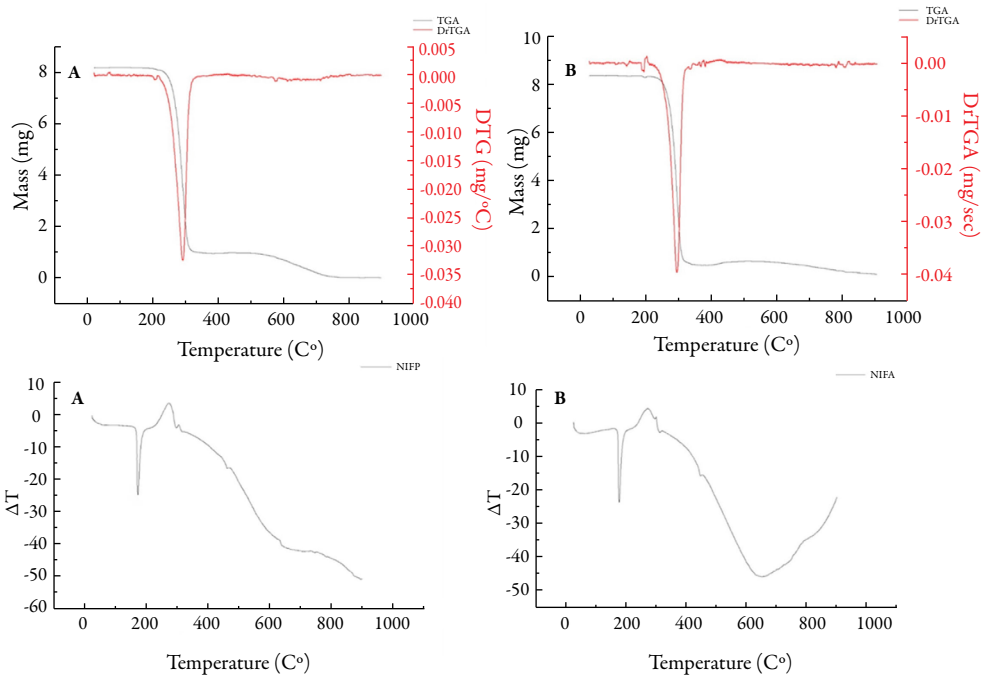

Figure 4. TG/DTG and DTA curves for Nifedipine: NIFP (A) and NIFA (B).

description of the other peaks detected was found in the literature, being associated only with drug decomposition [36].

The literature describes that nifedipine form I, more thermodynamically stable, has a melting range of 172 to 173 °C; form II has a melting point of approximately 163 °C and form III (metastable form) in the range 134 to 137 °C [9]. Thus, it is suggested that, in this study, the crystalline forms of nifedipine (NIFP1 and NIFA) are presented in nifedipine form I, being its most stable form.

Spectroscopic techniques such as X-ray diffraction (XRD) are useful for the identification of different (pseudo) polymorphs of an active pharmaceutical ingredient in dry powder formulations [37]. X-ray diffractograms for FURP1, FURP2 and FURA exhibited well-defined peaks (figure 5A). No significant differences were observed between sample profiles. The most intense peak occurred at 24.7° (2θ) for all samples. There were also peaks at 11.9°; 18.0°; 18.9°; 21.2°; 22.9°; 28.5° and 30.2° (2θ). These data corroborate the study by Shin and Kim and Garnero *et al.*, who showed the crystallinity of the compounds [38, 39]. However, other authors have described peaks at 24.8°; 21.2° and 22.9° (2θ) for furosemide form I [40-42]. Thus, it was noted that, for

the furosemide crystals studied (FURP1, FURP2 and FURA), similar profiles were evidenced to forms I and II of these drugs, according to table 2.

Table 2. Peaks exhibited by X-ray diffractometry for furosemide in this study and described in the literature.

	Angle (2θ)							
Shin and Kim [38]	18.0	18.9	24.7	28.6				
Garnero *et al.* [39]								
(Polymorph I)	18.2	21.2	22.9	24.8	29.3	29.7	30.5	31.6
(Polymorph II)	12.1	14.3	21.4	22.9	28.6			
This study	11.9	18.0	18.9	21.2	22.9	24.7	28.5	30.2

The diffractograms obtained for HCTZP and HCTZA were, to their greatest extent, superimposable (figure 5B), with more evident peaks at 19.13°; 28.78° and 35.96°, at the same angles (2θ) and the same intensity. The data obtained agreed with Souza *et al.* [1] and El-Gizawy *et al.* [43]. This fact can be explained, since Aceves-Hernández *et al.* [44] stated that there is no polymorphism for hydrochlorothiazide.

NIFP and NIFA showed intense peaks (figure 5C) at 16.09°; 19.56° and 24.62° (2θ), near to those found by Chinh *et al.* [45] and presented smaller peaks at 10.42°, 11.77°, 14.73°, 16.93°, 22.47° and 25.92° (2θ). However, Leite *et al.* [6] reported that pure nifedipine exhibits peaks at 10.6° and 11.9° (2θ), which were not found in any of the analyzed substances. Brown *et al.* [46] suggested that peak differences may be associated with the type of nifedipine treatment. These authors showed, from drug heating and cooling, a larger number of reduced peaks, associated with the formation of less organized structures. In addition, Leite *et al.* [6] also showed structural differences by X-ray diffractometry from the recrystallization of nifedipine using different solvents. Additionally, Grooff *et al.* [9] described that nifedipine form I exhibits prominent peaks at 8.2°, 10.5°, 11.7°, 16.2°, 24.7° and 26° (2θ) and form III at: 7.4°, 9.2°, 11.2°, 12.4°, 12.8°, 15.7°, 16.9°, 24.2° and 26.3°. From the results obtained in this study and comparing them with the literature and other results obtained by thermal analysis, it is stated that the studied nifedipine crystals are arranged in the form I of this drug.

Infrared spectroscopy is one of the most important analytical techniques available to drug analysis [11, 47, 48]. FTIR spectra obtained for FURP1, FURP2 and FURA exhibited bands at 1140, 1240, 1318, 1562, 1666, 3282, 3350, 3399 cm^{-1} (figure 6A). Garnero *et al.* [40] described that differences in the FTIR spectrum of furosemide forms I and II are observed in the zones between 3400-3200 and 1350-1100 cm^{-1}. These authors described that furosemide form I exhibits characteristic bands at 3398

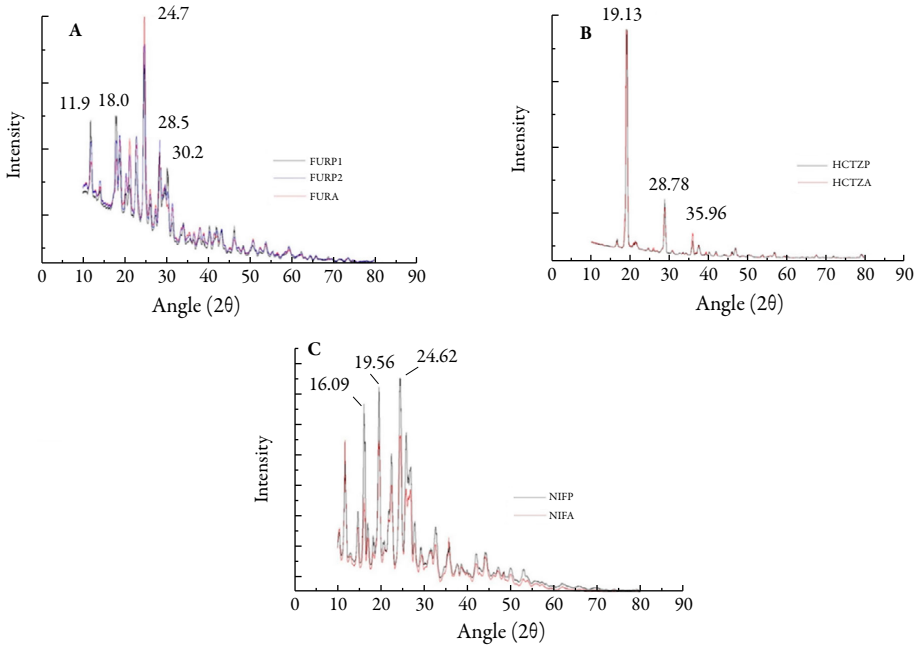

Figure 5. X-ray diffractograms: (A) furosemide (FURP1, FURP2 and FURA); (B) hydrochlorothiazide (HCTZP and HCTZA) and (C) nifedipine (NIFP and NIFA).

and 3284 cm^{-1} (NH sulfonamide stretch), 3352 cm^{-1} (secondary amine NH stretch) and 1141 cm^{-1} (symmetric stretch S= O), while form II exhibits bands at: 3345 cm^{-1} (secondary amine NH stretch), 3251 cm^{-1} (NH sulfonamide stretch) and 1337 and 1169 cm^{-1} (asymmetric and symmetric stretch S= O, respectively). Doherty and York [49] suggested that the unit cell of a furosemide crystal, it has an intermolecular hydrogen bonding network involving the sulfonamide group. Moreover, they argued that furosemide II data revealed an alteration in vibrations associated with the sulfonamide group, suggesting a change in the hydrogen bonding sequence within the crystal. Thus, this polymorph may be the result of a molecular conformational change and, consequently, crystalline packaging of the drug. Therefore, it was observed that the crystals (FURP1, FURP2 and FURA) are in forms (I and II) of this drug.

The drugs analyzed (HCTZP and HCTZA) exhibited bands in the FTIR spectra (figure 6B) at 1148, 1317, 1519, 1596, 3165, 3264 and 3359 cm^{-1}. In addition, small bands could be observed at 1021, 1057, 1121, 2836 and 2946 cm^{-1}. El-Gizawy *et al.* [43] described bands at 3363, 3264 and 3172 cm^{-1} for the NH group stretch and at 3098 cm^{-1} for the CH stretch. In addition, bands referring to the CH_2 group stretch at wave numbers 2964 and 2863 cm^{-1} have also been described: at stretching

vibrations C= C at 1604 and 1519 cm^{-1}. The bands for group SO_2 were displayed at 1329 cm^{-1} (asymmetric stretching vibrations) and 1171 and 1060 cm^{-1} (symmetric stretching vibrations). Sonpal *et al*. [50] observed a band at 3354 cm^{-1}, which was assigned to the stretching of NH bonds and 1570 cm^{-1}, corresponding to the folding of this group into pure hydrochlorothiazide. Therefore, HCTZP and HCTZA are in accordance with the data described in the literature for hydrochlorothiazide. No differences were observed between drug bands (reference and sample). Thus, the presence of polymorphism for hydrochlorothiazide was not characterized.

FTIR spectra for NIFP and NIFA (figure 6C) indicated characteristic bands of N-H and C-H stretch vibrations at 3324 and 2953 cm^{-1} [51]. The peak at 1678 cm^{-1} was assigned to the carbonyl styrene vibrations, while the peak at 1647 cm^{-1} and the absorption region at 792-857 cm^{-1} were attributed to the C= C stretching and flexural vibrations in the benzene ring. Some characteristic peaks at 1527 and 1494 cm^{-1} were assigned to flexural vibrations of the NH and NO_2 groups. In addition, symmetric and asymmetric C-O stretching vibrations in ester groups were also found at 1120 and 1224 cm^{-1}, respectively [45, 51]. Therefore, the presence of FTIR polymorphism for the analyzed nifedipine crystals was not observed. These results corroborate those obtained by thermal analysis and X-ray diffraction, in this study.

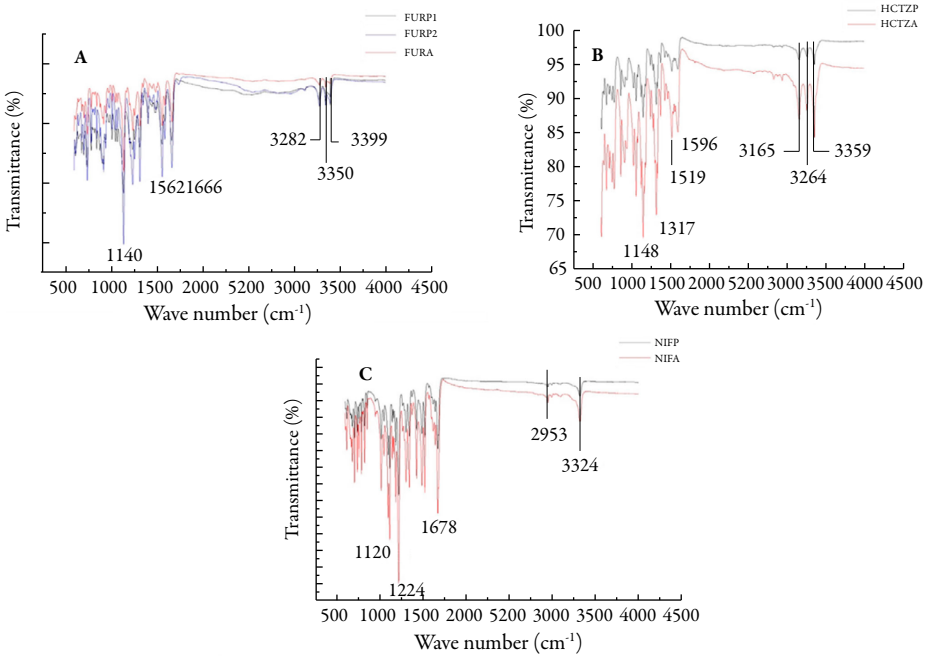

Figure 6. FTIR spectra: (A) furosemide (FURP1, FURP2 and FURA); (B) hydrochlorothiazide (HCTZP and HCTZA) and (C) nifedipine (NIFP and NIFA).

Scanning electron microscopy is widely used for observation of the microstructural characteristics of solids in drug analysis [52, 53]. The FURP1 crystals had a thin, elongated morphology of uniform size and the appearance of blades. For FURP2, smaller, finer divided needle-shaped crystals were visualized. Moreover, for FURA, the crystals were presented without a definite morphological formation and of varying sizes. These results corroborate that there is a morphological difference between the furosemide crystals studied (figure 7A) and the literature [54].

The micrographs obtained for HCTZP (figure 7B) showed large crystals (tile shapes) of uniform size and low thickness. For HCTZA, the crystals were large elongated parallelepipeds, with uniform sizes [15]. After morphological analysis of nifedipine crystals, NIFP and NIFA (figure 7C) were found to have varied sizes and undefined shapes. No other studies characterizing the morphology of pure nifedipine crystals were found in the literature.

Morphological differences observed for furosemide, hydrochlorothiazide and nifedipine crystals can be associated with differences in mass, size, shape, degree of compaction, bulk density and contact surface. Such differences may interfere with thermal analysis, X-ray diffraction and FTIR, as well as drug dissolution since the dissolution rate is dependent on the contact surface between the solid and the solvent.

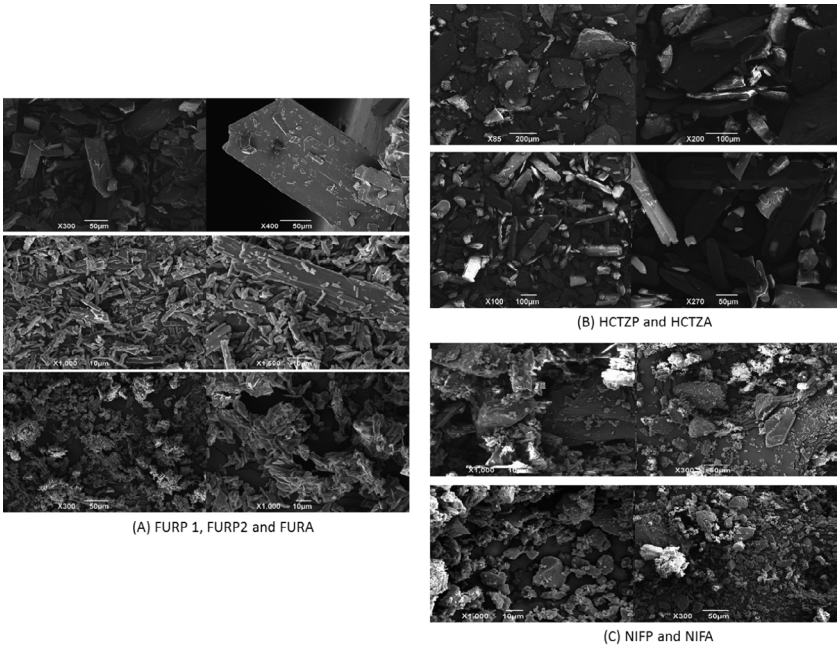

Figure 7. Micrographs obtained by SEM for: (A) furosemide (FURP1, FURP2 and FURA); (B) hydrochlorothiazide (HCTZP and HCTZA) and (C) nifedipine (NIFP and NIFA).

Validation of the analytical method

Table 3 shows analytical validation parameters of the proposed methods for the determination of Furosemide (FUR), Hydrochlorothiazide (HCTZ) and Nifedipine (NIF). No interference from the matrix components occurred. The linear correlation coefficients were adequate (> 0.990), showing acceptable linearity for the methods. The normality test (Shapiro-Wilk) performed in residues presented no statistically significant results (p-value < 0.05). The LOD and LOQ values were obtained for all drugs, in the range of 0.19 to 0.43 and 0.58 to 1.32 μg/mL, respectively. Precision (RSD <10 %) and accuracy (RE between 98.77 to 108.27 %) were adequate.

Table 3. Analytical validation parameters of UV-Vis methods for the determination of furosemide (FUR), hydrochlorothiazide (HCTZ) and nifedipine (NIF).

Parameter	Furosemide (FUR)	Hydrochlorothiazide (HCTZ)	Nifedipine (NIF)
Calibration equation	y= 0.0147x - 0.0272	y= 0.0279x - 0.0259	y= 0.0071x + 0.0067
Linear range, in μg mL^{-1}	5 - 50	5 - 30	2 - 16
r value	0.9997	0.9992	0.9985
Limit of detection (LOD), μg mL^{-1}	0.36	0.19	0.43
Limit of quantification (LOQ), μg mL^{-1}	1.10	0.58	1.32
Precision (%)*	0.16 - 1.21	0.24 - 0.81	2.92 - 4.78
Exatidão (%)*	98.77 - 102.95	98.99 - 108.27	100.03 - 104.25

* Precision and accuracy of the methods were evaluated by calculating relative standard deviation (RSD %) and relative error percentage (RE %), respectively, for six determinations of FUR (5, 25 and 50 μg mL^{-1}), HCTZ (5, 17.5 and 30 μg mL^{-1}), and NIF (2, 10 and 16 μg mL^{-1}) over 2 days, under the same experimental conditions.

Dissolution studies

Physical tests, such as average weight, friability, and disintegration, are essential for drug quality assessment. The evaluation of weight variation allows verifying if solid pharmaceutical forms (tablets and capsules) of the same batch have uniform weight, i. e. homogeneity, but does not provide information about the uniformity of drug content in each form. Disintegration test is used to check if tablets disintegrate within the specified time limit (usually, 30 minutes) when subjected to the action of the specific apparatus under described experimental conditions [28]. Friability is the tendency of a tablet to lose particles of its composition due to abrasion and mechanical shock [55, 56].

Quality control of medicines is essential for the industry and pharmacy compounding. In Brazil, "similar" drug products contain the same active ingredient and has the same concentration, pharmaceutical form, route of administration, posology, and therapeutic indication, and is equivalent to the medicine registered in the federal agency responsible for sanitary surveillance, and may differ only in characteristics related to the size and shape of the product, shelf-life, packaging, labeling, excipients and vehicle, and similar drugs must always be identified by trade name or brand [23]. Pharmacy Compounding Accreditation Board provides a standardized system for evaluating and validating quality-control techniques performed by compounding pharmacies voluntarily [57].

All analyzed drugs (reference, similar, generic, and compounded) presented weight uniformity, friability and disintegration within the limits recommended by the Brazilian and American Pharmacopoeias, satisfactorily fulfilling the physical quality control tests (table 4).

Table 4. Average weight, friability, and disintegration for furosemide (FUR) and hydrochlorothiazide (HCTZ) tablets and nifedipine (NIF) capsules.

Test	Furosemide (FUR)	Hydrochlorothiazide (HCTZ)	Nifedipine (NIF)
Average weight (g)	R (0.119) G (0.198) S (0.182)	R (0.111) G (0.126) S (0.150)	R (0.367) C (0.141)
Friability (%)	R (0.00) G (0.06) S (0.14)	R (0.50) G (0.21) S (0.17)	-
Disintegration (minutes/seconds)	R (23") G (3') S (5'43")	R (1'28") G (30") S (8'53")	R (11'54") C (6'09")

Reference (R); generic (G); similar (S); compounded (C); minutes ('); seconds (").

The disintegration of a drug is a physical phenomenon and is directly influenced by several factors associated with both formulation (excipients, for example, disintegrants) and production parameters (granulation, porosity, and compression force) [58]. The results suggest that the disintegration times of tablets and capsules are closely linked to these factors, since the use of different excipients in the formulations was observed. Compressive force, among other factors related to the powder compression process, is relevant for friability variations in tablets [59]. Lima *et al.* [60] observed that, in addition to compressive strength, moisture content was able to change the frictional resistance of hydrochlorothiazide tablets.

In vitro dissolution testing is an important tool used for development, control, and approval of generic dosage forms and can be used to predict the *in vivo* performance of certain products [61]. These tests show pharmaceutical equivalence (same biopharmaceutical specifications of the test and reference products), which is relevant, given the possibility of interchangeability between drug products [62]. The Brazilian and United States Pharmacopoeias recommend that not less than 80 and 60% of the furosemide (40 mg) and hydrochlorothiazide (25 mg) tablets, label amount must dissolve within 30 minutes. For nifedipine (10 mg) capsules, not less than 80% of the drug label amount must dissolve within 20 minutes.

One of the required pharmaceutical equivalence tests is the comparison of similar and generic drug release profiles to that of a reference drug. Drug dissolution profiles may be distinct due to differences in formulations and manufacturing processes, but the differences must not compromise the bioequivalence of the product [63]. Figure 8 shows the levels of furosemide, hydrochlorothiazide and nifedipine, in the dissolution media as a function of time (minutes).

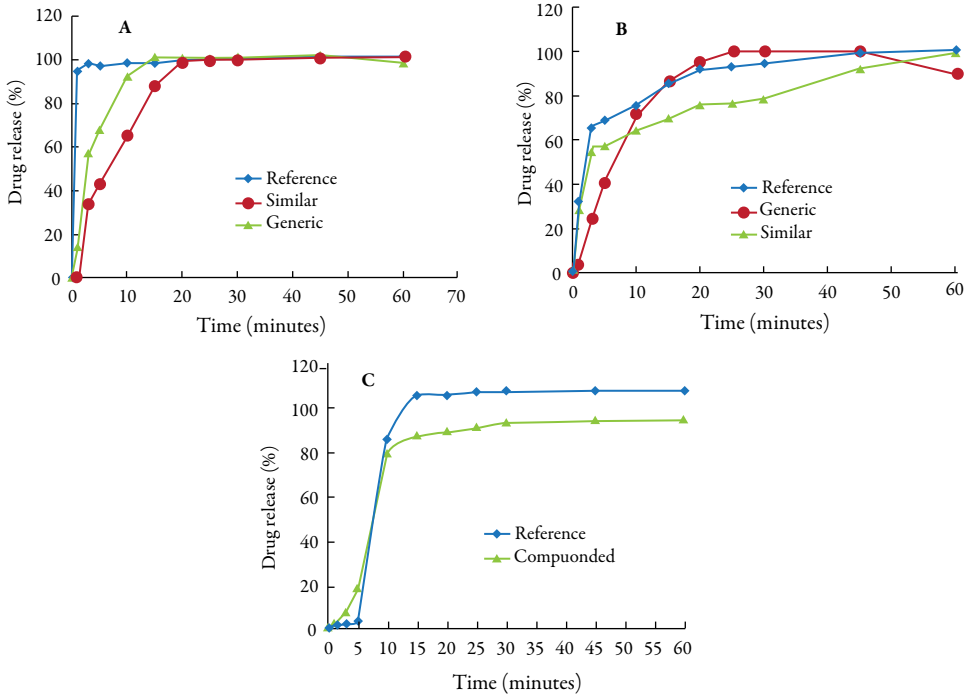

Figure 8. Comparative dissolution profiles: (A) furosemide tablets (40 mg); (B) hydrochlorothiazide tablets (25 mg) and (C) nifedipine capsules (10 mg) (Brazilian and United States Pharmacopoeias recommendations).

For furosemide tablets, dissolution was very fast, i.e. over 85% of the stated amount was obtained within 15 minutes. Therefore, the similarity factor (f2) was not calculated for any drug containing 40 mg furosemide. After 20 minutes of testing, drug concentration stabilization was observed in the dissolution medium (approximately 100% drug release). For hydrochlorothiazide, the similarity factor (f2) was calculated since the similar drug did not release 85% of the drug within 15 minutes [64]. As an established criterion for drugs to be considered pharmaceutical equivalents, f2 must be within the range of 50 to 100. Therefore, it is concluded that the similar drug (f2= 48.74) is not equivalent to the reference drug.

For nifedipine capsules, R and C products showed variations in drug release as a function of time. In the first 10 minutes, there was a similar behavior (release of ≥ 80% of nifedipine stated on product labels) and the similarity factor (f2) was not calculated. After this point, product C released the drug more slowly compared to product R, reaching approximately 94%. This difference may be mainly associated with the difference in excipients and manufacturing technology since the reference capsule had a liquid content in which the drug was already solubilized [65]. These authors evaluated the influence of excipients on nifedipine release, in compounded capsules, and obtained several formulations for the composition of this drug. None of the formulations was able to release the drug adequately, obtaining values below the recommended by the Brazilian Pharmacopoeia. From the pharmacotechnical point of view, it is emphasized that the solvent (Glycerol) present in the R product formulation may have led to an increase in the drug yield rate, playing a fundamental role in the dissolution profile of Nifedipine. In addition, Maria & Santinho [66] highlighted that the exposure time of nifedipine to light can influence the production of compounded drugs. Since this drug is photosensitive, the formation of dihydronifedipine and nitrosodihydronifedipine may occur, which have little or no pharmacological activity.

In order to obtain comparative data between the studied drugs, the dissolution efficiency values were calculated (% DE), as shown in table 5, as a tool for comparing dissolution profiles, from the values obtained from the area under the curve (ASC) of drug dissolution profiles (reference, similar, generic and compounded).

For furosemide tablets (40 mg), the results are in accordance with the literature [26, 67, 68] and suggest that the differences observed in dissolution profiles of products containing 40 mg furosemide may be mainly associated with manufacturing technology (use of excipients, granulation type, compressive strength, etc.) and, moreover, the size and morphology of drug particles. For tablets (reference, similar and generic) containing 25 mg hydrochlorothiazide, the values obtained differed from the literature, where DE ranged from 26.62 to 42.13% [27, 69]. Lee *et al.* [70] suggested that

Table 5. Dissolution efficiency values (% DE) for furosemide (FUR), hydrochlorothiazide (HCTZ) and nifedipine (NIF) within 30 minutes using the trapezoid method.

Furosemide (FUR)	Hydrochlorothiazide (HCTZ)	Nifedipine (NIF)
R (98.00) G (86.30) S (74.30)	R (95.81) G (77.00) S (53.90)	R (61.90) C (59.40)

Reference (R); generic (G); similar (S); compounded (C).

differences between samples in hydrochlorothiazide dissolution profiles (25 mg) are associated with drug properties (low solubility and permeability), granule size, crystal morphology, formulations, and industrial techniques. No data was found in the literature on dissolution efficiency of Nifedipine (10 mg) using similar methods.

Conclusions

Physicochemical characterization by TGA, XDR, FTIR, and SEM analysis for FUR, HCTZ, and NIF (raw materials and pharmaceutical formulations) showed differences and similarities between the medicines of each group studied. In the thermal events related to mass loss, they exhibited a significant difference. No presence of polymorphisms was observed for HCTZ and NIF, while by FTIR and DRX, polymorphs (I and II) were noted for FUR samples. It was also possible to infer about the presence of the organic groups that proved their molecular structures, and considerable differences were found in crystal morphological structures.

FUR and HCTZ tablets exhibited similar dissolution profiles with very rapid release to the pharmaceutical specialties (reference, similar and generic). For HCTZ tablets, the similar drug (f2= 48.74) is not equivalent to the reference drug. NIF capsules (reference and compounded), in 10 minutes, showed a release ≥80% of stated on product labels. The results obtained in this study suggest that the quality parameters and drug dissolution profiles may have been influenced by the morphology and size of the crystals, excipients, and technological processes for obtaining tablets and capsules. In this study, simple, rapid, and efficient UV-Vis methods were developed and validated for determination of raw materials and pharmaceutical formulations containing FUR, HCTZ and NIF.

Acknowledgments

The authors are grateful for the financial support received from Bahia State Research Support Foundation (FAPESB). Coordination for the Improvement of Higher Education Personnel-Brazil (CAPES), Brazilian National Council for Scientific and Technological Development (CNPq), State University of Bahia (UNEB), the Program for Technological Development in Tools for Health PDTIS-FIOCRUZ for use of Electron Microscopy Service; CPqGM facilities and Research Group: Biopharmaceutics and Drugs.

Disclosure statement

The authors declare that there are no conflicts of interest.

References

1. S.S. Anacleto, M.M.C. Borges, H. L. de Oliveira, A. R. Vicente, E. C. de Figueiredo, M.A.L. de Oliveira, B.J.P. Borges, M.A. de Oliveira, W.S. Borges, K.B. Borges, Evaluation of physicochemical properties as supporting information on quality control of raw materials and veterinary pharmaceutical formulations, *J. Pharm. Anal.,* **8**, 168-175 (2018).

2. M. Kesik-Brodacka, Progress in biopharmaceutical development, *Biotechnol. Appl. Biochem.,* **65**, 306-322 (2018).

3. D. Dahlgren, H. Lennernäs, Intestinal permeability and drug absorption: predictive experimental, computational and in vivo approaches, *Pharmaceutics*, **11**, E411 (2019).

4. A.F. Santos Júnior, I.S. Barbosa, V.L. Santos, R.L. Silva, E. Caetite Junior, Test of dissolution and comparison of in vitro dissolution profiles of coated ranitidine tablets marketed in Bahia, Brazil, *Braz. J. Pharm. Sci.*, **50**, 83-89 (2014).

5. M.K. Trivedi, K.K. Sethi, P. Panda, S. Jana, A comprehensive physicochemical, thermal, and spectroscopic characterization of zinc (II) chloride using X-ray diffraction, particle size distribution, differential scanning calorimetry, thermogravimetric analysis/differential thermogravimetric analysis, ultraviolet-visible, and Fourier transform-infrared Spectroscopy, *Int. J. Pharm. Investig.*, **7**, 33-40 (2017).

6. R.S. Leite, R.O. Macedo, S.M. Torres, C.C.N. Batista, L.O. Baltazar, S.A. Lima Neto, F.S. Souza, Evaluation of thermal stability and parameters of dissolution of nifedipine crystals, *J. Therm. Anal. Calorim.*, **111**, 2117-2123 (2013).

7. R.C. Silva, F.S. Semaan, C. Novák, E.T.G. Cavalheiro, Thermal behavior of furosemide, *J. Therm. Anal. Calorim.*, **111**, 1933-1937 (2013).

8. M.A. Oliveira, M.I. Yoshida, E.C.L. Gomes, Thermal analysis applied to pharmaceuticals and pharmaceutical formulations in the pharmaceutical industry, *Quím. Nova*, **34**, 1224-1230 (2011).

9. D. Grooff, M.M. De Villiers, W. Liebenberg, Thermal methods for evaluating polymorphic transitions in nifedipine, *Thermochim. Acta*, **454**, 33-42 (2007).

10. I. Jendrzejewska, P. Zajdel, E. Pietrasik, Z. Barsova, T. Goryczka, Application of X-ray powder diffraction and differential scanning calorimetry for identification of counterfeit drugs, *Monatsh. Chem.*, **149**, 977-985 (2018).

11. S.C. Jagdale, V.N. Jadhav, A.R. Chabukswar, B.S. Kuchekar, Solubility enhancement, physicochemical characterization and formulation of fast-dissolving tablet of nifedipine-betacyclodextrin complexes, *Braz. J. Pharm. Sci.*, **48**, 131-145 (2012).

12. M. Gallignani, R.A. Rondón, J.F. Ovalles, M.R. Brunetto, Transmission FTIR derivative spectroscopy for estimation of furosemide in raw material and tablet dosage form, *Acta Pharm. Sin. B*, **4**, 376-383 (2014).

13. C. Sharma, P.N. Badyal, R.K. Rawal, Simultaneous estimation of hydrochlorothiazide, hydralazine hydrochloride, and reserpine using PCA, NAS, and NAS-PCA, *Sci. Pharm.*, **83**, 599-610 (2015).

14. S.K. Dinakaran, B. Alluria, K.R. Annareddy, V.S. Ayyagari, H. Avasarala, R. Kakaraparthy, P.K. Chintamaneni, R. Gadi, Spectrophotometric method development and validation for atorvastatin calcium and nifedipine HCl in bulk and tablet dosage form using absorption ratio method assay of atorvastatin and nifedipine, *J. Pharm. Res.*, **7**, 666-669 (2013).

15. E. Vaculikova, A. Cernikova, D. Placha, M. Pisarcik, P. Peikertova, K. Dedkova, F. Devinsky, J. Jampilek, Preparation of hydrochlorothiazide nanoparticles for solubility enhancement, *Molecules*, **21**, 1005 (2016).

16. M.H. Shariare, M.A. Altamimi, A.L. Marzan, R. Tabassum, B. Jahan, H.M. Reza, M. Rahman, G.U. Ahsan, M. Kazi, In vitro dissolution and bioavailability study of furosemide nanosuspension prepared using design of experiment (DoE), *Saudi Pharm. J.*, **27**, 96-105 (2019).

17. Y. Tsume, D.M. Mudie, P. Langguth, G.E. Amidon, G.L. Amidon, The biopharmaceutics classification system: subclasses for in vivo predictive dissolution (IPD) methodology and IVIVC, *Eur. J. Pharm. Sci.*, **57**, 152-163 (2014).

18. G.L. Amidon, H. Lennernas, V.P. Shah, J.R. Crison, A theoretical basis for a biopharmaceutic drug classification: the correlation of in vitro drug product dissolution and in vivo bioavailability, *Pharm. Res.*, **12**, 413-420 (1995).

19. R. Ghadi, N. Dand, BCS class IV drugs: highly notorious candidates for formulation development, *J. Control. Release*, **248**, 71-95 (2017).

20. C.C. Chung, Biopharmaceutical innovation system and the influence of policies: the case of Taiwan (2000-2008), *Int. J. Health Policy Manag.*, **1**, 125-130 (2013).

21. J. Cook, W. Addicks, Y.H. Wu, Application of the biopharmaceutical classification system in clinical drug development—an industrial view, *AAPS J.*, **10**, 306-310 (2008).

22. National List of Essential Medicines (RENAME) 2020, Ministry of Health of Brazil, URL: http://portalarquivos2.saude.gov.br/images/pdf/2019/dezembro/24/Rename-2020-final.pdf, accessed December 2019.

23. Brazilian Health Surveillance Agency (ANVISA), *Concepts and definitions of medicines*, Ministry of Health of Brazil, URL: http://portal.anvisa.gov.br/medicamentos/conceitos-e-definicoes, accessed December 2019.

24. C. Barata-Silva, R.A. Hauser-Davis, A.L.O. Silva, J.C. Moreira, Challenges to drug quality control in Brazil, *Cad. Saúde Colet.*, **25**, 362-370 (2017).

25. *Brazilian Pharmacopeia,* 6rd ed., Brazilian Health Surveillance Agency (ANVISA), Brasília, Brazil, 2019.

26. M.S. Ferreira, L.C.M.G. Viana, R.A. Matos, R.R. Sá, F.A.S. Silva, M.D. Mota, E.C.L. Cazedey, H.I.F. Magalhães, A.F. Santos Júnior, Comparative in vitro analysis of dissolution profiles of furosemide tablets marketed in Bahia, Brazil, *Lat. Am. J. Pharm.*, **35**, 2064-2070 (2016).

27. L.C.M.G. Viana, M.S. Ferreira, M.D. Mota, H.I.F. Magalhães, A.F. Santos Júnior, Study of dissolution profiles and disintegration of tablets containing hydrochlorothiazide marketed in Bahia, Brazil, *Lat. Am. J. Pharm.*, **34**, 2010-2015 (2015).

28. *The United States Pharmacopeia*, 41rd ed. (USP 41), United States Pharmacopeial Convention, Rockville, Maryland, USA, 2018.

29. K.A. Khan, The concept of dissolution efficiency, *J. Pharm. Pharmacol.*, **27**, 48-49 (1975).

30. Brazilian Health Surveillance Agency (ANVISA), *Resolution of the Board of Directors* - RDC No. 166., Ministry of Health of Brazil, URL: https://www20.anvisa.gov.br/coifa/pdf/rdc166.pdf, accessed December 2019.

31. International Conference on Harmonization (ICH), *Technical Requirements for Registration of Pharmaceuticals for Human Use - Validation of Analytical Procedures: Text and Methodology Q2(R1)*, URL: https://database.ich.org/sites/default/files/Q2_R1__Guideline.pdf, accessed January 2020.

32. R.A. Saber, A.K. Attia, W.M. Salem, Thermal analysis study of antihypertensive drugs telmisartan and cilazapril, *Adv. Pharm. Bull.*, **4**, 283-287 (2014).

33. L.C.S. Cides, A.A.S. Araújo, M. Santos-Filho, J.R. Matos, Thermal behaviour, compatibility study and decomposition kinetics of glimepiride under isothermal and non-isothermal conditions, *J. Therm. Anal. Calorim.*, **84**, 441-445 (2006).

34. C.M.P. Souza, J.A.B. Santos, A.L. Nascimento, J.V. Chaves Júnior, F.J.L. Ramos Júnior, S.A. Lima Neto, F.S. Souza, R.O. Macedo, Thermal analysis study of solid dispersions hydrochlorothiazide, *J. Therm. Anal. Calorim.*, **131**, 681-689 (2018).

35. R.O. Macedo, T.G. Nascimento, J.W.E. Veras, Comparison of generic hydrochlorothiazide formulations by means of TG and DSC coupled to a photovisual system, *J. Therm. Anal. Calorim.*, **64**, 757-763 (2001).

36. R.O.C. Filho, P.I.B.M. Franco, E.C. Conceição, M.I.G. Leles, Stability studies on nifedipine tablets using thermogravimetry and differential scanning calorimetry, *J. Therm. Anal. Calorim.*, **97**, 343-347 (2009).

37. K. Egusa, F. Okazaki, J. Schiewe, U. Werthmann, M. Wolkenhauer, Identification of polymorphic forms of active pharmaceutical ingredient in low-concentration dry powder formulations by synchrotron X-Ray powder diffraction, *Drugs R D.*, **17**, 413-418 (2017).

38. S. Shin, J. Kim, Physicochemical characterization of solid dispersion of furosemide with TPGS, *Int. J. Pharm.*, **251**, 79-84 (2003).

39. C. Garnero, A.K. Chattah, M. Longhi, Stability of furosemide polymorphs and the effects of complex formation with β-cyclodextrin and maltodextrin, *Carbohyd. Polym.*, **152**, 598-604 (2016).

40. C. Garnero, A.K. Chattah, M. Longhi, Supramolecular complexes of maltodextrin and furosemide polymorphs: a new approach for delivery systems, *Carbohyd. Polym.*, **94**, 292-300 (2013).

41. M.M. Villiers, J.G. Watt, A.P. Lötter, Kinetic study of the solid-state photolytic degradation of two polymorphic forms of Furosemide, *Int. J. Pharm.*, **88**, 275-283 (1992).

42. Y. Matsuda, E. Tatsumi, Physicochemical characterization of furosemide modifications, *Int. J. Pharm.*, **60**, 11-26 (1990).

43. S.A. El-Gizawy, M.A. Osman, M.F. Arafa, G.M. El Maghraby, Aerosil as a novel co-crystal co-former for improving the dissolution rate of Hydrochlorothiazide, *Int. J. Pharm.*, **478**, 773-778 (2015).

44. J.M. Aceves-Hernández, E. Agacino-Valdés, M. Paz, J. Hinojosa-Torres, Experimental and theoretical study of the conformational analysis of Hydrochlorothiazide, *J. Mol. Struct.*, **786**, 1-8 (2006).

45. N.T. Chinh, N.T.T. Trang, N.V. Giang, D.T.M. Thanh, T.T.X. Hang, N.Q. Tung, C.Q. Truyen, P.M. Quan, P.Q. Long, T. Hoang, *In vitro* nifedipine release from poly(lactic acid)/chitosan nanoparticles loaded with nifedipine, *J. Appl. Polym. Sci.*, **133**, 43330 (2016).

46. M.E. Brown, B.D. Glass, M.S. Worthington, Binary systems of nifedipine and various cyclodextrins in the solid state. Thermal, FTIR, XRD studies, *J. Therm. Anal. Calorim.*, **68**, 631-646 (2002).

47. M. Gallignani, R.A. Rondón, J.F. Ovalles, M.R. Brunetto, Transmission FTIR derivative spectroscopy for estimation of furosemide in raw material and tablet dosage form, *Acta Pharm. Sin. B*, **4**, 376-383 (2014).

48. A.A. Bunaciu, H.Y. Aboul-Enein, S. Fleschin, Application of Fourier transform infrared spectrophotometry in pharmaceutical drugs analysis, *Appl. Spectrosc. Rev.*, **45**, 206-219 (2010).

49. C. Doherty, P. York, Fresemide crystal forms; solid state and physicochemical analyses, *Int. J. Pharm.*, **47**, 141-155 (1988).

50. R.N. Sonpal, P.K. Shelat, A.N. Lalwani, Solubility enhancement of hydrochlorothiazide using a novel drug-drug solid dispersion technology, *Int. J. Pharm. Sci. Nanotech.*, **8**, 2924-2936 (2015).

51. R. Razzaq, N.M. Ranjha, Z. Rashid, B. Nasir, Preparation, and evaluation of novel pH-sensitive poly(butyl acrylate-co-itaconic acid) hydrogel microspheres for controlled drug delivery, *Adv. Polym. Tech.*, **37**, 21663 (2018).

52. R.G. Ricarte, T.P. Lodge, M.A. Hillmyer, Detection of pharmaceutical drug crystallites in solid dispersions by transmission electron microscopy, *Mol. Pharmaceutics*, **12**, 983-990 (2015).

53. A. Mantas, A.T. Mihranyan, Immediate-release nifedipine binary dry powder mixtures with nanocellulose featuring enhanced solubility and dissolution rate, *Pharmaceutics*, **11**, E37 (2019).

54. M.H. Sadr, H. Nabipour, Preparation and identification of furosemide nanoparticles, *J. Basic Appl. Sci. Res.*, **3**, 666-670 (2013).

55. F. Osei-Yeboah, C.C. Sun, Validation and applications of an expedited tablet friability method, *Int. J. Pharm.*, **484**, 146-155 (2015).

56. S. Paul, C.C. Sun, The suitability of common compressibility equations for characterizing plasticity of diverse powders, *Int. J. Pharm.*, **532**, 124-130 (2017).

57. A. Pignato, C.R. Birnie, Analysis of compounded pharmaceutical products to teach the importance of quality in an applied pharmaceutics laboratory course, *Am. J. Pharm. Educ.*, **78**, 61 (2014).

58. A.D. Rajkumar, G.K. Reynolds, D. Wilson, S. Wren, M.J. Hounslow, A.D. Salman, Investigating the effect of processing parameters on pharmaceutical tablet disintegration using a real-time particle imaging approach, *Eur. J. Pharm. Biopharm.*, **106**, 88-96 (2016).

59. L.A.L. Soares, P.C. Schmidt, G.G. Ortega, P.R. Petrovick, Effect of compression strength and speed on the properties of tablets containing high concentration of dry plant extract, *Acta Farm. Bonaerense*, **22**, 147-154 (2003).

60. A.C. Lima, D.C. Michelin, M.R.C. Santos, M.O. Paganelli, R.F. Ignácio, M.V. Chaud, Compression force and humidity on hydrochlorothiazide dissolution profile, *Acta Farm. Bonaerense*, **25**, 104-107 (2006).

61. O. Anand, L.X. Yu, D.P. Conner, B.M. Davit, Dissolution testing for generic drugs: an FDA perspective, *AAPS J.*, **13**, 328-335 (2011).

62. D. Rumel, S.A. Nishioka, A.A.M. Santos, Drug interchangeability: clinical approach and consumer's point of view, *Rev. Saude Publica*, 40, 921-927 (2006).

63. J. Menegola, M. Steppe, E.E.S. Schapoval, Dissolution test for citalopram in tablets and comparison of in vitro dissolution profiles, *Eur. J. Pharm. Biopharm*., 67, 524-530 (2007).

64. Brazilian Health Surveillance Agency (ANVISA), *Resolution of the Board of Directors (RDC) N.° 31*, Ministry of Health of Brazil, URL: http://portal.anvisa.gov.br/documents/33880/2568070/res0031_11_08_2010.pdf/5e157d15-d3d5-4bb9-98db-5667e4d9e0c8, accessed December 2019.

65. K.J. Souza, P.V. Aléssio, A.J.P.S. Gomes, Specific excipient development for prepared nifedipine capsules masterfully: part I, *Rev. Cienc. Farm. Básica Apl.*, **30**, 257-261 (2009).

66. E.K. De Maria, A.J.P.S. Gomes, Nifedipine manipulated or pharmaceutical specialty? *In vitro* study, *Rev. Eletronica Farm.*, **5**, 31-36 (2008).

67. G.S. Silveira, L.D. Silva, V.C.F. Mosqueira, J. Souza, Biopharmaceutical evaluation of reference, generic, similar and magisterial medicines containing furosemide, one lower solubility and lower permeability drug, *Rev. Bras. Farm.*, **92**, 306-313 (2011).

68. M.A. Lamolha, A.C.P. Rodrigues, B.C. Silva, F.C. Granata, G.S. Podavin, J.C.O. Lima, Evaluation of pharmaceutical equivalence of furosemide 40mg tablets, *Rev. Bras. Farm.*, **93**, 17-21 (2012).

69. F. Mahle, F. Goelzer, J. Adriano, M. Felippe, N. Vier, R.B.G. Carli, T. Rosa, A.G. Couto, R.M. Lucinda-Silva, Evaluation of the tablet dissolution profile of hydrochlorothiazide marketed in Brazil, *Rev. Cienc. Farm. Basica Apl.*, **28**, 265-271 (2007).

70. M.S. Lee, C.L. Huang, S.H. Huang, Y.P. Chen, C.J. Chen, K.C. Wen, A comparative study on the dissolution profiles of commercial hydrochlorothiazide tablets, *J. Food Drug. Anal.*, **10**, 18-24 (2002).

How to cite this article

M.S. Ferreira, G.A.C. Teles Júnior, C.M.R. Carvalho Júnior, F.S. Dias, W.S.D. Santos Júnior, M.O.G. Souza, A.F. Santos Júnior, Evaluation of physicochemical properties and dissolution studies on quality control of low water solubility drugs (raw materials and pharmaceutical formulations), *Rev. Colomb. Cienc. Quím. Farm.*, **49**(2), 329-354 (2020).

Artigo de pesquisa tecnológica / *http://dx.doi.org/10.15446/rcciquifa.v49n2.89507*

Determinação espectrofotométrica de Cobre(II) em aguardente de mandioca (Tiquira)

Rayone Wesly Santos de Oliveira[1]*, Paulo Roberto Barros Gomes[2], Joelkson Diniz Ribeiro[1], Jonas Batista Reis[1], Maria Alves Fontenele[3], Gustavo Oliveira Everton[2], Wellington da Silva Lyra[4], Hilton Costa Louzeiro[5], Maria do Livramento de Paula[6], Victor Elias Mouchrek Filho[1]

[1]Laboratório de Pesquisa em Óleo Essenciais, Universidade Federal do Maranhão, São Luís, Maranhão, Brasil.

[2]Diretoria de Ensino, Instituto Federal de Educação Ciência e Tecnologia do Pará, Campus Paragominas, Pará, Brasil.

[3]Laboratório de Cereais, Universidade Federal do Maranhão, Campus Avançado, Imperatriz, Maranhão, Brasil.

[4]Universidade Federal da Paraíba,Campus João Pessoa, João Pessoa, Paraíba, Brasil.

[5]Coordenação de Licenciatura em Ciências Naturais, Universidade Federal do Maranhão, Campus Pinheiro, Pinheiro, Maranhão, Brasil.

[6]Departamento de Farmácia, Universidade Federal do Maranhão, São Luís, Maranhão, Brasil.

*Autor para correspondência: Correio eletrônico: rayone_santos@yahoo.com.br

Recebido: 29 ade abril de 2019

Revisado: 27 de abril de 2020

Aceto: 28 de abril de 2020

Resumo

A pesquisa descreve a reação espectrofotométrica do complexo Cu(II)–PAN (1-(2-piridilazo)-2-naftol) e determina a concentração de cobre (II) em aguardente de mandioca (Tiquira). Para isso, dimensionamos a reação para os estudos de absorção do complexo, pH, estabilidade, proporção estequiométrica, interferentes, correlação e recuperação. Após essa etapa, determinamos a concentração de cobre(II) em cinco amostras de bebidas destiladas artesanalmente de cinco municípios do Estado do Maranhão. O resultados mostram que o complexo absorve em 548 nm em pH 6, é estável em um tempo de 7 horas em proporções estequiométrica mínima de 1:1 do ligante e metal, possui limite de detecção em $3{,}3 \times 10^{-2}$ mg L^{-1}, faixa de linearidade de 1×10^{-6} a 1×10^{-5} mol L^{-1}, correlação (R^2= 0,9990), desvio padrão=0,0035 e recuperação em 104,54 ± 7,01 e os principais íons interferentes são o ferro (III) e o cobalto (II). Na aguardente, constatamos que o teor de cobre está acima do permitido pela legislação brasileira.

Palavras-chave: Espectrofotometria de absorção molecular UV, cobre(II), aguardente de mandioca, (1-(2-piridilazo)-2-naftol).

Summary

Spectrophotometric determination of Copper (II) in manioc spirit (Tiquira)

The search describes the spectrophotometric reaction of the Cu (II)-PAN (1-(2-pyridilazo) -2-naphthol) complex and determines the concentration of copper (II) in manioc spirit (Tiquira). For this, we dimensioned the reaction for the studies of complex absorption, pH, stability, stoichiometric ratio, interferences, correlation, and recovery. After this step, we determined the concentration of copper (II) in five samples of beverages distilled artisanal from five municipalities of the State of Maranhão. The results show that the complex absorbs at 548 nm at pH 6, is stable at a time of 7 hours in minimum 1:1 stoichiometric proportions of the binder and metal, has a detection limit in 3.3×10^{-2} mg L^{-1}, range ($R^2 = 0.9990$), standard deviation= 0.0035 and recovery at 104.54 ± 7.0, and the main interfering ions are iron (III) and cobalt (II). In the brandy, we find that the copper content is above that allowed by Brazilian legislation.

Key words: UV molecular absorption spectrophotometry, copper (II), cassava liquor, (1-(2-pyridylazo)-2-naphthol).

Introdução

Os diferentes tipos de aguardentes produzidos no mundo (bebidas alcoólicas destiladas) são obtidos a partir de matérias-primas ricas em carboidratos. No Brasil, destaca-se a aguardente obtida do destilado alcoólico simples de cana-de-açúcar ou pela destilação de mosto fermentado de cana ou a obtida da mandioca (*Manihot esculenta* Crantz). A primeira é mais conhecida como cachaça, sendo a segunda, comum no Maranhão, conhecida como Tiquira. Independentemente da aguardente, todas deverão atingir graduação alcoólica entre 38º GL e 54º GL, estando, dessa forma, de acordo com a legislação brasileira [1, 2].

O processo de obtenção da Tiquira envolve quatro etapas. A primeira consiste na lavagem, descasco, ralação e prensamento da mandioca para eliminar parte da umidade (cerca de 50%). Na segunda, a massa é esfarelada e distribuída em chapas metálicas aquecidas a lenha para obtenção dos beijus que até então, são guardados à sombra em local quente e úmido em tanques de madeira (coxos) cobertos com água, forrado com folhas de bananeira e/ou palmeira, onde permanecem até o crescimento dos fungos originários da flora microbiana natural. Na terceira, os beijus são macerados e recolocados

no coxo para fermentar em um período médio de quatro a seis dias [1]. Na quarta e última etapa, ocorre a destilação, que é puramente artesanal, onde o destilado é condicionado em alambique de cobre e este é submetido ao aquecimento direto que deve ser controlado para evitar a formação de produtos pirogenados e o sabor de "queimado".

Embora a Tiquira possua um cheiro característico, cujo aroma é formado pela mistura de vários álcoois, ácidos carboxílicos, ésteres, aldeídos e aminas, além de íon amônio [3, 4], esta bebida precisa atender a legislação para certificação de sua qualidade quanto ao risco de contaminação por cobre. A legislação brasileira e a Americana determinam que a concentração desse metal em bebidas destiladas sejam no máximo, respectivamente, 5 e 2 mg L^{-1} [2, 5]. Nesse caso, para manter o controle de qualidade, a AOAC (Association of Official Analytical Chemists) recomenda o método espectrométrico de absorção atômica em chamas [6]. No entanto, o uso desse método é limitado e com isso outros métodos foram desenvolvidos a fim de determinar esse metal nessas bebidas.

Assim, dentre os métodos que já foram utilizados para essa finalidade estão: espectrometria de absorção atômica sequencial rápida [7], espectrometria de absorção atômica de forno grafite [8], potenciometria [9] e absorção molecular UV vis, sendo este último utilizando o reagente biquinolina [10]. No entanto, na maioria dos métodos ou das reações utilizados possuem desvantagens, devido ao custo elevado dos equipamentos, o uso de grande quantidade de solvente, reagente e o tratamento prévio das amostras. Isso de alguma forma contraria os preceitos da química verde [11]. Portanto, diante dessas situações, esse estudo descreve as características da reação de complexação do cobre(II) com o reagente 1-(2-piridilazo)-2-naftol (PAN) e determina a concentração desse metal em aguardente de mandioca (Tiquira) por espectrofotometria de absorção molecular UV Vis.

Metodologia

Espectrofotômetro e acessórios

As medidas espectrofotométricas foram conduzidas em um espectrofotômetro UV-Vis modelo HP8452A, equipado com monitor HP, modelo 386116 e impressora HP modelo 500.

Solução de 1-(2-piridilazo)-2-naftol (PAN)

Devido à baixa solubilidade do reagente PAN em água, ele foi dissolvido em uma solução alcoólica (50%) para obtenção de uma solução com concentração 1×10^{-3} mol L^{-1}. Em seguida, a solução foi em estocada em frascos de polietileno e conservamos a temperatura de 15 °C.

Soluções tampão

A solução tampão acetato de sódio/ácido acético foi preparada a partir de uma solução estoque de CH_3COONa de concentração 2 mol L^{-1} e outra solução de CH_3COOH 2 mol L^{-1}. Para o estudo do efeito da variação do pH no complexo Cu(II)-PAN, os valores de pH foram variados com misturas dessas duas soluções até pH= 6,0. Já no estudo da variação do pH na faixa alcalina usou-se solução tampão de NH_4Cl/NH_4OH (cloreto de amônio/hidróxido de amônio), preparada a partir de misturas previamente calculadas das suas soluções padrão de 2 mol L^{-1}.

Soluções dos metais

Preparou-se as soluções estoque de Ni(II), Fe(III), Cd(II), Co(III), Pb(II) e Zn(II), com concentração de 1×10^{-2} mol L^{-1} e Cu(II) com concentração de 1×10^{-3} mol L^{-1}. Efetuou-se diluições em tampão CH_3COONa/CH_3COOH (acetato de sódio/ácido acético), pH 6,0 com força iônica ajustada para 0,2 mol L^{-1}. Para evitar a degradação, as soluções estoque foram acondicionadas e mantidas a temperatura de 15 °C para posterior preparo das soluções.

Coleta das amostras

As diversas amostras de Tiquira foram selecionadas dos principais municípios maranhenses produtores dessa aguardente. Todas são originadas de fabricantes que obtém o seu produto de forma artesanal. Coletou-se cinco amostras oriundas do município de São Domingo, Cabeceira da Cruz, Anapurus, Brejo e Santa Quitéria, no período de maio a junho de 2002. Observamos a localização dos principais municípios produtores de Tiquira na figura 1.

Observa-se na tabela 1 as informações referentes à coleta das amostras e o respectivo teor alcoólico. As amostras foram coletadas de acordo com descrições da técnica de coleta para aguardentes [12]. Posteriormente foram estocadas a temperatura ambiente, após acidificação com ácido nítrico e de acordo com as recomendações para análise de traços metálicos [13].

Tabela 1. Dados das coletas de Tiquira.

Local de coleta	Amostra	Teor alcoólico (°GL)
Nina Rodrigues	01	51
Santana do Maranhão	02	53
Brejo	03	54
Anapurus	04	53
Santa Quitéria do Maranhão	05	51

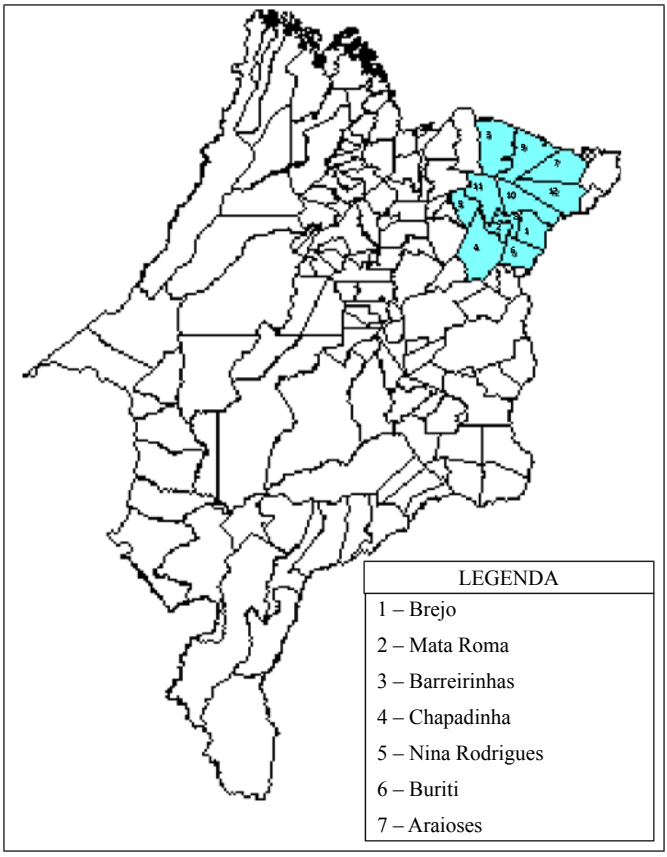

Figura 1. Localização dos principais municípios produtores de Tiquira.

Digestão das amostras

A digestão de cada amostra foi realizada em ácido nítrico e ácido perclórico na proporção de 2:1, respectivamente. Neste procedimento, retirou-se uma alíquota de 100 mL da amostra e transferiu-se para um balão de destilação com capacidade de 250 mL contendo esferas de vidro. Em seguida, adicionou-se 200 μL de ácido nítrico concentrado e colocamos para destilar durante 30 minutos em sistema fechado (refluxo). Transcorrido esse tempo, desconectou-se o balão do condensador e até a temperatura baixar, quando então adicionou-se mais 100 μL do ácido nítrico e 150 μL do ácido perclórico concentrado e colocando novamente para refluxo por mais 30 minutos. Após essa etapa, desconectou apenas o condensador deixando que o conteúdo do balão reduzisse a cerca de 5% do volume da amostra, quando então adicionou-se 30 mL de água deionizada e colocando novamente para evaporar. Seguido esse passo, o material foi resfriado e transferido, quantitativamente, para um balão volumétrico de

100 mL, aferindo-se logo em seguida. As amostras digeridas foram guardadas em frascos de polietileno (125 mL de capacidade), previamente rotulados, e conservadas em geladeira para posterior análise.

Análise estatística

A avaliação estatística do conjunto de dados encontrados nas análises para quantificação de Cu(II), foi utilizado a análise estatística convencional envolvendo a média aritmética (x), desvio padrão (SD), desvio padrão relativo (SD%) e o coeficiente de probabilidade a 95%.

Resultados e discussão

Caracterização espectrofotométrica do sistema Cu(II)-PAN

As bandas de absorção do íon Cobre (Cu^{+2}), o ligante PAN e do complexo Cu(II) -PAN divergem. O íon cobre(II) absorve em 240 nm, a solução do ligante PAN, de cor vermelha, em 474 nm e o complexo Cu(II)-PAN, de cor rosa, em 548 nm (figura 2).

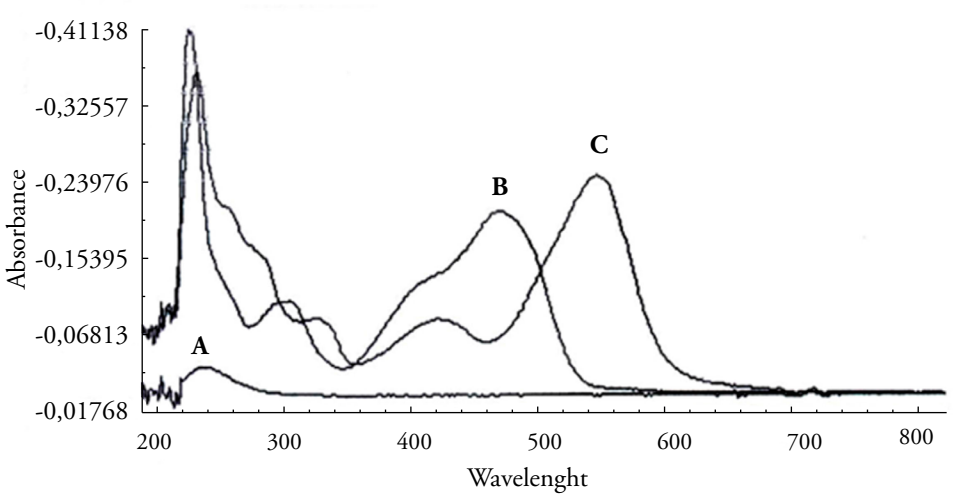

Figura 2. Sobreposição das bandas de absorção. (A) Cu^{+2} - 1,0 mol L^{-1}, (B) reagente PAN - 1,0 mol L^{-1} e (C) Complexo Cu(II) - PAN - 1,0 mol L^{-1}.

Efeito do pH

As absorbâncias da solução do complexo Cu(II)-PAN (metal e ligante, ambos 1,0 × 10^{-5} mol L^{-1}) possuem variações na faixa de pH. Observa-se a maior absorção em pH 6, que foi no tampão NaAc/HAc (pH 3,5 a 6,0). No entanto, valores de pH acima

(NH4Cl/NH4OH - 7,5 a 9,0) e abaixo desse valor, respectivamente, reduzem a absorbância desse complexo (figura 3).

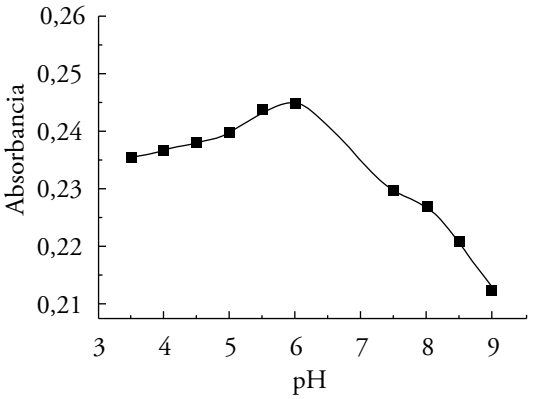

Figura 3. Efeito do pH sobre a absorção da solução do complexo Cu(II)-PAN 1,0 × 10^{-5} mol L^{-1} em tampão NaAc/HAc (faixa de 3,5 a 6,0) e tampão NH_4Cl/NH_4OH (faixa de 7,5 a 9,0), ambos em intervalos de pH de 0,5 unidades.

Efeito da concentração do metal (Cu^{+2}) e do ligante

Pode-se observar o efeito da concentração do metal e do ligante a partir do método univariado. Variou-se a concentração do metal de 2,0 × 10^{-6} a 1,4 × 10^{-5} mol L^{-1} em tampão NaAc/HAc (pH 6,0), enquanto manteve-se constante a concentração do ligante em 1 × 10^{-5} mol L^{-1}. À medida que aumenta a concentração do metal, verifica um aumento na absorbância do complexo formado (figura 4 (B)) até a proporção de 1:1. Quando as concentrações do ligante e metal se igualaram, houve uma sobreposição ponto a ponto da concentração de Cu^{+2} igual a 1,4 × 10^{-5} mol L^{-1}, sobre a anterior (1,2 × 10^{-5} mol L^{-1}). Além disso, observa-se a presença do ponto isosbéstico (@500 nm), caracterizando que o sistema é constituído por dois cromóforos interconvertíveis e que há um equilíbrio entre as duas formas, ligante e complexo [14].

Na figura 5, apresentamos os espectros obtidos em tampão NaAc/HAc, pH 6,0, quando manteve a concentração do metal constante em 1 × 10^{-5} mol L^{-1} e variou-se a concentração do ligante de 1 × 10^{-6} a 1,10^{-5} mol L^{-1}, é visto um aumento na absorvência à medida que aumentávamos a concentração do ligante.

Na figura 6, observamos a saturação de bandas do ligante a partir da concentração 2 × 10^{-5} mol L^{-1}. Para a ocorrência é necessário manter fixo a concentração do metal em 1,10^{-5} mol L^{-1} e variar a concentração do ligante de 1 × 10^{-6} a 4 × 10^{-5} mol L^{-1}. Portanto, a banda mais viável é aquela no qual a concentração do PAN é 1 × 10^{-5} mol L^{-1}, uma vez que em concentrações superiores estão há saturação e consequentemente mascaramento.

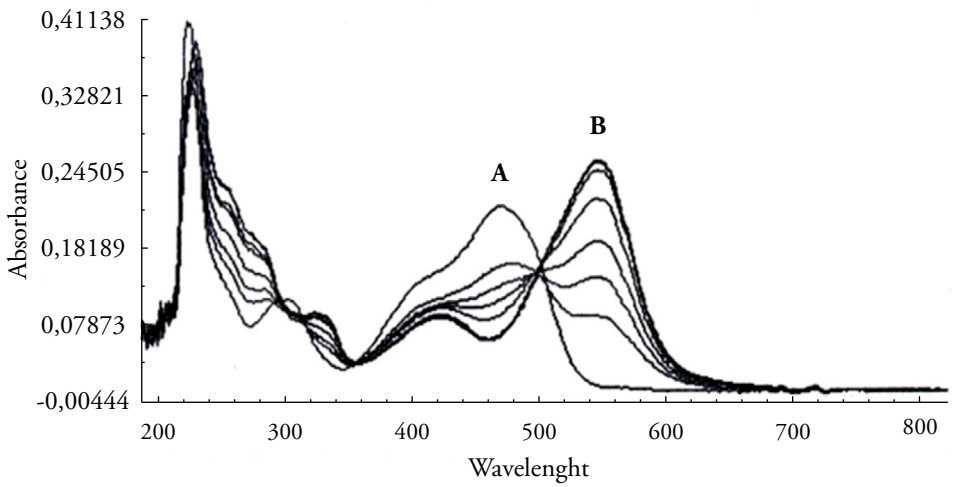

Figura 4. Espectros de absorção: Ligante PAN (A); complexo Cu(II)-PAN (B), mantendo-se constante a concentração do ligante em 1×10^{-5} mol L^{-1} e variando-se a concentração do metal (2×10^{-6} a $1{,}4 \times 10^{-5}$ mol L^{-1}), em tampão NaAc/HAc, pH 6,0.

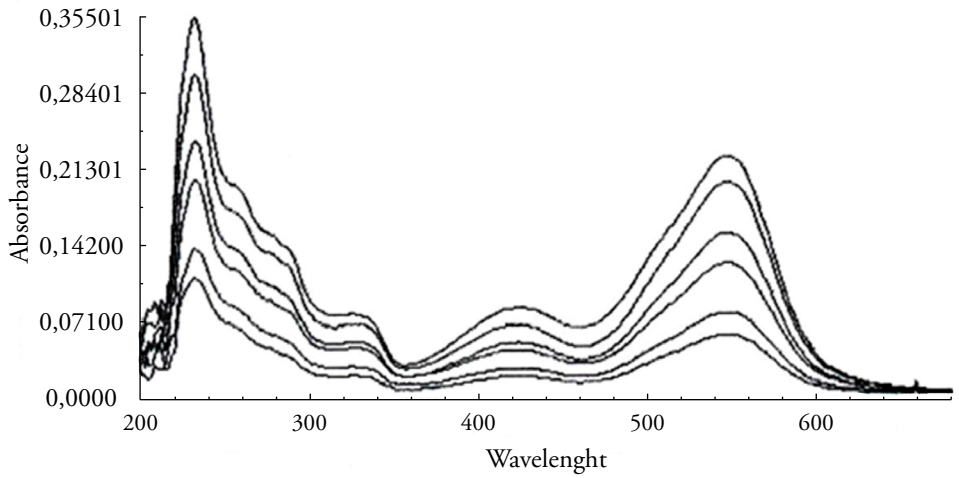

Figura 5. Espectros de absorção do complexo Cu(II)-PAN obtidos mantendo-se constante a concentração do metal em 1×10^{-5} mol L^{-1} e variando-se a concentração do ligante em 1×10^{-6} a 1×10^{-5} mol L^{-1}, em tampão NaAc/HAc, pH 6,0.

Efeito do tempo

O sucesso de um método analítico onde há formação de complexo está no tempo necessário para sua formação e na estabilidade em função do tempo. Para o sistema em estudo, observamos que a formação do complexo Cu(II)-PAN é instantânea, após a

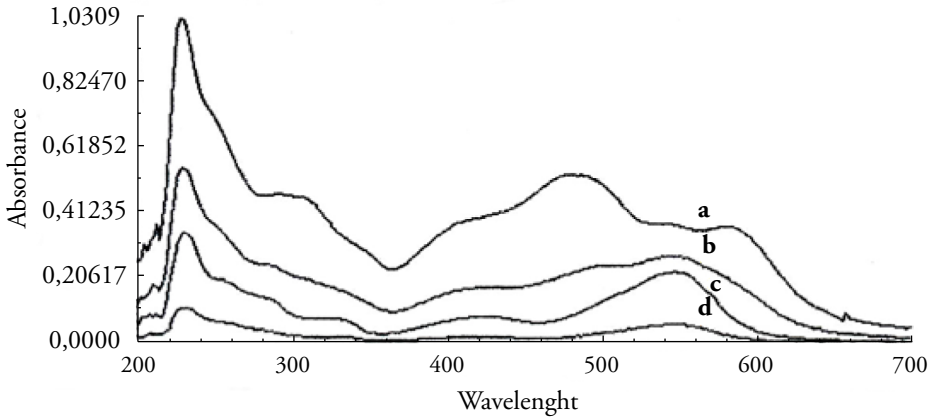

Figura 6. Bandas de Aborção do Complexo Cu(II)-PAN em diferentes concentrações do ligante PAN. (a) 4 × 10^{-5} mol L^{-1}; (b) 2 × 10^{-5} mol L^{-1}; (c) 1 × 10^{-5} mol L^{-1} e (d) 1 × 10^{-6} mol L^{-1}.

mistura das soluções de Cu(II) e PAN, ambos na concentração de 1,0 × 10^{-5} mol L^{-1} em tampão NaAc/HAc e pH 6,0. Contudo, ao realizarmos o estudo da estabilidade desse composto em um tempo de 420 minutos (7 horas), observa-se que este é estável (figura 7). Portanto, o composto não sofre degradação ao longo do tempo.

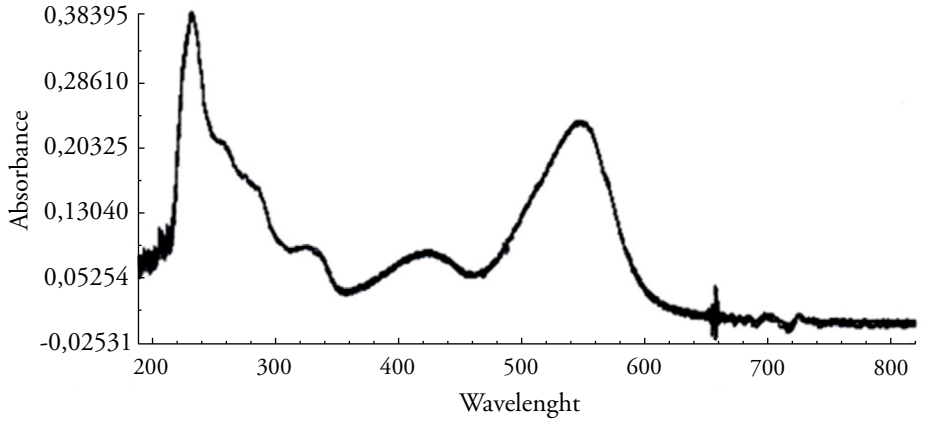

Figura 7. Estabilidade do complexo Cu(II)-PAN em função do tempo. [Cu(II)]= 1 × 10^{-5} mol L^{-1}; [PAN]= 1 × 10^{-5} mol L^{-1}; tampão NaAc/HAc, pH 6,0; tempo: 0 a 7 h.

Proporção estequiométrica

A quantidade estequiométrica do metal e do ligante na formação do complexo Cu(II)-PAN pelo método da Razão Molar foram avaliadas. O método consiste na relação entre a absorbância de uma série de soluções do complexo e a razão molar (R) entre a con-

centração do ligante (L) e a do metal (M) [15]. Tais medidas são obtidas mantendo-se a concentração do metal constante em 1×10^{-5} mol L^{-1} e variando-se a concentração do ligante.

Na figura 8, apresentamos os dados experimentais referentes à aplicação do método da Razão Molar ao sistema Cu(II)-PAN. Os resultados mostram que a razão estequiométrica para o sistema Cu(II)-PAN na formação do complexo é 1:1. Esse valor foi determinado após o rebatimento do ponto de extrapolação das tangentes, passando pelo ponto a partir do qual a curva muda de inclinação, até o eixo da razão molar. Tal proporção encontra-se dentro do esperado para metais de transição, embora o PAN seja um ligante tridentado [16, 17].

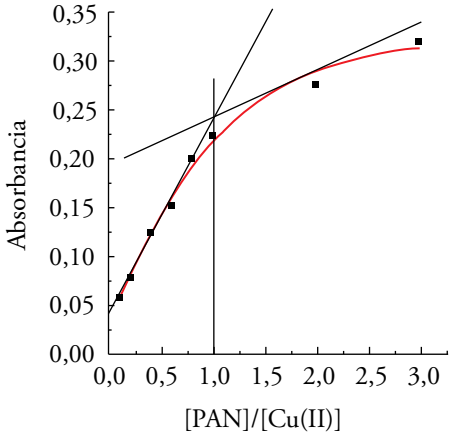

Figura 8. Curva da razão molar do complexo Cu(II)-PAN, concentração do metal constante em 1×10^{-5} mol L^{-1} e do ligante variando de 1×10^{-6} a 4×10^{-5} mol L^{-1} em tampão NaAc/HAc, pH 6,0, volume final 10 mL.

Estudo da interferência de cátions metálicos

O estudo da influência de íons no sinal analítico é de importância relevante em química analítica e é dirigido muito em função da matriz à qual o procedimento é aplicado. No presente trabalho o procedimento proposto e otimizado foi avaliado na determinação de cobre em solução padrão. A interferência foi avaliada para os íons metálicos possivelmente presentes na matriz estudada (Tiquira), podendo ser proveniente de fontes tais como: adubos químicos, processamento, armazenamento e água utilizada no processo [18]. A possível interferência pode ser devido à facilidade de formarem complexos com o PAN [17, 19], competindo desta forma com o íon Cu(II) no processo de complexação [20]. Os íons metálicos escolhidos no estudo da interferência foram: Cd(II), Co(III), Ni(II), Pb(II), Fe(III) e Zn(II) e os resultados são apresentados na tabela 2.

Tabela 2. Efeito da presença de outros cátions metálicos na resposta espectrofotométrica do Cu(II) em tampão acetato/ácido acético, pH 6,0 e concentração de Cu(II) 1×10^{-5} mol L^{-1}.

ÍON	C_M / $C_{CU(II)}$	SINAL
Co(III)	<10 ≥10	n.i i
Zn(II)	≤100	n.i.
Ni(II)	≤100	n.i.
Fe(III)	<100 ≥100	n.i. i.
Cd(II)	≤100	n.i.
Pb(II)	≤100	n.i.

C_M / $C_{cu(II)}$= concentração do metal/concentração do íon cobre; n.i.= não interfere; i.= interfere.

Avaliamos a interferência a partir da sobreposição dos espectros obtidos dos íons em diferentes concentrações com a do complexo Cu(II)-PAN (oriundo da mistura estequiométrica de metal e ligante, ambos $1 \prime 10^{-5}$ mol L^{-1}). Os estudos foram conduzidos adicionando-se soluções padrão dos íons metálicos escolhidos à solução de Cu(II). Em seguida, o ligante era adicionado [21]. Observamos que a presença dos íons Zn(II), Ni(II), Cd(II) e Pb(II) não interferiram significativamente no sinal analítico até uma concentração de 100 vezes maior que a concentração do íon Cu(II) em tampão NaAc/HAc, pH 6,0. Já o íon Fe(III) interferiu em uma concentração 100 vezes maior que a de Cu(II) de modo a mascarar a banda do complexo Cu(II)-PAN, enquanto que o íon Co (III) interferiu em uma concentração de 10 vezes maior que a concentração do íon Cu(II), diminuindo a banda de absorção do complexo Cu(II)-PAN.

Curva analítica

A curva analítica foi obtida através da plotagem da absorbância lida em relação à concentração de Cu(II). Dessa forma, os resultados desse são: faixa de linearidade de $1 \prime 10^{-6}$ a $1 \prime 10^{-5}$ mol L^{-1}, coeficiente de correlação $(R)^{2=}$ 0,9990 e desvio padrão= 0,0035.

Avaliação estatística do procedimento analítico proposto

A credibilidade e desempenho de um método ou procedimento analítico dependem, em grande parte, da avaliação estatística dos resultados obtidos nas análises, tendo-se como parâmetros a exatidão (recuperação), precisão (reprodutibilidade) e os limites de detecção [22].

A avaliação da exatidão foi baseada nas medidas de recuperação do cobre em amostras contendo concentrações variadas e conhecidas do analito [23]. Dessa forma, para o estudo da recuperação de Cu(II) utilizamos o método de adição padrão (tabela 3), onde a amostra utilizada teve o teor de Cu(II) previamente determinado por Espectrofotometria de Absorção Atômica.

Tabela 3. Avaliação estatística de recuperação de Cu(II) (método de adição padrão) para 95 % de probabilidade em tampão NaAc/HAc pH 6,0.

N.°	Cu(II) adicionado (mol L^{-1})	Cu(II) recuperado (mol L^{-1})	Recuperação (%)	Erro absoluto (mol L^{-1})	Erro relativo (%)	Fator de correlação (r)
1	$2{,}00 \times 10^{-6}$	$2{,}15 \times 10^{-6}$	107,50	$0{,}15 \times 10^{-6}$	7,50	0,9995
2	$1{,}50 \times 10^{-6}$	$1{,}59 \times 10^{-6}$	106,00	$0{,}09 \times 10^{-6}$	6,00	0,9986
3	$2{,}50 \times 10^{-6}$	$2{,}45 \times 10^{-6}$	98,00	$0{,}05 \times 10^{-6}$	2,00	0,9997
4	$1{,}50 \times 10^{-6}$	$1{,}60 \times 10^{-6}$	106,67	$0{,}10 \times 10^{-6}$	6,67	0,9952
$\overline{x}$			104,54 ± 7,01			
S			4,41			
S (%)			4,22			

$\overline{x}$ = média com desvio padrão; S= desvio padrão; S(%)= desvio padrão relativo.

Determinamos as percentagens de recuperação através da seguinte equação [23]:

$$\%recuperação = \frac{C(enc.)}{C(ad.)} \times 100 \qquad \text{Eq. (1)}$$

Onde *C(enc.)* significa concentração molar encontrada e C(ad.), concentração molar adicionada. Dessa forma, observamos que avaliação estatística mostrou recuperação na faixa de 98,00 a 107,50% e uma recuperação média de 104,54±7,01, adotando-se um limite de confiança de 95 %. Estes resultados validam o método proposto, uma vez que a recuperação ficou entre 80,00 a 110,00%, que é a razão considerada aceitável em estudo de confiança de um método [24], além de um baixo desvio padrão relativo 4,22%.

Avaliamos a precisão a partir do desvio padrão relativo (S(%)) das leituras feitas em 10 réplicas de cada amostra de Tiquira, realizadas no mesmo dia. Apresentamos na tabela 4 o resultado da repetibilidade e avaliação estatística. O desvio padrão relativo está entre 1,300 e 5,405, indicando que o método proposto possui boa precisão, já que

valores próximos de até 15 % são considerados aceitáveis na validação de um método analítico [24].

Tabela 4. Avaliação da repetibilidade do sinal analítico para o complexo Cu(II)-PAN em amostras de Tiquira, tampão NaAc/HAc, pH 6,0 (n= 10).

N.°	Absorbância (λ= 548nm)				
	Amostra 01	**Amostra 02**	**Amostra 03**	**Amostra 04**	**Amostra 05**
1	0,087	0,089	0,078	0,048	0,077
2	0,095	0,089	0,080	0,049	0,077
3	0,086	0,091	0,074	0,049	0,076
4	0,086	0,092	0,077	0,049	0,077
5	0,088	0,087	0,073	0,053	0,077
6	0,092	0,089	0,070	0,050	0,077
7	0,088	0,089	0,073	0,050	0,077
8	0,089	0,089	0,070	0,051	0,077
9	0,094	0,088	0,069	0,050	0,077
10	0,090	0,086	0,072	0,049	0,077
$\overline{x}$	0,090 ± 0,002	0,089 ± 0,001	0,074 ± 0,003	0,050 ± 0,001	0,077 ± 0,001
S	0,003	0,002	0,004	0,001	0,001
S(%)	3,333	2,247	5,405	2,000	1,300

$\overline{x}$= média com desvio padrão; S= desvio padrão; S(%)= desvio padrão relativo.

Calculamos a concentração mínima detectável a partir da equação 2, utilizando os resultados da curva analítica (curva padrão).

$$LD = \frac{K \cdot SD}{m} \qquad \text{Eq. (2)}$$

Onde K é uma constante e corresponde a três vezes o valor do ruído a partir do qual o valor lido pode ser considerado sinal analítico. No presente estudo o valor encontrado de SD (desvio padrão absoluto) e m (coeficiente angular) foram, respectivamente 0,0035 e 20251. Da Equação 2 calculamos o limite de detecção (LD) cujo resultado foi 3,3 × 10^{-2} mol L^{-1}. Portanto, na tabela 5 mostramos um resumo das condições experimentais da reação de complexação.

Tabela 5. Condições experimentais recomendadas para a determinação de Cu(II) por espectrofotometria UV-Vis.

Condições experimentais	Especificações
Comprimento de onda do complexo Cu(II)-PAN (nm)	548
pH	6,0
Tampão	Acetato de sódio/ácido acético
Faixa ideal de trabalho (mol L^{-1})	$1,0 \times 10^{-6}$ a $1,0 \times 10^{-5}$
Catión metálico	Cu(II)
Limite de detecção (mol L^{-1})	$3,3 \times 10^{-2}$

Aplicação do procedimento analítico proposto para a determinação de cobre em aguardente de mandioca (Tiquira)

O procedimento proposto foi aplicado para determinar a concentração de cobre em cinco amostras de Tiquira provenientes de municípios do Maranhão, cujas análises foram feitas em triplicatas. Na figura 9, apresentamos a curva analítica e os espectros de absorção referente à amostra 04 analisada pelo método da adição padrão. Como podemos observar, cada espectro apresentou bandas com boa resolução, indicando que outros íons metálicos, por venturas existentes na amostra, estão em quantidades inferiores ou iguais à concentração de interferência. Observamos ainda que a curva construída a partir dos espectros possui boa linearidade.

Na tabela 6, apresentamos a comparação entre os teores médios de Cu(II) em mg L^{-1} das cinco amostras analisadas com os valores encontrados por Espectrometria de Absorção Atômica (AAS) com o método proposto. Observamos que das cinco amostras de Tiquira analisadas, a de Nina Rodrigues (amostra 01) foi a que apresentou maior erro relativo, enquanto que as demais, com erro entre 5,76% a 11,11%, estão dentro da faixa aceitável [25], demonstrando que o método proposto pode ser considerado preciso. Assim, as concentrações de Cu(II) encontrada em todas as amostras estão acima da concentração máxima de $7,87 \times 10^{-5}$ mol L^{-1} (5,0 mg L^{-1}), recomendada pela legislação vigente [2].

Descrevemos as características química da reação de complexação do Cu(II)-PAN a partir do método espectrofotométrico UV Vis. Como demonstrado, o complexo formado possui absorção máxima em 548nm, é estável em pH, levemente, ácido (pH= 6) e reage na proporção de 1:1 na relação do metal Cu(II) com o ligante PAN. Em relação ao método, este apresentou bons resultados na correlação, recuperação e desvio padrão. Apesar dos bons resultados no dimensionamento do método, constatamos que a concentração de cobre em Tiquira estava acima da máxima permitida pela legislação brasileira.

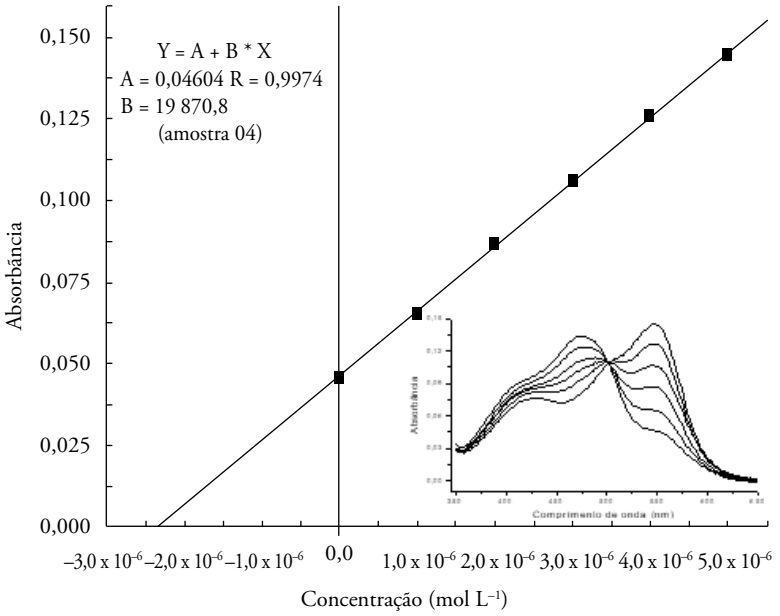

Figura 9. Curva de adição padrão de Cu(II) e espectros de absorção da amostra 04. [Cu(II)]= 10, 20, 30, 40 e 50 × 10^{-6} mol L^{-1} em tampão NaAc/HAc, pH 6,0, λ máx= 548 nm com [PAN]= 1 ′ 10^{-5} mol L^{-1}. *Figura interna*: espectros de absorção sobrepostos com adição padrão de Cu(II).

Tabela 6. Dados da média da concentração de Cu(II) encontrado nas cinco amostras de Tiquira através do método proposto por adição padrão e a comparação como os resultados obtidos pela Espectrometria de Absorção Atômica (AAS).

Amostra	Concentração média de cobre pelo método proposto (mg L^{-1})	Concentração de cobre por AAS (mg L^{-1})	Erro relativo (%)
01	13,53	10,61	27,52
02	14,42	13,09	10,16
03	9,60	8,64	11,11
04	7,88	8,64	8,80
05	8,26	7,81	5,76

Existem vários métodos disponíveis para determinar cobre em cachaça ou aguardente, mas o método recomendado apresenta limitações. A AOAC (Association of Official Analytical Chemists) recomenda a espectrometria de absorção com chamas (do inglês FAAS). Nesse método, as soluções padrão são preparadas em meio alcoólico (50% v/v) e as leituras são feitas de modo direto sem ajuste da graduação alcoólica para construção

da curva analítica de 0 a 0,96 mg L^{-1}. No entanto, como há efeito da matriz, o método foi modificado, substituindo-se a curva de calibração por método de adição de padrões [26]. Apesar dessa modificação ajudar na determinação de cobre em aguardente, o método recomendado pela AOAC apresenta limitações, tais como: faixa linear de trabalho pequena e menor frequência analítica [27].

Apesar das limitações do método recomendado, observamos que os resultados do nosso estudo para as amostras de Tiquira apresentaram erros relativos aceitáveis (tabela 6) quando comparado com o método recomendado pela AOAC. Portanto, o método que propomos mostra-se uma alternativa ao método recomendado.

Embora o método proposto seja inovador, simples e prático para determinar cobre em Tiquira, este não é o único que foi realizado pelo método espectrofotométrico UV Vis e com o reagente PAN. No estudo realizado por [28], os autores utilizaram o sistema ternário homogêneo água, etanol e metilisobutilcetona (MIC) e dissolveram o reagente nesse solvente. No entanto, a diferença do nosso trabalho está na matriz, que nesse caso foi a aguardente de mandioca, enquanto o deles estão na aguardente de cana-açúcar. Portanto, os resultados do nosso estudo complementam aos que já se tem a respeito da determinação de cobre em aguardente.

Conclusão

A partir do método espectrofotométrico UV vis e da reação de complexação, descrevemos o comportamento do complexo PAN-Cu (II) e a determinação do teor de cobre em aguardente de mandioca. Do complexo PAN-Cu (II), conclui que absorção é maior em meio fracamente ácido, possui estabilidade em um tempo de 7 horas, proporções estequiométricas mínima de 1:1 do ligante e metal, os principais íons interferentes são o ferro (III) e o cobalto (II). Na aguardente, constatamos que o teor de cobre está acima do permitido pela legislação brasileira.

Agradecimentos

Os autores agradecem ao CNPQ e a FAPEMA por financiarem esta pesquisa.

Conflito de interesse

Os autores declaram que não há conflito de interesses.

Referências

1. E. Aquarone, *Alimentos e bebidas produzidos por fermentação*, Edgard Blucher, 1983, p. 227.
2. Brasil Ministério da Agricultura, Pecuária e Abastecimento, *Instrução Normativa n°. 13*, de 29 de junho de 2005, URL: http://extranet.agricultura.gov.br/sislegis-consulta/consultarLegislacao.do?operacao=visualizar&id=12386, acessado em janeiro de 2019.
3. L.G.S. Andrade, *Determinação de cobre, aldeídos, álcoois, acetato de etila, ácidos carboxílicos e carbamato de etila em Tiquira (aguardente de mandioca) produzida no Estado do Maranhão*, Dissertação (Mestre em Química Analítica), Universidade Federal do Maranhão, 1999, p. 101.
4. L.R. Polastro, L.M. Boso, L.G. Andrade-Sobrinho, B.S. Lima-Neto, D.W. Franco, Compostos nitrogenados em bebidas destiladas: cachaça e Tiquira, *Ciênc. Tecnol. Aliment*, **21**, 78-81 (2001).
5. D.R. Cardoso, B.S. Lima-Neto, D.W. Franco, R.F. do Nascimento, Influência do material do destilador na composição química das aguardentes de cana, Parte II, *Quím. Nova*, **26**, 165-169 (2003).
6. A.A. Chemists, W Horwitz, *Official methods of analysis*, 15th ed., AOAC International, Arlington VA, 1990, Vol. I, p. 489.
7. K. Miranda, A.G. Dionísio, E.R. Pereira Filho, Copper determination in sugar cane spirits by fast sequential flame atomic absorption spectrometry using internal standardization, *Microchem. J.*, **96**, 99-101 (2010).
8. N.M. Caldas, S.R. Oliveira, J.A. Gomes-Neto, Feasibility of internal standardization in the direct and simultaneous determination of As, Cu and Pb in sugar-cane spirits by graphite furnace atomic absorption spectrometry, *Anal. Chim. Acta*, **636**, 1-5 (2009).
9. I.L. Küchler, F.A.M. Silva, Método potenciométrico para determinação de cobre em cachaça, *Quím. Nova*, **22**, 339-341 (1999).
10. S.A. do Nascimento Rocha, A.F. Dantas, H.V. Jaeger, A.C. Costa, E.S. Leão, M.R. Gonçalves, Spectrofotometric determination of copper in sugar cane spirit using biquinoline in the presence of ethanol and Triton X-100, *Spectrochim. Acta Part A: Mol. Biomol. Spectroscopy*, **71**, 1414-1418 (2008).

11. E.J. Lenardão, R.A. Freitag, M.J. Dabdoub, A.C.F. Batista, C.C. da Silveira, " Green Chemistry"- Os 12 princípios da química verde e sua inserção nas atividades de ensino e pesquisa, *Quím. Nova*, **26**, 123-129 (2003).

12. K.Z. Braĭnina, *Stripping voltammetry in chemical analysis*, John Wiley & Sons, Incorporated, Michigan, 1974, p. 222.

13. P. Barbeira, N. Stradiotto, Differential pulse anodic stripping determination of Pb and Cu traces in tropical alcoholic drinks, *Anais Assoc. Bras. Quim.*, **45**, 97-101 (1996).

14. G.W. Ewing, *Métodos Instrumentais de Análise Química*, Edgard Blücher, São Paulo, 1972, Vol. II, p. 312.

15. D.T. Sawyer, J.M. Beebe, W.R. Heineman, *Chemistry experiments for instrumental methods*, John Wiley & Sons, 1984, p. 448.

16. J. Gao, B. Peng, H. Fan, J. Kang, X. Wang, Spectrophotometric determination of palladium after solid-liquid extraction with 1-(2-pyridylazo)-2-naphthol at 90 °C, *Talanta*, **44**, 837-842 (1997).

17. A.E. Visser, S.T. Griffin, D.H. Hartman, R.D. Rogers, Naphthol-and resorcinol -based azo dyes as metal ion complexants in aqueous biphasic systems, *J. Chromatogr. B: Biomed. Sci. Applic.*, 7**43**, 107-114 (2000).

18. E.A.N. Fernandes, Determinação de Cálcio, Cobre, Cromo, Ferro, Magnésio, Manganês, Potássio, Sódio e Zinco em Etanol por Espectrometria de Absorção Atômica, Dissertação (Energia Nuclear na Agricultura), Escola Superior de Agricultura "Luiz de Queiroz", 1981, p. 86.

19. S. Shibita, K. Goto, R. Nakashima, Spectrophotometric determination of iron in high-purity yttrium oxide with 1-(2-pyridylazo)-2-naphthol, *Anal. Chim. Acta*, **46**, 146-148 (1969).

20. L.D. Coo, T.J. Cardwell, R.W. Cattrall, S.D. Kolev, Spectrophotometric study of the solubility and the protolytic properties of 1-(2-pyridylazo)-2-naphthol in different ethanol–water solutions, *Anal. Chim. Acta*, **360**, 153-159 (1998).

21. Z. Marczenko, *Spectrophotometric Determination of Elements*, Prentice Hall Europe, England, 1976.

22. J.E. Mouchreck Filho, *Potencialidades analíticas do 4-(2-piridilazo)-resorcinol e sua aplicação na determinação de cobre(ii) por espectrofotometria uv-vis em material biológico: sururu (Mytella falcata) e ostra (Crassostrea rhizophorae) do estuário Bacanga-São luís*, Dissertação (Química), Universidade Federal do Maranhão, 2000.

23. M.J. Cardone, S.A. Willavize, M.E. Lacy, Method validation revisited: A chemometric approach, *Pharm. Res.*, **7**, 154-160 (1990).

24. R. Caulcutt, R. Boddy, *Statistics for analytical chemists*, Chapman & Hall, London 1995, p. 264.

25. D. MacDougall, F.J. Amore, G.V. Cox, *et al.*, Guidelines for data acquisition and data quality evaluation in environmental chemistry, *Anal. Chem*, **52**, 2242-2249 (1980).

26. F.A. Honorato, R.S. Honorato, M.F. Pimentel, M.C.U. Araujo, Analytical curve or standard addition method: how to elect and design--a strategy applied to copper determination in sugarcane spirits using AAS, *Analyst*, **127**, 1520-1525 (2002).

27. D.A. Skoog, F.J. Holler, T.A. Nieman, *Princípios de Análise Instrumental*, 5 ed., Bookman, Porto Alegre, 2002, p. 836.

28. J.C. Souza, A.T. Toci, M.A. Beluomini, S.P Eiras, Spectrophotometric betermination of Copper (II) in sugarcane spirit using 1-(2-pyridylazo)-2-naphthol and a homogeneous ternary mixture of the solvents water, ethanol and methyl isobutyl ketone. *Rev. Virtual Quim.*, **8**, 687-701 (2016).

Como citar este artigo

R.W. Santos de Oliveira, P.R. Barros-Gomes, J.D. Ribeiro, J.B. Reis, M. Alves-Fontenele, G. Oliveira-Everton, W. da Silva-Lyra, H. Costa-Louzeiro, M. do Livramento de Paula, V.E. Mouchrek Filho, Determinação espectrofotométrica de Cobre(II) em aguardente de mandioca (Tiquira), *Rev. Colomb. Cienc. Quím. Farm.*, **49**(2), 355-373 (2020).

Scientific research article / *http://dx.doi.org/10.15446/rcciquifa.v49n2.89516*

Study of the antifungal activity of ibuprofen and its association with amphotericin B or ketoconazole against *Candida* spp.

Paula Mariane Silva Sousa[1], Jefferson Rodrigues Nóbrega[2], Laísa Vilar Cordeiro[3], Francisco Patricio de Andrade Júnior[4], Wylly Araújo de Oliveira[5]

[1]Academic Unit of Health, Education and Health Center, Federal University of Campina Grande, 58175-000, Cuité, Paraíba, Brazil. E-mail: paullamaryanne@hotmail.com

[2]Academic Unit of Health, Education and Health Center, Federal University of Campina Grande, 58175-000, Cuité, Paraíba, Brazil. E-mail: jeffersonrodriguesn@hotmail.com

[3]PhD student of Programa de Pós-Graduação em Produtos Naturais e Sintéticos Bioativos at Universidade Federal da Paraíba, 58033-455, João Pessoa, Paraíba, Brazil. E-mail: laisavilar@gmail.com

[4]Master in Natural and Synthetic Bioactive Products at Universidade Federal da Paraíba, 58033-455, João Pessoa, Paraíba, Brazil. E-mail: juniorfarmacia.ufcg@outlook.com

[5]Professor PhD at Universidade Federal de Campina Grande, 58429-900, Cuité, Paraíba, Brazil. E-mail: wylly@ufcg.edu.br

Received: 9 September 2019

Revised: 5 May 2020

Accepted: 5 May 2020

Summary

The objective was evaluating the antifungal activity of ibuprofen alone and when associated with amphotericin B or ketoconazole against *Candida* species. Strains of *C. albicans*, *C. tropicalis*, *C. guilliermondii*, *C. krusei* and *C. parapsilosis* were used. The minimum inhibitory concentration (MIC) was determined by the microdilution method and the association study performed through the checkerboard assay. The concentration of 512 μg/mL inhibited approximately 65% of the tested strains, while against 35% of the strains presented MIC values above 2048 μg/mL. Associations of ibuprofen with amphotericin B against *C. tropicalis* and ibuprofen with ketoconazole against *C. krusei* showed synergistic effect. Antagonistic effects were evidenced in the combination of ibuprofen with amphotericin B against *C. guilliermondii* and *C. albicans*, as well as in the association of ibuprofen with ketoconazole against *C. albicans* and *C. tropicalis*. Through the experiments, it was found that ibuprofen showed antifungal activity against most of the *Candida* species tested. The combinations of ibuprofen and antifungals had synergistic effects. However, antagonistic results were evidenced in the association with ibuprofen, which would make clinical applicability difficult. Therefore, studies of this combined activity should be investigated, considering that this association may be positive for antifungal therapy.

Key words: *Candida*, ibuprofen, antifungals, association.

Resumen

Estudio de la actividad antifúngica del ibuprofeno y su asociación con anfotericina B o ketoconazol contra *Candida* spp.

El objetivo fue evaluar la actividad antifúngica del ibuprofeno solo y asociado con anfotericina B o ketoconazol contra especies de *Candida*. Se utilizaron cepas de *C. albicans*, *C. tropicalis*, *C. guilliermondii*, *C. krusei* y *C. parapsilosis*. La concentración inhibitoria mínima (MIC) se determinó mediante el método de microdilución y el estudio de asociación fue realizado a través del ensayo de checkboard. La concentración de 512 μg/mL inhibió aproximadamente el 65% de las cepas analizadas, mientras 35% de las cepas presentaron valores de MIC superiores a 2048 μg/mL. Las asociaciones de ibuprofeno con anfotericina B contra *C. tropicalis* e ibuprofeno con ketoconazol contra *C. krusei* mostraron un efecto sinérgico. Se evidenciaron efectos antagonistas en la combinación de ibuprofeno con anfotericina B contra *C. guilliermondii* y *C. albicans*, así como en la asociación de ibuprofeno con ketoconazol contra *C. albicans* y *C. tropicalis*. Se descubrió, a través de los experimentos, que el ibuprofeno mostró actividad antifúngica contra la mayoría de las especies de *Candida* probadas. Las combinaciones de ibuprofeno y antifúngicos tuvieron efectos sinérgicos. Sin embargo, se evidenciaron resultados antagónicos en la asociación con ibuprofeno, lo que dificultaría la aplicabilidad clínica. Por lo tanto, los estudios de esta actividad combinada deben investigarse, considerando que esta asociación puede ser positiva para la terapia antimicótica.

Palabras clave: *Candida*, ibuprofeno, antifúngicos, asociación.

Resumo

Estudo da atividade antifúngica do ibuprofeno e sua associação com anfotericina B ou cetoconazol contra *Candida* spp.

O objetivo do estudo foi avaliar a atividade antifúngica do ibuprofeno sozinho e quando associado com anfotericina B ou cetoconazol contra espécies de Candida. Foram utilizadas cepas fúngicas de *C. albicans*, *C. tropicalis*, *C. guilliermondii*, *C. krusei* e *C. parapsilosis*, entre isolados clínicos e cepas padrão. A concentração inibitória mínima (CIM) foi determinada pela técnica de microdiluição e o estudo de associação realizado

através do ensaio checkerboard. A concentração de 512 μg/mL foi capaz de inibir, aproximadamente, 65% das cepas ensaiadas, enquanto que 35% das estirpes apresentaram valores da CIM acima de 2048 μg/mL. Associações do ibuprofeno com anfotericina B contra *C. tropicalis* e ibuprofeno mais cetoconazol contra *C. krusei* mostraram efeito sinérgico. Efeitos antagônicos foram evidenciados na combinação do ibuprofeno com anfotericina B contra *C. guilliermondii* e *C. albicans*, como também na associação do ibuprofeno com cetoconazol contra *C. albicans* e *C. tropicalis*. Por meio dos experimentos, pôde-se afirmar que o ibuprofeno exerceu atividade antifúngica contra a maioria das espécies de *Candida* ensaiadas. Os efeitos das combinações entre o ibuprofeno e os antifúngicos promoveram efeitos sinérgicos. No entanto, resultados antagônicos foram evidenciados na associação com o ibuprofeno, o que dificultaria aplicabilidade clínica. Logo, estudos dessa atividade combinada devem ser investigados, pois esta associação pode traçar pontos positivos na terapia antifúngica.

Palavras-chave: *Candida*, ibuprofeno, antifúngicos, associação.

Introduction

Candida species are commensal fungi that live on the skin and the oral, vaginal and intestinal mucous membranes of the human body. The genus Candida is related to a wide range of clinical manifestations, mainly when the immune defense mechanisms of the individual are compromised by several risk factors, including the use of corticosteroids, systemic antibiotics, internal medical devices, total parenteral nutrition, surgeries and others [1-3]. Although the most prevalent species of this genus involved in invasive fungal infections is *C. albicans*, infections caused by non-*albicans* species have increased significantly, further raising a worrying scenario because such infections are often more severe, rapidly progressive, treatment-refractory and associated the highest mortality and morbidity [1, 4]. Antifungals available to treat infections caused by *Candida* spp. include topical or systemic drugs, showing fungistatic or fungicidal action [5]. However, the low number of antifungal drugs available, the high rates of resistant microorganisms, as well as the inherent toxicity of these drugs have underlined the importance for researching new strategies that lead to effective treatments for the control of fungal infections [6, 7]. With this propose, recent studies have focused on the association between conventional non-antifungal pharmacological agents and conventional antifungal agents [8-12].

Ibuprofen is a non-steroidal anti-inflammatory inhibitor of cyclooxygenase (COX-1 and COX-2) isoenzymes, which specifically blocks mammalian prostaglandin biosynthesis [13]. This anti-inflammatory is classically used due to its antipyretic,

analgesic, and anti-inflammatory effects [14]. The antimicrobial potency of ibuprofen has been demonstrated in its ability to reverse resistance related to efflux pump activity in *C. albicans* [15]. Recently, ibuprofen showed *in vitro* antifungal activity against *Cryptococcus* [16]. Based on this, the present study aimed to evaluate the antifungal activity of ibuprofen alone and when associated with amphotericin B or ketoconazole against *Candida* species.

Materials and methods

Strains

For this study, 14 *Candida* strains were used, including clinical isolates (LM) and standard strains (American Type Culture Collection - ATCC). Amongst them, *C. albicans* (LM-13, LM-410, LM-178, LM-703, ATCC 76485, ATCC 40042); *C. tropicalis* (LM-10, ATCC 13803); *C. guilliermondii* (LM-703, LM-103); *C. krusei* (LM-120, LM-13); *C. parapsilosis* (ATCC 22019, ATCC 20019). All strains were provided by the Mycology Laboratory of the Federal University of Paraíba, João Pessoa-PB, Brazil.

Substances

The substances to which antifungal activity was performed were ibuprofen, amphotericin B and ketoconazole. In addition, sabouraud dextrose agar (SDA) and RPMI-1640 broth were purchased from Difco laboratories and Inlab, respectively. All substance solutions were prepared only at the time of testing by dissolving them in sterile distilled water with the addition of 50 µL dimethylsulfoxide (DMSO). DMSO controls were tested at the same concentrations.

Inoculum

Suspensions were prepared from fresh *Candida* fungal cultures, kept in SDA, and incubated at 37 °C for 24-48h. After this period, colonies of these cultures were suspended in 4 mL of sterile saline (0.85%). Finally, these suspensions were homogenized, and the turbidity was adjusted to 0.5 McFarland scale. Thus, the final inoculum concentration obtained was 1-5 x 10^6 CFU/mL [17, 18].

Minimum inhibitory concentration (MIC)

MIC determination of ibuprofen and antifungals was performed by the 96-well plate microdilution technique. Initially, 100 µL of double concentrated RPMI-1640 was added to the wells of the plate. Then 100 µL of the substance was distributed in the first-row wells of the plate. Through a serial dilution in the ratio of 2, concentrations

ranged from 2048 to 8 μg/mL for ibuprofen and from 512 to 0.0625 μg/mL for antifungals. Then 10 μL of the inoculum was added to each well. Finally, the plates were incubated at 37 °C and read after 24-48 h, observing the presence or absence of visible fungal growth [17-20]. Then 20 μL of 1% 2,3,5-triphenyltetrazolium chloride (TTC) (Sigma-Aldrich®) was added to each well of the plate to prove fungal growth and the plate incubated for a further 12 h [21]. The MIC of the tested drugs was defined as the lowest concentration capable of producing visible inhibition of fungal growth, as indicated by TTC. The following controls were tested: negative controls (RPMI-1640 only) and positive controls (RPMI-1640 and microorganism) to evaluate medium sterility and inoculum viability, respectively. All assays were performed in triplicate [17-20].

Drug association

The association assay between ibuprofen and antifungals was conducted using the checkerboard method [22]. Initially, 100 μL of double concentrated RPMI-1640 was added to the wells of the plate. Then 50 μL of ibuprofen at different concentrations (MICx8, MICx4, MICx2, MIC, MIC/2, MIC/4 and MIC/8) were added horizontally and 50 μL amphotericin B or ketoconazole, also at different concentrations (MICx8, MICx4, MICx2, MIC, MIC/2, MIC/4 and MIC/8) were added vertically to the plate. Thus, different ibuprofen concentrations were tested in the presence of various antifungal concentrations individually. Subsequently, 20 μL of the corresponding inoculum, previously adjusted to 0.5 McFarland scale, were added. The plates were incubated at 37 °C and read after 24-48 h to observe the presence or absence of visible fungal growth [22], as indicated after 12 h of the addition of 20 μL of 1% TTC [21]. All assays were performed in triplicate and the negative (RPMI-1640 only) and positive (RPMI-1640 and microorganism) controls tested.

The effect produced between the combination of anti-inflammatory and amphotericin B or ketoconazole was determined by the fractional inhibitory concentration index (FICI). This index was calculated by the sum of fractional inhibitory concentrations (FIC), where FIC_A= (MIC of substance A in combination)/(MIC of substance A alone) and FIC_B= (MIC of substance B in combination)/(MIC of substance B alone), thus FICI= FIC_A + FIC_B. The association was defined as synergistic for FICI ≤ 0.5, as additive for 0.5 <FICI<1, as indifferent for 1 ≤ FICI < 4, and as antagonistic for FICI ≥ 4 [23, 24].

Results and discussion

The MIC values of ibuprofen against *Candida* species are shown in table 1.

Table 1. MIC (μg/mL) of ibuprofen against *Candida* spp.

Strains	Ibuprofen
C. albicans	
LM-13	32
LM-410	128
LM-178	128
LM-703	256
ATCC 76485	32
ATCC 40042	>2.048
C. tropicalis	
LM-10	128
ATCC 13803	>2.048
C. guilliermondii	
LM-703	512
LM-103	>2.048
C. krusei	
LM-120	>2.048
LM-13	>2.048
C. parapsilosis	
ATCC 22019	128
ATCC 20019	512

>: MIC higher than the concentrations tested.

The results were quite variable, showing a higher antifungal activity against *C. albicans* strains, different from that observed for *C. krusei* where ibuprofen showed lower activity. The concentration of 512 μg/mL inhibited approximately 65% of the tested strains, whereas against 35% of the strains the MIC values were above 2048 μg/mL.

Table 2 presents the MIC for antifungals against the various strains tested.

Amphotericin B showed the best activity, where the concentration of 2 μg/mL was able to inhibit 100% of the strains. Ketoconazole presented MIC ranging from 0.125 to 64 μg/mL. From the individual antifungal MIC, it was possible to make the

Table 2. MIC (μg/mL) antifungals against *Candida* spp.

Strains	Amphotericin B	Ketoconazole
C. albicans		
LM-13	0.5	64
C. tropicalis		
ATCC 13803	2	0.5
C. guilliermondii		
LM-703	0.5	0.125
C. krusei		
LM-120	2	64
C. parapsilosis		
ATCC 20019	2	0.5

associations with ibuprofen. The results of the combination of ibuprofen and amphotericin B against *Candida* strains are shown in table 3.

Table 3. Minimum inhibitory concentration (MIC) in the combination; fractional inhibitory concentration (FIC); and fractional inhibitory concentration index (FICI) of the association between ibuprofen and amphotericin B against *Candida* spp.

Strains	MIC (μg/mL) in combination		FIC of drugs		FICI	Result
	Ibuprofen	Amphotericin B	Ibuprofen	Amphotericin B		
C. albicans LM-13	256	0.25	8	0.5	8.5	Antagonism
C. tropicalis ATCC 13803	512	0.25	0.25	0.125	0.375	Synergism
C. guilliermondii LM-703	4096	4	8	8	16	Antagonism
C. krusei LM-120	512	1	0.25	0.5	0.75	Additivity
C. parapsilosis ATCC 20019	256	0.25	0.5	0.125	0.625	Additivity

The association of ibuprofen with amphotericin B against *C. tropicalis* ATCC 13803 showed a synergistic effect. Additivity was observed in the combinations against *C. krusei* LM-20 and *C. parapsilosis* ATCC 20019. Antagonism was evidenced in 40% of the combinations.

Table 4 shows the effects of the combination of ibuprofen and ketoconazole against *Candida* spp.

Table 4. Minimum inhibitory concentration (MIC) in the combination; fractional inhibitory concentration (FIC); and fractional inhibitory concentration index (FICI) of the association between ibuprofen and ketoconazole against *Candida* spp.

Strains	MIC (μg/mL) in combination		FIC of drugs		FICI	Result
	Ibuprofen	Amphotericin B	Ibuprofen	Amphotericin B		
C. albicans LM-13	128	8	4	0.125	4.125	Antagonism
C. tropicalis ATCC 13803	256	4	0.125	8	8.125	Antagonism
C. guilliermondii LM-703	64	0.125	0.125	1	1.125	Indifference
C. krusei LM-120	256	8	0.125	0.125	0.25	Synergism
C. parapsilosis ATCC 20019	256	0.25	0.5	0.5	1	Indifference

Different forms of interactions between anti-inflammatory and ketoconazole were observed, among them: synergism in 20% of the associations, indifference in 40% and, finally, 40% of the combinations had an antagonistic effect. Non-steroidal anti-inflammatory drugs (ibuprofen, indomethacin, diclofenac sodium and acetylsalicylic acid) are therapeutic options for *Candida*-related infections by inhibiting COX-1 and/or COX-2 that are involved in prostaglandin E_2 biosynthesis, which is a virulence factor in promoting fungal colonization and chronic infections [25].

Studies conducted to evaluate the antimicrobial activity of ibuprofen have shown antibacterial action against methicillin-resistant *Staphylococcus aureus* (MIC 2500 μg/mL), *Salmonella choleraesuis*, *Pseudomonas aeroginosa*, *Klebsiella pneumoniae*, *Escherichia coli* (MIC> 5000 μg/mL) [26], and antifungal activity against *Trichosporon asahii* (MIC 500 to 2000 μg/mL) [9], besides inhibiting the growth of 10 clinical isolates of *Candida*, among them *C. albicans*, *C. krusei*, *C. tropicalis* and *C. guilliermondii*, with MIC value similar to that found in this study [27].

The effect of the association with ibuprofen has been investigated in several studies, including synergism in 43.5% of the combinations of ibuprofen and amphotericin B against *Fusarium* spp. strains [28], this same association showed indifferent results against *Aspergillus* spp. [29]. Recently, this association showed synergistic effects in 86.67% and indifferent effects in 13.33% of the associations against clinical isolates

of *Trichosporon asahii* [9]. Amphotericin B leads to rapid death of fungal cells by causing plasma membrane damage when interacting with ergosterol, resulting in pore formation, surface adsorption and ergosterol extraction from the fungal membrane [30]. Ketoconazole interferes with ergosterol synthesis, which prevents the conversion of lanosterol to ergosterol by inhibiting 14α-demethylase enzyme of cytochrome P450 [31]. In addition to a major problem in the eradication of nosocomial infections, resistance to these drugs is multifactorial and causes several complications in therapy [32]. For this reason, it could be useful to increase the effectiveness of these drugs through combinations with non-antifungal medicines.

Conclusions

This study showed that ibuprofen exerted antifungal activity against most *Candida* species tested, and this information provides more enlightened expectations for future studies that detail the mechanisms of action and resistance involved to ensure its clinical applicability in the treatment of fungal infections caused by *Candida* spp. The combinations of ibuprofen and antifungals promoted synergistic effects. However, antagonistic results were evidenced too, which would hinder its clinical applicability in this case. Therefore, studies of this combined activity should be investigated, as the use of these combinations would bring positive points in antifungal therapy.

Acknowledgment

The authors are gratefully acknowledged to Conselho Nacional de Desenvolvimento Científico e Tecnológico (CNPq) by financial support.

Disclosure statement

No potential conflict of interest was reported by the authors.

References

1. A. Mehta, S.V. Date, Determination of incidence of different *Candida* spp. in clinical specimens and characterisation of *Candida* species isolates, *Indian J. Microbiol. Res.*, **23**(4), 342-351 (2016).

2. G.D. Brown, D.W. Denning, S.M. Vevitz, Tackling human fungal infections, *Science*, **336**(6082), 647 (2012).

3. O. Gudlaugsson, S. Gillespie, K. Lee, V.J. Berg, J. Hu, S. Messer, *et al.*, Attributable mortality of nosocomial candidemia revisited, *Clin. Infect. Dis.*, **37**(9), 1172-1177 (2003).

4. M. Pfaller, D. Neofytos, D. Diekema, N. Azie, H.U. Meier-Kriesche, S.P. Quan, *et al.*, Epidemiology and outcomes of candidemia in 3648 patients: data from the prospective antifungal therapy (PATH Alliance®) registry, 2004–2008, *Diagn. Microbiol. Infect. Dis.*, **74**(4), 323-331 (2012).

5. S. Sharifynia, H. Badali, M.S. Sorkherizi, M.R. Shidfar, A. Hadian, S. Shahrokhi, *et al.*, *In vitro* antifungal susceptibility profiles of *Candida albicans* complex isolated from patients with respiratory infections, *Acta Med. Iran.*, **54**(6), 376-381 (2016).

6. S. Silva, M. Negri, M. Henriques, R. Oliveira, D.W. Williams, J. Azeredo, *Candida glabrata*, *Candida parapsilosis* and *Candida tropicalis*: biology, epidemiology, pathogenicity and antifungal resistance, *FEMS Microbiol. Ver.*, **36**(2), 288-305 (2012).

7. S.B. Paula, T.F. Bartelli, V. Di Raimo, J.P. Santos, A.T. Morey, M.A. Bosini, *et al.*, Effect of eugenol on cell surface hydrophobicity, adhesion, and biofilm of *Candida tropicalis* and *Candida dubliniensis* isolated from oral cavity of HIV-infected patients, *Evid. Based Complement. Alternat. Med.*, **2014**, ID 505204 (2014).

8. P.T. Venturini, L. Rossato, F. Chassot, T.J. Keller, B.F. Piasentin, M.J. Santurio, *et al.*, *In vitro* synergistic combinations os pentamidine, polymyxin B, tigecycline and tobramycin with antifungal agents against *Fusarium* spp, *J. Med. Microbiol.*, **65**(8), 770-774 (2016).

9. S. Yang, Y. Liao, L. Cong, X. Lu, R. Yang, *In vitro* interactions between non-steroidal anti-inflammatiry drugs and antifungal agents against planktonic and biofilm forms of *Trichosporon asahii*, *PLoS One*, **11**(6), e0157047 (2016).

10. L.Y.S. Holbrook, A. Garzan, K.E, Dennis, K.S. Shrestha, S. Garneau-Tsodikova, Repurposing antipsychotic drugs into antifungal agents: Synergistic combinations of azoles and bromperidol derivatives in the treatment of various fungal infections, *Eur. J. Med. Chem.*, **139**, 12-21 (2017).

11. L. Gao, X. Ding, Q. Liu, Q. Wu, T. Zeng, Y. Sun, *In vitro* interactions between target of rampamycin kinase inhibitor and antifungal agents against *Aspergillus species*, *Antimicrob. Agents Chemother.*, **60**(6), 3813-3816 (2016).

12. L. Gao, Y. Sun. in vitro interactions of antifungal agents and tacrolimus against Aspergillus biofilms. *Antimicrob Agents Chemother*, 59, 11, (2015).

13. E. Rusu, I. Sarbu, D. Pelinescu, I. Nedelcu, T. Vassu, C. Cristescu, *et al.*, Influence of associating nonsteroidal anti-inflammatory drugs with antifungal compounds on viability of some *Candida* strains, *Romanian J. Infec. Dis.*, **17**, 2 (2014).

14. S. Costa-de-Oliveira, M.I Miranda, A. Silva-Dias, P.A Silva, G.A Rodrigues, C. Pina-Vaz, Ibuprofen potentiates the *in vivo* antifungal activity of fluconazole against *Candida albicans* murine infection, *Antimicrob. Agents Chemother.*, **59**(7), 4289–4292 (2015).

15. C. Pina-Vaz, F. Sansonetti, A.G. Rodrigues, J. Martinez-de-Oliveira, A.F. Fonseca, P.A. Mardh, Antifungal activity of ibuprofen alone and in combination with fluconazole against *Candida* species, *J. Med. Microbiol.*, **49**(9), 831-840 (2000).

16. A.O. Ogundeji, H.C. Pohl, M.O. Sebolal, Repurposing of aspirin and ibuprofen as candidate anti-*Cryptococcus* drugs. *Antimicrob. Agents Chemother.*, **60**(8), 4799-808 (2016).

17. L. Cleeland, E. Squires, Evaluation of new antimicrobials in vitro and experimental animal infections, in: *Antibiotics in laboratory medicine*, 3rd ed., edited by: Y. Lorian, Williams & Wilkins, Baltimore, 1991, p. 739-788.

18. F. Hadacek, H. Greger, Testing of antifungal natural products: methodologies, comparability of results and assay choice, *Phytochem. Anal.*, **11**(3), 137-147 (2000).

19. National Committee for Clinical Laboratory Standards, *Reference method for broth dilution antifungal susceptibility testing of yeasts: approved standard*, 2nd ed., NCCLS, Wayne, 2008, 29 p.

20. J.N. Eloff, A sensitive and quick microplate method to determine the minimal inhibitory concentration of plant extracts for bacteria, *Planta Med.*, **64**(8), 711-713 (1998).

21. E.V. Costa, S.D. Teixeira, F.A Marques, M.C.T Duarte, C. Delarmelina, M.L.B. Pinheiro, *et al.*, Chemical composition and antimicrobial activity of the essential oils of the Amazon Guatteriopsis species, *Phytochemistry*, **69**(9), 1895-1899 (2008).

22. R.L. White, D.S. Burgess, M. Mandruru, J.A. Bosso, Comparison of three different *in vitro* methods of detecting synergy: time-kill, checkerboard and E-test, *Antimicrob. Agents Chemother.*, **40**(8), 1914–1918 (1996).

23. R.E. Lewis, D.J. Diekema, A.S. Messer, M.A. Pfaller, M.E. Klepser, Comparison of Etest, chequerboard dilution and time-kill studies for the detection of synergy or antagonism between antifungal agents tested against *Candida* species, *J. Antimicrob. Chemother.*, **49**, 345–351 (2002).

24. J. Correa-Royero, V. Tangarife, C. Durán, E. Stashenko, A. Mesa-Arango, *In vitro* antifungal activity and cytotoxic effect of essential oils and extracts of medicinal and aromatic plants against *Candida krusei* and *Aspergillus fumigatus*, *Braz. J. Pharm.*, **20**(5), 734-741 (2010).

25. E.E. Nash, B.M. Peters, P.I. Fidel, M.C. Noverr, Morphology-independent virulence of *Candida* species during polymicrobial intra-abdominal infections with *Staphylococcus aureus*, *Infect. Immun.*, **84**(1), 90–98 (2015).

26. L.W.E. Chan, Y.Z. Yee, I. Raja, Y.K.J Yap, Synergistic effect of non-steroidal anti-inflammatory drugs (NSAIDs) on antibacterial activity of cefuroxime and chlotamphenicol against methicillin-resistant *Staphylococcus aureus*, *J. Glob. Antimicrob. Resist.*, **10**, 70-74 (2017).

27. C. Pina-Vaz, F. Sansonetty, G.A. Rodrigues, J. Martinez-de-Oliveira, F.A. Fonseca, P. Mardh, Antifungal activity of ibuprofen alone and in combination with fluconazole against *Candida* species, *J. Med. Microbiol.*, **49**(9), 831-840 (2000).

28. T.P. Venturini, L. Rossato, T.B. Spader, G.R. Tronco-Alves, M.I. Azevedo, C.B. Weiler, *et al.*, *In vitro* synergisms obtained by amphotericin B and voriconazole associated with non-antifungal agents against *Fusarium* spp, *Diagn. Microbiol. Infect. Dis.*, **71**(2), 126-130 (2011).

29. L. Li-Juan, C. Wei, X. Hui, W. Zhe, L. Ruo-Yu, L. Wei, Antifungal activity of ibuprofen against *Aspergillus* species and its interaction with common antifungal drugs, *Chinese J. Mycol.*, **123**, 19 (2010).

30. K. Lohner, Antimicrobial mechanisms: a sponge against fungal infections, *Nat. Chem. Biol.*, **10**(6), 411-412. (2014).

31. K.H. Greenblatt, J. D. Greenblatt. Liver injury associated with ketoconazole: Review of the published evidence. *J Clin Pharmacol*, 54, 12, (2014).

32. C. Ceresa, M. Rinaldi, L. Fracchia, Synergistic activity of antifungal drugs and lipopeptide AC7 against *Candida albicans* biofilm on silicone, *AIMS Bioengineering*, **4**(2), 318-334 (2017).

How to cite this article

P.M. Silva-Sousa, J. Rodrigues-Nóbrega, L. Vilar-Cordeiro, F.P. de Andrade Júnior, W. Araújo de Oliveira, Study of the antifungal activity of ibuprofen and its association with amphotericin B or ketoconazole against *Candida* spp., *Rev. Colomb. Cienc. Quím. Farm.*, **49**(2), 374-386 (2020).

Artículo de investigación clínica / *http://dx.doi.org/10.15446/rcciquifa.v49n2.89677*

Evaluación de la publicidad de medicamentos en los principales medios televisivos, radiofónicos y escritos en Costa Rica

Yenifer Corrales-Cubillo[1]*, Nathalie Saborío-Quesada[1], Ramsés Alfaro-Mora[2]

[1]Escuela de Farmacia, Universidad Latina de Costa Rica, San José, Costa Rica.

[2]Dirección de Investigación, Universidad Latina de Costa Rica, San José, Costa Rica.

*Correo electrónico: corralesjennifer73@yahoo.es

Recibido: 20 de abril de 2020

Revisado: 8 de mayo de 2020

Aceptado: 9 de mayo 2020

Resumen

La presente investigación evaluó la publicidad de medicamentos en los principales medios televisivos, radiofónicos y escritos en Costa Rica para conocer la información que se transmite al consumidor. Los medios de comunicación son interesantes objetos de estudios porque son usados por las industrias como una herramienta para poder llegar al consumidor. Este es un estudio observacional, descriptivo de tipo transversal, se realizó una encuesta a la población estudiantil de la Universidad Latina de Costa Rica y con la misma se hizo una observación de las pautas publicitarias en la radio, periódicos y la televisión en diferentes horarios. En la investigación se determinó que la mayoría de los anuncios encontrados en los diferentes medios de comunicación carecieron de ciertas disposiciones solicitadas por el reglamento. Las faltas que se encontraron fueron: composición del producto (principios activos), casa fabricante, categoría del producto, presentaciones disponibles. Se demostró que las regulaciones en la parte de la promoción de un medicamento son de gran importancia para poder proteger a los consumidores, porque las ganancias de las industrias farmacéuticas dependen en gran medida de su mercadotecnia. La promoción de productos busca aumentar las ganancias, sin embargo, si esto no se hace correctamente podría haber una mala utilización de los medicamentos.

Palabras clave: Publicidad, medicamentos, reglamento, medios de comunicación.

Summary

Evaluation of drug advertising in the main television, radio, and written media in Costa Rica

This research evaluated drug advertising in the main television, radio, and written media in Costa Rica to find out the information that is transmitted to the consumer. The media are interesting objects of study because they are used by industries as a tool to reach the consumer. This is an observational, descriptive cross-sectional study, a survey was conducted of the student population of the Universidad Latina de Costa Rica and with it an observation was made of the advertising patterns on radio, newspapers, and television at different times. The investigation determined that most of the advertisements found in the different media lacked certain provisions requested by the regulation. The faults found were product composition (active ingredients), manufacturer, product category, available presentations. Regulations in the promotion part of a drug have been shown to be of great importance to protect consumers, because the profits of the pharmaceutical industries depend largely on their marketing. The promotion of products seeks to increase profits, however, if this is not done correctly there could be a misuse of medications.

Keywords: Advertising, medications, regulations, media.

Introducción

Los medios de comunicación son de gran importancia para las industrias, ya que son una herramienta para hacer llegar el mensaje al receptor. La publicidad es una rama de las comunicaciones que forma parte del proceso de mercadotecnia. Esta es un método para enviar un mensaje de un patrocinador, a través de un canal de comunicación formal, a la audiencia deseada [1].

En Costa Rica, según una encuesta realizada por el Ministerio de Ciencias, Tecnologías y Comunicaciones, el 72,3% de la población posee televisión por suscripción [2]. Esto es un buen indicador de que gran parte de los costarricenses tiene acceso a la televisión, por lo que dicho medio de comunicación es de gran utilidad para promocionar productos a la población. Este medio fue utilizado para esta investigación, de igual manera se va a emplear el periódico y la radio para determinar qué información se le está enviando a los consumidores.

La publicidad de medicamentos es algo que se debe tomar con seriedad porque dependiendo del mensaje que se le haga llegar al público podría generar que los consumidores

se automediquen. La información de los anuncios publicitarios describe diferentes síntomas de las enfermedades, y esto incita a la adquisición del medicamento y a la automedicación [3].

El Estado tiene un papel importante, en relación con la propaganda de medicamentos, al velar por la protección de la sociedad y que se cumpla lo estipulado en la legislación vigente [4, 5]. Por tal razón, lo que se buscó con el presente proyecto fue evaluar la publicidad de medicamentos a través de los medios televisivos, radiofónicos y escritos para conocer qué información se transmite al consumidor en Costa Rica.

Metodología

Se presenta un estudio observacional, descriptivo de tipo transversal, donde se evaluó la publicidad de medicamentos en los principales medios radiofónicos, televisivos y escritos en Costa Rica, según los gustos de la población universitaria. Se hizo una encuesta a una muestra de 220 universitarios. Las preguntas facilitaron la determinación de las preferencias según los medios de comunicación que los estudiantes frecuentaban. Estas determinaron si utilizaban los medios de comunicación como televisión, radio y periódicos enumerándolos del 1 al 3 según la frecuencia de uso, donde el 1 será el más frecuente el 3 el menos frecuente, además se determinó la edad, sexo, la carrera, si emplean los medios de comunicación, los canales de televisivos de no paga más usados, así como los periódicos y la radio que empleaban con más frecuencia.

La segunda parte de la investigación consistió en seguir los programas radiales, televisivos y periódicos, de acuerdo con las preferencias de los estudiantes según la encuesta. Se eligieron 3 periódicos, 3 canales televisivos y las 3 frecuencias radiofónicas más frecuentadas por parte del estudiantado. Luego se recolectaron los periódicos durante la semana del 26 de agosto al 1 de septiembre del 2019 y de esta manera se examinó la información correspondiente en cada uno.

Posteriormente, se recolectó los datos de la radio, se grabó por 3 semanas, en 2 horarios distintos cada emisora. La primera emisora fue en la semana del 16 al 22 de septiembre del 2019, luego la semana del 23 al 29 de septiembre del 2019, y por último en fechas del 30 de septiembre al 06 de octubre del 2019. El primer horario fue de 7:00 a 8:00 a. m. y el segundo horario de 7:00 a 8:00 p. m.

El último medio de comunicación analizado correspondió a la televisión. El estudio se llevó a cabo con grabaciones de los 3 canales televisivos seleccionados durante 3 semanas, en 2 horarios distintos cada canal. Se realizaron las grabaciones en la semana del 7 al 13 de octubre del 2019, la segunda semana fue del 14 al 20 de octubre del 2019 y la

última semana correspondió al 21 al 27 de octubre del 2019, grabando en el horario de 7:00 a 8:00 a. m. y un segundo horario de 7:00 a 8:00 p. m.

Para evaluar cada uno de los anuncios obtenidos en los diferentes horarios y medios de comunicación se creó un instrumento como parámetro de medición, el cual se puede observar en la tabla 1, esta nos permitió determinar las características presentes en cada anuncio publicitario y precisar si cada pauta cumple con el Reglamento de Publicidad en Costa Rica, este es regulado por el Ministerio de Salud de Costa Rica [6]. El cálculo y análisis de datos se realizó mediante el uso de las herramientas tecnológicas Winepi 2.0 y MS Excel® versión 2016.

Tabla 1. Tabla ejemplificadora de las variables usadas para la evaluación de los anuncios publicitario.

Regulación de la publicidad de medicamentos		
Variable	**Cumple**	**No cumple**
La publicidad de medicamentos de venta libre no deberá:		
Incluir información sobre posología (dosis)		
Emplear técnicas publicitarias que puedan confundir e inducir a los menores de edad al consumo de los medicamentos		
Omitir las leyendas: "Antes de consumir este medicamento, lea la información de la etiqueta" y "Todo medicamento posee efectos secundarios"		
Utilizar imágenes o elementos que induzcan a error al consumidor		
Hacer uso de declaraciones o testimonios de usuarios del producto que no coincidan con las indicaciones aprobadas en el registro del medicamento.		
La publicidad de medicamentos no declarados como de venta libre, que esté dirigida al público en general, se limitará a señalar las siguientes características del mismo		
Nombre comercial		
Indicación(es), y características atribuibles al producto aprobada(s) por el ministerio		
Presentaciones disponibles		
Forma farmacéutica		
Composición del producto (principios activos)		
Casa fabricante		
Categoría del producto		

Regulación de la publicidad de medicamentos		
Variable	**Cumple**	**No cumple**
Deberá incluir en forma visual o auditiva, según el medio de comunicación empleado:		
Todo medicamento posee efectos secundarios		
Este medicamento requiere receta médica		
Consulte con su médico		
Indicar número de oficio de aprobación de la publicidad		

Resultados

Se aplicaron 220 encuestas a hombres 71 (32 %) y mujeres 149 (68 %) con una edad media de 22 años, una desviación estándar de un 8,8991, un error típico de la 0,6013 y un rango de 47, donde la mínima fue de 17 y la máxima de 64. En la tabla 2 se puede observar las diferentes tendencias que existen por carrera universitaria, correspondientes a cada uno de los medios de comunicación, así como los datos de preferencia según sexo. Entre los resultados obtenidos a través de la encuesta se logró identificar 3 periódicos de preferencia por la población estudiantil. Para las emisoras radiales la más frecuentada fue 101.1 FM, seguida de 104.7 FM y 102.7 FM. En el caso de los canales televisivos los estudiantes prefieren 3 canales nacionales, al igual que los periódicos. La diferencia entre los totales generales observados en la tabla 2 es resultado de la pérdida de datos, por motivo, de la falta de contestación de ciertos encuestados. La preferencia de uso según los resultados de las encuestan posicionan a la televisión como el medio más frecuentado (94,5%), seguida por la radio (58,3%) y finalmente el periódico (25,6%).

Tabla 2. Información básica obtenida de las encuestas.

Variable	**Uso de televisión**		**Uso de radio**		**Uso de periódico**	
Carreras	**Sí (%)**	**No (%)**	**Sí (%)**	**No (%)**	**Sí (%)**	**No (%)**
Ciencias de salud	158 (72,5)	12 (5,5)	127 (58,3)	43 (19,7)	56 (25,6)	114 (52,8)
Ciencias de educación	22 (10,1)		19 (8,7)	3 (1,4)	15 (6,9)	5 (2,3)
Ciencias jurídicas	10 (4,6)		8 (3,7)	2 (0,9)	5 (2,3)	5 (2,3)
Arquitectura	2 (0,9)		2 (0,9)			2 (0,9)
Ingenierías	7 (3,2)		7 (3,2)			7 (3,2)
Periodismo	7 (3,2)		7 (3,2)		6 (2,7)	1 (0,5)
Totales	206 (94,5)	12 (5,5)	170 (78)	48 (22)	82 (38)	134 (62)
Total general	**218 (100)**		**218 (100)**		**216 (100)**	

Nota: los porcentajes totales están calculados con base a la muestra de 220 sujetos.

En la tabla 3 como resultado de la contabilización de los anuncios en cada uno de los medios evaluados se observó que, aunque la cantidad de publicidad encontrada es alta en cada medio, no se logró encontrar un porcentaje de anuncios de medicamentos relevante.

Tabla 3. Publicidad de medicamentos en los medios de comunicación de preferencia por los estudiantes.

Medios de comunicación		**Total de anuncios generales semanal**	**Total de anuncios de medicamentos semanal**	**Cantidad total de anuncios (100)**	**Porcentajes de anuncios de medicamentos (%)**
Periódicos	Periódico 1	1031	01	1032	0,10
	Periódico 2	531	0	531	0
	Periódico 3	137	0	137	0
Radio	Emisora 1	118	18	136	13,24
	Emisora 2	44	07	51	16
	Emisora 3	69	0	0	0
Televisión	Canal nacional 1	221	16	237	6,75
	Canal nacional 2	289	13	302	4,50
	Canal nacional 3	208	0	208	0

En la tabla 4 se presentan los productos encontrados y analizados de los diferentes medios de comunicación. El único anuncio en periódicos, en el cual se observó que no cumple con el reglamento de publicidad por falta de información. Los anuncios en radio por lo general no cumplieron de forma adecuada lo que se estipula en el reglamento.

Para anuncios televisivos se puede visualizar pautas publicitarias de medicamentos de venta libre que no cumplieron con el reglamento a pesar de que presentan menos regulaciones hasta publicidad de medicamentos que no son de venta libre y decidieron omitir lo solicitado por el reglamento.

Discusión

Estudios señalan que las fuentes de información de los jóvenes son la familia, los amigos y los medios de comunicación. De los 3 medios de comunicación en estudio, la

Tabla 4. Totales de anuncios en medios de comunicación y observaciones según acatamiento al reglamento de publicidad de medicamentos en Costa Rica.

Categoría	Producto	Cumple	No cumple	Observaciones
Antiinflamatorios no esteroideos	Diclofenaco en combinación		X	Omiten presentaciones disponibles, forma farmacéutica, composición de producto, casa fabricante y categoría del producto.
	Naproxeno sódico		X	Indican la dosificación con respecto al medicamento (prohibido para medicamentos de venta libre). Omitieron las leyendas: "Antes de consumir este medicamento, lea la información de la etiqueta" y "Todo medicamento posee efectos secundarios".
	Diclofenaco con Tiocolchicósido		X	No cumple prácticamente con nada.
	Ácido acetilsalicílico 650 mg	X		Cumple con lo solicitado por el reglamento de publicidad de medicamentos de venta libre.
	Ácido acetilsalicílico 100 mg		X	Omitieron las leyendas: "Antes de consumir este medicamento, lea la información de la etiqueta" y "Todo medicamento posee efectos secundarios".
	Naproxeno en combinación		X	No cumple en su publicidad ya que indica la dosificación con respecto al medicamento.
Antihistamínicos	Fexofenadina		X	Omitieron categoría del producto y presentaciones disponibles.
	Cetirizina en combinación		X	Omitieron composición del producto (principios activos), casa fabricante, categoría del producto, presentaciones disponibles.
Antigripales	Paracetamol, amantadina en combinación		X	Omiten las leyendas: "Antes de consumir este medicamento lea la información de la etiqueta" y "Todo medicamento posee efectos secundarios".

(*Continúa*)

Tabla 4. Totales de anuncios en medios de comunicación y observaciones según acatamiento al reglamento de publicidad de medicamentos en Costa Rica.

Categoría	Producto	Cumple	No cumple	Observaciones
Descongestionante	Inhalador		X	Omiten nombre comercial, indicación(es), y características atribuibles al producto aprobada(s) por el ministerio, presentaciones disponibles, forma farmacéutica, composición del producto (principios activos), casa fabricante, categoría del producto.
Antitusivo	Hederá Hélix L.		X	Omiten las leyendas que exige la ley como lo son: "Antes de consumir este medicamento lea la información de la etiqueta" y "Todo medicamento posee efectos secundarios".
Vacuna	Virus del Papiloma Humano		X	Omiten nombre comercial, indicación(es), y características atribuibles al producto aprobada(s) por el ministerio. Forma farmacéutica, composición del producto, leyendas "Todo medicamento posee efectos secundarios", "Este medicamento requiere receta médica" y "Consulte con su médico", casa fabricante.
Antimicótico	Clotrimazol		X	Omitieron composición del producto (principios activos), categoría del producto.
Antiagruras	Bicarbonato de sodio y potasio en combinación	X		Cumplió con lo solicitado por el reglamento de medicamentos de venta libre.

televisión es la que presenta los mayores porcentajes de uso, esto coincide con el reporte en lo reportado en la literatura [7]. En Costa Rica el medio de comunicación que menos frecuencia se usó reporta en la población universitaria es el periódico. La Universidad de Salamanca (2010) indica que los índices de lectura de prensa se están reduciendo y lo hacen de manera especialmente significativa entre los lectores más jóvenes [8]. El consumo de medios por parte de este sector de la población difiere mucho de generaciones anteriores y es de prever que seguirá por ese camino en las generaciones futuras,

cuyo acceso a la información de actualidad estará cada vez más mediatizado por las innovaciones tecnológicas.

El medio de comunicación preferido por los estudiantes universitarios después de la televisión es la radio. Según Martínez y Prata [9], "el objetivo de todo proceso de comunicación es llegar al destinatario, ya que lo contrario sería un ejercicio estéril de emisión y de derroche de energías que se perderían en el aire". Los casos recopilados demuestran que la radio permanece activa en este objetivo y en la reinvención de las formas en que dialoga con su audiencia, porque encuentra nuevos lenguajes y formas de construir y consolidar sus comunidades de oyentes.

Es evidente la falta de interés por parte de las industrias farmacéuticas de explotar los periódicos como medio de comunicación, ya que se contabilizaron un total de 1760 anuncios semanales entre los tres medios de comunicación, solo hubo un anuncio de medicamentos en prensa, este es un porcentaje demasiado bajo, 0,060%, esto por no decir que es un porcentaje despreciable. El anuncio encontrado incumplió con el reglamento de publicidad, pues solamente hacían referencia a una promoción (oferta por compra del producto). Es evidente que el periódico es un medio que presenta poco interés para generar publicidad por medicamentos en Costa Rica. Quizás la falta de interés de las industrias farmacéuticas está muy relacionada al desinterés de la población en adquirir un periódico para leerlo. Según el Instituto Nacional de Estadística y Censos (INEC) [10], una de las razones por las que las personas no leen un periódico es por desinterés o simplemente no es de su agrado, también manifiestan que una segunda razón es por la falta de tiempo y como una última opción consideran que el sitio para conseguirlos queda lejos.

En el caso de la radio hay un escenario más alentador en comparación con el periódico, pues este si refleja más interés por parte de la industria farmacéutica para dar a conocer sus productos. La industria farmacéutica usa la radio porque es de fácil acceso para los consumidores, además de considerarse uno de los medios más usados desde la antigüedad. La música que se usa en los mensajes publicitarios rompe la línea narrativa del discurso y crea en el oyente un estado de curiosidad que le hace prestar una mayor atención al mensaje publicitario, quizá por ello la radio sea un medio muy usado para hacer llegar la publicidad [11].

Con respecto de los 3 medios analizados el que presenta más anuncios a la semana y de igual manera más anuncios de medicamentos es la Radio. Al analizar cada uno de los anuncios de medicamentos en las diferentes emisoras se encontró que muchas veces se omiten las leyendas que son consideradas de interés o relevantes como: "Antes de consumir este medicamento lea la información de la etiqueta" y "Todo medicamento posee efectos secundarios", y esto claramente atenta contra la reglamentación nacional, y

puede tener implícito posibles efectos nocivos sobre la población. Al omitir las leyendas anteriormente indicadas no se concientiza a las personas del uso de los medicamentos, aunque sean de venta libre, los medicamentos tienen un riesgo al generar un efecto no deseado o incluso una intoxicación, por tal razón debe hacerse publicidad que no omita información de relevancia para los consumidores y les recuerde la importancia de leer las etiquetas de cada medicamento y tomar las medidas pertinentes para usar los mismos.

Respecto a la publicidad en televisión es prohibido hacer referencia a la dosificación y en algunos casos se ejemplifican el uso de 2 pastillas como dosis, inclusive se comparan algunos medicamentos indicando que: "2 pastillas (principio activo naproxeno) son igual de fuertes que 8 de otras". Se debe hacer referencia a que los anuncios de fármacos que son de venta libre no necesitan la aprobación del Ministerio de Salud para ser publicados, ya que, conforme al *Reglamento para la autorización y control sanitario de la publicidad de productos de interés sanitario N.º 36868-S*: "Artículo 17. La publicidad o promoción de los medicamentos estará sujeta a la aprobación previa del ministerio. A excepción de los declarados de venta libre cuya fiscalización se realizará a *posteriori*". Por tal razón se podría deducir que existe la posibilidad que todavía no hayan sido analizados y por ende se presente ese "error" en la publicidad, la cual podría generar confusión en los consumidores a la hora de la dosificación del mismo [12].

El caso de mayor relevancia, de la situación antes descrita, corresponde al de diclofenaco con tiocolchicósido, este no es un medicamento de venta libre, por ende, necesita la autorización por parte del Ministerio de Salud para poder ser publicado, sin embargo, genera dudas ya que en su anuncio no cumplió con las disposiciones del reglamento para los medicamentos que no son de venta libre, para el momento en que se realizó el análisis.

La mayoría de los anuncios de televisión en su mayoría incumplían con las disposiciones solicitadas por el reglamento, aunque contaban con el permiso del Ministerio Salud. El resultado obtenido nos hace ver que las regulaciones en la promoción de un medicamento son importantes para proteger a los consumidores. En las industrias farmacéuticas, las ganancias van a depender de su mercadotecnia, y para aumentarlas por medio de la promoción, donde podrían generar sino se hace correctamente una mala utilización de los medicamentos.

La fiscalización de la promoción de medicamentos está lejos de ser perfecta, la Organización Mundial de la Salud (OMS), en 2013 encontró que solo 20% de los países poseía regulación farmacéutica, también poco menos de la mitad de los 89 países informaron que tenían alguna manera de regularla, sin embargo, se dice que el problema es la cantidad de tiempo y esfuerzo que invierte el personal encargado de dichas regulaciones [13].

En Costa Rica, el reglamento de publicidad de medicamentos menciona que:

> En caso de existir una propaganda o publicidad que incumpla con una o más disposiciones del presente reglamento, la Dirección de Regulación de la Salud presentará la respectiva denuncia ante la Comisión Nacional del Consumidor para que proceda conforme lo establece la Ley N.º 7472 y su reglamento [14]. Asimismo, en el caso que se presuma la existencia de un ilícito penal se dará parte a los órganos judiciales competentes.

Además:

> El incumplimiento a las disposiciones establecidas en este reglamento dará lugar a la aplicación de las sanciones y medidas especiales que señala la Ley General de Salud N.º 5395 del 30 de octubre de 1973, en respeto al debido proceso y derecho a defensa al administrado [6].

Entre las sanciones encontradas según la Ley de Promoción de la Competencia y Defensa Efectiva del Consumidor N.° 7475 se menciona la siguiente sanción, en donde se castigará con una multa de diez a cuarenta veces el menor salario mínimo mensual establecido en la Ley de Presupuesto Ordinario de la República, por la desobediencia al artículo 34. Obligaciones del comerciante inciso m, por el incumplimiento con lo dispuesto en las normas de calidad y las reglamentaciones técnicas de acatamiento obligatorio [15]. Según la Ley General de Salud N.° 5395

> Artículo 382.- Será reprimido de veinte a sesenta días multa el que hiciere publicidad o propaganda engañosa o ambigua que pueda ser perjudicial para la salud de las personas o que pueda inducir a error al público en asuntos relativos a la conservación o recuperación de la salud, a menos que el hecho constituya delito [15].

De esta manera podemos darnos cuenta de que sí existen disposiciones que castigan las infracciones al reglamento, aunque las pautas publicitarias no están completas muchas obtuvieron la respectiva autorización del Ministerio de Salud para ser trasmitidas, por tanto, la publicidad depende del criterio del ente regulador [15].

Con dicha investigación se logró determinar que Costa Rica no es la excepción al incumplimiento del reglamento sobre la publicidad de medicamentos, como se ha demostrado en investigaciones realizadas en otros países, uno de ellos Colombia, donde González-Acuña *et al.*, identificaron que un porcentaje importante de publicaciones incumplían algunos de los criterios establecidos por el Instituto Nacional de Vigilancia de Medicamentos y Alimentos (Invima) y la OMS [16]. También Vacca [17] logró identificar que en otros países latinoamericanos se incluían las indicaciones

del fármaco y un 70% omitían información sobre los efectos adversos, además mencionaban indicaciones no aprobadas por la autoridad sanitaria. Lo que sucede en Costa Rica es una situación que se repite en muchos países, y que no se debe ver como algo poco frecuente. Esto es un ejemplo para tratar de mejorar en dicho tema y acoplarse de manera más rigurosa a las reglas establecidas por los reglamentos vigentes.

Como se ha dejado notar en la presente investigación, una limitación del tiempo para poder visualizar, leer o escuchar por más tiempo la información que se brinda en los diferentes medios de comunicación, como sugerencia se debería de realizar una investigación con horarios más amplios, para así analizar más publicidad generada en diferentes horas del día, que quizás son más afluentes para los medios y factibles para las industrias. De esta manera se obtendría una mayor cantidad de anuncios de medicamentos que bien podrían ser analizados y que se encuentran fuera del horario en que se llevó a cabo esta investigación.

Finalmente, la televisión es el medio de comunicación de mayor consumo por la población universitaria, según los resultados esto puede tener influencia en las mujeres y principalmente estudiantes del ámbito de salud. De la misma manera el análisis de los otros medios de comunicación, como lo es la radio y el periódico indicaron que las mujeres siguen siendo el género que más uso les da a los medios de comunicación con respecto a los hombres. La radio es el medio más utilizado para generar publicidad de medicamentos, seguida por la televisión. En el caso del periódico no se evidencia publicidad por parte de la industria farmacéutica. Debe resaltarse que los anuncios de medicamentos no lograron cumplir con el reglamento de publicidad, según la legislación costarricense. Se debe de generar más conciencia de la falta de una legislación más estricta por parte de los entes regulatorios para las pautas publicitarias para que las personas le puedan dar a los medicamentos el uso correcto.

Contribución de autores

Yenifer Corrales-Cubillo: diseño del estudio, recolección de datos, análisis de datos y escritura del manuscrito. Nathalie Saborío-Quesada: recolección de datos y análisis de datos. Ramsés Alfaro- Mora: concepción del estudio, diseño del estudio, escritura del manuscrito y aprobación final.

Conflicto de interés

Los autores no declaran tener conflicto de interés.

Referencias

1. T. Rusell, R. Lane, *Publicidad*, 12 ed., Editorial Prentice Hall, México, 1993.

2. Ministerio de Ciencia, Tecnología y Telecomunicaciones, *Acceso y uso de los servicios de telecomunicaciones en Costa Rica*, URL: https://www.micit.go.cr/?option=com_content&view=article&id=9886%3Amicitt-presenta-los-resultados-de-la-encuesta-de-acceso-y-uso-de-los-servicios-de-telecomunicaciones-en-costa-rica-2015&catid=40&Itemid=630

3. L. Porras-Alvarado, R. Vargas, E. Jara-Tenorio, Ministerio de Economía, Industria y Comercio, *Diagnóstico del mercado de medicamentos*, Costa Rica, URL: http://reventazon.meic.go.cr/informacion/estudios/2015/medicamentos.pdf., 2015.

4. S. Forner, M. Santos da Silva, F. Stolf-Brzozowski, Instituto Salus, *Publicidad de medicamentos, automedicación y ética farmacéutica: una tríada farmacéutica*, Salud y Fármacos, Disponible en: http://www.saludyfarmacos.org/lang/es/boletin-farmacos/boletines/feb2013/publicidad-de-medicamentos-automedicacin-y-tica-farmacutica-una-trada-farmacutica/, 2013.

5. B. Erickson, *La publicidad*, 2 ed., Editorial Playor, Madrid, 2001.

6. Sistema Costarricense de información Jurídica, *Reglamento para la autorización y control sanitario de la publicidad de productos de interés sanitario*, URL: http://www.pgrweb.go.cr/scij/Busqueda/Normativa/Normas/nrm_texto_completo.aspx?param1=NRTC&nValor1=1&nValor2=71585&nValor3=86939&strTipM=TC, 2000.

7. S. Reigosa, Televisión y adolescencia: valores y aspiraciones académico-profesionales, *Revista Española de Orientación y Psicopedagogía*, **20**(2), 174-183 (2009).

8. P. Sonia, ¿Por qué los jóvenes no leen periódicos? Análisis y propuestas, II Congreso Internacional Comunicación 3.0, 4 y 5 de octubre de 2010, Universidad de Salamanca, URL: http://campus.usal.es/~comunicacion3punto0/comunicaciones/080.pdf, 2010.

9. M. Martínez-Costa, N. Prata, La radio en busca de su audiencia: hacia una escucha diversificada y multiplataforma, *Intercom-RBCC (São Paulo)*, **40**(3), 109-128 (2017).

10. Instituto Nacional de Estadística y Censos, Costa Rica, *El 92,4% de los habitantes del país ven televisión*, URL: http://inec.cr/noticia/el-924-de-los-habitantes-del-pais-ven-television

11. D. Cagua, D. Cisneros, D. Chilliquinga, A. Bilbao, B. Molina, A. Obando, A. Fernández, Influencia de la publicidad radial y televisiva en Sangolquí, Ecuador, *Lecturas: Educación Física y Deportes, Revista Digital (Buenos Aires)*, **20**(211), 1-11 (2015).

12. D. Alfaro-Monge, Causas y consecuencias de la automedicación: Experiencia de 10 adultos mayores del Cantón de Grecia durante el I trimestre de 2016, *Pro Veritatem*, **2**(2), 8-28 (2016).

13. OMS, Perspectivas políticas de la OMS sobre medicamentos, 2000-2003, URL: https://apps.who.int/iris/bitstream/handle/10665/66775/WHO_EDM_2000.4_spa.pdf;sequence=1, 2003.

14. Sistema Costarricense de información Jurídica, Costa Rica, *Ley General de Salud*, URL: http://www.pgrweb.go.cr/scij/Busqueda/Normativa/Normas/nrm_resultado_simple.aspx?param1=NER&param2=1&param3=FECHA&param4=DESC&param5=Ley%20General%20de%20Salud, 1973.

15. Sistema Costarricense de información Jurídica, Costa Rica, *Ley de promoción de la competencia y defensa efectiva del consumidor*, URL: https://www.pgrweb.go.cr/scij/Busqueda/Normativa/Normas/nrm_texto_completo.aspx?param1=NRTC&nValor1=1&nValor2=26481&nValor3=92463&strTipM=TC, 1994.

16. A.A. González-Acuña, L.D. Vargas-Zapata, J.J. López-Gutiérrez, Evaluación de la publicidad de medicamentos y suplementos dietarios en un canal de televisión dentro de la franja horaria central, *Rev. Colomb. Cienc. Quím. Farm.*, 47(2), 169-183 (2018).

17. C. Vacca, C. Vargas, M. Cañas, L. Reveiz, Publicidad y promoción de medicamentos: regulaciones y grado de acatamiento en cinco países de América Latina, *Rev. Panam. Salud Pub.*, **29**(2), 76-83 (2011).

Como citar este artículo

Y. Corrales-Cubillo, N. Saborío-Quesada, R. Alfaro-Mora, Evaluación de la publicidad de medicamentos en los principales medios televisivos, radiofónicos y escritos en Costa Rica, *Rev. Colomb. Cienc. Quím. Farm.*, **49**(2), 387-400 (2020).

Scientific research article / *http://dx.doi.org/10.15446/rcciquifa.v49n2.89704*

Talinum paniculatum: a plant with antifungal potential mitigates fluconazole-induced oxidative damage-mediated growth inhibition of *Candida albicans*

Cláudio Daniel Cerdeira[1]*, Jeferson J. da Silva[2a], Manoel F. R. Netto[2b], Marcelo F. G. Boriollo[2c], Gabriel O. I. Moraes[1a], Gérsika B. Santos[1b], Luis F. C. dos Reis[3], Maísa R. P. L. Brigagão[1c]

[1]Department of Biochemistry (DBc), Institute of Biomedical Sciences (IBS), Federal University of Alfenas (UNIFAL-MG), Alfenas, 37130-001, Minas Gerais (MG), Brazil.

[2]Laboratory of Microbiology and Immunology, Department of Oral Diagnostic, Dental school of Piracicaba, State University of Campinas (FOP/UNICAMP), Piracicaba, 13414-903, São Paulo (SP), Brazil.

[3]Laboratory of Medicinal Plants, UNIFAL-MG, Alfenas, 37130-001, MG, Brazil.

Corresponding author E-mail address: [1]daniel.cerdeira.84@gmail.com, Orcid ID: https://orcid.org/0000-0002-7242-8028.

Other authors' e-mails: [2a] jefersonbiomed@hotmail.com, [2c]manoelfrn@hotmail.com, marcelofgb@yahoo.com.br, [1a]gabriel.g8@gmail.com, [1b]gersika.santos@unifenas.br, [3]luis_cunhaz@yahoo.com.br, [1c]maisaunifal@gmail.com

Received: 3 March 2019

Revised: 13 May 2020

Accepted: 14 May 2020

Summary

Aims: This study investigated the bioactivity of the crude leaf extract (CLE) and fractions hexane (HX) and ethyl acetate (EtOAc) from *Talinum paniculatum* alone and in association with fluconazole (FLC) against reference strain and clinical isolates of FLC-resistant *Candida albicans*. Furthermore, the antioxidant capability, chemical composition of this plant, and the effect's underlying mechanisms were evaluated. **Methods:** The antifungal activity was evaluated using checkerboard assay to establish the minimum inhibitory (MIC) and minimum microbicidal concentrations (MMC). During FLC and plant products challenges, the reactive oxygen species (ROS) generation (hydroxyl radicals [HO•]) were detected in *C. albicans* cells using the membrane-permeable fluorescent probes APF and HPF. High-performance liquid chromatography (HPLC) profile, quantitative analysis of antioxidant compounds, and free radical scavenging activity (DPPH assay) tests were performed. **Results:** The CLE and fractions presented outstanding antifungal activity and selectivity against *C. albicans* cells but had no synergistic effects with FLC. The MIC values for CLE and its fractions against *C. albicans* reference strain were in the order of HX (31.25 $\mu g\,ml^{-1}$) < EtOAc (62.5 $\mu g\,ml^{-1}$) < CLE (500 $\mu g\,ml^{-1}$), and

against FLC-resistant *C. albicans* HX (125 $\mu g\,ml^{-1}$) = EtOAc < CLE (500 $\mu g\,ml^{-1}$). CLE and its fractions had more potent antifungal activities than FLC against the clinical isolates. Moreover, fungicidal effects for these plant products were demonstrated against FLC-resistant *C. albicans*, which further confirmed an antifungal potential. Conversely, during association, plant products were shown to cause an increase in FLC MIC anywhere from 2- to 16-fold. FLC exposure led to an increase in the steady-state levels of ROS ($HO^{\bullet}$) in *C. albicans* cells. Next, we found that the increases in FLC MICs were owing to action of antioxidants containing-CLE and its fractions in preventing FLC-induced ROS-mediated growth inhibition of *C. albicans*. **Conclusion:** *T. paniculatum* can be a source of bioactive compounds with antifungal potential. However, because of the common use of its edible leaf, caution is advised during therapy with FLC (since it can decrease FLC susceptibility).

Key words: Antimicrobial resistance, *Candida albicans*, susceptibility, reactive oxygen species, *Talinum paniculatum*, fluconazole.

Resumen

Talinum paniculatum: una planta con potencial antifúngico atenúa la inhibición del crecimiento de *Candida albicans* mediada por el daño oxidativo inducido por fluconazol

Objetivos: este estudio investigó la bioactividad del extracto de hoja en bruto (EHB) y las fracciones hexano (HX) y acetato de etilo (AcOEt) de *Talinum paniculatum* solo y en asociación con fluconazol (FLC) contra cepas de referencia y aislados clínicos de *Candida albicans* resistente a FLC. Además, evaluó la capacidad antioxidante, la composición química de esta planta y los mecanismos subyacentes del efecto fungicida. **Métodos:** la actividad antifúngica se evaluó mediante microdilución en caldo para establecer las concentraciones inhibitorias mínimas (CIM) y microbicidas mínimas (CMM). Durante el tratamiento con FLC y productos vegetales se detectó la generación de especies reactivas de oxígeno (ERO) (radicales hidroxilo [$HO^{\bullet}$]) en células de *C. albicans* utilizando las sondas fluorescentes permeables a la membrana APF y HPF. El perfil de cromatografía líquida de alta resolución (CLAR), el análisis cuantitativo de compuestos antioxidantes y el ensayo DPPH fueron evaluados. **Resultados:** el EHB y las fracciones presentaron una excelente actividad antifúngica y selectividad contra las células de *C. albicans*, pero no tuvieron efectos sinérgicos con FLC. Los valores de CIM para EHB y sus fracciones contra la cepa referencia de *C. albicans* fueron del orden de: HX (31,25 $\mu g\,ml^{-1}$) < AcOEt (62,5 $\mu g\,ml^{-1}$) < EHB (500 $\mu g\,ml^{-1}$), y contra C. albicans resistente a FLC: HX (125 $\mu g\,ml^{-1}$)= AcOEt < EHB (500 $\mu g\,ml^{-1}$). EHB y sus fracciones fueron más potentes antifúngicos que

FLC contra los aislados clínicos. Además, estos productos vegetales tienen efectos fungicidas contra *C. albicans* resistentes a FLC, esto confirmó el potencial antifúngico. Por el contrario, durante la asociación se demostró que los productos vegetales causan un aumento en la CIM de FLC de 2 a 16 veces. La exposición a FLC aumentó los niveles de ERO (HO•) en las células de *C. albicans*. Los aumentos en las CIM de FLC se debieron a la acción de los antioxidantes presentes en EHB y sus fracciones para prevenir la inhibición del crecimiento mediada por ERO inducida por FLC en *C. albicans*. Conclusión: *T. paniculatum* puede ser una fuente de compuestos bioactivos con potencial antifúngico. Sin embargo, debido al uso común de su hoja comestible, se recomienda usarla con precaución durante la terapia con FLC (ya que puede disminuir la susceptibilidad a FLC).

Palabras clave: Resistencia a los antimicrobianos, *Candida albicans*, especies reactivas de oxígeno, *Talinum paniculatum*, fluconazole.

Introduction

Over the last few decades, the relentless increase of antimicrobial resistance and multidrug resistance (AMR/MDR) in microorganisms has been observed in low-, middle-, and high-income countries and has resulted in mortality rates in patients who have hospital- or community-associated infections (HAI/CAI) reaching numbers comparable to the pre-antimicrobial era [1-4]. The ever-increasing incidence of AMR/MDR combined with a weak pipeline of new antimicrobial agents launching on the market has created a great threat to the successful management of infectious diseases as well as a major global public health problem [5-7].

Since the early 1980s, AMR has risen to alarming levels in *Candida albicans* (i.e., elevated MICs to azoles and cross-resistance to related antifungal agents) –a frequent pathogen of immunologically compromised individuals, but an even more common commensal fungus from the microbiome of healthy humans–, and the severity of candidiasis caused by antimicrobial-resistant *C. albicans* strains has increased over the years due to clinical interactions, such as the use of corticosteroids, immunosuppressive agents, radiotherapy, and anti-tumoral chemotherapy [1, 2, 8]. Furthermore, the spread of resistance, emergence of highly virulent and pathogenic strains of *C. albicans* that commensally colonize 30-70% of healthy individuals, and formation of biofilms underlie chronic and recurrent infections accordingly have increased the ability of this microorganism to cause disease, further aggravating the issue of AMR/MDR. These factors are, at least partially, responsible for the high invasive fungal infections (IFIs) and mortality rates from *C. albicans* infections [2].

Approximately 400 000 life-threatening infections caused by *C. albicans* are reported per year worldwide. In the United States, from the estimated 46 000 healthcare-associated *C. albicans* infections reported each year, 3400 are caused by Fluconazole-resistant *C. albicans*, with approximately 220 deaths. In this context, regarding level of concern, Fluconazole-resistant *C. albicans* is today recognized by the centers for disease control and prevention (CDC) as a "serious threat" to people's health, the second major threat into one of three threat categories: urgent, serious, and concerning. In Brazil, the real data are still underestimated, but studies have showed a considerable prevalence of Fluconazole-resistant *C. albicans* infections, and besides the natural process of AMR/MDR, the inadequate antimicrobial use (most from food production) is the single most important factor leading to antibiotic resistance in this country [9-12].

The serious threat of AMR/MDR in *C. albicans* strains represents a current public health problem and poses a burgeoning need for new antifungal agents that can tackle AMR/MDR as well as novel antifungal agent deployment strategies are imperative and urgent, to address the issue of AMR/MDR [6,9-13]. Moreover, new antifungal mechanisms are a field to be explored against the broad antifungal resistance seen in epidemiology. Among the approaches to cope with AMR, plants have been used for medicinal purposes long before recorded history [14]. *Talinum paniculatum* (Jacq.) Gaertner (*Talinaceae* family) is commonly known in Brazil as "Erva-gorda" and "Língua-de-vaca", or Jewels of Opar and Ginseng Java worldwide. Nowadays, this plant is widely spread throughout the world and all Brazilian territories. Its edible leaves are succulent subshrub and make an excellent addition to salads, among other culinary purposes (a non-conventional edible leaf) [15].

In folk medicine, *T. paniculatum* is used to treat several pathological conditions including headaches, ulcers, and diarrhea; as an emollient for fighting gastrointestinal disorders; and used topically to combat a broad spectrum of wounds and skin infections. Furthermore, it is used to ease digestion, moisten the lungs, as an aphrodisiac, and to promote breast milk production [15, 16]. Studies have demonstrated the phytochemical constitution [17] and several bioactivities of this plant and its metabolites, including antibacterial and antifungal [18], estrogenic [19], antifertility [20], antinociceptive [21], and the induction of uterine contractility [16].

Over the past decade, intense investigation revealed that the action of antibiotics with specific targets into microbial cells can be accompanied by oxidative stress (i.e., mainly via an increase in respiratory chain–dependent reactive oxygen/nitrogen species [ROS/RNS] production), which is considered a common mechanism of antibiotic-mediated cell death (referred to as "unified mechanism of killing"), as those seen during the killing of *C. albicans*, *Staphylococcus aureus*, *Escherichia coli*, *Mycobacterium*

tuberculosis, and *Pseudomonas aeruginosa* [22-25]. Recently, a great number of antibiotics have been demonstrated to stimulate the production of ROS in microbial cells [22-25]. More specifically, studies conducted by Kobayashi *et al*. [26]; Silva *et al*. [23]; and Mahl *et al*. [22] have shown a participation of ROS in antifungal mechanism of fluconazole (FLC)–the first-line antifungal treatment agent against *C. albicans* infections–and other azoles, resulting in oxidative DNA damage-mediated cell death [9].

Additionally, in recent years, studies have shown that the interaction between plant product and antibiotic can increase the minimum inhibitory concentration (MIC) of some antibiotics, so that their actions could be hampered by antioxidants containing-plant products [27, 28]. This effect could be from a previous decrease in oxidants; thus, compromising the mechanisms of antibiotic-induced ROS/RNS-mediated cell death, such as ROS-induced guanine pool oxidation that leads to double-strand DNA breaks and cell death. This might also have consequences *in vivo*, reducing the pharmacokinetics, efficacy, and even safety of antibiotics and leading to microbial resistance, causing high medical costs during treatment and higher risk of death for patients [27, 28].

In that way, reductive stress caused by antioxidants has been investigate in the non-communicable diseases, for example, cardiovascular disease and cancer (i.e., via down regulation of Nrf2 pathways), and communicable diseases, for example, infectious diseases (i.e., via a decrease in oxidants generated in phagocytic cells) [29, 30]. However, the influence of reductive stress on the susceptibility of microorganisms to antibiotics remains poorly explored. Moreover, to the best of the authors' knowledge, there are no reports about the influence of *T. poaniculatum* on the susceptibility of *C. albicans* to FLC. The elucidation of possible interactions between antioxidants-rich foods and antibiotic is important because of many nutrition products and medicines –including the leaves from *T. paniculatum* that are often used as a green leafy vegetable for human consumption– may interact with antibiotics during medical treatment and modify their action hence having a great impact on clinical practice and patient outcomes.

Based upon the above, we evaluated the antifungal activity of the crude leaf extract (CLE), fractions hexane (HX), and ethyl acetate (EtOAc) from *T. Paniculatum*, alone or in association with the azole antifungal FLC, against reference and FLC-resistant *C. albicans* strains. We also investigated the influence of the CLE, HX, and EtOAc from *T. paniculatum* during the action of FLC against these strains with focus on oxidative/reductive stress. Furthermore, chemical constituents and antioxidant activity of these plant products were checked.

Methodology

Chemicals

Fluconazole (FLC); Roswell Park Memorial Institute (RPMI)-1640 *medium;* 3-(N-morpholine) propanesulfonic acid (MOPS); Ascorbic acid; Benzoic acid (≥ 99.5%); Chlorogenic acid (≥ 95.0%); Caffeic acid (≥ 98.0% HPLC); Ferulic acid (≥ 98.0%); 2,3,5-Triphenyl-2H-tetrazolium chloride (TTC) were purchased from Sigma-Aldrich, St. Louis, MO, USA. 2-[6-(4'-Hydroxy)phenoxy-3H-xanthen-3-on-9-yl] benzoic acid (HPF); and 2-[6-(4'-amino)phenoxy-3H-xanthen-3-on-9-yl]benzoic acid (3′-p-(aminophenyl) fluorescein, APF) were acquired from Life Technologies. Nutriente Agar (Difco); Sabouraud Dextrose Agar (SDA, BD Difco™); Agar/broth Brain Heart Infusion (BHI, HiMedia Laboratories); 3-(4,5-dimethylthiazolyl-2)-2,5-diphenyltetra-zolium bromide (MTT Ultrapure, USB Corp., Cleveland, OH); Dimethyl sulfoxide (DMSO, Neon Comercial); Tryptone Soy Agar (TSA, Oxoid Ltd, London, UK); Sodium chloride 0.9% (145 mM NaCl); Phosphate-buffered saline (PBS, pH 7.4): NaCl (120 m*M*), KH_2PO_4 (1.7 m*M*), Na_2HPO_4 (8.3 m*M*) e KCl (5 m*M*). Others used chemicals and solvents were of analytical grade. The reagents were sterilized in an autoclave (whenever possible) or by filtration (Millipore Corporation, hydrophilic Durapore® PVDF, 0.22 μm, Ø 47 mm).

Ethics statement

This study did not involve any endangered or protected species and no specific permits were required for the described studies. Botanical material from *T. paniculatum* was collected in an area, with access permitted to researchers.

Candida albicans from human subjects were obtained in a previous approved study (FOP/UNICAMP Institution Review Board approved protocol #082/2014) after obtaining an informed consent, in compliance with the relevant laws, institutional guidelines, and ethical standards of the Declaration of Helsinki.

Plant material

Provenience

The leaves from *T. paniculatum* were collected in the mornings of June, near the town of Fama, MG, Brazil (Geographic coordinates obtained from GPS observations: 21º 24' 53.4" S; 45º 52' 15.8'' W). The climate of this region is classified as humid temperate, with a hot summer and a dry winter (type Cwa in the Köppen classification). A voucher specimen was deposited in the UALF Herbarium at the Federal University of Alfenas (UNIFAL-MG) after proper taxonomic identification (sample #2338).

Crude leaf extract (CLE) and fractions (EtOAc and HX) from T. paniculatum

The dried leaf powder (200 g) from *T. paniculatum* was percolated (with an alcohol to water ratio of 7:3) at 1.0 mL/min/kg. After fluid extraction, the fluid was placed in a rotary evaporator under reduced pressure and at a temperature of 45 °C to completely remove the alcohol. The extract was then lyophilized to completely remove water and obtain the dry extract, hereafter referred to as CLE (17.0% yield). To obtain the fractions, the dried extract (CLE) was subjected to a liquid-liquid partition with hexane (1:1, v/v [4×]) or ethyl acetate (1:1, v/v [6×]), yielding hexane (HX) or ethyl acetate (EtOAc) fractions, and a final residue termed the aqueous fraction (this last not used in this study) [18]. At time of their use, the CLE or fractions were solubilized in DMSO (at the concentrations used for solubilization in this study, DMSO does not display antifungal, cytotoxic, antioxidant, or other activities here evaluated) and adjusted at used concentrations.

Antifungal activity

Strains

C. albicans (ATCC® 90028 and ATCC 10231) used in this study were from the American Type Culture Collection (ATCC, Manassas, VA). Antibiotic-resistant *C. albicans* were isolated from clinical source (patients with orofacial cleft), as shown in table 1 and identified as previously reported [31]. AMR in the isolates were interpreted for FLC against *C. albicans* according to document M27A3 (CLSI, 2008) of the Clinical and Laboratory Standards Institute (CLSI), where FLC MIC ≤ 16 μg ml^{-1}= sensitive, MIC 16–32 μg ml^{-1}=intermediate, and MIC ≥ 64 μg ml^{-1}= resistant [32].

Table 1. Used microorganisms, clinical sources, identification, and code.

Microorganism	**Code**	**Source**	**Identification methods**	**Primers (PCR)***
C. albicans	Sample 1	Clinical isolates**	PCR***/MEE	OK3 (forward 5′ - ATG TAT TCA TTA ATC AAA TCA - 3′); OK4 (reverse 5′ - ATT TAA AAA ACA ACG GAC AT - 3′)
C. albicans	Sample 2	Clinical isolates	PCR/MEE Microsatellite loci****	

Microsatellite loci**	**Primers F (forward) e R (reverse)**
CAI (noncoding region) $(CAA)_{32}$	5′ ATG CCA TTG AGT GGA ATT GG (F) 5′ AGT GGC TTG TGT TGG GTT TT (R)
CDC3 (cell division cycle protein) $(AGTA)_8$	5′ CAG ATG ATT TTT TGT ATG AGA AGA A (F) 5′ CAG TCA CAA GAT TAA AAT GTT CAA G (R)

(*Continued*)

Table 1. Used microorganisms, clinical sources, identification, and code.

Microorganism	Code	Source	Identification methods	Primers (PCR)*
CPH1 (Ste 12-like transcription factor) $(CAA)_5(CAG)_1(CAA)_3$... $(CAA)_5(CAG)_5(CAA)_3$				5′ GCC ATG GGA TAT CAA AGC (F) 5′ CTT GGT AAT GCC ACC GCC (R)
ERK1 (extracellular-signal-regulated kinase) $(CAGGCT)a(CAAGCT)_b$ ...$(CAA)_c$...$(GCCGCA)_d$...$(CTT)_e$				5′ CGA CCA CGT CAT CAA TAC AAA TCG (F) 5′ CGT TGA ATG AAA CTT GAC GAG GGG (R)
KRE6 (1,6-glucan synthesis) $(AAT)_n$				5′ CAA GCT TAT AGT GGC TAC TA (F) 5′- CCA ACA CTG ATA CAT CTC G (R)
LOC4 (anonymouslocus) $(GAA)_6$				5′ GTA ATG ATT ACG GCA ATG AC (F) 5′ AGA ACG ACG TGT ACT ATT GG (R)
MNT2 (mannosyltransferase) $(CTT)_5$				5′ GCC AAT ACT GGA AAC TGT GCC (F) 5′ CGG GCT AAA GTG ACA AAT GTG GC (R)
ZNF1 (zinc finger transcription factor) $(CAA)_{8\text{-}11}$				5′ CCA TTA CAG CTG AAC CAG CGA GGG (F) 5′ CGC TAG GTA ACC TAC AGA TTG TGG C (R)

MEE: Multilocus Enzyme Electrophoresis; PCR: Polymerase Chain Reaction; *These species-specific primers for *C. albicans* were used to amplify a DNA fragment of approximately 1,644 bp (PHR1 gene); **Origin: from children with cleft lip and palate; ***Conditions: Amplifications were conducted using an initial program for DNA denaturation at 95 °C for 5 minutes, followed by 30 cycles at 95 °C for 20 seconds (denaturation), 50 °C for 1 minute (annealing), and 72 °C for 1½ minute (extension). The final cycle was conducted at 72 °C for 10 minutes for the final extension; ****(*i*) CAI: initial program for DNA denaturation at 95 °C for 5 minutes, followed by 30 cycles at 94 °C for ½ minute (denaturation), 60 °C for ½ minute (annealing), and 72 °C for 1 minute (extension). The final cycle was conducted at 72 °C for 7 minutes for the final extension, (*ii*) CDC3: initial program for DNA denaturation at 95 °C for 5 minutes, followed by 35 cycles at 95 °C for 1 minute (denaturation), 52 °C for 1 minute (annealing) and 72 °C for 1 minute (extension). The final cycle was conducted at 72 °C for 7 minutes for the final extension, (*iii*) ERK1, KRE6, LOC4 and ZNF1: initial program for DNA denaturation at 95 °C for 5 minutes, followed by 35 cycles at 95 °C for 1 minute (denaturation), 55 °C for 1 minute (annealing) and 72 °C for 1 minute (extension). The final cycle was conducted at 72 °C for 5 minutes for the final extension, (*iv*) CPH1 and MNT2: initial program for DNA denaturation at 94 °C for 5 minutes, followed by 40 cycles at 94 °C for 1 minute (denaturation), 50 °C for 1 minute (annealing) and 72 °C for 1 minute (extension). The final cycle was conducted at 72 °C for 5 minutes for the final extension [31].

Minimum inhibitory concentration and determination of synergistic action

Both plant product (CLE, HX and EtOAc from *T. paniculatum*) and FLC were tested to determine the MIC values against the two resistant *C. albicans* strains, as well as against the reference strain of *C. albicans*, using the broth checkerboard microdilution assay, following the CLSI document M27A3 (CLSI, 2008) [32]. The tests were performed on 96-well microplates (flat-bottom, Corning Inc., NY) containing 100 mL of RPMI-1640 broth (plus phenol red, 1.04% [w/v] of glutamine, 2% [w/v] of glucose, and without bicarbonate) per well, buffered with 165 mM MOPS (pH 7.0 at 25 °C). Afterwards, the CLE or the fractions (EtOAc or HX) were diluted into the wells (the concentration range used was 4000-1.95 $\mu g\,ml^{-1}$ for the CLE, and 500-0.244 $\mu g\,ml^{-1}$ for fractions), either alone or coupled with FLC (final concentrations ranged from 32000 to 15.6 $\mu g\,ml^{-1}$). Microbial suspensions (cultures during the exponential growth phase after an overnight incubation) were centrifuged (900×g for 6 min, 5810R Centrifuge, Eppendorf, NY, USA) and the pellet diluted in sodium chloride 0.9%, and then spectrophotometrically adjusted at 1×10^4 colony-forming units (CFUs)/mL^{-1} ($OD_{530=}$ 0.1= 5×10^6 CFUs/mL^{-1}, further diluted). Afterwards, 10 µL of inoculum were added to the wells.

The plates were then incubated at 37 °C for 48 hours. After the incubation period, readings were performed visually as previously determined [18], wherein the presence of turbidity in the wells was considered indicative of microbial growth, further confirmed using the specific dye TTC to evaluate the metabolic activity of *C. albicans* cells. The $MIC_{99.9}$ of the CLE, fractions (EtOAc or HX) or FLC alone, and all isoeffective combinations (plant product plus FLC) were defined when the growth of the microorganism was inhibited at the lowest concentration relative to the untreated control. The growth control was composed of 100 µL of RPMI-1640 (as above specified) and 10 µL of inoculum. The extract control was composed of 100 µL RPMI-1640 and 100 µL of the CLE or fraction (EtOAc or HX) and the sterility control contained only 100 µL of RPMI-1640.

Minimum microbicidal concentration

The minimum microbicidal concentration (MMC) was defined as the lowest concentration of antibiotic/extract/fractions that killed 99.9% of the original inoculums from each well where growth inhibition occurred in the analysis of MIC/Synergism. For each strain of *C. albicans*, MBC values were determined by removing 100 µl of microbial suspension from each well demonstrating no microbial growth and inoculating them with three serial dilutions of 1:10 onto nutrient agar in plates (plus 2% [w/v] of glucose; Petri plates, 90×15 mm) and then maintaining them at room temperature for complete absorption. After that, the plates were incubated at 37 °C for 48 hours.

Finally, colony counts were performed to determine which concentrations presented microbicidal (fungicidal) or microbistatic (fungistatic) action.

Evaluation of the amount of intracellularly-generated oxidants in C. albicans

The quantification of hydroxyl radicals ($HO^{\bullet}$) generated under the different treatments was performed using the probe APF (highly specific toward $HO^{\bullet}$) and HPF [33]. First, reference strain of *C. albicans* (ATCC 10231) was grown overnight on BHI. Next, microbial suspensions (in exponential-phase growth) were centrifuged (900×g for 6 min) and the pellet diluted in sodium chloride 0.9% and spectrophotometrically adjusted. Afterwards, *C. albicans* cells (1×10^4 CFUs/mL^{-1}) were added on wells of a 96-well microplate and previously treated (for 10 min) with CLE (100 μg ml^{-1}) or fractions (EtOAc [50 μg ml^{-1}] or HX [50 μg ml^{-1}]). After that, FLC treatments (10 μg ml^{-1}) were performed. The control group was comprised of untreated microorganisms. Finally, *C. albicans* cells were loaded with the membrane-permeable fluorescent probes APF or HPF (25 μM, dissolved in DMSO) for 30 min in the dark at 35 °C and then immediately readings took place every 30 minutes over the next 18 hours, using a Varian Cary Eclipse *spectrofluorometer* ($\lambda_{excitation}$=500 nm; $\lambda_{emission}$=520 nm). The results were recorded as arbitrary fluorescent units (AFU) and the fluorescence intensity of the probe is proportional to the amount of ROS ($HO^{\bullet}$).

Cell-free assays

Antioxidant activity of the CLE and fractions from *T. paniculatum.*

The free radical scavenging ability of the CLE and fractions was measured using the 2,2-Diphenyl-1-picrylhydrazyl (DPPH) assay [34]. The results were reported in percentage (%) of $DPPH^{\bullet}$ scavenging activity inhibition.

Quantitative analysis and Chemical characterization of T. paniculatum

Quantitative analysis

The Folin Ciocalteu reagent was used to determine the total polyphenols content of the CLE and fractions according to Fattahi *et al.* [34]. As a standard, gallic acid was used. From the calibration curve, total polyphenol content was expressed in terms of gallic acid equivalent per gram of sample (mg/g).

Chemical characterization of T. paniculatum

High-performance liquid chromatography (HPLC) was performed for analysis of the CLE from *T. paniculatum* using a Shimadzu UFLC 20A CLC-ODS (250-4.6 mm, C18 column and 5 μm particle sizes). Mobile phases were composed of (A) 0.5%

aqueous acetic acid and (B) 0.5% acetic acid in methanol. It was used the mobile phases (A:B) for separation with a linear gradient from 0 to 60 minutes (90:10 to 0:100), solvent flow rate of 1.0 Ml/min, and an injection volume of 25 μL at a concentration of 1 mg/ml. We used the photodiode array detection (DAD) with UV light at 268 nm and the LC solution software (Shimadzu) for data collection. Ascorbic acid, benzoic acid, chlorogenic acid, caffeic acid, and ferulic acid were used as standards.

Data analysis

Results were from three replicates from three independent experiments and values are presented as mean ± SD. To assess the interactions between the CLE, HX, or EtOAc and FLC, the data obtained from the checkerboard microdilution assays were analyzed by a nonparametric model based on the no-interaction theory known as the Loewe additivity model (LA). Using the LA-based model, the nonparametric approach of the model-fractional inhibitory concentration index (FICI) was calculated as follows: FICA= MICAB/MICA and FICB= MICBA/MICB, where MICA and MICB are the MICs of samples A (FLC) and B (extract or fraction) when acting alone, and MICAB and MICBA are the MICs of samples A and B when acting in combination, respectively; thus, the FICI values were expressed as follows: FICA + FICB. "Synergy" was defined as an FICI ≤ 0.5, while "antagonism" was defined as an FICI value > 4.0. A FICI between 0.5 and 1.25 was considered as "Additive effect", while between 1.25 and 4 was considered to have "No interaction" [35-37]. According to the ratio of MMC/MIC, we reported the type of antifungal action displayed by the sample. If the ratio of MMC/MIC= 1 or 2, the effect was considered fungicidal, but if the ratio of MMC/MIC= 4 or 16, the effect was defined as fungistatic [38]. The Selectivity Index (SI) was calculated as follows: SI= $CC_{90}/MIC_{99.9}$, being CC_{90} adopted from our previous study [18]. The significance of difference was analyzed by one-way ANOVA and a Tukey post-test (BioEstat 5.0, Belém, Pará, Brazil, 2007). Significance was accepted at $p<0.05$ (α= 5%), unless indicated otherwise. Structural elucidation of compounds from *T. paniculatum* was performed by interpreting the second mass spectra order upon the fragmentation patter assumption. Structures depicted in this study were constructed on ACD/Labs (Advanced Chemistry Development Inc., version 6.0).

Results

MIC and MBC values for the CLE, EtOAc, and HX from *T. paniculatum*

As observed in **table 2**, high MIC values were observed with FLC measured against the isolates, in which both isolates of *C. albicans* were resistant to this antifungal agent (MIC ≥ 64 $\mu g\,ml^{-1}$). The MIC and MMC values for the CLE, EtOAc, HX, and FLC,

measured against the reference strains of *C. albicans* and FLC-resistant *C. albicans* strains are presented in **table 2**. It was found that for FLC-resistant *C. albicans*, the MIC of both EtOAc and HX was 150 μg ml^{-1}, whereas the MIC against the reference strain was 31.5 μg ml^{-1} for HX and 62.5 μg ml^{-1} for EtOAc. The CLE presented MIC value of 500 μg ml^{-1} against all of *C. albicans* strains. The EtOAc was as effective as FLC against the reference strain of *C. albicans*, whereas this fraction was more effective (< MIC) than FLC against the two FLC-resistant *C. albicans* (clinical isolates). HX fraction had lower MIC values than FLC against all of *C. albicans* strains. The CLE was more effective than FLC against the two antibiotic-resistant *C. albicans*, but not against the reference strain of *C. albicans*.

MIC and MBC values for the associations between plant product (CLE, EtOAc, and HX) and FLC, and FICI from the associations

The interactions from associations between plant products (CLE, EtOAc, or HX from *T. Paniculatum*) and FLC against *C. albicans*, were investigated. As demonstrated in **table 2,** treatment of *C. albicans* using the CLE, EtOAc, or HX alone, resulted in outstanding MIC values (the lowest MIC values). However, when the mixture of extract/fraction and antifungal agent was assayed to determine the type of interaction between the two compounds, FLC MICs increased 2- to 16-fold (table 3), whereas some fractions MICs were shown to be decreased as an effect experienced during these associations. Taken together, data from tables 2 and 3 were interpreted as the FICI values (table 3) in which there was no synergy for any of associations between plant product and antifungal agent. The observed effects for the associations were: "additive effect" (2 associations), "no interaction" (5 associations), or "antagonism" (5 associations).

Antifungal effects/actions for the crude leaf extract (CLE) and fractions

In table 2, it is also shown that the CLE displayed fungicidal action against antibiotic-resistant *C. albicans* (sample 1). There was a fungicidal action from both EtOAc and HX against antibiotic-resistant *C. albicans*, but only HX presented this effect against the two samples (1 and 2), whereas the effect of EtOAc against sample 1 of the antibiotic-resistant *C. albicans* and both fractions against the reference strain of *C. albicans* were fungistatic. Therefore, the EtOAc and HX fractions not only presented the lowest MIC values, but also presented fungicidal action.

Selectivity index (SI) for the CLE and fractions from *Talinum paniculatum*

The results of the SI are presented in table 4 and the best ones were 17.7 and 4.42 (HX against the reference strain of *C. albicans*), 4.85 (EtOAc against the reference strain of *C. albicans*), and 2.76 (CLE against all strains of *C. albicans*).

Table 2. Minimum inhibitory concentration (MIC) and minimum microbicidal concentration (MMC) for the alone crude leaf extract (CLE) and fractions from *Talinum paniculatum* and fluconazole against *Candida albicans* and the types of antimicrobial effects.

Microorganisms	*C. albicans* (ATCC 90028)				*C. albicans* (sample 1)				*C. albicans* (sample 2)			
Extract/ Fraction/ Antibiotic	MIC ($\mu g\,ml^{-1}$)	MMC ($\mu g\,ml^{-1}$)	MMC/ MIC	Antimicrobial Effect	MIC ($\mu g\,ml^{-1}$)	MMC ($\mu g\,ml^{-1}$)	MMC/ MIC	Antimicrobial Effect	MIC ($\mu g\,ml^{-1}$)	MMC ($\mu g\,ml^{-1}$)	MMC/ MIC	Antimicrobial Effect
CLE	500	N	N/A	N/A	500	1000	2	Fungicidal	500	1000	2	Fungicidal
EtOAc	62.5	250	4	Fungistatic	125	125	1	Fungicidal	125	250	2	Fungicidal
HX	31.25	250	8	Fungistatic	125	500	4	Fungistatic	125	125	1	Fungicidal
Fluconazole	62.5	250	4	Fungistatic	2000	8000	4	Fungistatic	2000	16000	8	Fungistatic

Antimicrobial Action: Fungicidal

Fungistatic

For plants products: MIC up to 100 $\mu g\,ml^{-1}$ = promising inhibitory potential, MIC between 100 and 625 $\mu g\,ml^{-1}$ = moderate inhibitory activity [18]. Fractions from the CLE of *Talinum paniculatum*; EtOAc = Ethyl acetate fraction and HX = Hexane fraction; *C. albicans:* samples 1 and 2 are clinical isolates from children with cleft lip and palate*; C. albicans*: 5×10^4 CFU/mL^{-1}; Antimicrobial resistance (AMR) classification: Fluconazole MIC ≤ 8 $\mu g\,ml^{-1}$ = Sensitive, MIC 16-32 $\mu g\,ml^{-1}$ = Intermediate, MIC ≥ 64 $\mu g\,ml^{-1}$ = Resistant [32]. *In vitro* phenotypic "tolerance" has also been defined as an MBC that is ⩾32 times the MIC; Ratio MMC/MIC = 1 or 2 → Effect was considered as microbicidal; Ratio MMC/MIC = 4 or 16 → Effect was defined as microbistatic according to Konaté *et al.*, [38]. N: Inhibition of microbial growth was not observed at maximum concentration (4000 $\mu g\,ml^{-1}$); N/A: Not applicable due to absence as for the inhibition of microbial growth at maximum concentration.

Table 3. Results for the contribution of each compound or plant product in the final MIC value during the association between (1) plant product (Crude leaf extract [CLE], EtOAc, or HX) from *Talinum paniculatum* and (2) antibiotic (Fluconazole) against *Candida albicans*, correspondent fractional inhibitory concentration index (FICI), and interpretation of the FICIs from the associations with the resulting interaction type.

	C. albicans (ATCC 90028)				*C. albicans* (sample 1)				*C. albicans* (sample 2)			
	Concentration ($\mu g\,ml^{-1}$)*		FICI		Concentration ($\mu g\,ml^{-1}$)		FICI		Concentration ($\mu g\,ml^{-1}$)		FICI	
Association	(1)	(2)		Interpretation	(1)	(2)		Interpretation	(1)	(2)		Interpretation
(1) CLE + (2) Fluconazole	625	1000	>4	Antagonism	1000	16000	>4	Antagonism	1000	16000	>4	Antagonism
(1) EtOAc + (2) Fluconazole	3.9	250	>4	Antagonism	62.5	4000	2.5	No interaction	31.25	2000	1.25	Additive effect
(1) HX + (2) Fluconazole	1.9	125	2	No interaction	62.5	4000	2.5	No interaction	62.5	4000	2.5	No interaction
(1) EtOAc + (2) HX	1000	1000	1	Additive effect	125	125	2	No interaction	62.5	62.5	1	Additive effect

Interaction index interpretation: Antagonism; No interaction; Additive effect

*Concentration of each substance in the associations between the (1) crude leaf extract (CLE)/fraction (EtOAc, or HX) from *Talinum paniculatum* and (2) antibiotic (Fluconazole) or (1) fraction and (2) fraction in which no microbial growth was observed; Fractions from the CLE of *Talinum paniculatum*; EtOAc = Ethyl acetate fraction and HX = Hexane fraction; FICI data interpretation from the interactions/associations: 'synergy' (FICI ≤0.5), 'additive effect' (FICI > 0.5-1.25), 'no interaction' (FICI > 1.25–4.0), and 'antagonism' (FICI > 4.0) [35-37].

Chemical characterization, antioxidant property, and total polyphenol content of *T. paniculatum*

Here, we identified compounds likely to be related to the bioactivities. To support the increase in MIC values of FLC in the association with plant products, table 5 shows the antioxidant activity and the total polyphenols content of the CLE and fractions. EtOAc and HX fractions presented higher polyphenols contents and the best results as for antioxidant activity. Table 6 shows some compounds identified by HPLC (retention time in minutes, compared to standards) and illustrates the proposed structures. Figure 1 presents the chromatogram of the CLE, which renders the identified structures drawn on it (compounds also depictured in table 6).

Table 4. Selectivity Index (SI) for the crude leaf extract (CLE) and fractions from *Talinum paniculatum.*

Extract/ Fraction	CLE		EtOAc		HX	
Sample Results						
	MIC	**SI**	**MIC**	**SI**	**MIC**	**SI**
C. albicans (ATCC 90028)	500	2.76	62.5	4.85	31.25	17.7
C. albicans (sample 1)	500	2.76	125	2.42	125	4.42
C. albicans (sample 2)	500	2.76	125	2.42	125	4.42

SI:= $CC_{90}/MIC_{99.9}$; MIC: $\mu g\,ml^{-1}$; Fractions from the CLE of *Talinum paniculatum*; EtOAc= Ethyl acetate fraction and HX= Hexane fraction; CC_{90} data from our previous paper [18].

Table 5. Polyphenols content and antioxidant activity for the crude leaf extract (CLE) and fractions from *Talinum paniculatum.*

Extract/Fraction	CLE	EtOAc	HX
Polyphenols content			
Gallic acid equivalent[1]	20.38[a]	56[b]	52[b]
Antioxidant activity			
DPPH• radical scavenging activity (%)	31.93[a]	77.5[c]	47.98[b]
Ascorbic acid (90.45)			
BHT (63.8)			

Fractions from the CLE of *Talinum paniculatum*; EtOAc= Ethyl acetate fraction and HX= Hexane fraction; [1]gallic acid equivalent per gram of sample (mg/g); [abc]Means followed by the same letter (row) do not differ statistically by the Tukey's test (α= 5%).

Table 6. Chemical compounds found in the crude leaf extract (CLE) and fractions from *Talinum paniculatum*.

Compound	Sample	HPLC Retention time (min)	MS** *m/z* (m^2/z)	MS** *m/z* (m^2/z) (second order mass spectra)	Activities/interactions (references)	Structure
Campesterol	CLE: + EtOAc: + HX:+	----	401	207, 147, and 121	Antifungal [39] Antibacterial [39] Antioxidant [40] Antibiotic interaction: ----	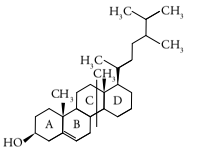
Stigmasterol	CLE: + EtOAc: + HX: +	----	413	207 and 269	Antifungal [39] Antibacterial [39] Antioxidant [40] Antibiotic interaction: ----	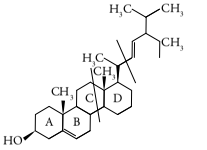
Sitosterol	CLE: + EtOAc: + HX: +	----	415 (M+H)	223, 267, and 355	Antifungal [39] Antibacterial [39] Antioxidant [40] Antibiotic interaction: ----	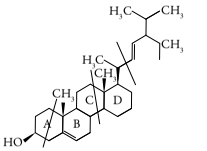
Ascorbic acid	CLE: + EtOAc: ---- HX: ----	3.2	176	----	Antifungal no activity[b], [41] Antibacterial [42,43] Antioxidant [41] Antibiotic interaction [44]	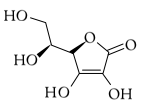
Benzoic acid	CLE: + EtOAc: ---- HX: ----	14.5	122	----	Antifungal [45] Antibacterial [46] Antioxidant [47] Antibiotic interaction [48, 49]	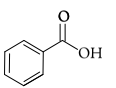

(*Continúa*)

Table 6. Chemical compounds found in the crude leaf extract (CLE) and fractions from *Talinum paniculatum*.

Compound	Sample	HPLC Retention time (min)	MS** *m/z* (m^2/z)	MS** *m/z* (m^2/z) (second order mass spectra)	Activities/interactions (references)	Structure
Chlorogenic acid[c]	CLE: + EtOAc: ---- HX: ----	15	354	----	Antifungal [50] Antibacterial [51,52] Antioxidant [53] Antibiotic interaction [54]	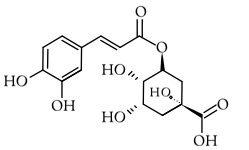
Caffeic acid	CLE: + EtOAc: ---- HX: ----	16.5	180	----	Antifungal [55] Antibacterial [56-57] Antioxidant [53, 57] Antibiotic interaction [49]	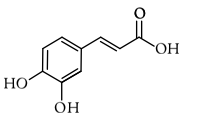
Ferulic acid	CLE: + EtOAc: ---- HX: ----	19	194	----	Antifungal [58] Antibacterial [52, 59] Antioxidant [60] Antibiotic interaction [54]	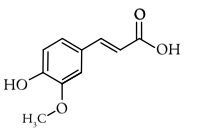

+: presence of the compound; ----: not evaluated; [a] mixture of sterols (Campesterol, **S**tigmasterol, and Sitosterol); [b] up to 250 μg ml^{-1}; [c] MIC of 80 μg ml^{-1} against *C. albicans*; *Interaction between polyphenolic compounds and antibiotics has been reported. Fractions from the CLE of *Talinum paniculatum*; EtOAc= Ethyl acetate fraction and HX= Hexane fraction. HPLC: High performance liquid chromatography; MS: Mass spectrometry: data from our previous paper [18].

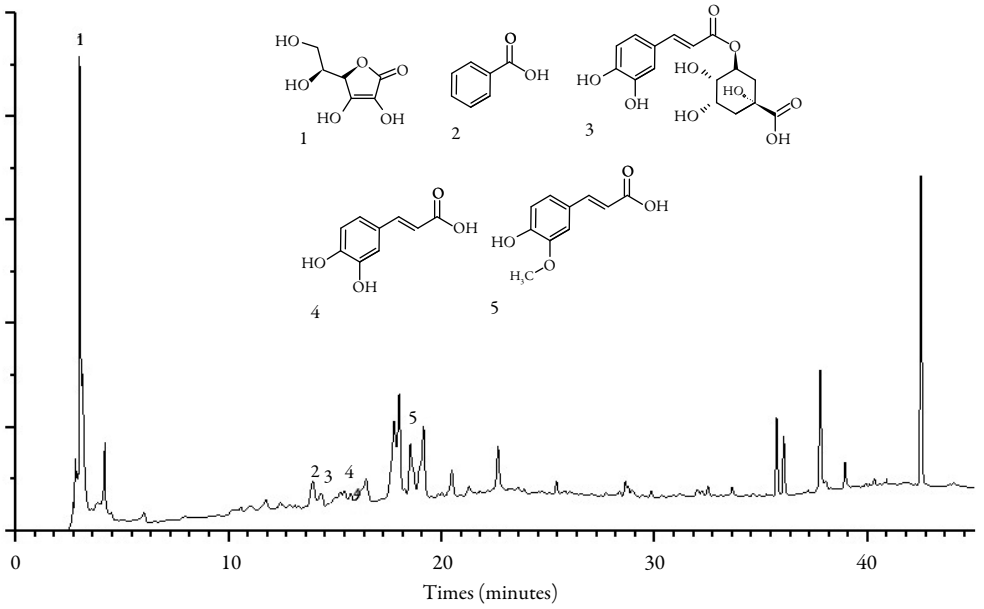

Figure 1. High performance liquid chromatography (HPLC) of the crude leaf extract (CLE) from *Talinum paniculatum*. Based on the peaks at each retention time (minutes) for the sample, related to the used standards, the separation permitted the identification of the following structures: 1: Ascorbic acid, Molar mass (MM)= 176.12 g.mol^{-1}; 2: Benzoic acid, MM= 122.12 g.mol^{-1}; 3: Chlorogenic acid, MM= 354.31 g.mol^{-1}; 4: Caffeic acid, MM= 180.16 g.mol^{-1}; 5: Ferulic acid, MM= 194.18 g.mol^{-1}.

Influence of the CLE, EtOAc, and HX from *T. paniculatum* upon oxidants in *C. albicans*

To explain the increase in MIC values of FLC, when in association with plant products, we performed tests to evaluate the influence of the CLE, EtOAc, and HX from *T. paniculatum* on the levels of oxidants (HO$^{\bullet}$) generated by *C. albicans* cells. The results are shown in figure 2. Increased ROS levels in *C. albicans* cells after FLC exposure was observed (over 18 h), as part of the antifungal action. On the other hand, decreased ROS levels were constated over the 18 h of exposure to FLC, when a previous treatment with plant product (CLE, EtOAc, or HX) was performed. CLE induced the greatest decrease in ROS levels, significant relative to *C. albicans* cells exposed to FLC, *per se*.

Discussion

In this study, we demonstrated that the CLE, EtOAc, and HX from *T. paniculatum* present outstanding antifungal activity against *C. albicans*, with "moderating" or "promising" inhibitory potential [18]. The CLE and its fractions (EtOAc and

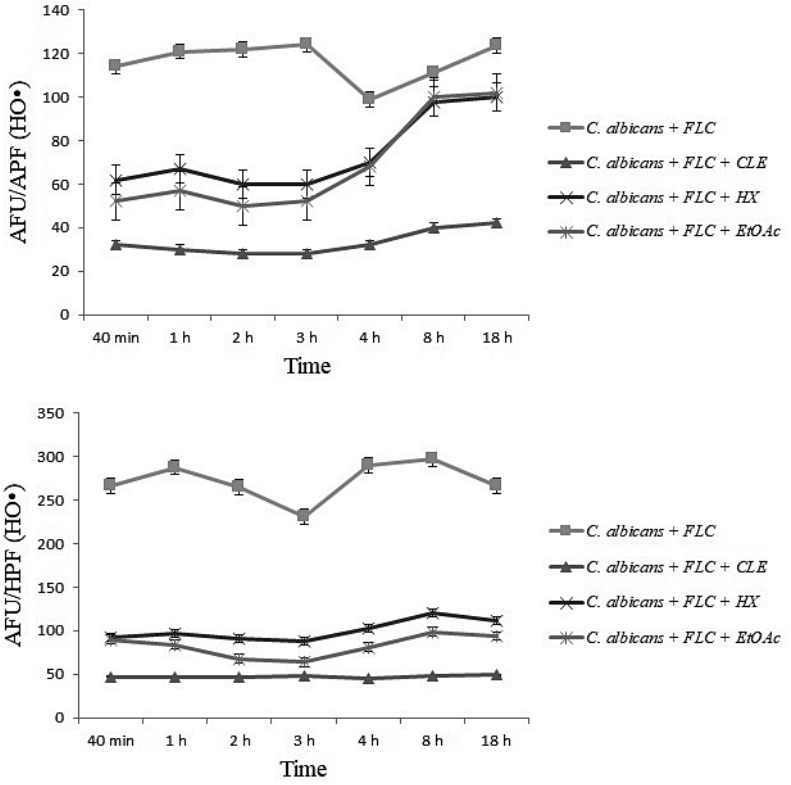

Figure 2. Levels of hydroxyl radicals (HO•) in *Candida albicans* cells generated by alone fluconazole (FLC) or during the associations with plant products. CLE: crude leaf extract from *Talinum paniculatum*; EtOAc= Ethyl acetate fraction and HX= Hexane fraction. AFU: arbitrary fluorescent units.

HX) promoted growth inhibition of the reference strain of *C. albican*s (fungistatic effect). Against FLC-resistant *C. albicans*, the cell death was the principal outcome of the treatments (fungicidal effect). With focus on a selectivity of *T. paniculatum* against *C. albicans* cells, outstanding SI values were observed for the CLE, EtOAc, and HX against both clinical isolates of FLC-resistant *C. albicans* and reference strain of *C. albicans*. A previous work has shown notable SI values of *T. paniculatum* toward *C. albicans* cells (ATCC 10231) and other microorganisms [18].

The pathogenic potential (overgrowth) of *C. albicans* arises *after* a break in homeostasis and depends on factors of both the human host, for example, immunosuppression, and the microorganism, for example, virulence of the strain. Thus, in these cases, the invasion of *C. albicans* into vital sites of immunocompromised patients causes the so-called IFI (sometimes life-threatening infections) and accounts for the high mortality rates

from infectious diseases caused by this fungus [61, 62]. Here, the clinical isolates of *C. albicans* presented resistance to FLC, which is commonly used to treat *C. albicans* infections. The LE, HX, and EtOAc fractions from *T. paniculatum* presented significant inhibitory activity against clinical isolates of *C. albicans*. Moreover, the activity of terpenes, sterols (compounds found in *T. paniculatum*), and plant products with high terpenes/sterols contents were also demonstrated against *Candida* species [18, 63].

In vivo, even on antibiotic action, the killing of pathogens in humans requires a competent immune system. The immunocompetent host is usually far better equipped to eliminate *C. albicans* than an immunosuppressed host. Therefore, it is especially desirable to have a truly microbicidal drug–one that absolutely kills the microorganisms–as a treatment option for immunosuppressed patients [64]. In this context, regarding the type of antifungal effect expected for the CLE and fractions from *T. paniculatum*, as seen here, and bearing in mind the clinical considerations above mentioned, the antimicrobial agents with fungicidal action are preferred to with fungistatic action.

Interestingly, the MIC and MBC values may vary for the actions of the CLE, EtOAc, and HX, as well as for FLC, as consequences of different AMR profiles of *C. albicans*, used in this study. Furthermore, differences between chemical compositions of the fractions or CLE (i.e., in part, from the differences in solvents used to extraction) and the association with antifungal may explain the effects found in this study, since the concentration of metabolites produced may produce a combination of antimicrobial effects or inactivation of FLC [65].

The different compounds in *T. paniculatum*, here evidenced by HPLC, explain the observed bioactivities, including the effects when there were associations between plant product and antifungal. As examples, chlorogenic acid, benzoic acid, caffeic acid, and ferulic acid, and phytosterols display antifungal activity [45, 46, 50-53, 55-59]. In contrast, isolated ascorbic acid does not have antifungal activity up to 250 $\mu g\,ml^{-1}$, as reported by Khalil *et al.* [41], but it displays outstanding antioxidant activity. These factors may, at least in part, contribute with the observed decrease in FLC MIC since ascorbic acid can have an outstanding antioxidant and hence it prevents FLC-induced oxidative damage. Apart from the phenolic content, other compounds present in *T. paniculatum* such as phytosterols take part in the redox control [40, 66, 67].

In this study we demonstrated for the CLE and fractions from *T. paniculatum* the presence of some compounds with outstanding antioxidant activity (some polyphenols and the most abundant plant phytosterols: campesterol, sitosterol, and stigmasterol), quantified polyphenols (flavonoids and tannins), and evidenced their antioxidant potential. It may justify–at least in part–the actions of these plant products to decrease MIC values of FLC. The process of fractioning CLE into HX or EtOAc concentrated

the polyphenols in these fractions, as seen in this study. This fact is also reflected in our results from MIC values and during the associations between plant product and FLC, since the outstanding MIC values for the alone HX fraction overcome the influence of its polyphenols content and antioxidant activity on FLC activity ("no interaction" when the associations were performed), while the greater polyphenols content and antioxidant activity of EtOAc fraction or a higher MIC values for the alone CLE influenced MIC values from the associations ("antagonism" from most associations).

We demonstrated that plant product can increase the MIC of FLC, the next question arising was whether antioxidants-containing plant product could potentially interfere with FLC susceptibility owing to a previous action upon ROS levels. The generation of ROS is an inevitable aspect of aerobic organism's life, so that, during oxygen (O_2) metabolism, by electron-transport chains and/or other mechanisms, O_2 is converted into $O_2^{\bullet-}$, that is spontaneously or enzymatically converted into H_2O_2. Consequently, in the Fenton reaction, H_2O_2 is further converted into the highly-reactive $HO^{\bullet}$ that can generate damage upon DNA. Under physiological conditions, steady-state levels of ROS are maintained in *C. albicans* cells, but the cell's homeostatic system can be disturbed, in the so-called oxidative stress, overly burdening the cell with ROS and leading to death. Thus, external factors, including antibiotic action, as here performed, can modify this redox balance, and it could explain why FLC-induced ROS/RNS-mediated *C. albicans* death/damage or growth inhibition is hampered by antioxidants-containing plant product.

Over the last few decades, controversies about the participation of intense ROS production during antibiotic action have generated discussion [68, 69]. Reinforcing the theory that high levels of ROS are induced during antibiotic action, the presence of some exogenous redox-active compounds with pro- or antioxidant activity, such as polyphenols and other plant products, can change the antibiotic action. It has been shown that antioxidants promote a diminution in the expression of genes related to ROS detoxification systems in microorganisms, reversing expectations of an increase in gene expression–a common consequence of oxidative stress induced by antibiotics– [27], as seen in cases of antibiotic resistance because of a higher oxidative stress tolerance in *C. albicans* [70] and *P. aeruginosa* biofilms [71]. As demonstrated here, we found that these increased FLC MICs were caused by antioxidant effects attributed to the plant products accordingly decreasing $HO^{\bullet}$; thus, mitigating FLC-induced growth inhibition or killing of *C. albicans*. As part of its antifungal action, FLC, *per se*, increased the levels of ROS ($HO^{\bullet}$) in *C. albicans* cells, whereas the association between plant product (CLE, EtOAc, or HX) and this antifungal agent caused a decrease in FLC-induced ROS which in turn generated an increase in MIC values (decreased sensitivity of *C. albicans* to FLC). Similarly, Smirnova *et al.* demonstrated that plant

polyphenols and crude extracts from the leaves of various plants decreased the antibacterial effect (increased MIC value) of ciprofloxacin against *E. coli*. This effect was also assigned by the author to an antioxidant action of the compounds/extracts [27].

Of great relevance, in this study, we considered intracellularly-generated and confined oxidants in *C. albicans* cells, so that we used membrane-permeable fluorescent probes that readily diffuse through the cell membrane and then are rapidly oxidized to highly fluorescent products. The treatments with the CLE, EtOAc, and HX were performed; and these plant products present antioxidant compounds able to cross a membrane. This is further supported in previous studies, in which non-polar compounds with antioxidant action have been described for this plant [17,18].

In this study, we detected elevated $HO^{\bullet}$ formation in *C. albicans* cells induced by FLC, which may, at least in part, explain the link between FLC treatment and oxidative damage in DNA (quantifying 8-oxo-7,8-dihydro-2′-deoxyguanosine [8-oxodG]), as found by Mahl *et al*. [22], since unlike the $O_2^{\bullet-}$ and H_2O_2, $HO^{\bullet}$ is highly reactive toward DNA and hence it could explain the FLC-dependent ROS-induced guanine pool oxidation leading to *C. albicans* death. In addition, recent evidence suggests that FLC induces oxidative DNA damage in *Candida tropicalis* after 24 hr of exposure, being this outcome of an earlier augmentation in ROS levels (oxidative stress) [23].

Here we demonstrated the generation of FLC-induced ROS in a reference strain of *C. albicans*. Silva *et al*. reported which fluconazole induced high levels of ROS only in susceptible strains of *C. tropicalis* [23]. However, different strains may differ in the sensitivity and response to oxidative stress because of a specific sensitivity to FLC. In addition, azole antifungals act in a time and concentration dependent-manner in these cases, and the associated generation of ROS after antifungal exposure to appear not to be directly related to them but by some by-products generated through their mechanisms of action [22]. Silva *et al*. [23] and Mahl *et al*. [22] have shown that resistance to FLC among *Candida* species can involve increased gene expression of products related to redox homeostasis systems, such as genes for the synthesis of antioxidant enzymes, GPx, Sod, and GST [70], provided that the antifungal activity of FLC has been reported to be dependent on an intensive ROS production, which generate DNA damage (consequence of an excessive farnesyl pyrophosphate formation) beyond the effects in inhibiting ergosterol biosynthesis and consequent changes in the fungal membrane. A recent study has also demonstrated that FLC at subinhibitory concentrations induced oxidative- and nitrosative-responsive genes *TRR1*, *GRE2*, and *YHB1*, and led to AMR profile in *C. albicans* and resistance to phagocytes [9].

In *C. albicans* cells, antioxidant-mediated protection against FLC may function in any of the two ways: chain-breaking or prevention. Thiourea, an antioxidant, was proved to protect *E. coli* from killing by norfloxacin, a fluoroquinolone antibiotic. Later, Keren *et al*. demonstrated that, at low concentrations of norfloxacin, thiourea, acting by diminishing ROS levels, protected *E. coli* cells from killing [28]. As also here observed, plant products provide protection against FLC-induced ROS/RNS-mediated *C. albicans* death.

To reinforce the plausible putative action of antioxidants as scavengers of ROS/RNS to prevent FLC activity, rather than other effects, Goswami *et al*. [44] demonstrated that wild type *E. coli* K-12 strain MG1655 has lower susceptibility toward different antibiotics (Ciprofloxacin, Ofloxacin, Streptomycin, Kanamycin, Gentamycin, Spectinomycin, Tetracycline, Chloramphenicol, Ampicillin, and Penicillin), when in the presence of antioxidants (10 mM glutathione or ascorbic acid). The results found here–protection of the *C. albicans* cells (using an experimental model of fungi [eukaryote microorganism]) by antioxidants-containing plant products against FLC–and those ones found by Goswami *et al*. (different antibiotics representing a wide diversity of mechanisms of action) against an experimental model of prokaryote microorganism (bacteria), may indicate a putative mechanism of antioxidants, as ROS scavengers, to interfere with the susceptibility of *C. albicans*, rather than, a pleiotropic effect.

The limitations of our study should be noted, which are the analysis of oxidative stress response just in exponential growth phase (i.e., yeast cells in exponential and stationary phase can respond in a different manner to oxidative stress) and a verification upon the *C. albicans* exposure to FLC more in-depth, under the influence of treatments with the CLE, HX, or EtOAc, and the correspondent *C. albicans* antioxidant response (analyses of the systems of ROS detoxification: *GPx*, *SOD*, and *GST* genes and related enzymes), total glutathione, and oxidative damage in DNA (since FLC-induced oxidative damage upon lipids and proteins appears to be no significant in this case) [22]. These tests could help to shed light whether the treatments are priming/modulating genes expressions/enzymes activities and/or whether they are creating direct antioxidant effects (most probably) or other types of interaction with FLC.

Taken together, our findings suggest that *T. paniculatum* presents potential for furthers studies to look at it as an antifungal. This plant presents low toxicity at concentrations of optimal antifungal activity (significant SI values). As a recommendation, additional studies are required to isolate new compounds with original antifungal actions through a bioassay-guided approach. Alternatively, a study could be conducted regarding the efficacy, safety, and pharmacokinetics for a herbal drug from *T. paniculatum* leaves to treat infectious diseases, including those caused by AMR, since the CLE from

T. paniculatum alone presents outstanding antifungal activity, its inability to have significant synergic effects with antibiotics notwithstanding.

Conversely, these findings also provide novel insights into redox regulation of *C. albicans* cells during the association between plant product and antifungal. We used an experimental model of antifungal action (FLC), demonstrating a plausible putative activity of antioxidants containing-plant products in preventing the effects of FLC by decreasing oxidants. Of clinical relevance, our data support the fact that some polyphenols and other antioxidant compounds, being a part of many nutrition products and medicines, may interact with antibiotics during medical treatment and modify their action. Therefore, since the dietary intake of *T. paniculatum* as a green leafy vegetable is common, a word of warning should be issued regarding the association between *T. paniculatum* and FLC, in face of the antagonistic effects here demonstrated; thus, during antibiotic therapy, the physician should take all this into account, since patients under FLC treatment parallel to an intake of this plant may cause a decrease in antifungal efficacy.

Nonetheless, these data should also prompt *in vivo* studies, focusing additional effects of exogenous products with antioxidants on the host/organism to observe resistance phenomenon and/or the failure of therapeutic regimens, since some combinations may increase the MIC of antibiotics *in vitro* and there is possibility for this also occurs *in vivo*–in addition to–be worthwhile to target these interactions between plant product and antibiotics and associated effect's underlying mechanisms as a means to enhance the killing efficacy of available antimicrobial agents.

Acknowledgment

The authors acknowledge Dr. Marcelo Polo for the identification of the plant material. This study was financed in part by the Coordenação de Aperfeiçoamento de Pessoal de Nível Superior - Brasil (CAPES) - Finance Code 001.

Author contributions

Conceived and designed the experiments: CDC. Performed the experiments: CDC MFRN JJS GOIM LFCR. Analyzed the data: CDC. Contributed reagents/materials/analysis tools: MFGB GBS MRPLB. Gave technical support and conceptual advice: GOIM MFGB MRPLB. Wrote the paper: CDC. Supervised the study: CDC MRPLB. Final approval of manuscript: CDC JJS MFRN MFGB GBS LFCR MRPLB.

Disclosure statement

No potential conflict of interest was reported by the authors.

References

1. F.C. Tenover, Mechanisms of antimicrobial resistance in bacteria, *Am. J. Med.*, **119**, S3-S10 (2006).

2. W. Liu, L.P. Li, J.D. Zhang, *et al*., Synergistic antifungal effect of glabridin and fluconazole, *PLoS ONE*, **9**, e103442 (2014).

3. J. Tanwar, D. Das, Z. Fatima, *et al*., Multidrug resistance: an emerging crisis, *Interdisc. Persp. Infect. Dis.*, **2014**, Article ID 541340, 7 (2014).

4. S. Baker, A return to the pre-antimicrobial era? *Science*, **347**, 1064-1066 (2015).

5. M.P. Brynildsen, J.A. Winkler, C.S. Spina, *et al*., Potentiating antibacterial activity by predictably enhancing endogenous microbial ROS production, *Nature Biotechnol.*, **31**, 160-165 (2013).

6. L. Imamovic, M.O.A. Sommer, Use of collateral sensitivity networks to design drug cycling protocols that avoid resistance development, *Sci. Translat. Med.*, **5**(204), 204 (2013).

7. M.A. Perros, Sustainable model for antibiotics, *Science*, **347**, 1062-1064 (2015).

8. L. García-Agudo, P. García-Martos, P. Marín-Casanova, *et al*., Susceptibility to fluconazole of clinical interest yeasts: new breakpoints, *Rev. Esp. Quimioter.*, **25**, 266-268 (2012).

9. D.M. Arana, C. Nombela, J. Pla, Fluconazole at subinhibitory concentrations induces the oxidative- and nitrosative-responsive genes TRR1, GRE2 and YHB1, and enhances the resistance of *Candida albicans* to phagocytes, *J. Antimicrob. Chemother.*, **65**, 54-62 (2010).

10. IOM (Institute of Medicine), *Antibiotic resistance: Implications for global health and novel intervention strategies*, The National Academies Press, Washington, D.C., 2010.

11. M.A. Kohanski, M.A. DePristo, J.J. Collins, Sub-lethal antibiotic treatment leads to multidrug resistance via radical-induced mutagenesis, *Mol. Cell*, **37**, 311-320 (2010).

12. Centers for Disease Control and Prevention (CDC), *Antibiotic Resistant Threats in the United States*, U.S. Department of Health and Human Services, Atlanta, GA, 2013, 114 p.

13. S.S. Grant, D.T. Hung, Persistent bacterial infections, antibiotic tolerance, and the oxidative stress response, *Virulence*, **4**, 273-283 (2013).

14. M.M. Cowan, Plant products as antimicrobial agents, *Clin. Microbiol. Rev.*, **12**, 564-582 (1999).

15. J. Caribe, J.M. Campos, *Plantas que ajudam o homem: guia prático para época*, Cultrix/Pensamento, São Paulo, 1991.

16. C. Sukwan, S. Wray, S. Kupittayanant, The effects of Ginseng Java root extract on uterine contractility in nonpregnant rats, *Physiol. Reports*, **2**, e12230 (2014).

17. H. Shimoda, N. Nishida, K. Ninomiya, *et al*., Javaberine A, new TNF-alpha and nitric oxide production inhibitor, from the roots of *Talinum paniculatum*, *Heterocycles*, **55**, 2043-2050 (2001).

18. L.F. Reis, C.D. Cerdeira, B.F. Paula, *et al*., Chemical characterization and evaluation of antibacterial, antifungal, antimycobacterial, and cytotoxic activities of *Talinum paniculatum*, *Rev. Inst. Med. Trop. Sao Paulo*, **57**, 397-405 (2015).

19. C. Thanamool, P. Papirom, S. Chanlun, *et al*., *Talinum paniculatum* (Jacq.) Gertn: a medicinal plant with potential estrogenic activity in ovariectomized rats, *Int. J. Pharm. Pharm. Sci.*, **5**, 478-485 (2013).

20. C. Thanamool, A. Thaeomor, S. Chanlun, *et al*., Evaluating the anti-fertility activity of *Talinum paniculatum* (Jacq.) Gaertnin female Wistar rats, *Aust. J. Plant Physiol.*, **7**, 1802-1807 (2013).

21. M.P.O. Ramos, G.D.F. Silva, L.P. Duarte, *et al*. Antinociceptive and edematogenic activity and chemical constituents of *Talinum paniculatum* willd, *J. Chem. Pharm. Res.*, **2**, 265-274 (2010).

22. C.D. Mahl, C.S. Behling, F.S. Hackenhaar, *et al*., Induction of ROS generation by fluconazole in *Candida glabrata*: activation of antioxidant enzymes and oxidative DNA damage, *Diagn. Microbiol. Infect. Dis.*, **82**, 203-208 (2015).

23. C.R. Silva, J.B.A. Neto, J.J.C. Sidrim, *et al*., Synergistic effects of amiodarone and fluconazole on *Candida tropicalis* resistant to fluconazole, *Antimicrob. Agents Chemother.*, **57**, 1691-1700 (2013).

24. I. Albesa, M.C. Becerra, P.C. Battan, *et al*., Oxidative stress involved in the antibacterial action of different antibiotics, *Biochem. Biophys. Res. Commun.*, **317**, 605-609 (2004).

25. M. Goswami, S.H. Mangoli, N. Jawal, Involvement of reactive oxygen species in the action of ciprofloxacin against *Escherichia coli*, *Antimicrob. Agents Chemother.*, **50**, 949-954 (2006).

26. D. Kobayashi, K. Kondo, N. Uehara, *et al*., Endogenous reactive oxygen species is an important mediator of miconazole antifungal effect, *Antimicrob. Agents Chemother.*, **46**, 3113-3117 (2002).

27. G. Smirnova, Z. Samoilova, N. Muzyka, *et al*., Influence of plant polyphenols and medicinal plant extracts on antibiotic susceptibility of *Escherichia coli*, *J. Appl. Microbiol.*, **113**, 192-199 (2012).

28. I. Keren, Y. Wu, J. Inocencio, L.R. Mulcahy, K. Lewis, Killing by bactericidal antibiotics does not depend on reactive oxygen species, *Science*, **339**, 1213-1216 (2013).

29. A.C. Brewer, S.B. Mustafi, T.V.A. Murray, *et al*., Reductive stress linked to small HSPs, G6PD, and Nrf2 pathways in heart disease, *Antioxid. Redox Signal.*, **18**, 1114-1127 (2013).

30. E. Piskounova, M. Agathocleous, M.M. Murphy, *et al*., Oxidative stress inhibits distant metastasis by human melanoma cells, *Nature*, **527**, 186-191 (2015).

31. J.J. da Silva, T.A. da Silva, H. de Almeida, M.F.R. Netto, C.D. Cerdeira, J.F. Höfling, M.F.G. Boriollo, *Candida* species biotypes in the oral cavity of infants and children with orofacial clefts under surgical rehabilitation, *Microb. Pathogen.*, **124**, 203-215 (2018).

32. Clinical and Laboratory Standards Institute (CLSI), *Reference method for broth dilution antifungal susceptibility testing of yeasts: Approved standard M27-A3*, 3rd ed., CLSI, Wayne, 2008.

33. K.I. Setsukinai, Y. Urano, K. Kakinuma, *et al*., Development of novel fluorescence probes that can reliably detect reactive oxygen species and distinguish specific species, *J. Biol. Chem.*, **278**, 3170-3175 (2003).

34. S. Fattahi, E. Zabihi, Z. Abedian, *et al*., Total phenolic and flavonoid contents of aqueous extract of *Stinging Nettle* and *in vitro* antiproliferative effect on Hela and BT-474 cell lines, *Int. J. Mol. Cell. Med.*, **3**, 102-107 (2014).

35. F.C. Odds, Synergy, antagonism, and what the chequerboard puts between them, *J. Antimicrob. Chemother.*, **52**, 1 (2003).

36. J. Meletiadis, S. Pournaras, E. Roilides, *et al.*, Defining fractional inhibitory concentration index cutoffs for additive interactions based on self-drug additive combinations, Monte Carlo simulation analysis, and *in vitro-in vivo* correlation data for antifungal drug combinations against *Aspergillus fumigatus*, *Antimicrob. Agents Chemother.*, **54**, 602-609 (2010).

37. O.P. Salin, L.L. Pohjala, P. Saikku, *et al.*, Effects of coadministration of natural polyphenols with doxycycline or calcium modulators on acute *Chlamydia pneumonia* infection *in vitro*, *J. Antibiotics*, **64**, 747-752 (2011).

38. K. Konaté, J.F. Mavoungou, A.N. Lepengué, *et al.*, Antibacterial activity against β-lactamase producing Methicillin and Ampicillin-resistants *Staphylococcus aureus*: fractional Inhibitory Concentration Index (FICI) determination, *Ann. Clin. Microbiol. Antimicrob.*, **11**, 18 (2012).

39. J.D. Tamokou, J.R. Kuiate, M. Tene, *et al.*, The antimicrobial activities of extract and compounds isolated from *Brillantaisia lamium*, *Iran. J. Med. Sci.*, **36**, 24-31 (2011).

40. Y. Yoshida, E. Niki, Antioxidant effects of phytosterol and its components, *J. Nutr. Sci. Vitaminol. (Tokyo)*, **49**, 277-280 (2003).

41. O.A.K. Khalil, O.M.M. de Faria Oliveira, J.C.R. Vellosa, *et al.*, Curcumin antifungal and antioxidant activities are increased in the presence of ascorbic acid, *Food Chem.*, **133**, 1001-1005 (2012).

42. M. Tajkarimi, S.A. Ibrahim, Antimicrobial activity of ascorbic acid alone or in combination with lactic acid on *Escherichia coli* O157:H7 in laboratory medium and carrot juice, *Food Control*, **22**, 801-804 (2011).

43. B.M. Abu-Ghazaleh, Effects of ascorbic acid, citric acid, lactic acid, NaCl, potassium sorbate and *Thymus vulgaris* extract on *Staphylococcus aureus* and *Escherichia coli*, *African J. Microbiol. Res.*, **7**, 7-12 (2013).

44. M. Goswami, S.H. Mangoli, N. Jawali, Antibiotics and antioxidants: Friends or foes during therapy? *BARC Newsletter*, **323**, 42-46 (2011).

45. A. López, D.S. Ming, G.H.N. Towers, Antifungal activity of benzoic acid derivatives from *Piper lanceaefolium*, *J. Nat. Prod.*, **65**, 62-64 (2002).

46. O. Drăcea, C. Larion, M.C. Chifiriuc, *et al*., New thioureides of 2-(4-methylphenoxymethyl) benzoic acid with antimicrobial activity, *Roum. Arch. Microbiol. Immunol.*, **67**, 92-97 (2008).

47. B. Velika, I. Kron, Antioxidant properties of benzoic acid derivatives against superoxide radical, *Free Radic. Antioxid.*, **2**, 62-67 (2012).

48. D.F. Basri, L.W. Xian, N.I.A. Shukor, *et al*., Bacteriostatic antimicrobial combination: Antagonistic interaction between epsilon-viniferin and vancomycin against methicillin-resistant *Staphylococcus aureus*, *BioMed Res. Int.*, **2014**, Article ID 461756, 8 (2014).

49. D.R. Oliveira, S.R. Tintino, M.F.B.M. Braga, *et al*., *In vitro* antimicrobial and modulatory activity of the natural products silymarin and silibinin, *BioMed Res. Int.*, **2015**, Article ID 292797, 7 (2015).

50. W.S. Sung, D.G. Lee, Antifungal action of chlorogenic acid against pathogenic fungi, mediated by membrane disruption, *Pure Appl. Chem.*, **82**, 219-226 (2010).

51. Z. Lou, H. Wang, S. Zhu, *et al*., Antibacterial activity and mechanism of action of chlorogenic acid, *J. Food Sci.*, **76**, M398-403 (2011).

52. M.J. Alves, I.C. Ferreira, H.J. Froufe, *et al*., Antimicrobial activity of phenolic compounds identified in wild mushrooms, SAR analysis and docking studies, *J. Appl. Microbiol.*, **115**, 346-357 (2013).

53. Y. Sato, S. Itagaki, T. Kurokawa, *et al*., *In vitro,* and *in vivo* antioxidant properties of chlorogenic acid and caffeic acid, *Int. J. Pharm.*, **403**, 136-138 (2011).

54. S. Hemaiswarya, M. Doble, Synergistic interaction of phenylpropanoids with antibiotics against bacteria, *J. Med. Microbiol.*, **59**, 1469-1476 (2010).

55. N.H. Aziz, S.E. Farag, L.A. Mousa, *et al*., Comparative antibacterial and antifungal effects of some phenolic compounds, *Microbios*, **93**, 43-54 (1998).

56. M.S. Barber, V.S. McConnell, B.S. DeCaux, Antimicrobial intermediates of the general phenylpropanoid and lignin specific pathways, *Phytochemistry*, **54**, 53-56 (2000).

57. D. Stojković, J. Petrović, M. Soković, *et al*., *In situ* antioxidant and antimicrobial activities of naturally occurring caffeic acid, p-coumaric acid and rutin, using food systems, *J. Sci. Food Agric.*, **93**, 3205-3208 (2013).

58. B.K. Sarma, U.P. Singh, Ferulic acid may prevent infection of *Cicer arietinum* by *Sclerotium rolfsii*, *World J. Microbiol. Biotechnol.*, **19**, 123-127 (2003).

59. A. Borges, C. Ferreira, M.J. Saavedra, *et al.*, Antibacterial activity and mode of action of ferulic and gallic acids against pathogenic bacteria, *Microb. Drug Resist.*, **19**, 256-265 (2013).

60. M. Srinivasan, A.R. Sudheer, V.P. Menon, Ferulic acid: Therapeutic potential through its antioxidant property, *J. Clin. Biochem. Nutr.*, **40**, 92-100 (2007).

61. F.L. Mayer, D. Wilson, B. Hube, *Candida albicans* pathogenicity mechanisms, *Virulence*, **4**, 119-128 (2013).

62. M.A. Rawashdeh, J.A. Ayesh, A.M. Darwazeh, Oral candidal colonization in cleft patients as a function of age, gender, surgery, type of cleft, and oral health, *J. Oral Maxillofac. Surg.*, **69**, 1207-1213 (2011).

63. S. Dalleau, E. Cateau, T. Bergès, *et al.*, *In vitro* activity of terpenes against *Candida* biofilms, *Int. J. Antimicrob. Agents*, **31**, 572-576 (2008).

64. J.R. Graybill, D.S. Burgess, T.C. Hardin, Key issues concerning fungistatic versus fungicidal drugs, *Eur. J. Clin. Microbiol. Infect. Dis.*, **16**, 42-50 (1997).

65. M.W. Biavatti, Synergy: an old wisdom, a new paradigm for pharmacotherapy, *Braz. J. Pharm. Sci.*, **45**, 371-378 (2009).

66. J.M. Choi, E.O. Lee, H.J. Lee, *et al.*, Identification of campesterol from *Chrysanthemum coronarium* L. and its antiangiogenic activities, *Phytother. Res.*, **21**, 954-959 (2007).

67. A.C. Holloway, S.W.J. Gould, M.D. Fielder, *et al.*, Enhancement of antimicrobial activities of whole and sub-fractionated white tea by addition of copper (II) sulphate and vitamin C against *Staphylococcus aureus*; a mechanistic approach, *BMC Complement. Altern. Med.*, **11**, 115 (2011).

68. Y. Liu, J.A. Imlay, Cell death from antibiotics without the involvement of reactive oxygen species, *Science*, **339**, 1210-1213 (2013).

69. D.J. Dwyer, P.A. Belenky, J.H. Yang, *et al.*, Antibiotics induce redox-related physiological alterations as part of their lethality, *Proc. Natl. Acad. Sci. USA*, **111**, E2100-E2109 (2014).

70. C.E.B. Linares, S.R. Giacomelli, D. Altenhofen, *et al*., Fluconazole and amphotericin-B resistance are associated with increased catalase and superoxide dismutase activity in *Candida albicans* and *Candida dubliniensis*, *Rev. Soc. Bras. Med. Trop.*, **46**, 752-758 (2013).

71. D. Nguyen, A. Joshi-Datar, F. Lepine, *et al*., Active starvation responses mediate antibiotic tolerance in biofilms and nutrient-limited bacteria, *Science*, **334**, 982-986 (2011).

How to cite this article

C.D. Cerdeira, J.J. da Silva, M.F.R. Netto, M.F.G. Boriollo, G.O.I. Moraes, G.B. Santos, L.F.C. dos Reis, M.R.P.L. Brigagão, *Talinum paniculatum*: a plant with antifungal potential mitigates fluconazole-induced oxidative damage-mediated growth inhibition of *Candida albicans*, *Rev. Colomb. Cienc. Quím. Farm.*, **49**(2), 401-431 (2020).

Scientific research article / *http://dx.doi.org/10.15446/rcciquifa.v49n2.89894*

Talinum paniculatum leaves with in vitro antimicrobial activity against reference and clinical strains of *Staphylococcus aureus* interfere with oxacillin action

Cláudio Daniel Cerdeira[a,1*], Jeferson J. da Silva[b,2], Manoel F. R. Netto[b,3], Marcelo F. G. Boriollo[b,4], Gérsika B. Santos[a,5], Luis F. C. dos Reis[c,6], Maísa R. P. L. Brigagão[a,7]

[a]Department of Biochemistry (DBc), Institute of Biomedical Sciences (IBS), Federal University of Alfenas (UNIFAL-MG), Alfenas, 37130-001, Minas Gerais (MG), Brazil.

[b]Laboratory of Microbiology and Immunology, Department of Oral Diagnostic, Dental school of Piracicaba, State University of Campinas (FOP/UNICAMP), Piracicaba, 13414-903, São Paulo (SP), Brazil.

[c]Laboratory of Medicinal Plants, UNIFAL-MG, Alfenas, 37130-001, MG, Brazil.

*Corresponding author e-mail address: daniel.cerdeira.84@gmail.com, Orcid ID: https://orcid.org/0000-0002-7242-8028

E-mail addresses: [1*]daniel.cerdeira.84@gmail.com, [2]jefersonbiomed@hotmail.com, [3]manoelfrn@hotmail.com, [4]marcelofgb@yahoo.com.br, [5]gersika.santos@unifenas.br, [6]luis_cunhaz@yahoo.com.br, [7]maisaunifal@gmail.com

Received: 3 March 2019

Revised: 13 May 2020

Accepted: 14 May 2020

Summary

Propose: We evaluated the antibacterial potential of the crude leaf extract (CLE) and fractions hexane (HX) and ethyl acetate (EtOAc) from *Talinum paniculatum* alone and in association with oxacillin (OXA) against OXA-resistant *Staphylococcus aureus* (ORSA, environment isolates) and OXA-sensitive *S. aureus* (OSSA, ATCC 25923). Furthermore, toxicity tests were performed. **Methods:** The antibacterial activity was evaluated through checkerboard assay (broth microdilution) to establish the minimum inhibitory (MIC) and minimum bactericidal concentrations (MBC). Toxicity test in mice was assessed. **Results:** The MIC values for the CLE and its fractions against ORSA and OSSA were in the order of HX (500 $\mu g\,ml^{-1}$) = EtOAc < CLE (4000 $\mu g\,ml^{-1}$). EtOAc and HX presented outstanding antibacterial activities against ORSA, and these fractions were bactericidal toward OSSA. Conversely, the associations between plant product (CLE, EtOAc, or HX) and OXA exhibited no synergistic effects. During these associations, there was an increase in OXA MICs anywhere from 2- to 4092-fold. The CLE presented absence of toxicity at a dose of 5 g kg^{-1} (*in vivo*). **Conclusion:** Although *T. paniculatum* be a good source

of bioactive compounds with antistaphylococcal potential, the researchers should be cautious, since its edible leaf may interfere with OXA therapy (mitigating OXA-induced growth inhibition or killing of *S. aureus* and enhancing *S. aureus* resistance).

Key words: Antimicrobial resistance, *Staphylococcus aureus*, reactive oxygen species, oxacillin, *Talinum paniculatum*.

Resumen

Las hojas de *Talinum paniculatum* con actividad antimicrobiana *in vitro* contra cepas de referencia y clínicas de *Staphylococcus aureus* interfieren con la acción de la oxacilina

Propósito: evaluamos el potencial antibacteriano del extracto de hoja en bruto (EHB) y las fracciones hexano (HX) y acetato de etilo (AcOEt) de *Talinum paniculatum* solo y en asociación con oxacilina (OXA) contra *Staphylococcus aureus* resistente a OXA (ORSA, ambientales) y *S. aureus* sensible a OXA (OSSA, ATCC 25923). Además, se realizaron pruebas de toxicidad. **Métodos:** la actividad antibacteriana se evaluó mediante microdilución en caldo para establecer las concentraciones inhibitorias mínimas (CIM) y bactericidas mínimas (CBM). Se evaluó la toxicidad en ratones. **Resultados:** los valores de CIM para el EHB y sus fracciones contra ORSA y OSSA fueron del orden de HX (500 $\mu g\,ml^{-1}$) = AcOEt < EHB (4000 $\mu g\,ml^{-1}$). AcOEt y HX presentaron actividades antibacterianas sobresalientes contra ORSA, y estas fracciones fueron bactericidas hacia OSSA. Por el contrario, las asociaciones entre el producto vegetal (EHB, AcOEt o HX) y OXA no mostraron efectos sinérgicos. Durante estas asociaciones, hubo un aumento en las CIM de OXA de 2 a 4092 veces. EHB no mostró toxicidad a una dosis de 5 $g\,kg^{-1}$. **Conclusión:** aunque *T. paniculatum* es una buena fuente de compuestos bioactivos con potencial antiestofilocócico, los investigadores deben ser cautelosos, ya que su hoja comestible puede interferir con la terapia con OXA (mitigando la inhibición del crecimiento inducida por OXA o la muerte de *S. aureus* y promoviendo resistencia bacteriana).

Palabras clave: Resistencia a los antimicrobianos, *Staphylococcus aureus*, oxacilina, *Talinum paniculatum*.

Introduction

Infectious diseases remain among the leading causes of morbidity and mortality in the world. Moreover, antimicrobial (AMR) and multidrug (MDR) resistance have risen to

alarming levels in *Staphylococcus aureus* (i.e., chiefly to penicillin and cross-resistance to other ß-lactams). From the global burden associated with AMR/MDR in microorganisms, most frequent are the threat to therapeutics, prolonged illness, decreased effectiveness, creating easy targets for immunocompromised conditions, high medical costs, and high mortality rates [1-4].

Indeed, the accelerating growth and global expansion of oxacillin (OXA) resistant *S. aureus* (ORSA) strains and hospital (HAI) or community (CAI) associated infections related to them are ultimately both a global public health problem and a critical problem in clinical settings where immunocompromised patients or those who have had surgical wounds are present. Resistance to current antibiotics has limited the therapeutic armory to treat *S. aureus* infections [6, 7].

In that way, approaches such as screening of plant products alone or in combination with antibiotics that can tackle AMR/MDR have been extensively reported [7-11]. Plants have been used in folk medicine since ancient times, and the chemical diversity and therapeutic potential are great reasons for the current interest taken in them [10]. *Talinum paniculatum* (Jacq.) Gaertner (Talinaceae family) is a plant widely spread throughout the world, commonly known as "Erva-gorda" and "Língua-de-vaca" in Brazil or Tu-ren-shen in Traditional Chinese Medicine [12]. Its green leafy is a non-conventional vegetable for human consumption [12]. Furthermore, several biological activities have been attributed to *T. paniculatum* and its bioactive compounds, including antibacterial and antifungal [7], estrogenic [13], antifertility [14], antinociceptive [15], and other effects: on uterine contractility and those related in folk medicine [12, 16, 17].

Over the last two decades, the underlying mechanism of action for the bactericidal ß-lactam antibiotics (including OXA) against a broader set of microorganisms has been shown to be overt dependent of reactive oxygen species (ROS) accumulation [18-20]. On this knife's edge, OXA-induced ROS-associated damage to proteins and/or DNA contribute to *S. aureus*' loss of viability, even when there is increased expression of systems of ROS detoxification (i.e. condition that characterizes the so-called oxidative stress) [21-23]. Indeed, β-lactams (including OXA) can generate oxidative stress-induced autolysis. Besides these factors, oxidative stress tolerance-induced antibiotic resistance in *S. aureus* biofilms with a maintenance of the steady-state levels of ROS in *S. aureus* cells, has been described [21-27].

Despite the controversy and opposing viewpoints over the mechanism of ROS accumulation behind the activity of antibiotics, OXA activity could be hampered by providing microbial cells with exogenous antioxidants, as attested in previous studies [20, 28-31]. Moreover, antioxidants could prime (priming) microbial cells to

counteract the oxidative stress induced by antibiotics [1, 22, 24, 32, 33]. Therefore, the elucidation of possible interactions between antioxidants-rich foods and antibiotic is important because of many nutrition products and medicines, including the leaves from *T. paniculatum* that are often used as a green leafy vegetable for human consumption, may occur during medical treatment and modify the action of the antibiotic hence this could have a great impact on clinical practice and patient outcomes [7, 12].

In this study, we evaluated the antistaphylococcal potential of the extract and fractions from the leaves of *T. paniculatum* alone or in association with the ß-lactam antibiotic OXA against ORSA and OXA-sensitive *S. aureus* (OSSA). Furthermore, a possible toxicity of *T. paniculatum* (*in vivo*) was checked.

Materials and methods

Chemicals

Oxacillin (OXA); Mueller Hinton broth (MHB); 7-Hydroxy-3H-phenoxazin-3-one 10-oxide (Resazurin) were purchased from Sigma-Aldrich, St. Louis, MO, USA. Nutriente Agar (Difco); Agar/broth Brain Heart Infusion (BHI, HiMedia Laboratories); Dimethyl sulfoxide (DMSO, Neon Comercial); Solutions: Sodium chloride 0.9% (145 mM NaCl); Phosphate-buffered saline (PBS, pH 7.4): NaCl (120 mM), KH_2PO_4 (1.7 mM), Na_2HPO_4 (8.3 mM) e KCl (5 mM). Other chemicals and solvents were analytical grade. The reagents were sterilized into an autoclave (whenever possible) or by filtration (Millipore Corporation, hydrophilic Durapore® PVDF, 0.22 μm, Ø 47 mm).

Ethics statement

This study did not involve any endangered or protected species and no specific permits were required for the described studies. Botanical material from *T. paniculatum* was collected in a particular area, with access permitted to researchers.

All animal experiments were carried out in strict accordance with the recommendations of the *Guide for the Care and Use of Laboratory Animals* (National Institutes of Health [NIH], Washington DC: The National Academy Press, 2011). The animals were gently conceded from a previous approved study by the ethics committee on the use of animals (CEUA) of the Federal University of Alfenas (protocol #490/2013).

Plant material and preparation of the crude leaf extract and its fractions

T. paniculatum leaves were collected in the mornings of June, near the town of Fama, MG state, Brazil (Geographic coordinates obtained from GPS observations: 21° 24' 53.4" S; 45° 52' 15.8'' W). The climate of this region is classified as humid temperate,

with a hot summer and a dry winter (type Cwa in the classification of Köppen). A voucher specimen was deposited in the UALF Herbarium at Federal University of Alfenas (UNIFAL-MG), after identification and taxonomic authentication by a botanical (Herbarium number 2338). The collected *T. paniculatum* leaves were weighed, arranged in thin layers, and dried in a circulating air oven at 40 °C for eleven days (250 h), aiming at a stable and constant weight to be reached. The final percentage of dry mass was 5.26%. The material underwent through a rough division followed by a spray obtained in a Wiley mill. After grinding, the size of the powder particles was measured according to WHO, as shown in table 1 [34]. The dried leaf powder (200 g) from *T. paniculatum* was percolated (with an alcohol to water ratio of 7:3) at 1.0 mL/min/kg. After fluid extraction, the fluid was placed in a rotary evaporator under reduced pressure and at a temperature of 45 °C. The extract was then lyophilized to completely remove water and obtain the dry extract, hereafter referred to as CLE (17.0% yield). To obtain the fractions, the dried extract was subjected to a liquid-liquid partition with hexane (1:1, v/v [4×]) and ethyl acetate (1:1, v/v [6×]), yielding hexane (HX), ethyl acetate (EtOAc), and a final residue termed the aqueous fraction. During this process, the solvents, hexane, and ethyl acetate, are removed. The CLE or fractions were solubilized in DMSO (which at used concentration does not present antimicrobial activity) and adjusted at used concentrations.

Table 1. Diameters of the mesh chosen to perform the powder grain size of leaves from *Talinum paniculatum*.

Mesh (n. º)	Average Diameter (µm)	Mass (g)	Percentage (%)
20	850	0.56	0.46
25	710	2.33	1.94
35	500	28.46	23.57
45	355	28.38	23.50
60	250	35.66	29.52
0	-	25.38	21.01
Total		120.77	

Activity against S. aureus

Strains

Reference strains of *S. aureus* were from the American Type Culture Collection (*Staphylococcus aureus subsp. aureus* [ATCC® 25923™ and 6538], Manassas, VA, USA). The two ORSA isolates were from clinical environment and identified as shown in

table 2. The classification of AMR in *S. aureus* was as following: OXA MIC ≤ 2 μg ml^{-1}= Sensitive and ≥ 4 μg ml^{-1}= resistant [35].

Table 2. Used microorganisms, clinical sources, identification, and code.

Microorganism	Code	Source		Identification methods
S. aureus	Sample G11.39	Environment isolates from air at a dental clinicz		Multiplex PCR
S. aureus	Sample G11.19	Environment isolates from air at a dental clinic		Multiplex PCR
Loci	**Oligonucleotides: Primers F (forward) e R (reverse)**		**Size of the amplicons**	**Purpose/interpretation**
mecA1	5' TGG CTA TCG TGT CAC AAT CG 3' (F) 5' CTG GAA CTT GTT GAG CAG AG 3' (R)		310 bp	Resistance profile: ORSA (+) OXA-sensitive *S. aureus* (-)
femA1	5' CTT ACT TAC TGG CTG TAC CTG 3' (F) 5' ATG TCG CTT GTT ATG TGC 3' (R)		686 bp	ORSA identification (level of OXA resistance): ORSA (+)
IS431[A]	5' AGG ATG TTA TCA CTG TAG CC 3' (F) 5' GAT GTA CAA TGA CAG TCA GG 3' (R)		444 bp	Class C1 *mec g*ene complex: ORSA: (+)

[A]Insertion sequence.

Genomic DNA: Clinical isolates of *S. aureus* was grown in Luria-Bertani medium (pH 7, Laboratory Bottles, Hamburg, Germany) for 16 hrs at 35 °C with continuous shaking (150 r.p.m). Then, bacteria were washed two times with Tris-buffered saline (TBS: 50 mM Tris HCl pH 8.0, 100 mM EDTA, 150 mM NaCl), followed by a centrifugation at 1500 × *g* (Centrifuge 5417R, Eppendorf do Brasil Ltda., São Paulo, SP, Brasil) for 5 min. The resulting *S. aureus* cells containing-pellet was incubated at 37 °C for 30 min and cells were lysed in 500 μL TBS containing SDS (1% m/v), 100 μg lysostaphin (Sigma Chemical Co., St. Louis, MO, USA) and 100 μg RNAse (Sigma Chemical Co., St. Louis, MO, USA) into Eppendorf Thermomixer® comfort (Eppendorf™, Hamburg, Germany). The final lysed *S. aureus* cells were added with 200 μg proteinase K (Sigma Chemical Co., St. Louis, MO, USA) and 200 μg lysozyme (Sigma Chemical Co., St. Louis, MO, USA). Next, after the addition of phenol:chloroform:isoamyl alcohol (25:24:1), a high-speed centrifugation (12000 ′ *g* for 10 min) was performed and the culture supernatants underwent a further centrifugation, and then resuspended in chloroform:isoamyl alcohol (24:1). Genomic DNA was pelleted by subsequent addition of ethanol at –20 °C for 30 min and centrifugation at 12000 × *g* for 10 min, dried at 30 °C for 90 min, and solubilized in 500 μL TE buffer (10 mM Tris, 1 mM EDTA, pH 8) and stored at –20 °C. **PCR multiplex assays** - PCR was performed using the following set up: 100 ng genomic DNA in assay buffer (20 mM Tris HCl pH 8.4, 50 mM KCl), 1.5 mM $MgCl_2$, 0.2 mM of each dNTP, 100 pmol of each primer (described in **table 1**), and 1.5 U Taq DNA polymerase (Invitrogen™ Brasil Ltda.) were mixed and underwent to an initial program for DNA denaturation at 92 °C for 3 min, followed by 30 cycles at 92 °C for 1 min (denaturation), 56 °C for 1 min (annealing) and 72 °C for 1 min (extension). The final cycle was performed at 72 °C for 5 min for the final extension. **Amplicons patterns** - The PCR products in loading buffer (10% v/v glycerol, 0.083% m/v bromophenol blue, 0.083% m/v xylene cyanol in H_2O milliQ) were analyzed on a 2% agarose gel (prepared with TBE buffer 0.5′: 445 mM

trizma base, 445 mM boric acid, and 10 mM EDTA) and 0.5 μg mL^{-1} ethidium bromide) using horizontal gel electrophoresis apparatus (Sunrise™ 96), with a voltage at 5 V cm^{-1} of gel length (Thermo EC 3000-90 power supply, Thermo Electron Corporation, Milford, MA, United States) and a continuous gradient (TBE buffer 0.5×) for 3 hrs. The gels were visualized by UV light at 300 nm (Electronic UV Transilluminator mod. EB-40, Ultra Lum. Inc., Paramount, CA). Images were captured with a Photodocumentation System (Mod. DP001. FDC version 10; Vilber Lourmat, Marne la Vallée, France) and analyzed with a PhotoCapt MW (version 10.01 for Windows; Vilber Loumat, Marne la Vallée, France). *S. aureus* ATCC® 43300 (methicillin resistant *S. aureus*–MRSA), ATCC® 25923 (methicillin sensitive *S. aureus*–MSSA) and a maker of DNA (100 bp DNA, Ladder Cat. # 15628-019, Invitrogen) were used as controls.

Minimum Inhibitory Concentration (MIC) and determination of interactions between plant product and OXA

The MIC values were determined using the broth checkerboard microdilution assay on 96-well microplates (flat-bottom, Corning Inc., NY) containing 100 mL of MHB, following the CLSI document (M7-A6) [35, 36]. CLE or fractions (EtOAc or HX) were diluted into the wells (at final concentrations ranging from 4000 to 1.95 μg ml^{-1} [CLE], and from 500 to 0.244 μg ml^{-1} [fractions]), either alone or coupled with OXA (from 8000 to 3.9 μg ml^{-1}). *S. aureus* suspensions (cultures of ORSA [isolates] or OSSA [ATCC® 25923™] during the early exponential growth phase, after an overnight incubation on BHI) were centrifuged (900 × g for 6 min), the pellet diluted in sodium chloride 0.9%, and then spectrophotometrically adjusted at OD_{625} = 0.1 = 1 × 10^8 CFU mL^{-1} (further diluted, 1 × 10^5 CFU mL^{-1} final concentration). Afterwards, 10 μL of inoculums were added to the wells. The plates were then incubated at 37 °C for 24 hours. Finally, readings were performed visually as previously determined [7], wherein the presence of turbidity in the wells was considered indicative of microbial growth and a specific dye (resazurin 0.01%) was used to evaluate the metabolic activity of the microorganism. The MIC of the CLE, fractions (EtOAc or HX) or OXA alone, and all isoeffective combinations (association between plant product and OXA) were defined when the growth of the microorganism was inhibited at the lowest concentration. The growth control was composed of 100 μL of MHB and 10 μL of inoculum. The extract control was composed of 100 μL of MHB and 100 μL of the CLE or fraction (EtOAc or HX) and the sterility control contained only 100 μL of MHB.

Minimum Bactericidal Concentration (MBC)

The MBC was defined as the lowest concentration of OXA/extract/fractions that killed 99.9% of the original inoculums from each well where growth inhibition occurred in the analysis of MIC/Synergism. For each strain of ORSA and OSSA, MBC values were determined by removing 100 μl of microbial suspension from each well demonstrating no microbial growth and inoculating them with three serial dilutions of 1:10 on Petri plates (90 × 15 mm) containing the nutrient agar. Then, the plates were

incubated at 35 °C for 24 h. After that, colony counts were performed to determine which concentrations showed bactericidal or bacteriostatic effect.

Toxicity test: in vivo acute toxicity

Adult male Swiss mice weighing 30 to 45 g were obtained from the Central Animal Facility of the Federal University of Alfenas and housed in a controlled 12 h light/dark cycle at 23 °C and received water and food *ad libitum*. The acute toxicity in mice ($n = 10$) was performed with an oral dose of 5 g kg^{-1} of the CLE. During a seven-day period with adequate acclimatization (21 °C) and food and water given to the mice, *ad libitum*, the following parameters were assessed: hyperactivity, sedation, changes in stool characteristics (consistency), and food and water intake [37].

Data analysis

MIC and MBC values were from two replicate wells from two independent experiments. To assess the interactions between the CLE, HX, or EtOAc and OXA, the data obtained from the checkerboard microdilution assays were analyzed as previously described. The model-fractional inhibitory concentration index (FICI) was calculated as follows: FICA = MICAB/MICA and FICB = MICBA/MICB, where MICA and MICB are the MICs of samples A and B when acting alone, and MICAB and MICBA are the MICs of samples A and B when acting in combination, respectively. A and B represent the treatments (exposures) under investigation (i.e., A: can be an extract or fraction and B: OXA); then, FICI = FICA + FICB. "Synergy" was defined as an FICI ≤ 0.5, while "antagonism" was defined as an FICI value > 4.0. An FICI between 0.5 and 1.25 was considered to have an "additive effect" and between 1.25 and 4 "no interaction" [38, 39]. According to the ratio of MBC/MIC, the type of antimicrobial action displayed by each treatment was considered. If the ratio of MBC/MIC = 1 or 2, the effect was considered bactericidal, but if the ratio of MMC/MIC = 4 or 16, the effect was defined as bacteriostatic [40]. The selectivity index (SI) was calculated as follows: $SI = CC_{90}/MIC_{99.9}$, being CC_{90} adopted from our previous study [7].

Results

MIC and MBC values for OXA and the CLE, EtOAc, and HX from *T. paniculatum*

The MIC and MBC values for OXA and CLE, EtOAc, and HX against OSSA and the two clinical samples are shown in table 3. Increased MIC values were demonstrated for OXA against the isolates (samples G11.39 and G11.19, both resistant to this antibiotic [MIC ≥ 4 μg ml^{-1}]), confirming the ORSA profiles. We found MIC values of 500 μg ml^{-1} for EtOAc and HX and 4000 μg ml^{-1} for CLE against both OSSA and ORSA. The CLE was as effective as OXA against one of the isolates (sample G11.39). Both EtOAc and HX were more effective (lower MICs) than OXA against the two ORSA isolates.

Table 3. Minimum inhibitory (MIC) and minimum bactericidal (MBC) concentrations for the crude leaf extract (CLE) and fractions from *Talinum paniculatum* and for Oxacillin against *Staphylococcus aureus* and the types of antibacterial effects.

Microorganisms	*S. aureus* (ATCC 25923)				*S. aureus* (sample G11.39)				*S. aureus* (sample G11.19)			
Extract/ fraction/ antibiotic	MIC ($\mu g ml^{-1}$)	MBC ($\mu g ml^{-1}$)	MBC/ MIC	Antibacterial effect	MIC ($\mu g ml^{-1}$)	MBC ($\mu g ml^{-1}$)	MBC/ MIC	Antibacterial effect	MIC ($\mu g ml^{-1}$)	MBC ($\mu g ml^{-1}$)	MBC/ MIC	Antibacterial effect
CLE	4000	N	N/A	N/A	4000	N	N/A	N/A	4000	N	N/A	N/A
EtOAc	500	500	1	Bactericidal	500	N	N/A	N/A	500	N	N/A	N/A
HX	500	500	1	Bactericidal	500	N	N/A	N/A	500	N	N/A	N/A
Oxacillin	3.91	7.813	2	Bactericidal	4000	N	N/A	N/A	62.5	1000	16	Bacteriostatic

Antimicrobial Action: Bactericidal

Bacteriostatic

For plants products: MIC up to 100 $\mu g ml^{-1}$ = promising inhibitory potential, MIC between 100 and 625 $\mu g ml^{-1}$ = moderate inhibitory activity [7]. Fractions from the CLE of *Talinum paniculatum*; EtOAc = Ethyl acetate fraction and HX= Hexane fraction; *S. aureus:* samples G11.39 and G11.19 are from clinical environment*; S. aureus*: 5 ′ 10^5 CFU mL^{-1}; Antimicrobial resistance (AMR) classification: OXA MIC ≤ 2 $\mu g ml^{-1}$ = sensitive and ≥ 4 $\mu g ml^{-1}$ = resistant [35]. Ratio MBC/MIC = 1 or 2 → Effect was considered as bactericidal; Ratio MBC/MIC = 4 or 16 → Effect was defined as bacteriostatic [40]. N: inhibition of microbial growth was not observed at maximum used concentration; N/A: not applicable due to absence of an MBC value.

Antistaphylococcal effects for the CLE and fractions

In table 3, it is shown that the fractions EtOAc and HX showed bactericidal effects against OSSA and ORSA. MBC values were not observed for the CLE and fractions at maximum concentrations used in this study, 4000 $\mu g\,ml^{-1}$ and 500 $\mu g\,ml^{-1}$, respectively, against ORSA strains.

Final MIC values for the associations between plant product (CLE, EtOAc, and HX) and OXA, and FICI values from these associations

The associations between plant products (CLE, EtOAc, or HX from *T. Paniculatum*) and OXA, were investigated. As demonstrated in table 3, the treatment of OSSA or ORSA with CLE, EtOAc, or HX, resulted in outstanding MIC values (low MIC values). On the other hand, when the association between plant product (extract/fraction) and OXA was performed (table 4), OXA MICs increased 2- to 4092-fold, whereas the MICs of each fraction decreased up to 1020-fold. Taken together, data from tables 3 and 4 were interpreted as FICI values (table 4), which demonstrated that there was no synergy for any of the associations. The most common effect for the associations was "no interaction" (8 associations).

***In vivo*/*in vitro* toxicity data for *T. paniculatum* and selectivity index (SI)**

Of clinical relevance, the CLE from *T. paniculatum* did not present an acute toxicity at a dose of 5 $g\,kg^{-1}$ (table 5). In table 5, the results of the SI are also presented, and the best ones were from CLE against both OSSA (3.45) and ORSA (3.45).

Discussion

In this study, we first demonstrated that the CLE from *T. paniculatum* and its fractions (EtOA and HX) have antibacterial activity against OSSA and ORSA, and a bactericidal effect for the fractions against OSSA. Currently, resistance to ß-lactam antibiotics in *S. aureus* is a global and serious health threat, even in the clinical environment such as the healthcare settings, places where the ORSA strains used in this study were isolated [4, 41, 42]. Thus, new antimicrobials are urgently needed.

Over the last few decades, the screening of plants seems to be a good option for possible sources of new compounds with original antistaphylococcal action, including studies that evaluate the association between plant product and antibiotic [7, 43-45]. *T. paniculatum* was here evaluated because of previous studies about the antimicrobial activity against medically relevant strains of bacteria and fungi; the popular use in folk medicine, and the culinary use [7]. The antimicrobial activity for members of the *Talinaceae* family or related families have also been described [46, 47].

Table 4. Results for the contribution of each compound or plant product in the final MIC value during the association between (1) plant product (Crude leaf extract [CLE], EtOAc, or HX) from *Talinum paniculatum* and (2) Oxacillin against *Staphylococcus aureus*, correspondent Fractional inhibitory concentration index (FICI), and interpretation of the FICIs from the associations with the resulting type of interaction.

Microorganisms	***S. aureus* (ATCC 25923)**				***S. aureus* (sample G11.39)**				***S. aureus* (sample G11.19)**			
	Concentration ($\mu g\,ml^{-1}$)*		FICI		Concentration ($\mu g\,ml^{-1}$)		FICI		Concentration ($\mu g\,ml^{-1}$)		FICI	
Association	(1)	(2)		Interpretation	(1)	(2)		Interpretation	(1)	(2)		Interpretation
(1) CLE + (2) Oxacillin	4000	16000	>4	Antagonism	4000	16000	>4	Antagonism	4000	16000	>4	Antagonism
(1) EtOAc + (2) Oxacillin	0.49	7.8	2	No interaction	500	8000	3	No interaction	7.8	125	2	No interaction
(1) HX + (2) Oxacillin	0.49	7.8	2	No interaction	500	8000	3	No interaction	7.8	125	2	No interaction
(1) EtOAc + (2) HX	250	250	1	Additive effect	500	500	2	No interaction	500	500	2	No interaction

Interaction index interpretation: Antagonism; No interaction; Additive effect

Fractions from the CLE of *Talinum paniculatum*; EtOAc = Ethyl acetate fraction and HX = Hexane fraction; *Concentration of each substance in the associations between the (1) crude leaf extract (CLE)/fraction (EtOAc, or HX) from *Talinum paniculatum* and (2) oxacillin or (1) fraction and (2) fraction in which no microbial growth was observed; FICI data interpretation from the interactions/associations: 'synergy' (FICI ≤ 0.5), "Additive effect" (FICI > 0.5–1.25) 'no interaction' (FICI > 1.25–4.0), and 'antagonism' (FICI > 4.0) [38-39].

Table 5. Selectivity index (SI) for the crude leaf extract (CLE) and fractions, and *in vivo* toxicity data for the CLE from *Talinum paniculatum*.

Extract/ Fraction	**CLE**		**EtOAc**		**HX**	
Selectivity index						
	MIC	SI	MIC	SI	MIC	SI
S. aureus (ATCC 25923)	400	3.45	500	0.6	500	1.1
S. aureus (sample G11.39)	400	3.45	500	0.6	500	1.1
S. aureus (sample G11.19)	400	3.45	500	0.6	500	1.1
Toxicity	CLE		EtOAc		HX	
In vivo (mice)	Absence at 5 gkg^{1}		----		----	

SI: = $CC_{90}/MIC_{99.9}$; MIC: $\mu g\,ml^{-1}$; fractions from the CLE of *Talinum paniculatum*; EtOAc = ethyl acetate fraction and HX = hexane fraction.

As for the selectivity toward microbial cells, data have demonstrated a low toxicity for *T. paniculatum* leaves on other cells *in vitro*, justifying the antimicrobial potential of this plant [7]. We showed the selectivity of plant products from *T. paniculatum* toward *S. aureus* cells. Moreover, we found absence of an *in vivo* toxicity for *T. paniculatum* leaves at a dose of 5 $mg\,kg^{-1}$.

The screening for the antimicrobial activities of plant products alone, or in association with antibiotic, have been reported in myriad papers that document the effects against different microorganisms, including human pathogens [3, 30, 39, 40, 45, 48-51]. As seen in this study, decreased OXA lethality was observed for the association between plant products and antibiotic, and our results are in line with some previous reports [20, 31, 52]. About this context, the "one drug, one target, one disease" approach has for some time remained the conventional pharmaceutical approach to the search of drugs and treatment strategies. However, this paradigm has been gradually shifted toward the adoption of combination therapies as well as possible interactions between drug and food.

Contrarily to a desirable synergistic action between plant product and OXA, in this study was demonstrated that such associations caused an augmentation in OXA MICs. In this context, a putative action of antioxidants-containing plant product upon ROS levels should be considered. The action of some antibiotics have shown dependence on intense ROS accumulation and associated oxidative stress (i.e., OXA produces ROS

that promotes growth inhibition or kills *S. aureus*), and other studies have pointed that antioxidants-containing plant products and isolated antioxidant compounds can decrease the susceptibility of microorganisms to antimicrobials, including *S. aureus* to ß-lactam and other antistaphylococcal drugs [20, 31, 52-55].

Other evidences indicate a role of harnessing oxidative stress as an interesting way to enhance the killing efficacy of OXA and other antistaphylococcal drugs, regardless of macromolecular or drug-target interaction (the main antibiotic mode-of-action in interfering with cell wall biosynthesis), aside from the importance of new insights into the mechanisms behind signaling pathways in *S. aureus* to control the redox balance and develop high-level AMR/MDR [23, 56, 57]. A metabolic response of *S. aureus* toward oxidative stress caused by penicillin has been proposed through up-regulation of an environmental sensing and other gene, countering oxidative damage coupled with other effects generated by this ß-lactam antibiotic [29, 58]. Moreover, a successful response of *S. aureus vis-à-vis* oxidative stress imposed by antibiotics includes overproduction of antioxidant pigments, overexpression of detoxifying enzymes (such as superoxide dismutase [Sod], catalase and peroxiredoxin AhpC) and genes and enzymes related to DNA protection and repair (including *mrgA* response and pyrophosphohydrolase activity of MutT to remove oxidized guanine [8-oxoG or GO lesion] from the nucleotide pool), and an augmentation in protein damage repair (overexpression of thioredoxin).

It is well-known that ß-lactam antibiotics induce an increase in oxygen consumption to form superoxide ($O_2^{\bullet-}$) as a by-product via different pathways (such as the metabolism-related NADH depletion, the tricarboxylic acid (TCA) cycle, the electron transport chain, damage of iron sulphur clusters in proteins, and stimulation of the Fenton reaction). The production of $O_2^{\bullet-}$ allows the formation of other ROS, including hydrogen peroxide (H_2O_2), and the derivatives $HO^{\bullet}$ (via Fenton chemistry) and/or peroxinitrite ($ONOO^-$, via nitric oxide [•NO] biosynthesis pathways [58-60]. Moreover, while *S. aureus* Sod and catalases can enzymatically degrade $O_2^{\bullet-}$ and H_2O_2, respectively, no cellular detoxification mechanism is described for $HO^{\bullet}$, and this oxidant can avidly attack the DNA [59-61]. Thus, high-levels $HO^{\bullet}$ and the effects of blocking $HO^{\bullet}$ accumulation (controls) can interfere with MIC and MBC values of antistaphylococcus agents (including OXA), as previously reported [20]. In this context, these factors may, at least partially, explain the link between $HO^{\bullet}$ accumulation and oxidative DNA damage, as seen to a broader set of antibiotics and against different microorganisms [59-65], also explaining how antibiotic lethality is enhanced by amplifying basal ROS production and how antioxidants containing-plant products can interfere with this process [53]. In that way, we have reasons to believe that the prevention of OXA-induced ROS-mediated growth inhibition or killing of

S. aureus is related to a mechanism in which the levels/concentrations of compounds in *T. paniculatum* generate an effect "purely antioxidant" within *S. aureus* cells.

Taken together, our findings suggest that the alone CLE, HX and EtOAc from *T. paniculatum* present antistaphylococcal potential for furthers studies, *in vitro* involving other strains of *S. aureus* and *in vivo*. However, a word of warning should be issued regarding the *in vivo* association between *T. paniculatum* and OXA and the use of *T. paniculatum* should be phased out during OXA treatment. These *in vitro* effects carry *in vivo* implications and caution is required, since patients under OXA treatment parallel to the intake of leaves or herbal drug preparations from *T. paniculatum* may cause a decrease in OXA efficacy (jeopardizing therapeutic). Our data supports the fact that antioxidants containing-plant products, being a part of many nutrition products and medicines, may interact with OXA during antibiotic therapy and modify its action, causing resistance phenomenon or the failure of therapeutic regimens. However, to support this idea, these data should be investigated further, and the physician should take all this into account.

Acknowledgments

The authors acknowledge Dr. Marcelo Polo for the identification of the plant material. This study was financed in part by the Coordenação de Aperfeiçoamento de Pessoal de Nível Superior - Brasil (CAPES)-Finance Code 001.

Author contributions

Conceived and designed the experiments: CDC. Performed the experiments: CDC MFRN JJS LFCR. Analyzed the data: CDC. Contributed reagents/materials/analysis tools: MFGB GBS MRPLB. Gave technical support and conceptual advice: MFGB MRPLB. Wrote the paper: CDC. Supervised the study: CDC MRPLB. Final approval of manuscript: CDC JJS MFRN MFGB GBS LFCR MRPLB.

Disclosure statement

No potential conflict of interest was reported by the authors.

References

1. A. Jousselin, W.L. Kelley, C. Barras, *et al*., The *Staphylococcus aureus* thiol/oxidative stress global regulator Spx controls *trfA*, a gene implicated in cell wall antibiotic resistance, *Antimicrob. Agents Chemother.*, **57**, 3283-3292 (2013).

2. IOM (Institute of Medicine), *Antibiotic resistance: Implications for global health and novel intervention strategies*, The National Academies Press, Washington, D.C., 2010.

3. J.E.C. Betoni, R.P. Mantovani, L.N. Barbosa, *et al*., Synergism between plant extract and antimicrobial drugs used on *Staphylococcus aureus* diseases, *Mem. Inst. Oswaldo Cruz*, **101**, 387-390 (2006).

4. Centers for Disease Control and Prevention (CDC), *Antibiotic Resistant Threats in the United States*, U.S. Department of Health and Human Services, Atlanta, GA, 2013, p. 114.

5. E.D. Brown, Is the GAIN Act a turning point in new antibiotic discovery? *Can. J. Microbiol.*, **59**, 153-156 (2013).

6. H. Peng, C. Li, S. Kadow, *et al*., Acid sphingomyelinase inhibition protects mice from lung edema and lethal *Staphylococcus aureus* sepsis, *J. Mol. Med. (Berlin)*, **93**, 675-689 (2015).

7. L.F. Reis, C.D. Cerdeira, B.F. Paula, *et al*., Chemical characterization and evaluation of antibacterial, antifungal, antimycobacterial, and cytotoxic activities of *Talinum paniculatum*, *Rev. Inst. Med. Trop. Sao Paulo*, **57**, 397-405 (2015).

8. N. Gallucci, M. Oliva, E. Carezzano, *et al*., Terpenes antimicrobial activity against slime producing and non-producing staphylococci, *Mol. Med. Chem.*, **21**, 132-136 (2010).

9. J. Nadarajah, M.J. Lee, L. Louie, *et al*., Identification of different clonal complexes and diverse amino acid substitutions in penicillin-binding protein 2 (PBP2) associated with borderline oxacillin resistance in Canadian *Staphylococcus aureus* isolates, *J. Med. Microbiol.*, **55**, 1675-1678 (2006).

10. A. Shirwaikar, R. Govindarajan, A.K.S. Rawat, Integrating complementary and alternative medicine with primary health care, *Evid. Based Complement. Alternat. Med.*, **2013**, Article ID 948308, 3 (2013).

11. Z. Meng, C. Sop, Y. Xuefu, *et al*., Characteristics of baicalin synergy with penicillin or notopterygium ethanol extracts against *Staphylococcus aureus*, *Tsinghua Sci. Technol.*, **11**, 459-461 (2006).

12. J. Caribe, J.M. Campos, *Plantas que ajudam o homem: guia prático para época*, Cultrix/Pensamento, São Paulo, 1991.

13. C. Thanamool, P. Papirom, S. Chanlun, *et al*., *Talinum paniculatum* (Jacq.) Gertn: a medicinal plant with potential estrogenic activity in ovariectomized rats, *Int. J. Pharm. Pharm. Sci.*, **5**, 478-485 (2013).

14. C. Thanamool, A. Thaeomor, S. Chanlun, *et al*., Evaluating the anti-fertility activity of *Talinum paniculatum* (Jacq.) Gaertnin female Wistar rats, *Aust. J. Plant Physiol.*, **7**, 1802–1807 (2013).

15. M.P.O. Ramos, G.D.F. Silva, L.P. Duarte, *et al*. Antinociceptive and edematogenic activity and chemical constituents of *Talinum paniculatum* willd, *J. Chem. Pharm. Res.*, **2**, 265-274 (2010).

16. C. Sukwan, S. Wray, S. Kupittayanant, The effects of Ginseng Java root extract on uterine contractility in nonpregnant rats, *Physiol. Rep.*, **2**, e12230 (2014).

17. H. Shimoda, N. Nishida, K. Ninomiya, *et al*., Javaberine A, new TNF-alpha and nitric oxide production inhibitor, from the roots of *Talinum paniculatum*, *Heterocycles*, **55**, 2043-2050 (2001).

18. T.V. Chittezham, L.C. Kinkead, A. Janssen, *et al*., A dysfunctional tricarboxylic acid cycle enhances fitness of *Staphylococcus epidermidis* during β-lactam stress, *mBio*, **4**, e00437-13 (2013).

19. A. Krawczyk-Balska, J. Marchlewicz, D. Dudek, *et al*., Identification of a ferritin-like protein of *Listeria monocytogenesis* a mediator of β-lactam tolerance and innate resistance to Cephalosporins, *BMC Microbiol.*, **12**, 278 (2012).

20. Y. Liu, X. Liu, Y. Qu, *et al*., Inhibitors of reactive oxygen species accumulation delay and/or reduce the lethality of several antistaphylococcal agents, *Antimicrob. Agents Chemother.*, **56**, 6048-6050 (2012).

21. R. Pechous, N. Ledala, B.J. Wilkinson, *et al*., Regulation of the expression of cell wall stress stimulon member gene msra1 in methicillin-susceptible or -resistant *Staphylococcus aureus*, *Antimicrob. Agents Chemother.*, **48**, 3057-3063 (2004).

22. K. Singh, V.K. Singh, Expression of four methionine sulfoxide reductases in *Staphylococcus aureus*, *Int. J. Microbiol.*, **2012**, Article ID 719594, 8 (2012).

23. K. Poole. Bacterial stress responses as determinants of antimicrobial resistance, *J. Antimicrob. Chemother.*, **67**, 2069-2089 (2012).

24. P. Belenky, J.D. Ye, C.B.M. Porter, *et al*., Bactericidal antibiotics induce toxic metabolic perturbations that lead to cellular damage, *Cell Rep.*, **13**, 968-980 (2015).

25. K. W. Bayles, The biological role of death and lysis in biofilm development, *Nat. Rev. Microbiol.*, **5**, 721-726 (2007).

26. T. Uehara, T. Dinh, T.G. Bernhardt, LytM-domain factors are required for daughter cell separation and rapid ampicillin-induced lysis in *Escherichia coli*, *J. Bacteriol.*, **191**, 5094-5107 (2009).

27. D. Nguyen, A. Joshi-Datar, F. Lepine, *et al.*, Active starvation responses mediate antibiotic tolerance in biofilms and nutrient-limited bacteria, *Science*, **334**, 982-986 (2011).

28. M. Goswami, S.H. Mangoli, N. Jawal, Involvement of reactive oxygen species in the action of ciprofloxacin against *Escherichia coli*, *Antimicrob. Agents Chemother.*, **50**, 949-954 (2006).

29. D.J. Dwyer, P.A. Belenky, J.H. Yang, *et al.*, Antibiotics induce redox-related physiological alterations as part of their lethality, *Proc. Natl. Acad. Sci. USA*, **111**, E2100-E2109 (2014).

30. I. Keren, Y. Wu, J. Inocencio, *et al.*, Killing by bactericidal antibiotics does not depend on reactive oxygen species, *Science*, **339**, 1213-1216 (2013).

31. M. Goswami, S.H. Mangoli, N. Jawali, Antibiotics and antioxidants: Friends or foes during therapy? *BARC Newsletter*, **32**, 42-46 (2011).

32. I. Albesa, M.C. Becerra, P.C. Battan, *et al.*, Oxidative stress involved in the antibacterial action of different antibiotics, *Biochem. Biophys. Res. Commun.*, **317**, 605-609 (2004).

33. S.S. Grant, D.T. Hung, Persistent bacterial infections, antibiotic tolerance, and the oxidative stress response, *Virulence*, **4**, 273-283 (2013).

34. World Health Organization (WHO), *Quality control methods for medicinal plant materials*, Geneva, 1998.

35. J. Meng, G. He, H. Wang, *et al.*, Reversion of antibiotic resistance by inhibiting mecA in clinical methicillin-resistant Staphylococci by antisense phosphorothioate oligonucleotide, *J. Antibiot. (Tokyo)*, **68**, 158-164 (2015).

36. Clinical and Laboratory Standards Institute (CLSI), *Methods for dilution antimicrobial susceptibility tests for bacteria that grow aerobically, Approved standard M7-A6*, 6th ed., CLSI, Wayne, 2003.

37. B.F. Paula, L.F.C. Reis, C.D. Cerdeira, *et al*., Pharmacological evaluation of the anti-inflammatory and antinociceptive effects of the hydroethanolic extract of the leaves of *Raphanus sativus* (L.) var. oleifera metzg in mice, *J. Pharm. Biol.*, **6**, 27-33 (2016).

38. F.C. Odds, Synergy, antagonism, and what the chequerboard puts between them, *J. Antimicrob. Chemother.*, **52**, 1 (2003).

39. J. Meletiadis, S. Pournaras, E. Roilides, *et al*., Defining fractional inhibitory concentration index cutoffs for additive interactions based on self-drug additive combinations, Monte Carlo simulation analysis, and *in vitro -in vivo* correlation data for antifungal drug combinations against *Aspergillus fumigatus*, *Antimicrob. Agents Chemother.*, **54**, 602-609 (2010).

40. K. Konaté, J.F. Mavoungou, A.N. Lepengué, *et al*., Antibacterial activity against β-lactamase producing methicillin and ampicillin-resistants *Staphylococcus aureus*: fractional Inhibitory Concentration Index (FICI) determination, *Ann. Clin. Microbiol. Antimicrob.*, **11**, 18 (2012).

41. J. Nadarajah, M.J. Lee, L. Louie, *et al*., Identification of different clonal complexes and diverse amino acid substitutions in penicillin-binding protein 2 (PBP2) associated with borderline oxacillin resistance in Canadian *Staphylococcus aureus* isolates, *J. Med. Microbiol.*, **55**, 1675-1683 (2006).

42. S. Petti, A. Polimeni, Risk of methicillin-resistant *Staphylococcus aureus* transmission in the dental healthcare setting: a narrative review, *Infect. Control Hosp. Epidemiol.*, **32**, 1109-1115 (2011).

43. M.M. Cowan, Plant products as antimicrobial agents, *Clin. Microbiol. Rev.*, **12**, 564-582 (1999).

44. L.J. Bessa, A. Palmeira, A.S. Gomes, *et al*., Synergistic effects between thioxanthones and oxacillin against methicillin-resistant *Staphylococcus aureus*, *Microb. Drug Resist. (Larchmont, N.Y.)*, **21**, 404-415 (2015).

45. S. Hemaiswarya, A.K. Kruthiventi, M. Doble. Synergism between natural products and antibiotics against infectious diseases, *Phytomedicine*, **15**, 639-652 (2008).

46. R. Londonkar, H.B. Nayaka, Phytochemical and antimicrobial activities of *Portulaca oleracea* L., *J. Pharm. Res.*, **4**, 3553 (2011).

47. N. Savithramma, S. Ankanna, M.L. Rao, *et al*., Studies on antimicrobial efficacy of medicinal tuberous shrub *Talinum cuneifolium*, *J. Environ. Biol.*, **33**, 775-780 (2012).

48. Y. Han, Synergic anticandidal effect of epigallocatechin-O-gallate combined with amphotericin B in a Murine model of disseminated Candidiasis and its anticandidal mechanism*, Biol. Pharm. Bull.*, **30**, 1693-1696 (2007).

49. T. Inui, Y. Wang, S. Deng, *et al*., Counter-current chromatography-based analysis of synergy in an anti-tuberculosis ethnobotanical, *J. Chromatogr. A*, **1151**, 211-215 (2007).

50. L. Sun, S. Sun, A. Cheng, *et al*., *In vitro* activities of retigeric acid B alone and in combination with azole antifungal agents against *Candida albicans*, *Antimicrob. Agents Chemother.*, **53**, 1586-1591 (2009).

51. M.S.A. Khan, I. Ahmad, Antibiofilm activity of certain phytocompounds and their synergy with fluconazole against *Candida albicans* biofilms, *J. Antimicrob. Chemother.*, **67**, 618-621 (2012).

52. G. Smirnova, Z. Samoilova, N. Muzyka, *et al*., Influence of plant polyphenols and medicinal plant extracts on antibiotic susceptibility of *Escherichia coli*, *J. Appl. Microbiol.*, **113**, 192-199 (2012).

53. M.P. Brynildsen, J.A. Winkler, C.S. Spina, *et al*., Potentiating antibacterial activity by predictably enhancing endogenous microbial ROS production, *Nature Biotechnol.*, **31**, 160-165 (2013).

54. R.M. Perera, N. Bardeesy, When antioxidants are bad, *Nature*, **475**, 43-44 (2011).

55. M.C. Becerra, I. Albesa, Oxidative stress induced by ciprofloxacin in *Staphylococcus aureus*, *Biochem. Biophys. Res. Commun.*, **297**, 1003-1007 (2002).

56. D.J. Dwyer, M.A. Kohanski, J.J. Collins, Role of reactive oxygen species in antibiotic action and resistance, *Curr. Opin. Microbiol.*, **12**, 482-489 (2009).

57. D.J. Dwyer, J.J. Collins, G.C. Walker, Unraveling the physiological complexities of antibiotic lethality, *Annu. Rev. Pharmacol. Toxicol.*, **55**, 313-332 (2015).

58. R. Gaupp, N. Ledala, G.A. Somerville, Staphylococcal response to oxidative stress, *Front. Cell. Infect. Microbiol.*, **2**, 1-19 (2012).

59. H. Van Acker, T. Coenye, The role of reactive oxygen species in antibiotic-mediated killing of bacteria, *Trends Microbiol.*, **25**, 456-466 (2017).

60. M.A. Kohanski, D.J. Dwyer, B. Hayete, *et al*., A common mechanism of cellular death induced by bactericidal antibiotics, *Cell*, **130**, 797-810 (2007).

61. B. Balasubramanian, W.K. Pogozelski, T.D. Tullius, DNA strand breaking by the hydroxyl radical is governed by the accessible surface areas of the hydrogen atoms of the DNA backbone, *Proc. Natl. Acad. Sci. USA*, **95**, 9738-9743 (1998).

62. X. Wang, X. Zhao, Contribution of oxidative damage to antimicrobial lethality, *Antimicrob. Agents Chemother.*, **53**, 1395-1402 (2009).

63. T.R. Sampson, X. Liu, M.R. Schroeder, *et al*., Rapid killing of *Acinetobacter baumannii* by polymyxins is mediated by a hydroxyl radical death pathway, *Antimicrob. Agents Chemother.*, **56**, 5642-5649 (2012).

64. S.S. Grant, B.B. Kaufmann, N.S. Chand, *et al*., Eradication of bacterial persisters with antibiotic-generated hydroxyl radicals, *Proc. Natl. Acad. Sci. USA*, **109**, 12147-12152 (2012).

65. J.J. Foti, B. Devadoss, J.A. Winkler, *et al*., Oxidation of the guanine nucleotide pool underlies cell death by bactericidal antibiotics, *Science*, **336**, 315-319 (2012).

How to cite this article

C.D. Cerdeira, J.J. da Silva, M.F.R. Netto, M.F.G. Boriollo, G.B. Santos, L.F.C. dos Reis, M.R.P.L. Brigagão, *Talinum paniculatum* leaves with *in vitro* antimicrobial activity against reference and clinical strains of *Staphylococcus aureus* interfere with oxacillin action, *Rev. Colomb. Cienc. Quím. Farm.*, **49**(2), 432-451 (2020).

Mini-review article / *http://dx.doi.org/10.15446/rcciquifa.v49n2.89898*

EGFR and HER2 small molecules inhibitors as potential therapeutics in veterinary oncology

Juan Martín Cadena García[1,2]*, Carlos Eduardo Giraldo Murillo[1], Manuela Ramos Jaramillo[3]

[1]Universidad de Caldas, Facultad de Ciencias Agropecuarias, Departamento de Salud Animal, Calle 65 N.° 26-10, Manizales, Colombia. Código postal: 170001.

[2]Universidad de Santa Rosa de Cabal (UNISARC), Facultad de Ciencias Agropecuarias, Santa Rosa de Cabal, Colombia.

[3]Universidad de Caldas, Facultad de Ciencias Exactas y Naturales, Calle 65 No 26-10, Manizales, Colombia.

*Corresponding author E-mail address: : juan.cadena@ucaldas.edu.co

Received: 17 August 2019

Revised: 10 April 2020

Accepted: 14 May 2020

Summary

EGFR and HER2 receptors are crucial signaling molecules tyrosine kinase involved in human cancer. Aberrant signaling is associated with a variety of cancers, frequently with poor prognosis. Currently, EGFR and HER2 receptors are being targeted by small molecules, which offer a huge benefit to those patients afflicted by aggressive forms of cancer, improving their prognosis. Both human and canine cancers share molecular, biological, histopathological, and clinical similarities, including EGFR and HER2 expression in some forms of cancer. However, despite the use of one tyrosine kinase inhibitor approved to treat canine mastocytoma, canine cancers overexpressed EGFR and HER2 do not yet have targeted therapy, leading to high morbidity and mortality. Targeting EGFR and HER2 receptors in canine cancers using comparative approaches in human cancer could lead to better outcomes.

Key words: Human cancer, veterinary cancer, EGFR, HER2, inhibitors.

Resumen

Inhibidores EGFR y HER2 como tratamientos potenciales en oncología veterinaria

El receptor de factor de crecimiento epidérmico (Epidermal growth factor receptor, EGFR) y el receptor 2 del factor de crecimiento epidérmico (HER2 epidermal growth factor receptor 2) son moléculas señalizadoras cruciales pertenecientes a la familia de proteínas tirosina quinasa involucradas en el cáncer en humanos. La señalización aberrante de dichos receptores se encuentra asociada con una variedad de tumores, frecuentemente asociados a mal pronóstico. Actualmente, EGFR y HER2 son tratados específicamente a través de pequeñas moléculas inhibidoras, las cuales ofrecen un gran beneficio a aquellos pacientes que padecen formas agresivas de cáncer, y de esta manera su pronóstico mejora. Tanto el cáncer en medicina humana como veterinaria comparte similitudes moleculares, biológicas, histopatológicas y clínicas, las cuales incluyen la expresión tanto de EGFR y HER2 en algunas formas de cáncer. Sin embrago, a pesar del uso de un inhibidor tirosina quinasa aprobado para el manejo del mastocitoma canino los tumores que se caracterizan por la sobreexpresión de EGFR y HER2 aún no cuentan con un inhibidor específico, lo cual conduce a alta morbilidad y mortalidad.

Palabras clave: Cáncer humano, cáncer en veterinaria, EGFR, HER2, inhibidores.

Introduction

Cancer is the most important cause of death in dogs worldwide [1-3]. As observed in human patients EGFR and HER2 receptors, tyrosine kinase receptors that play a fundamental role in the control of fundamental transduction and signaling cellular pathways involved in cell survival, cell proliferation, angiogenesis, cell adhesion, cell motility, development, and organogenesis, their dysregulation can result in both development and progression of a variety of tumors [4, 5]. Their overexpression and amplification are associated with poor prognosis in both species, however by contrast with human medicine, small animal veterinary oncology lacks small molecule inhibitors targeting EGFR and HER2, despite the evidence of *in vitro* activity in canine cancer cell lines of some approved EGFR and HER2 small molecule inhibitors for use in humans [6, 7], in which using inhibitors can provide better prognosis. The objective of this literature research was to review and discuss the role of EGFR and HER2 in the biology of both human and veterinary cancer, and the potential benefit of using EGFR and HER2 small molecule inhibitors in veterinary practice.

EGFR AND HER2 STRUCTURE

EGFR (epidermal growth factor receptor) and HER2, belong to the ErbB subclass of tyrosine kinases receptors (RTKs), one of the most studied signaling proteins and signaling transduction pathways regulators in biology [8-11]. EGFR was the first HER receptor identified as tyrosine kinase receptors a revolutionary discovery [8]. The coding genes of these receptors are EGFR/ERBB1/HER1, ERBB2/HER2/NEU, and can be found in two different chromosomes [12]. Under normal conditions, EGFR and HER2 are expressed by epithelial, mesenchymal, neuronal, cardiac, and mammary tissues [13-15].

The structure presents the typical kinase bi-lobed folding. The N-terminal lobe contains mainly β-strands and a one α-helix, whereas the C-terminal lobe is mostly α-helical [16]. The two lobes are connected through a flexible hinge region and separated by a cleft functioning as docking site for ATP [16].

Globally, EGFR and HER2 consist of an extracellular domain, a single hydrophobic transmembrane α-helix, a juxtamembrane segment, and a catalytic domain with tyrosine kinase activity [12]. ErBb family members exist as monomers, the ligand binding to the extracellular domain results in the formation of either homo or heterodimers, a process that activates the catalytic cytoplasmic domain and the C-terminal phosphorylation initiates further downstream signaling pathways [8].

Although EGFR can HER2 is the preferred dimerization partner to all the other members, the heterodimers forming with HER1 and HER3 manifest a strong signaling activity [8, 10, 17]. The binding domains of ErbB family are stimulated by eleven polypeptide growth factor ligands distributed in 4 subgroups, which results in the formation of dimers [18]. In contrast to EGFR, HER2 receptors are unable to bind growth factors physiologically. However, HER2 can form functional homodimers under non-physiological expression, an important phenomenon in carcinogenesis [19].

EGFR AND HER2 SIGNALING PATHWAYS

EGFR and HER2 signaling pathways correspond to complex networks, their specificity and potency are determined by several factors, and however, the most important determinant is the variety of binding proteins associated with the carboxy-terminal tail from each member of the family [20]. The autophosphorylated sites are determined both by the ligand identity and by the heterodimer partner [20]. HER2 can binds to a much quantity of phosphotyrosine-binding proteins in contrast to other receptors

of the ErbB family [21]. Additionally, EGFR and HER2 heterodimers present higher affinity and broader specificity to various ligands than other heterodimeric receptor complexes in this family, and have slow rates of growth-factor dissociation, slow endocytosis and more recycle to the cell surface [22, 23]. This confers potent mutagenic signaling [24] due to the recruitment of multiple signaling pathways [10]. Ras (Ras/Raf/MEK/ERK1/2 pathway), phospholipase C (PLCγ), Shc-activated mitogen-activated protein kinase (MAPK) and STAT (signal transducer and activator of transcription) proteins, especially STAT3 and STAT5 pathway are common targets of all the family ligands and PI3K/AKT are activated by the majority of the active dimers [5, 8, 25, 26]. The activation of simultaneous signaling cascades, including the MAPK pathway, the stress-activated protein cascade, protein kinase C (PKC) and the Akt pathway results in activation of transcriptional activity in the nucleus [8]. This variety of process involves both the proto-oncogenes fos, myc and Sp1 and Egr1 a family of zinc-finger-containing transcription factors and GA-binding protein (GABP) one of the Ets family members [25].

EGFR and HER2 signaling pathways play fundamental roles in cell survival, cell proliferation, angiogenesis, cell adhesion, cell motility, development, and organogenesis [5, 25]. However, their aberrant signaling results in key events leading to cancer development and progression [18].

EGFR, HER2, AND ONCOGENESIS

EGFR and HER2 dysregulation represent a potent oncogenic trigger [12, 27, 28]. The underlying mechanisms leading to this dysregulated activity include extracellular and cytoplasmatic domains mutations, which cause increased biosynthesis and levels of ErbB proteins. These mechanisms are tumor-specific [28].

Through receptors deregulation matrix metalloproteinases (MMPs) process its ligands, facilitating autocrine activation and growth signals auto-sufficiency [1, 28]. Loss of suppressor genes functions results in EFGR and HER receptors recycling, phenomena that induces the insensibility to growth inhibition [12, 28]. PI3K and STAT signaling inhibit apoptosis, a potent mechanism regulator of cellular survival, additionally, STAT and MAPK signaling provide to cells with unlimited replicative potential [12]. Both STAT3 activation and vascular endothelial growth factor (VEGFR) transactivation results in sustained angiogenesis [29]. Finally, PLCγ, MAPK and MMP pathways are associated with invasion and metastasis [12, 30].

EGFR AND HER2 EXPRESSION IN HUMAN CANCERS

When EGFR and HER2 are deregulated, they can become potent oncogenic triggers [5, 31]. Resulting effects from aberrant EGFR and HER2 signaling pathways induce the hallmarks of cancer (self-sufficiency in growth signals, inhibitory signals insensitivity, apoptosis evasion, angiogenesis, unlimited replication, invasive potential, and metastasis) [31, 32]. Deregulated receptors induce self-ligands processing, and hence, can establish autocrine-signaling loops, which provides EGFR and HER2 the ability to generate their own growth signals [5]. Frequently, loss of regulation occurs because of degradation evasion, and gain sustained signaling. Evasion results whether from increased reutilization or reduced degradation [33, 34]. Additionally, the loss of function of tumor suppressor proteins and constitutively activated receptors [35] increase the effect of inhibitory signals insensitivity [5].

Both amplification or overexpression of EGFR are frequently observed in breast cancer, non-small lung cancer [36], colorectal, urinary bladder, pancreatic, ovarian [18], head and neck squamous cell carcinoma [37, 38], renal [39], hepatocellular carcinoma [40], stomach [41], glioma, meningioma [42, 43], glioblastoma [44], and astrocytoma [8, 20], and they are associated with progression of disease, radiotherapy resistance, and poor survival [45, 46].

On the other hand, both amplification and overexpression of HER2 has been documented in breast and stomach cancer [47], salivary ducts carcinoma [48], ovarian cancer, pancreatic, cervical, endometrium, colon, glioblastoma, head and neck, non-small cell lung cancer, hepatocellular carcinoma, urinary bladder carcinoma, and pediatric osteosarcoma in variable degrees [49-52]. Its expression has been associated with an aggressive phenotype, highly metastatic degree, and poor prognosis [52].

EGFR AND HER2 EXPRESSION IN VETERINARY ONCOLOGY

Despite the role of EGFR and HER2 is well characterized in human medicine, in veterinary medicine is still in its early stages [53]. In veterinary oncology, several studies have documented the overexpression of EGFR and HER2 and its correlation with prognosis, however, these results have been in certain degree contradictory [54], hence further research is needed [5]. In veterinary cancer, EGFR expression has been demonstrated in a variety of cancer, including head and neck squamous cell carcinoma [55], hepatocellular carcinoma [56, 57] , astrocytoma [5, 43], and glioblastoma [58]. There is an increasing body of evidence about the function of EGFR either in normal and neoplastic mammary tissue in dogs, and its potential as a pharmacological target [59].

In canine mammary tumors, one of the most common in dogs a recent study reports the positive correlation between EGFR expression by immunohistochemistry with angiogenesis, histological grade of malignancy, mitotic grade, and clinical stage in canine mammary tumors [60]. Another research evaluated EGFR immunohistochemical expression in 138 tumor specimens, and revealed overexpression in 38 tissues (42.2%), this finding was associated with age, and tumoral size, and showed a relation between overexpression and malignant behavior [61]. Based on 5 molecular phenotypes established in breast cancer according to estrogens, progesterone, and HER2 status [62], in canine mammary tumors researchers have attempted to evaluate the potential of this system [62-64]. One of these studies have revealed 45 de 241 to triple negative (18.7%), 32 (71.1%) was positive to EGFR, and 13 (28.9%) was negative, and they were associated with pathological parameters (grade III, central necrosis, lymphatic infiltration, and high mitotic index) [62]. Another recent research has quantified EGFR in canine mammary tumors using ELISA in 75 specimens of 45 affected patients and 8 controls and demonstrated a statistically significant difference between both groups and a correlation with relapse, and distant metastasis during follow-up, and both reduced global survival and disease-free time. These findings provide the rationale to the implementation to therapeutic intervention, in particular in cases with aggressive behavior [65].

In HER2, its expression has been documented in diverse types of cancer in dogs, especially in canine mammary tumors, which exists larger emphasis, there exists a correlation between overexpression and malignant behavior [61, 66]. Additionally, certain evidence in other types of cancer, such as transitional cell carcinoma in urinary bladder [7, 67], and canine osteosarcoma, has also reported [68]. Clonal aberrations have been identified in the HER2 gene in some types of cancer in dogs [69].

EGFR AND HER2 TYROSINE KINASE INHIBITORS

All small molecules EGFR and HER2 inhibitors, gefitinib (Iressa®, AstraZeneca), erlotinib (Tarceva1®, OSI Pharmaceuticals), lapatinib (Tykerb®, GlaxoSmithKline), vandetanib (Caprelsa®, AstraZeneca), afatinib (Gilotrif®, Boehringer Ingelheim), neratinib (Nerlynx®, Puma Biotechnology, Inc), and dacomitinib (Vizimpro®, Pfizer), belong to quinazoline scaffold binding and occupying adenine of adenosine triphosphate (ATP) pocket, and are one of the most largest groups of RTKs inhibitors approved [70]. The members of this group are classified in reversible belong to the first generation, and irreversible belong to the second generation. EGFR and HER2 inhibitors are further categorized into four types based on the conformation of the binding pocket and the Asp-Phe-Gly (DFG) motif [71, 72] from type I to type V [70].

First generation of EGFR and HER2 inhibitors

Lapatinib

Lapatinib distosylate monohydrate (Tykerb®, GlaxoSmithKline) an oral small molecule reversible inhibitor [73] that targets both EGFR and HER2, was approved by the FDA in March 2007 to be used in combination with capecitabine (Xeloda®; Roche) for patients with metastatic breast cancer overexpressing HER2 and who have received prior therapy including an anthracycline, a taxane and trastuzumab [14]. Lapatinib binds the kinase ATP-binding cleft of EGFR on its inactive conformation in contrast to other HER family inhibitors (erlotinib and gefitinib) that exhibit type I inhibition mechanism [70], additionally uses an allosteric pocket formed by the conformation change of the DFG motif [74]. Lapatinib binds with the inactive conformation of HER4 and HER2 due shares the same contacting residues between both [75], its EGFR, HER2, and HER4 inhibition leads to inhibition of substrate phosphorylation and blocks MAPK and PI3K/Akt and treated cells depending on tumor type can undergo either apoptosis or growth arrest [73].

Second generation of EGFR and HER2 inhibitors

Neratinib

Neratinib maleate (Nerlynx®, Puma Biotechnology, Inc), is an irreversible small molecule inhibitor initially designed to target specifically HER receptor using a model of homology for the catalytic domain [76]. Neratinib binds covalently with a cysteine residue in the adenosine triphosphate (ATP)-binding pocket of HER receptor kinases (Cys773 in EGFR and Cys805 in HER2), which is tough as a property to compete with the high concentration of ATP and provide prolongs inhibition of kinase catalytic activity [77]. It is considered as a pan-HER inhibitor because the cysteine residue required for binding is conserved in these three HER receptors [78]. Neratinib inhibits phosphorylation of MAPK [77], retinoblastoma gene product, blocks cell cycle progression, cyclin D1 expression, increase p27 levels (an inhibitor of cell cycle progression), which result in G1-S arrest and an increase in cells with sub-G1 DNA content, associated with apoptosis [77]. Nerlynx® is indicated as adjuvant treatment of patients with early stage HER2-overexpressed following adjuvant trastuzumab-based therapy [79].

Afatinib

Afatinib, an aniline-quinazoline, is an oral, potent irreversible EGFR and HER2 inhibitor oral. Quinazoline ring binds to catalytic domain as observed with

inhibitors EGFR and HER2 [80] [81] According to efficacy on in vitro and in vivo assays in lung cancer [82, 83] afatinib was approved in 2013 as Gilotrif ®, Boehringer Ingelheim Pharmaceuticals, Inc, to the therapy of non-small cell lung cancer. Its potency in vitro is better than gefitinib and lapatinib due to covalent nature [82]. Afatinib has been effective to a variety of cell lines of breast cancer (BT-474, SUM190-PT, SUM 149-PT y T47D). In fact, this finding was crucial to elucidate its action against Her3, associated with the ability to confer cellular survival to cancer cells throughout the PI3K/Akt pathway [84]. Afatinib has demonstrated synergistic activity to mTOR inhibitor rapamycin and trastuzumab [83], and longer duration of action in vitro in contrast with reversible inhibitors erlotinib, gefitinib y lapatinib [82, 85]. Nowadays the potential role of afatinib as adjuvant therapy with paclitaxel in breast cancer is investigated, however, the results have not yet released [86]. In breast cancer, afatinib has been administered because of HER2 inhibition with promising results in HER overexpressing patients with combination to first-line therapies [87]. Adverse effects documented are very similar to those observed with lapatinib (diarrhea and skin reactions).

Dacomitinib

Dacomitinib inhibits irreversibly EGFR, HER2, and HER4. Its preclinical efficacy was demonstrated only on EGFR T790M, and some HER2 cell lines [88-90]. In both phases, I and II, dacomitinib was safe and efficient in patients with non-small cell lung cancer, even compared with patients treated with erlotinib [91]. Adverse effects observed in different trials are diarrhea, dermatitis acneiform, and other types of skin toxicities, and stomatitis [91]. In 2018 was approved the first-line treatment of patients with metastatic non-small cell lung cancer (NSCLC) with epidermal growth factor receptor (EGFR) exon 19 deletion or exon 21 L858R substitution mutations.

Comparative oncology: opportunities for both species

The insights in the molecular and genomic research of cancer have improved the understanding about the similarities between humans and dogs and have led to the concept of comparative oncology, which has the objective to accelerate simultaneously the cancer drug development in both species [92]. Whole canine genome sequence and assembly released in 2005 and improved in 2014 has revealed strong similarities in genes implied in cancer development and progression [93, 94]. Additionally, it is widely accepted that both humans and dogs share certain features in cancer, including determined risk factors, such as age, hormonal, environmental influence, histological types, overexpression of a variety of biomarkers such as cellular proliferation

(Ki67, AgNor), p53 mutations, EGFR, MMPs, cyclooxygenase 2 (COX2), molecular, clinical behaviors and outcomes, however also exist significant differences [95-98].

Tyrosine kinase inhibitors in veterinary oncology

Actually, in veterinary oncology only exists one small molecule inhibitor of RTKs approved to clinical use in canine patients by FDA, toceranib phosphate (Palladia®, Pfizer Animal Health), an oral small molecule inhibitor targeting VEGFR2, platelet-derived growth factor receptor (PDGFRα) and c-kit [99]. Due Palladia® has structural similarity with Sunitinib® an oral small molecule inhibitor targeting VEGFR2, VEGFR3, PDGFRα/β, KIT, CSF1R, FLT-3, and RET, probably has an additional activity to these molecules [100]. Toceranib phosphate was initially developed as an antiangiogenic drug, however, due to its wider pharmacological profile that includes KIT and FLT-3 causes antitumor activity [101].

Its first clinical efficacy in canine cancer patients was a phase 1 clinical trial, which included 57 dogs with diverse temporal types including sarcomas, carcinomas, melanomas, myelomas, and mastocytomas. The response in 16 patients was observed: 6 with complete response and 10 with partial response and stable disease. This study documented a biological activity of 54% [99].

After its FDA approved licensed in June 2009, has been utilized as an extra label in other temporal types that failed to standard treatments, including metastatic osteosarcoma, anal sacs adenocarcinoma, thyroid carcinoma, head, and neck carcinoma, and nasal carcinoma documented clinical benefit in 63 of 85 dogs [102]. Additionally, have been documented responses in a case of [103], synergistic activity with piroxicam in transitional and squamous cell carcinoma and with vinblastin in mastocytoma [104, 105].

In combination with radiotherapy its efficacy was evaluated, was observed the objective response in 76.4%, 58.8% of canine patients achieved a complete response and 17.6% partial response, which suggest clinical benefit [106].

Imatinib (Gleevec®, Novartis) an oral small molecule inhibitor targeting Bcr/Abl, platelet-derived growth factor (PDGF) and stem cell factor (SCF) c-kit in human patients with chronic myelogenous leukemia (CML), myelodysplastic/myeloproliferative diseases, aggressive systemic mastocytosis, hypereosinophilic syndrome and/or chronic eosinophilic leukemia (CEL), dermatofibrosarcoma protuberans, and malignant gastrointestinal stromal tumors (GIST), demonstrated tolerance in canine patients [107-109].

An interesting *in vitro* study with Gefitinib (Iressa1®, AstraZeneca), an oral small molecule inhibitor targeting EGFR, conducted in a cellular line of CMT (REM134) demonstrated a favorable effect in cellular proliferation, migration. Additionally, other small molecule inhibitors such as AG825, which targeting HER2 and GW583340, which targeting EGFR and ERBB2, have documented activity, with the potential use in veterinary oncology clinical trials [*6*].

Conclusions

As documented in human cancer, in canine patients the aberrant expression of EGFR and HER2 receptors constitute a potent oncogenic trigger, however in canine patients still clearly unresolved the expression patterns and the precise molecular structure, which limit its inclusion in validated clinical trials. Despite the increasing evidence of the biological activity of EGFR and HER2 small molecule inhibitors using in human medicine in canine cancer cell lines, their clinical use not have been yet received special attention, in contrast to toceranib phosphate and masitinib mesylate in veterinary oncology. Actually, there is an increasing interest in developing targeted therapies in veterinary oncology. The *in vitro* efficacy documented regarding some small molecule tyrosine kinase inhibitors, can constitute an interesting starting point to initiate the investigation of therapeutic potential to target EGFR and HER2 in veterinary cancer and then improve the clinical outcomes, survival rates, and optimize health quality of life of these patients. Veterinary cancer high prevalence requires targeted therapies, and the routinely uses of EGFR and HER2 small molecules inhibitors represent an excellent opportunity to address this worldwide problem that affects dogs.

Disclosure statement

No potential conflict of interest was reported by the authors.

References

1. V.J. Adams, K.M. Evans, J. Sampson, J.L.N. Wood, Methods and mortality results of a health survey of purebred dogs in the UK, *J. Small Anim. Pract.*, **51**(10), 512-524 (2010).

2. J.M. Fleming, K.E. Creevy, Mortality in North American dogs from 1984 to 2004: An investigation into age-, size-, and breed-related causes of death, *J. Vet. Intern. Med.*, **25**(2), 187-198 (2011).

3. A. Egenvall, A. Nødtvedt, J. Häggström, B. Ström-Holst, L. Möller, B.N. Bonnett, Mortality of life-insured Swedish cats during 1999 –2006: Age, breed, sex, and diagnosis, *J. Vet. Intern. Med.*, **23**(6), 1175-1183 (2009).

4. P. Blume-Jensen, T. Hunter, Oncogenic kinase signalling, *Nature*, **411**, 355-365 (2001).

5. G.T. Bergkvist, D.A. Yool, Epidermal growth factor receptor as a therapeutic target in veterinary oncology, *Vet. Comp. Oncol.*, **9**(2), 81-94 (2011).

6. M.E. Gray, S. Lee, A.L. Mcdowell, *et al.*, Dual targeting of EGFR and ERBB2 pathways produces a synergistic effect on cancer cell proliferation and migration *in vitro*, *Vet. Comp. Oncol.*, **15**(3), 890-909 (2017).

7. K. Sakai, S. Maeda, K. Saeki, *et al.*, Anti-tumour effect of lapatinib in canine transitional cell carcinoma cell lines, *Vet. Comp. Oncol.*, **16**(4), 642-649 (2018).

8. R. Roskoski, Jr., The ErbB/HER family of protein-tyrosine kinases and cancer, *Pharmacol. Res.*, **79**, 34-74 (2014).

9. M.A. Lemmon, J. Schlessinger, Cell signaling by receptor tyrosine kinases, *Cell*, **141**(7), 1117-1134 (2010).

10. A. Citri, Y. Yarden, EGF – ERBB signalling : towards the systems level, *Nat. Rev. Mol. Cell Biol.*, **7**, 505-516 (2006).

11. P. Littlefield, L. Liu, V. Mysore, Y. Shan, D.E. Shaw, N. Jura, Structural analysis of the EGFR /HER3 heterodimer reveals the molecular basis for activating HER3 mutations, *Sci. Signal.*, **7**(354), ra114 (2014).

12. G.T. Bergkvist, D.A. Yool, Epidermal growth factor receptor as a therapeutic target in veterinary oncology, *Vet. Comp. Oncol*., **9**(2), 81-94 (2011).

13. N.E. Hynes, H.A. Lane, ERBB receptors and cancer: the complexity of targeted inhibitors, *Nat. Rev. Cancer*, **5**(5), 341-354 (2005).

14. B. Moy, P. Kirkpatrick, S. Kar, P. Goss, Lapatinib, *Nat. Rev. Drug Discov.*, **6**(6), 431-432 (2007).

15. R. Nahta, G.N. Hortobagyi, F.J. Esteva, Growth factor receptors in breast cancer: potential for therapeutic intervention, *Oncologist*, **8**(1), 5-17 (2003).

16. K. Aertgeerts, R. Skene, J. Yano, *et al.*, Structural analysis of the mechanism of inhibition and allosteric activation of the kinase domain of HER2 protein, *J. Biol. Chem.*, **286**(21), 18756-18765 (2011).

17. E. Tzahar, H. Waterman, X. Chen, *et al.*, A hierarchical network of interreceptor interactions determines signal transduction by Neu differentiation factor/neuregulin and epidermal growth factor, *Mol. Cell. Biol.*, **16**(10), 5276-5287 (1996).

18. R. Roskoski, Jr., The ErbB/HER receptor protein-tyrosine kinases and cancer, *Biochem. Biophys. Res. Commun.*, **319**(1), 1-11 (2004).

19. R. Ghosh R, A. Narasanna S.E. Wang, *et al.*, Trastuzumab has preferential activity against breast cancers driven by HER2 homodimers, *Cancer Res.*, **71**(5), 1871-1882 (2011).

20. Y. Yarden, M.X. Sliwkowski, Untangling the ErbB signalling network, *Nat. Rev. Mol. Cell. Biol.*, **2**(2), 127-137 (2001).

21. R.B. Jones, A. Gordus, J.A. Krall, G. Macbeath, A quantitative protein interaction network for the ErbB receptors using protein microarrays, *Nature*, **439**, 168-174 (2006).

22. A.E. Lenferink, R. Pinkas-Kramarski, M.L. van de Poll, *et al.*, Differential endocytic routing of homo- and hetero-dimeric ErbB tyrosine kinases confers signaling superiority to receptor heterodimers, *EMBO J.*, **17**(12), 3385-3397 (1998).

23. J. Baulida, M.H. Kraus, M. Alimandi, P. Paolo, D. Fiore, G. Carpenter, All ErbB receptors other than the epidermal growth factor receptor are endocytosis impaired (*), *J. Biol. Chem.*, **271**(9), 5251-5257 (1996).

24. R. Pinkas-kramarski, L. Soussan, H. Waterman, *et al.*, Diversification of Neu differentiation factor and epidermal growth factor signaling by combinatorial receptor interactions, *EMBO J.*, **15**(10), 2452-2467 (1996).

25. G. Lurje, H.J. Lenz, EGFR signaling and drug discovery, *Oncology*, **77**(6), 400-410 (2009).

26. T. Bowman, R. Garcia, J. Turkson, R. Jove, STATs in oncogenesis, *Oncogene*, **19**(21), 2474-2488 (2000).

27. S.P. Soltoff, L.C. Cantley, p120cbl is a cytosolic adapter protein that associates with phosphoinositide 3-kinase in response to epidermal growth factor in PC12 and other cells, *J. Biol. Chem.*, **271**(1), 563-567 (1996).

28. R. Zandi, A.B. Larsen, P. Andersen, M.T. Stockhausen, H.S. Poulsen, Mechanisms for oncogenic activation of the epidermal growth factor receptor, *Cell Signal*, **19**(10), 2013-2023 (2007).

29. G. Niu, K.L. Wright, M. Huang, *et al.*, Constitutive Stat3 activity up-regulates VEGF expression and tumor angiogenesis, *Oncogene*, **21**, 2000-2008 (2002).

30. D. Hanahan, R.A. Weinberg, Hallmarks of cancer: The next generation, *Cell*, **144**(5), 646-674 (2011).

31. S. Ménard, S.M. Pupa, M. Campiglio, E. Tagliabue, Biologic and therapeutic role of HER2 in cancer, *Oncogene*, **22**(42), 6570-6578 (2003).

32. D. Hanahan, R.A. Weinberg, The hallmarks of cancer, *Cell*, **100**(1), 57-70 (2000).

33. A. Sorkin, L.K. Goh, Endocytosis and intracellular trafficking of ErbBs, *Exp. Cell. Res.*, **315**(4), 683-696 (2009).

34. G. Levkowitz, H. Waterman, E. Zamir, *et al.*, c-Cbl/Sli-1 regulates endocytic sorting and ubiquitination o the epidermal growth factor receptor, *Genes Dev.*, **12**, 3663-3674 (1998).

35. S.J. Rogers, K.J. Harrington, P. Rhys-Evans, P. O-Charoenrat, S.A. Eccles, Biological significance of c-erbB family oncogenes in head and neck cancer, *Cancer Metastasis Rev.*, **24**(1), 47-69 (2005).

36. S.V. Sharma, D.W. Bell, J. Settleman, D.A. Haber, Epidermal growth factor receptor mutations in lung cancer, *Nat. Rev. Cancer*, **7**(3), 169-181 (2007).

37. M. Mrhalova, J. Plzak, J. Betka, R. Kodet, Epidermal growth factor receptor - its expression and copy numbers of EGFR gene in patients with head and neck squamous cell carcinomas, *Neoplasma*, **52**(4), 338-343 (2005).

38. B. Kumar, K.G. Cordell, J.S. Lee, *et al.*, Response to therapy and outcomes in oropharyngeal cancer are associated with biomarkers including human papillomavirus, epidermal growth factor receptor, gender, and smoking, *Int. J. Radiat. Oncol. Biol. Phys.*, **69**(2 Suppl.), 109-111 (2007).

39. J.R. Grandis, D.J. Tweardy, Elevated levels of transforming growth factor alpha and epidermal growth factor receptor messenger RNA are early markers of carcinogenesis in head and neck cancer, *Cancer Res.*, **53**, 3579-3584 (1993).

40. M. Sibilia, R. Kroismayr, B.M. Lichtenberger, A. Natarajan, M. Hecking, M. Holcmann, The epidermal growth factor receptor: from development to tumorigenesis, *Differentiation*, **75**(9), 770-787 (2007).

41. R. Terragni, A.C. Gardini, S. Sabattini, *et al.*, EGFR, HER-2 and KRAS in canine gastric epithelial tumors: A potential human model? *PLoS One*, **9**(1), e85388 (2014).

42. R.J. Higgins, P.J. Dickinson, R.A. Lecouteur, *et al.*, Spontaneous canine gliomas: Overexpression of EGFR, PDGFRα and IGFBP2 demonstrated by tissue microarray immunophenotyping, *J. Neurooncol.*, **98**(1), 49-55 (2010).

43. R. Thomas, S.E. Duke, H.J. Wang, *et al.*, "Putting our heads together": Insights into genomic conservation between human and canine intracranial tumors, *J. Neurooncol.*, **94**(3), 333-349 (2009).

44. H.K. Gan, A.H. Kaye, R.B. Luwor, The EGFRvIII variant in glioblastoma multiforme, *J. Clin. Neurosci.*, **16**(6), 748-754 (2009).

45. J. Baselga, Why the epidermal growth factor receptor? The rationale for cancer therapy, *Oncologist*, **7**(Suppl. 4), 2-8 (2002).

46. L. Milas, K.A. Mason, K.K. Ang, Epidermal growth factor receptor and its inhibition in radiotherapy: *In vivo* findings, *Int. J. Radiat. Biol.*, **79**(7), 539-545 (2003).

47. M. Yan, M. Schwaederle, D. Arguello, HER2 expression status in diverse cancers : review of results, *Cancer Metastasis Rev.*, **34**(1), 157-164 (2015).

48. M.D. Williams, D.B. Roberts, M.S. Kies, L. Mao, R.S. Weber, A.K. El-Naggar, Genetic and expression analysis of HER-2 and EGFR genes in salivary duct carcinoma: Empirical and therapeutic significance, *Clin. Cancer Res.*, **16**(8), 2266-2274 (2010).

49. M. Yan, B.A. Parker, R. Schwab, R. Kurzrock, HER2 aberrations in cancer: Implications for therapy, *Cancer Treat. Rev.*, **40**(6), 770-780 (2014).

50. F. Cappuzzo, L. Bemis, M. Varella-Garcia, HER2 mutation and response to trastuzumab therapy in non-small-cell lung cancer, *N. Engl. J. Med.*, **354**(24), 2619-2621 (2006).

51. H. Zhou, R. Randall, A. Brothman, T. Maxwell, C. Coffin, R. Goldsby, Expression in osteosarcoma increases risk of lung metastasis and can be associated with gene amplification, *J. Pediatr. Hematol. Oncol.*, **25**(1), 27-32 (2003).

52. N.J. Mason, J.S. Gnanandarajah, J.B. Engiles, *et al.*, Immunotherapy with a HER2-targeting listeria induces HER2-specific immunity and demonstrates potential therapeutic effects in a phase I trial in canine osteosarcoma**,** *Clin Cancer Res.*, **22**(17), 4380-4390 (2016).

53. C.A. London, Tyrosine kinase inhibitors in veterinary medicine, *Top. Companion Anim. Med.*, **24**(3), 106-112 (2009).

54. R. Klopfleisch, P. Klose, A.D. Gruber, The combined expression pattern of BMP2, LTBP4, and DERL1 discriminates malignant from benign canine mammary tumors, *Vet. Pathol.*, **47**(3), 446-454 (2010).

55. J.S. Looper, D.E. Malarkey, D. Ruslander, D. Proulx, D.E. Thrall, Epidermal growth factor receptor expression in feline oral squamous cell carcinomas, *Vet. Comp. Oncol.*, **4**(1), 33-40 (2006).

56. Z. Grabarević, M. Corić, S. Seiwerth, *et al.*, Comparative analysis of hepatocellular carcinoma in men and dogs, *Coll. Antropol.*, **33**(3), 811-814 (2009).

57. G. Stoica, H.-T. Kim, D.G. Hall, J.R. Coates, Morphology, immunohistochemistry, and genetic alterations in dog astrocytomas, *Vet. Pathol.*, **41**(1), 10-19 (2004).

58. D.L. Ipsitz, R.J.H. Iggins, G.D.K. Ortz, *et al.*, Glioblastoma multiforme: clinical findings, magnetic resonance imaging , and pathology in five dogs, *Vet. Pathol.*, **40**(6), 659-669 (2003).

59. A.A. Santos, A.J.F. Matos, Advances in the understanding of the clinically relevant genetic pathways and molecular aspects of canine mammary tumours. Part 2: Invasion, angiogenesis, metastasis and therapy, *Vet. J.*, **205**(2), 144-153 (2015).

60. M.I. Carvalho, M.J. Guimarães, I. Pires, *et al.*, EGFR and microvessel density in canine malignant mammary tumours, *Res. Vet. Sci.*, **95**(3), 1094-1099 (2013).

61. A. Gama, F. Gärtner, A. Alves, F. Schmitt, Immunohistochemical expression of Epidermal Growth Factor Receptor (EGFR) in canine mammary tissues, *Res. Vet. Sci.*, **87**(3), 432-437 (2009).

62. N.H. Kim, H.Y. Lim, K.S. Im, J.H. Kim, J.-H. Sur, Identification of triple-negative and basal-like canine mammary carcinomas using four basal markers, *J. Comp. Pathol.*, **148**(4), 298-306 (2013).

63. F. Sassi, C. Benazzi, G. Castellani, G. Sarli, Molecular-based tumour subtypes of canine mammary carcinomas assessed by immunohistochemistry, *BMC Vet. Res.*, **6**, 5 (2010).

64. A. Gama, A. Alves, F. Schmitt, Identification of molecular phenotypes in canine mammary carcinomas with clinical implications: Application of the human classification, *Virchows Arch.*, **453**(2), 123-132 (2008).

65. F.L. Queiroga, M.D. Perez-Alenza, A. González-Gil, G. Silván, L. Peña, J.C. Illera, Quantification of epidermal growth factor receptor (EGFR) in canine mammary tumours by ELISA assay: Clinical and prognostic implications, *Vet. Comp. Oncol.*, **15**(2), 383-390 (2017).

66. J. Martín de las Mulas, J. Ordás, Y. Millán, V. Fernández-Soria, S. Ramón y Cajal, Oncogene HER-2 in canine mammary gland carcinomas: An immunohistochemical and chromogenic in situ hybridization study, *Breast Cancer Res. Treat.*, **80**, 363-367 (2003).

67. F. Millanta, J. Impellizeri, L. McSherry, G. Rocchigiani, L. Aurisicchio, G. Lubas, Overexpression of HER-2 via immunohistochemistry in canine urinary bladder transitional cell carcinoma - A marker of malignancy and possible therapeutic target, *Vet. Comp. Oncol.*, **16**(2), 297-300 (2018).

68. A.F. Flint, L. U'Ren, M.E. Legare, S.J. Withrow, W. Dernell, W.H. Hanneman, Overexpression of the erbB-2 proto-oncogene in canine osteosarcoma cell lines and tumors, *Vet. Pathol.*, **41**(3), 291-296 (2004).

69. H. Murua-Escobar, K. Becker, J. Bullerdiek, I. Nolte, The canine ERBB2 gene maps to a chromosome region frequently affected by aberrations in tumors of the dog (*Canis familiaris*), *Cytogenet. Cell Genet.*, **94**(3-4), 194-195 (2001).

70. P. Wu, T.E. Nielsen, M.H. Clausen, FDA-approved small-molecule kinase inhibitors, *Trends Pharmacol. Sci.*, **36**(7), 422-439 (2015).

71. R.A. Norman, D. Toader, A.D. Ferguson, Structural approaches to obtain kinase selectivity, *Trends Pharmacol. Sci.*, **33**(5), 273-278 (2012).

72. M.E.M. Noble, J.A. Endicott, L.N. Johnson, Protein kinase inhibitors: insights into drug design from structure, *Science*, **303**(5665), 1800-1805 (2004).

73. A.J. Tevaarwerk, J.M. Kolesar, Lapatinib: A small-molecule inhibitor of epidermal growth factor receptor and human epidermal growth factor receptor-2 tyrosine kinases used in the treatment of breast cancer, *Clin. Therapeut.*, **31**(Part. 2), 2332-2348 (2009).

74. E.R. Wood, A.T. Truesdale, O.B. McDonald, *et al.*, A unique structure for epidermal growth factor receptor bound to GW572016 (Lapatinib): Relationships among protein conformation, inhibitor off-rate, and receptor activity in tumor cells, *Cancer Res.*, **64**(18), 6652-6659 (2004).

75. C. Qiu, M.K. Tarrant, S.H. Choi, *et al.*, Mechanism of activation and inhibition of the HER4/ErbB4 kinase, *Structure*, **16**(3), 460-467 (2008).

76. H.-R. Tsou, E.G. Overbeek-klumpers, W.A. Hallett, *et al.*, Optimization of 6,7-disubstituted-4-(arylamino)quinoline-3-carbonitriles as orally active, irreversible inhibitors of human epidermal growth factor receptor-2 kinase activity, *J. Med. Chem.*, **48**(4), 1107-1131 (2005).

77. S.K. Rabindran, C.M. Discafani, E.C. Rosfjord, *et al.*, Antitumor activity of HKI-272, an orally active, irreversible inhibitor of the HER-2 tyrosine kinase, *Cancer Res.*, **64**(11), 3958-3965 (2004).

78. A. Wissner, T.S. Mansour, The vevelopment of HKI-272 and related compounds for the treatment of cancer, *Arch. Pharm. Chem. Life Sci.*, **341**(8), 465-477 (2008).

79. S.R. Tiwari, P. Mishra, J. Abraham, Neratinib, a novel HER2-targeted tyrosine inhibitor, *Clin. Breast Cancer*, **16**(5), 344-348 (2016).

80. F. Solca, G. Dahl, A. Zoephel, *et al.*, Target binding properties and cellular activity of afatinib (BIBW 2992), an irreversible ErbB family blocker, *J. Pharmacol. Exp. Ther.,* **343**(2), 342-350 (2012).

81. R. Roskoski, Jr., ErbB/HER protein-tyrosine kinases: Structures and small molecule inhibitors, *Pharmacol. Res.*, **87**, 42-59 (2014).

82. S.A. Hurvitz, R. Shatsky, N. Harbeck, Afatinib in the treatment of breast cancer, *Expert Opin. Investig. Drugs*, **23**(7), 1039-1047 (2014).

83. D. Li, L. Ambrogio, T. Shimamura, *et al.*, BIBW2992, an irreversible EGFR/HER2 inhibitor highly effective in preclinical lung cancer models, Oncogene, 27(34), 4702-4711 (2008).

84. Y. Wu, Y. Zhang, M. Wang, *et al.*, Downregulation of HER3 by a novel antisense oligonucleotide, EZN-3920, improves the antitumor activity of EGFR and HER2 tyrosine kinase inhibitors in animal models, *Mol. Cancer Ther.*, **12**(4), 427-437 (2013).

85. A. Canonici, K. Pedersen, B. Browne, M. McDermott, N. Walsh, J. Crown, N. O'Donovan, Effect of afatinib alone and in combination with trastuzumab in HER2-positive breast cancer cell lines, *J. Clin. Oncol.*, **31**(15 Suppl.), 632 (2013).

86. R.L.N. Godone, G.M. Leitão, N.B. Araújo, C.H.M. Castelletti, J.L. Lima-Filho, D.B.G. Martins, Clinical and molecular aspects of breast cancer : Targets and therapies, *Biomed. Pharmacother.*, **106**, 14-34 (2018).

87. X. Zhang, P.N. Munster, New protein kinase inhibitors in breast cancer: afatinib and neratinib, *Expert Opin. Pharmacother.*, **15**(9), 1277-1288 (2014).

88. J.A. Engelman, K. Zejnullahu, C. Gale, *et al.*, PF00299804, an irreversible Pan-ERBB inhibitor, is effective in lung cancer models with EGFR and ERBB2 mutations that are resistant to gefitinib, *Cancer Res.*, **67**(24), 11924-11933 (2007).

89. A.J. Gonzales, K.E. Hook, I.W. Althaus, *et al.*, Antitumor activity and pharmacokinetic properties of PF-00299804 , a second-generation irreversible pan-erbB receptor tyrosine kinase inhibitor, *Mol. Cancer Ther.*, **7**(7), 1880-1889 (2008).

90. B.-C. Liao, C.-C. Lin, J.C.-H. Yang, Second and third-generation epidermal growth factor receptor tyrosine kinase inhibitors in advanced nonsmall cell lung cancer, *Curr. Opin. Oncol.*, **27**(2), 94-101 (2015).

91. S.S. Ramalingam, F. Blackhall, M. Krzakowski, *et al.*, Randomized phase II study of dacomitinib (PF-00299804), an irreversible pan-human epidermal growth factor receptor inhibitor, versus erlotinib in patients with advanced non-small-cell lung cancer, *J. Clin. Oncol.*, **30**(27), 3337-3344 (2012).

92. J. Singer, M. Weichselbaumer, T. Stockner, *et al.*, Comparative oncology: ErbB-1 and ErbB-2 homologues in canine cancer are susceptible to cetuximab and trastuzumab targeting, *Mol. Immunol.*, **50**(4), 200-209 (2012).

93. K. Lindblad-Toh, C.M. Wade, T.S. Mikkelsen, *et al.*, Genome sequence, comparative analysis and haplotype structure of the domestic dog, *Nature*, **438**(7069), 803-819 (2005).

94. M.P. Hoeppner, A. Lundquist, M. Pirun, et al., An improved canine genome and a comprehensive catalogue of coding genes and non-coding transcripts, *PLoS One*, **9**(3), e91172 (2014).

95. P. Rivera, H. von Euler, Molecular biological aspects on canine and human mammary tumors, *Vet. Pathol.*, **48**(1), 132-146 (2011).

96. S. Visan, O. Balacescu, I. Berindan-Neagoe, C. Catoi, *In vitro* comparative models for canine and human breast cancer, *Clujul Med.*, **89**(1), 38-49 (2016).

97. K.S. Borge, S. Nord, P. Van-Loo, *et al.*, Canine mammary tumours are affected by frequent copy number aberrations, Including amplification of MYC and loss of PTEN, *PLoS One*, **10**(5), e0126371 (2015).

98. F.L. Queiroga, T. Raposo, M.I. Carvalho, J. Prada, I. Pires, Canine mammary tumours as a model to study human breast cancer: most recent findings, *In Vivo*, **25**(3), 455-465 (2011).

99. C.A. London, A.L. Hannah, R. Zadovoskaya, *et al.*, Phase I dose-escalating study of SU11654, a small molecule receptor tyrosine kinase inhibitor, in dogs with spontaneous malignancies, *Clin. Cancer Res.*, **9**(7), 2755-2768 (2003).

100. G.S. Papaetis, K.N. Syrigos, Sunitinib: A multitargeted receptor tyrosine kinase inhibitor in the era of molecular cancer therapies, *BioDrugs*, **23**(6), 377-389 (2009).

101. C.A. London, Small molecule inhibitors in veterinary oncology practice, *Vet. Clin. North Am., Small Anim. Pract.*, **44**(5), 893-908 (2014).

102. C. London, T. Mathie, N. Stingle, *et al.*, Preliminary evidence for biologic activity of toceranib phosphate (Palladia®) in solid tumours, *Vet. Comp. Oncol.*, **10**(3), 194-205 (2012).

103. A. Marcinowska, J. Warland, M. Brearley, J. Dobson, A novel approach to treatment of lymphangiosarcoma in a boxer dog, *J. Small Anim. Pract.*, **54**(6), 334-337 (2013).

104. E. Chon, L. McCartan, L.N. Kubicek, D.M. Vail, Safety evaluation of combination toceranib phosphate (Palladia) and piroxicam in tumour-bearing dogs (excluding mast cell tumours): A phase I dose-finding study, *Vet. Comp. Oncol.*, **10**(3), 184-193 (2012).

105. C. Robat, C. London, L. Bunting, *et al.*, Safety evaluation of combination vinblastine and toceranib phosphate (Palladia®) in dogs: A phase I dose-finding study, *Vet. Comp. Oncol.*, **10**(3), 174-183 (2012).

106. K.S. Carlsten, C.A. London, S. Haney, R. Burnett, A.C. Avery, D.H. Thamm, Multicenter prospective trial of hypofractionated radiation treatment, toceranib, and prednisone for measurable canine mast cell tumors, *J. Vet. Intern. Med.*, **26**(1), 135-141 (2012).

107. L. Marconato, G. Bettini, C. Giacoboni, *et al*., Clinicopathological features and outcome for dogs with mast cell tumors and bone marrow involvement, *J. Vet. Intern. Med.*, **22**(4), 1001-1007 (2008).

108. M. Isotani, N. Ishida, M. Tominaga, *et al.*, Effect of tyrosine kinase inhibition by imatinib mesylate on mast cell tumors in dogs, *J. Vet. Intern. Med.*, **22**(4), 985-988 (2008).

109. O. Yamada, M. Kobayashi, O. Sugisaki, *et al.*, Imatinib elicited a favorable response in a dog with a mast cell tumor carrying a c-kit c.1523A>T mutation via suppression of constitutive KIT activation, *Vet. Immunol. Immunopathol.*, **142**(1-2), 101-106 (2011).

How to cite this article

J.M. Cadena-García, C.E. Giraldo-Murillo, M. Ramos Jaramillo, EGFR and HER2 small molecules inhibitors as potential therapeutics in veterinary oncology, *Rev. Colomb. Cienc. Quím. Farm.*, **49**(2), 452-471 (2020).

Artigo de pesquisa científica / *http://dx.doi.org/10.15446/rcciquifa.v49n2.89920*

A descrição matemática da detecção eletroquímica dos alcaloides do grupo da insubosina, assistida pelos novos triazóis com e sem composto de ligação

Volodymyr V. Tkach[1,2]*, Marta V. Kushnir[1], Sílvio C. de Oliveira[2], Volodymyr V. Parchenko[3], Vira M. Odyntsova[3], Ilona I. Aksyonova[3], Olga V. Luganska[4], Maryna M. Kornet[4], Yana G. Ivanushko[1], Petro I. Yagodynets´[1]

[1]Universidade Nacional de Chernivtsi, 58012, Rua de Kotsyubyns'ky, 2, Chernivtsi, Ucrânia.

[2]Universidade Federal de Mato Grosso do Sul, Av. Sen. Felinto. Müller, 1555, C/P. 549, 79074-460, Campo Grande, MS, Brasil.

[3]Universidade Estatal de Medicina de Zaporizhzhya, 69000, Av. de Maiakovs´ky, 26, Zaporizhzhya, Ucrânia.

[4]Universidade Nacional de Zaporizhzhya, Faculdade de Biologia, 69095, Rua de Zhukovs'ky, 66, Zaporizhzhya, Ucrânia.

*Autor para correspondência correio eletrônico: nightwatcher2401@gmail.com

Recebido: 31 de maio de 2018

Revisado: : 20 de maio de 2020

Aceto: 21 de maio de 2020

Resumo

Pela primeira vez, foi feita uma abordagem teórica do desempenho dos novos derivados triazólicos durante a determinação química dos alcaloides acridínicos do grupo insubosina, na presença de uma concentração pequena de um composto de ligação. A detecção eletroanalítica é realizada mediante um mecanismo híbrido, envolvendo ou não a formação de novos compostos iônicos. É possível mostrar que o estado estacionário é estabilzado, apesar de a região topológica, que lhe é correspondente, ser mais estreita que no caso da detecção mais comum. O comportamento oscilatório, neste caso, é mais provável que nos casos mais comuns, mas o fator adicional é relacionado apenas com a introdução de um composto de ligação.

Palavras-chave: Insubosina, triazóis, sensores eletroquímicos, compostos de ligação, estado estacionário estável.

Summary

The mathematical description for the electrochemical determination of insubosin alkaloid group, assisted by new triazoles with and without link compound

For the first time, a theoretical investigation of novel triazolic derivatives during the chemical determination of acridinic alkaloids of insubosin group in the presence of the presence of the small quantity of the link compound has been realized. The electrochemical determination is realized by a hybrid mechanism, involving or not the formation of novel ionic compounds. It is possible to show that the steady-state is stabilized, despite of the narrower correspondent topological region, while compared to the more common detection case. The oscillatory behavior is more probable than in more common cases, due to the introduction of the link compound.

Key words: UV Insubosine; triazoles; electrochemical sensors; link compounds; stable steady-state.

Introdução

As insubosinas A, B e C é um grupo de alcaloides acridínicos, recentemente isolados de *Streptomyces sp. IFM 11440.* [1]. Este composto contém fragmento da acridina com um grupo hidroximetila na posição 2 do anel e as hidroxilas nas posições 3, 4, ou em ambas (figura 1).

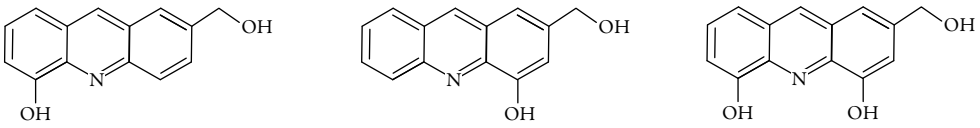

Figura 1. O grupo das insubosinas.

A insubosina B, possuindo a hidroxila na posição 4 mostrou uma atividade potente promotora de Ngn2-receptores. Essa atividade foi dependente de dose. Outrossim, o composto foi mais ativo que a baicalina, enquanto as insubosinas A e C, com a hidroxila na posição 5, não mostraram atividade significante [2, 3]. Sem embargo, a sua atividade biológica em outros aspectos não pode ser descartada. Geralmente, as acridinas

possuem atividades anti-inflamatória [4, 5], anticancerígena [6], antimicrobiana [7], antitubercular [8, 9], antiparasitária [10-12], entre outras. No entretanto, quando em excesso, os derivados acridínicos podem possuir efeitos tóxicos, incluindo o mutagênico e o teratogênico [13, 14]. Destarte, o desenvolvimento de um método de determinação eficiente do grupo insubosina é, deveras, uma tarefa atual.

Por ora, não há nenhum trabalho experimental acerca da determinação quantitativa do grupo insubosina, envolvendo métodos químicos ou eletroquímicos, à exceção de alguns trabalhos teóricos do nosso grupo [15, 16]. No entretanto, da sua composição química poder-se-ia julgar que os compostos deste grupo podem ser eletroquimicamente ativos. Outrossim, avaliar-se-ia a possibilidade de um processo eletroanalítico, baseado no elétrodo, modificado por um dos compostos triazólicos, descritos em [17, 18], com o possível uso de um dihalogenoderivado como composto de ligação.

Por outro lado, o desenvolvimento de novos processos eletroanalíticos requer a investigação teórica *a priori* do comportamento do sistema. Esta investigação permite resolver problemas como:

- A incerteza acerca de alguns detalhes do processo eletroanalítico (como se faz em condições concretas a eletrorredução, quais são os modificadores, que se poderiam usar lá).

- A possibilidade de aparição de instabilidades, características para a eletrooxidação de compostos orgânicos, inclusive a eletropolimerização [19-21].

Destarte, o objetivo geral deste trabalho é avaliar o desempenho da detecção eletroquímica das insubosinas por via de uma determinação anódica sobre os derivados triazólicos, usando um composto de ligação. Outrossim, o comportamento deste sistema comparar-se-á com o dos semelhantes [15, 16].

O sistema e o seu modelo

No caso do processo mais simples, a determinação das insubosinas far-se-á pela transferência dos dois prótons e dois elétrons através do sistema conjugado do derivado triazólico (figura 2)

Ao ser usado um composto de ligação, a imobilização da insubosibna far-se-á pelo nitrogênio piridínico do anel da acridina, sendo ele ligado com o do triazol, conforme a figura 3.

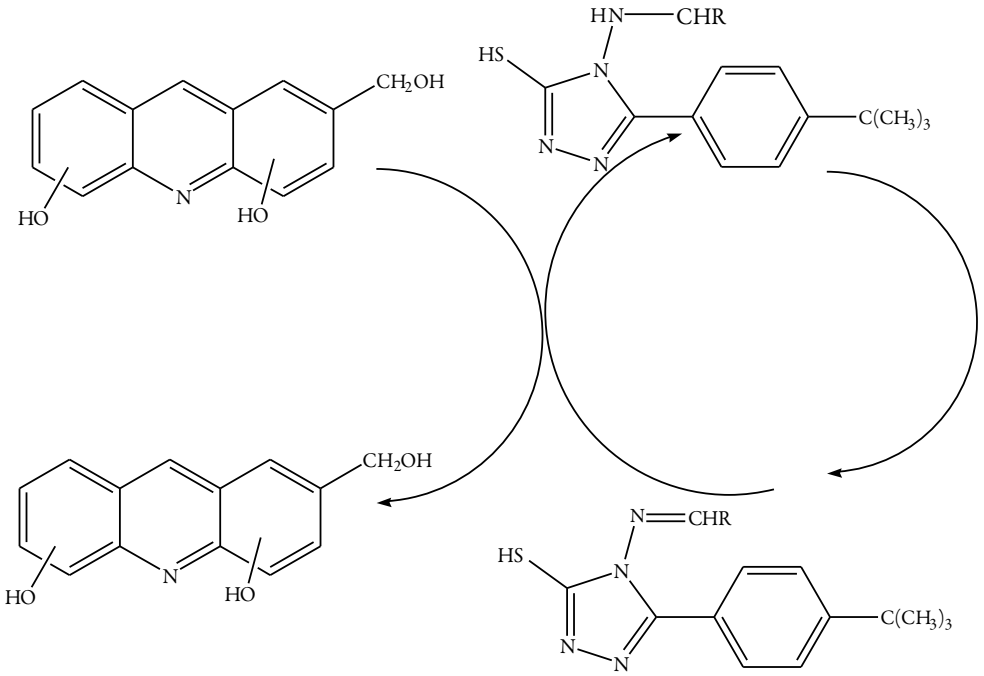

Figura 2. O esquema da determinação da insubosina, assistida por alguns derivados triazólicos.

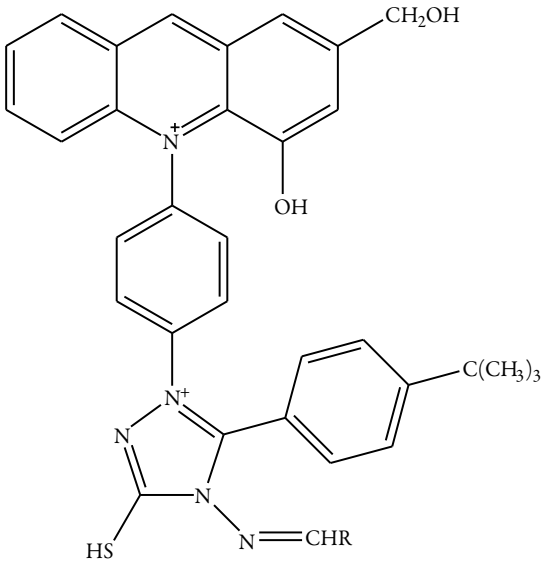

Figura 3. A imobilização da insubosina pelo triazol, com o uso de um composto de ligação.

Considerando que o derivado triazólico faz parte de um compósito polimérico condutor, introduzimos as três variáveis:

c: a concentração da insubosina na camada pré-superficial.

l: a concentração do composto de ligação na camada pré-superficial.

θ: o grau de recobrimento da superfície pelo polímero modificado.

Para simplificar a modelagem, supomos que o reator esteja agitando-se intensamente, o que nos deixa menosprezar o fluxo de convecção e as suas influências. Outrossim, supomos que o eletrólito de suporte esteja em excesso, o que nos permite menosprezar o fluxo de migração e as suas influências. Além disso, supomos que o perfil da distribuição de concentrações das substâncias na camada pré-superficial seja lineal, e a espessura da camada, estável, igual a δ.

É possível mostrar que o comportamento do sistema pode ser descrito pelo conjunto de equações diferenciais a seguir:

$$\begin{cases} \dfrac{dc}{dt} = \dfrac{2}{\delta}\left(\dfrac{D}{\delta}(c_0 - c) - r_d - r_l - r_{lat}\right) \\ \dfrac{dl}{dt} = \dfrac{2}{\delta}\left(\dfrac{D}{\delta}(l_0 - l) - r_l - r_{lat}\right) \\ \dfrac{d\theta}{dt} = \dfrac{1}{G}(r_l + r_d - r_{ox}) \end{cases} \quad (1)$$

Em que Δ e D são coeficientes de difusão do analito e do composto de ligação, c_0 e l_0 são as suas concentrações no interior da solução, r_d é a velocidade da oxidação direta, r_l, a velocidade da oxidação pelo composto da ligação, r_{lat} é a velocidade da reação lateral. As velocidades das respectivas reações podem ser calculadas conforme:

$$r_d = k_d c(1-\theta) \quad (2)$$

$$r_l = k_l c l (1-\theta)\exp(\alpha\theta) \quad (3)$$

$$r_{lat} = k_{lat} c^2 l \quad (4)$$

$$r_{ox} = k_{ox}\theta \exp\left(\frac{2F\varphi_0}{RT}\right) \quad (5)$$

Sendo os parâmetros k as constantes das respectivas reações, a o parâmetro que descreve a influência do processo da formação de novos compostos iônicos na dupla camada

elétrica (DCE), F é o número de Faraday, φ_0 é o salto do potencial, relativo ao potencial da carga zero, R é a constante universal de gases, T é a temperatura absoluta do vaso.

Em se tratando da questão comportamental, trata-se de um sistema interessante, cujo comportamento parece ser mais dinâmico que em [15-16], o que será discutido abaixo.

Resultados e discussão

Para investigar o comportamento do sistema com a determinação eletroanalítica da insubosina, analisamos o conjunto de equações diferenciais (1), havendo vista as relações algébricas (2-5), mediante a teoria de estabilidade linear. Os elementos estacionários da matriz funcional de Jacobi podem ser descritos como:

$$\begin{pmatrix} a_{11} & a_{12} & a_{13} \\ a_{21} & a_{22} & a_{23} \\ a_{31} & a_{32} & a_{33} \end{pmatrix} \tag{6}$$

em que:

$$a_{11} = \frac{2}{\delta}\left(-\frac{D}{\delta} - k_d(1-\theta) - k_l l(1-\theta)\exp(-\alpha\theta) - 2k_{lat} c\ l\right) \tag{7}$$

$$a_{12} = \frac{2}{\delta}\left(-c(1-\theta)\exp(-\alpha\theta) - k_{lat} c^2\right) \tag{8}$$

$$a_{13} = \frac{2}{\delta}\left(k_d c + k_l cl\exp(-\alpha\theta) - \alpha k_l cl(1-\theta)\exp(-\alpha\theta)\right) \tag{9}$$

$$a_{21} = \frac{2}{\delta}\left(-k_l l(1-\theta)\exp(-\alpha\theta) - 2k_{lat} c\ l\right) \tag{10}$$

$$a_{22} = \frac{2}{\delta}\left(-\frac{D}{\delta} - c(1-\theta)\exp(-\alpha\theta) - k_{lat} c^2\right) \tag{11}$$

$$a_{23} = \frac{2}{\delta}\left(k_l cl\exp(-\alpha\theta) - \alpha k_l cl(1-\theta)\exp(-\alpha\theta)\right) \tag{12}$$

$$a_{31} = \frac{1}{G}\left(k_d(1-\theta) + k_l l(1-\theta)\exp(-\alpha\theta)\right) \tag{13}$$

$$a_{32} = \frac{1}{G}\left(k_l c(1-\theta)\exp(-\alpha\theta)\right) \tag{14}$$

$$a_{33}=\frac{1}{G}\left(-k_l cl\exp(-\alpha\theta)+\alpha k_l cl(1-\theta)\exp(-\alpha\theta)-k_d c-k_{ox}\exp\left(\frac{2F\varphi_0}{RT}\right)-jk_{ox}\theta\exp\left(\frac{2F\varphi_0}{RT}\right)\right) \quad (14)$$

Observando as equações 7, 11 e 14, observamos que os elementos da diagonal principal da matriz contêm os elementos positivos, que são correspondentes à positiva conexão de retorno. Destarte, o *comportamento oscilatório*, neste caso, é possível. Outrossim, graças à presença da influência da reação de ligação na DCE, ela é mais provável que em casos mais simples da determinação eletroquímica assistida.

Além do elemento $-jk_{ox}\theta\exp\left(\frac{2F\varphi_0}{RT}\right)>0$, que descreve as influências desestabilizadoras do rearranjo da composição da camada pré-superficial, outro elemento positivo é o $\alpha k_l cl(1-\theta)\exp(-\alpha\theta)>0$, que descreve as influências na mesma camada da formação das novas formulações iônicas. As oscilações, neste caso, se esperam frequentes e de pequena amplitude.

Para investigar a estabilidade do estado estacionário, aplicamos ao conjunto de equações diferenciais 1 o critério de Routh-Hurwitz. Evitando as expressões grandes, introduzimos as novas variáveis, de modo que o determinante se descreve como:

$$\frac{4}{G\delta^2}\begin{vmatrix}-\kappa_1-\Lambda-\Sigma-\Phi & -\mathrm{X} & \Pi+\Xi\\ \Sigma-\Phi & -\kappa_2-\mathrm{X} & \Xi\\ \Lambda+\Sigma & -\mathrm{X} & -\Xi-\Pi-\mathrm{P}\end{vmatrix} \quad (15)$$

Abrindo os parênteses e aplicando a condição Det J<0, saliente do critério, nós obtemos o requisito de estabilidade, descrito como:

$$\begin{aligned}&-\kappa_1\left(\kappa_2\Xi+2\mathrm{X}\Xi+\kappa_2\Pi+\mathrm{X}\Pi+\kappa_2\mathrm{P}+\mathrm{X}\mathrm{P}\right)-\Lambda\left(2\mathrm{X}\Xi+\kappa_2\mathrm{P}+\mathrm{X}\mathrm{P}\right)\\&-\Sigma\left(4\mathrm{X}\Xi+\kappa_2\mathrm{P}+2\mathrm{X}\mathrm{P}+2\mathrm{X}\Pi\right)-\Phi\left(\kappa_2\Xi+\kappa_2\Pi-\mathrm{X}\Pi+\kappa_2\mathrm{P}\right)<0\end{aligned} \quad (16)$$

E esta equação é típica para processos eletroanalíticos, controlados pela difusão, tanto de analito, como do composto de ligação.

Neste sistema, o estado estacionário é fácil de estabelecer, mas a eficiência eletroanalítica, neste caso, é condicionada à concentração do composto de ligação, cujo excesso pode levar a reação lateral a acelerar-se. Satisfeito este requisito, o estado estacionário estável é correspondente à *instabilidade monotônica*, correspondente ao limite de

detecção do ponto de vista eletroanalítico, também é possível para este sistema, e as suas condições descrevem-se como:

$$\begin{aligned} &-\kappa_1\left(\kappa_2\Xi+2\mathrm{X}\Xi+\kappa_2\Pi+\mathrm{X}\Pi+\kappa_2\mathrm{P}+\mathrm{XP}\right)-\Lambda\left(2\mathrm{X}\Xi+\kappa_2\mathrm{P}+\mathrm{XP}\right)\\ &-\Sigma\left(4\mathrm{X}\Xi+\kappa_2\mathrm{P}+2\mathrm{XP}+2\mathrm{X}\Pi\right)-\Phi\left(\kappa_2\Xi+\kappa_2\Pi-\mathrm{X}\Pi+\kappa_2\mathrm{P}\right)=0 \end{aligned} \tag{17}$$

O papel do *composto de ligação* pode ser realizado por qualquer substância que contém dois grupos, capazes de reagir com nitrogênio piridínico. Formam-se, destarte, os dois sais. A formação do complexo como composto de ligação também é possível e descrever-se-á num dos nossos próximos trabalhos.

Conclusões

Da avaliação teórica do desempenho dos triazóis durante a determinação eletroanalítica do grupo das insubosinas pode-se concluir que:

- Não obstante a maior possibilidade das instabilidades oscilatória e monotônica, o sistema eletroanalítico pode ser oficiente, desde que o composto de ligação não esteja em excesso.
- O processo eletroanalítico, neste caso, é controlado pela difusão tanto do analito, como do composto de ligação.
- Haja vista as influências da formação de novos íons durante a reação do composto de ligação na estrutura da dupla camada elétrica, o comportamento oscilatório neste sistema é mais provável que nos semelhantes.

Conflito de interesse

Os autores declaram que não há conflito de interesses.

Referências

1. M.A. Arai, K. Koryudzu, M. Ishibashi, Insubosins A, B and C are acridine alkaloids, isolated from a culture of Streptomyces Sp. IFM 11440 with Ngn2 promoter activity, *J. Nat. Prod.*, **78**, 311-314 (2015).

2. M. Genicka-Kowalewska, G. Cholewinski, K. Dzierzbicka, Recent development in the synthesis and biological activity of acridine/acridone analogues, *RSC Adv.*, **7**, 15776-15804 (2017).

3. Y.L. Chen, C.M. Lu, I.L. Chen, *et al.*, Synthesis and anti-inflammatory evaluation of 9-anilinoacridine and 9-phenoxyacridine derivatives, *J. Med. Chem.*, **45**, 4689-4694 (2002).

4. L.V. Yartseva, S.G. Isayev, O.M. Svechnikova, Synthesis, physico-chemical properties, and biological activities of 9-acetylamino and arylamino derivatives of 5-nitroacridine, *Farm. Zh.*, **9**, 60-64 (2003).

5. S.A. Gamega, J.A. Spicer, G.J. Atwell, *et al.*, Structure-Activity Relationships for substituted bis(acridine-4-carboxamides): A new class of anticancer agents, *J. Med. Chem.*, **42**, 2383-2393 (1999).

6. M. Kaya, Y. Yildirir, G.Y. Celik, Synthesis and antimicrobial activities of novel bisacridine-1,8-dione derivatives, *Med. Chem. Res.*, **20**, 293-299 (2011).

7. E.I. Aly, A.H. Abadi, Synthesis and antitubercular activity of 6-chloro(unsubstituted)-2-methoxy-9-substituted acridine derivatives, *Arch. Pharmac. Res.*, **27**, 713-719 (2004).

8. R.P. Tripathi, S.S. Verma, J. Pandey. *et al.*, Search of antitubercular activities in tetrahydroacridines: Synthesis and biological evaluation, *Bioorg. Med. Chem. Lett.*, **16**, 5144-5147 (2006).

9. C. Di Giorgio, M. De Meo, J. Chiron, *et al.*, Synthesis and antileishmanial activities of 4,5-disubstituted acridines as compared to their 4-monosubstituted homologues, *Bioorg. Med. Chem.*, **13**, 5560-5568 (2005).

10. A. Kumar, K. Srivastava, S.R. Kumar, *et al.*, Synthesis of 9-anilinoacridine triazines as new class of hybrid antimalarial agents, *Bioorg. Med. Chem. Lett.*, **19**, 6996-6999 (2009).

11. V. Tomar, G. Bhattarchajee, Kamaluddin, *et al.*, Synthesis of new chalcone derivatives containing acridinyl moiety with potential antimalarial activity, *Eur. J. Med. Chem.*, **45**, 745-751 (2010).

12. G.W. Ware, *Reviews of Environmental Contamination and Toxicology*, 173, Springer Verlag, New York, 2002.

13. I.R. Ferguson, W.A. Denny, The genetic toxicity of acridines, *Mutat. Res.*, **258**, 123-160 (1991).

14. S.A. Wiegman, J.A. Termeer, T. Verheul, *et al.*, UV-absorbance dependent toxicity of acridine to the marine diatom *Phaeodactylum tricornutum*, *Env. Sci. Technol.*, **36**, 908-913 (2002).

15. V.V. Tkach, Y.G. Ivanushko, S.M. Lukanova, *et al.*, (9-triphenylphosphazo)acridine: Synthesis and theoretical modeling of electroanalytical action, *Appl. J. Env. Eng. Sci.*, **3**, 365-372 (2017).

16. V.V. Tkach, Y.G. Ivanushko, S.M. Lukanova, *et al.*, *The Ukrainian-Polish Conference in Membran and Sorption Processes and Technologies*, Kiev, December 14th, 2017.

17. I.I. Aksyonova, O.I. Panasenko, Y.G. Knysh, The properties of new salts of 2(5-adamantane-1-yl-4r-1,2,4-triazole-3-(ylthio)acetic acids in glucose tolerance test (em ucraniano), *Act. Probl. Med. Pharm. Sci.*, **18**, 17 (2015).

18. V.M. Odyntsova, Y.S. Pruglo, A.S. Gotsulya, *et al.*, Antihypoxic activity of the salts of 2(5-adamantane-1-yl-4r-1,2,4-triazole-3-(ylthio)acetic acids, *Zapor. J. Med.*, **2**, 96 (2014).

19. A. Stadnik, E.M. Caldas, A. Galli, F.J. Anaissi, Electrodo, modificado por CoO(OH) coloidal, aplicado na detecção do ácido oxálico, *Orbital. Elec. J. Chem.*, **7**, 122-130 (2015).

20. J.S. Bonini, F.Q. Mariani, E. Guimarães Castro, *et al.*, Partículas de CoO(OH), dispersas em pasta de carbono, aplicado na eletrooxidação de compostos fenólicos, *Orbital Elec. J. Chem.*, **7**, 318-326 (2015).

21. T. McQuade, A. Pullen, T.M. Swager, Conjugated polymer-based chemical sensors, *Chem. Rev.*, **100**, 2537-2574 (2000).

Como citar este artigo

V.V. Tkach, M.V. Kushnir, S.C. de Oliveira, V.V. Parchenko, V.M. Odyntsova, I.I. Aksyonova, O.V. Luganska, M.M. Kornet, Y.G. Ivanushko, P.I. Yagodynets, A descrição matemática da detecção eletroquímica dos alcaloides do grupo da insubosina, assistida pelos novos triazóis com e sem composto de ligação, *Rev. Colomb. Cienc. Quím. Farm.*, **49**(2), 472-481 (2020).

Technological research article / *http://dx.doi.org/10.15446/rcciquifa.v49n2.89923*

The selective obtaining of amyrins from Amazonian *Protium* oleoresins

Rosilene Gomes da Silva Ferreira[1], Fernanda Guilhon-Simplicio[2,*], Klenicy Kazumy de Lima Yamaguchi[3], Priscila Duarte de Lira[4], Tallita Marques Machado[2], Márcio Antônio Couto Ferreira[3], Valdir Florêncio da Veiga-Junior[5], Emerson Silva Lima[2]

[1]Escola Normal Superior, Universidade do Estado do Amazonas, 3578, Flores, 69050-010, Manaus, Amazonas, Brazil.

[2]Faculdade de Ciências Farmacêuticas, Universidade Federal do Amazonas, Setor Sul, Coroado, 69067-005, Manaus, Amazonas, Brazil.

[3]Instituto de Saúde e Biotecnologia, Universidade do Estado do Amazonas, 305, Urucu, 69460-000, Coari, Amazonas, Brazil.

[4]Departamento de Química, Instituto de Ciências Exatas, Universidade Federal do Amazonas, Setor Norte, Coroado, 69077-000, Manaus, Amazonas, Brazil.

[5]Departamento de Engenharia Química, Instituto Militar de Engenharia, 80, Urca, 22290-270, Rio de Janeiro, Brazil.

*Corresponding author E-mail address: fgsfarmaceutica@gmail.com

Received: 19 March 2019

Revised: 22 April 2020

Accepted: 22 May 2020

Summary

The oleoresin produced by species of genus *Protium* sp. is rich in alpha and beta-amyrins, two triterpenes with many pharmacogical activities. Considering the need to make the improved obtainment of these products feasible, this study sought to optimize techniques for the extraction and isolation of amyrins from resin. Two methods of extraction (maceration and sonication) with different solvents were compared to direct isolation from crude resin. The isolation of triterpenes was performed by chromatographic columns and the yields of extracts and fractions were analyzed by analysis of variance. The best extraction solvent for amyrins was hexane for both maceration and sonication methods (38.16±2.06% and 37.67±8.21%, respectively). There was no statistical difference between these methods and the direct method (32.05±2.40%). Additionally, the direct method is cheaper and more environmentally friendly. Thus, this study showed that it is possible to obtain a large quantity of amyrins by means of cheap, fast and ecological methods.

Key words: *Protium*, alpha and beta-amyrins, yielding extraction, extraction optimization.

Resumen

La obtención selectiva de amirinas a partir de oleorresinas de *Protium* amazónicas

La oleorresina producida por especies del género *Protium* sp. es rica en amirinas alfa y beta, dos triterpenos con muchas actividades farmacológicas. Esta investigación buscó optimizar las técnicas de extracción y aislamiento de amirinas de la resina para hacer factible la obtención mejorada de esos productos. Se compararon dos métodos de extracción (maceración y sonicación) con diferentes solventes con aislamiento directo de la resina cruda. El aislamento de los triterpenos se realizó mediante columnas cromatográficas y los rendimientos de extractos y fracciones fueron hechos mediante análisis de varianza. El mejor solvente para la extracción de amirinas fue el hexano para ambos métodos de maceración y sonicación (38,16±2,06% y 37,67±8,21%, respectivamente). No hubo diferencia estadística entre estos métodos y el método directo (32,05±2,40%). Además, el método directo es más barato y ecológico. De este modo, esta investigación demostró que es posible obtener una gran cantidad de amirinas a través de métodos rápidos, baratos y ecológicos.

Palabras clave: *Protium*, amirinas alfa y beta, rendimientos de extracción, optimización de extracción.

Introduction

The Amazon, with its enormous biodiversity, has a great potential of providing new products. In this context, the oleoresins produced by the *Protium* species (Burseraceae), commonly known as "breu branco", is very promising due to its medicinal and industrial potential [1]. This raw material is used in popular medicine as a healer, anti-inflammatory, analgesic, expectorant and for ulcer treatment. It is also commonly used as an incense and natural insecticide, as well as for caulking boats. Its main industrial application is as a perfume fixative [2-4].

The oleoresin is characterized by the substantial presence of terpenoids, especially triterpenes. Triterpenes have a wide structural diversity and can be tetracyclic or pentacyclic. Subclasses oleane and ursane, the most common pentacyclic in the class of triterpenoids, and euphanus [5], the most frequent tetracyclic in *Protium* species, are considered chemical markers of the genus [6]. Triterpenes are constituents that have captured much interest in recent years as their pharmacological potential was discovered, which gave rise to various therapeutic activities, being used for anticancer,

anti-inflammatory, antiepileptic, antiviral, antibacterial, antifungal, antidiuretic, giardicide treatments, and as an acetylcholinesterase inhibitor [7].

The major constituents of *Protium* resins are the pentacyclic triterpenes, alpha and beta-amyrins [2], which have been showing significant biological activity. The isolation or isomeric mixture of these substances and their derivatives have shown to be anti-inflammatory, antinociceptive, gastro- and hepatoprotective, antipruritic, antidementia, anxiolytic and antidepressant, hypoglycemic, and lipid-lowering agents [8-17], which have made them interesting molecules for studying drug development.

The large-scale isolation of active substances for use in pharmacological and chemical studies is an essential step toward the development of new medicines. Additionally, it is also necessary for discovering the active principle responsible for the therapeutic effect of crude extract. Several studies have been carried out to optimize extraction processes of bioactive substances. The most commonly used parameters are solvent type, extraction method, time, and temperature, according to the class of the substance of interest [18-20].

The standardization for obtaining bioactive substances on large scale allows the development of new biotechnological products for industrial application. In view of the need to find ways to improve the extraction yields of amyrins from *Protium* oleoresin, this work performed a factorial study aiming to optimize its isolation from commercial resins, which is considered a sustainable way for its production.

Methodology

Obtaining plant material

Samples of impure *Protium* resins were purchased at a traditional fair in Coari, Amazonas, Brazil. The samples were cleaned to remove impurities, such as mineral and vegetal residues, powdered in a porcelain mortar and stored in a refrigerator until the extraction procedure.

Extraction methods

The amyrin was obtained in three ways: direct method, using the crude resin fractioned directly in chromatographic column; maceration and sonication both using hexane, ethyl acetate, and ethanol (Labsynth, São Paulo, Brazil) as eluents. Then, all extracts obtained were fractioned by chromatographic column. All procedures were carried out in sextuplicate (figure 1).

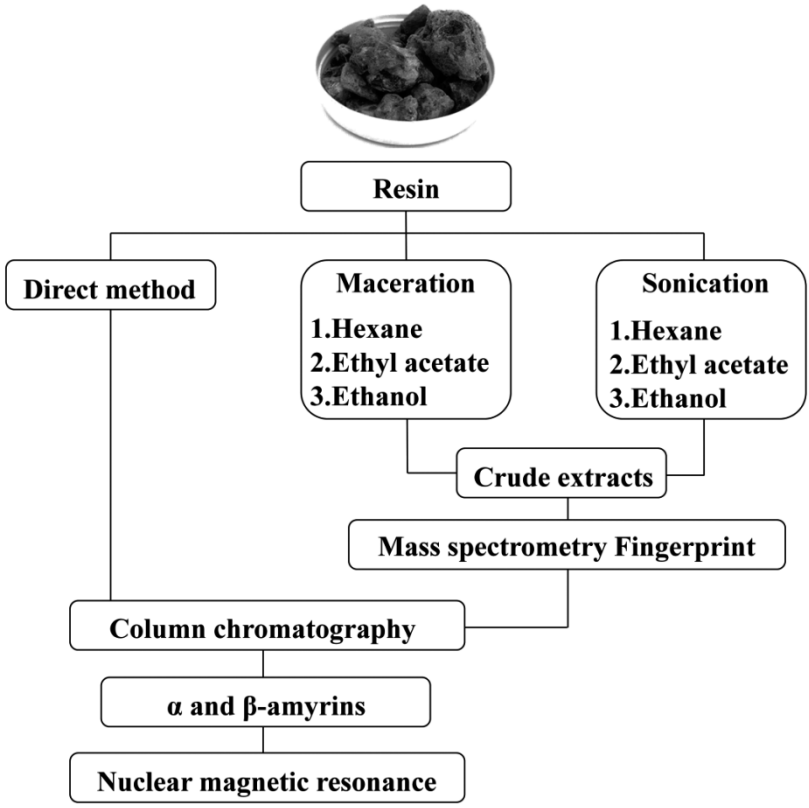

Figure 1. Experimental design of alpha and beta-amyrin extraction from different processes.

Obtainment and fractionation of the crude extracts

Cold maceration was carried out for a period of 72 h at a 1:10 (*m/v*) resin and extractive solvent ratio. After the extraction time, the material was subjected to simple filtration and subsequent removal of the solvent in a rotary evaporator under reduced pressure. After removing the solvent, the extract was fractionated in a chromatographic column.

Sonication extraction was performed on an ultrasound device (Ultrasonic Cleaner, Unique) for 20 min at a 1:10 (*m/v*) ratio of resin and extractive solvent. After the extraction time, the solution was subjected to filtration and evaporation, in the same manner as the previous methodology.

Chromatographic separation was performed in a glass column with a 2 cm internal diameter. One (1) cm of cotton was placed on the bottom base of the column. Then, 20 cm of silica gel (Silicycle G60 70-230 mesh) in height was added to the column and used as stationary phase, eluted with a 200 mL gradient of hexane and ethyl acetate at ratios: 95:5; 90:10; 80:20; 70:30; 60:40; 1:1 as mobile phase. The eluting was observed

under ultraviolet light (λ^{254}). The collected fractions (50 mL) were grouped according to the similarity observed by thin layer chromatography (TLC). Subsequently, the amyrin mixture was washed with acetone and methanol and the yield was calculated.

Direct extraction

The powdered resin (30 g) was subjected to column chromatography using silica gel as stationary phase and combinations of hexane, ethyl acetate, and methanol as mobile phases, as previously described. Eight (8) fractions were obtained. After solvent removal, the fractions were grouped according to the similarity in TLC for calculating the yield.

Electrospray ionization mass spectrometry fingerprint

All extracts were dissolved in methanol and ethyl acetate (J. T. Baker, Thermo Fisher Scientific, Massachusetts, USA) and analyzed by direct electrospray ionization mass spectrometry (ESI-MS) on an ion-trap mass spectrometer (LCQ Fleet, Thermo Fisher Scientific, Massachusetts, USA). The MS spectra were acquired at a mass/charge (*m/z*) range from 100 to 1000. Tentative identifications were performed by manual interpretation of the mass spectra.

Nuclear magnetic resonance (NMR)

Nuclear Magnetic Resonance ^{1}H and ^{13}C spectra were obtained on a 300 *MHz* equipment (Fourier 300 model, Bruker, Massachusetts, USA), using 550 μL of chloroform-d (Acros Organics, Massachusetts, USA) in a tube of 5 mm to solubilize 15 mg of sample.

Statistical analysis

The effect related to the type of extraction in the alpha and beta-amyrins yielding was evaluated by a factor analysis, considering: the extraction method (factor A), which varied in two levels (maceration and sonication); and the solvent (factor B), which varied in three levels (hexane, ethyl acetate, and ethanol). Data was presented in mean ± standard deviation and compared by analysis of variance (ANOVA) followed by the Tukey test, considering $p<0.05$ as statistically significant.

Results and discussion

Several methodologies are described for the preparation of extracts from plants, microorganisms or even animals (sponges) aiming at the isolation of their chemical constituents, as well as for obtaining them on a larger scale. Thus, different extractive methods and solvents were used to obtain the major constituents, alpha and beta-amyrins, in order to develop a process for large-scale obtainment and improved cost effectiveness.

Six yield measures (%) were obtained in each treatment or level of the experiment (table 1). The figure below shows the box graph (box plot) for each level of the variable yield in the two extraction types (maceration and sonication) with the three solvent types (figure 2A and 2B) and the correlation of the two extraction methods. A strong correlation between the type of solvent and yield was found (figure 2C).

Table 1. Yield of extracts obtained by different extraction methods.

Solvent	Extraction method	Yield (%)
Hexane	Maceration	21.43 ± 0.79^{b}
	Sonication	17.33 ± 0.80^{e}
Ethyl acetate	Maceration	79.17 ± 1.89^{a}
	Sonication	76.98 ± 1.49^{d}
Ethanol	Maceration	79.03 ± 1.67^{a}
	Sonication	44.96 ± 0.62^{c}

[a,b,c,d] interactions with the same letters do not significantly differ from one other at the 5% level of significance.

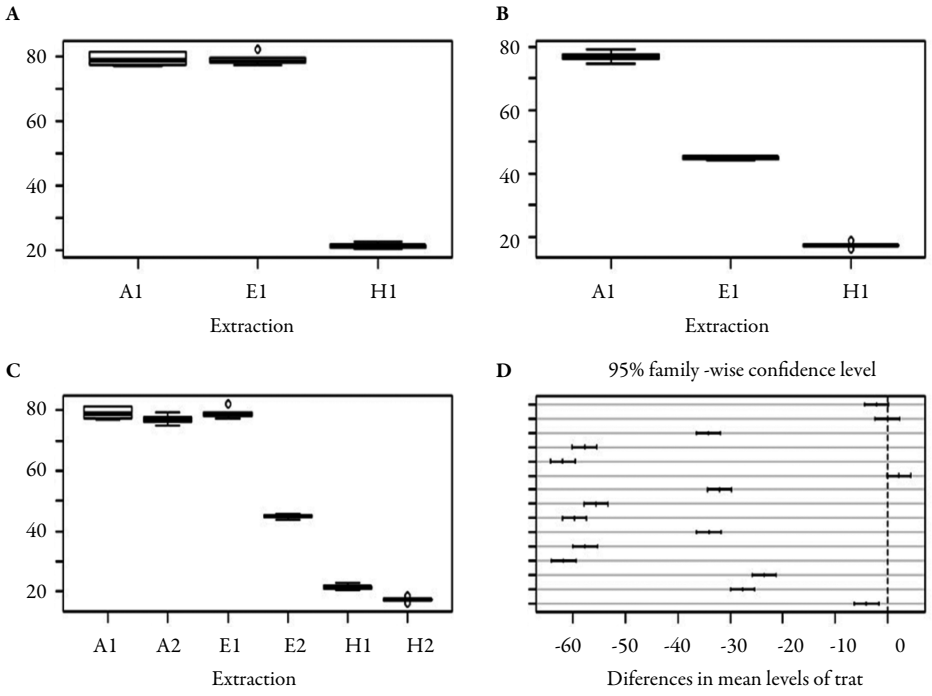

Figure 2. Analysis of the variance of yields in different extractions: (A) maceration (A1, E1 and H1); (B) sonication (A2, E2 and H2); (C) both methods; (D) differences in mean levels of methods. A1 and A2- ethyl acetate; E1 and E2- ethanol; H1 and H2-hexane.

The same delineation was used to evaluate the fraction yield of the columns where the substance of interest was identified. Then, the treatment with the best amyrin isolation yield was compared to the yield obtained through fractionation of the resin in column without any previous treatment.

By analyzing the yield of the substances obtained after the solvent extraction, a higher yield of pure substance was observed using solvent hexane as shown in table 2. The analysis of variance for the yield obtained in the columns showed that only the type of solvent significantly ($p < 0.05$) affects the resin yield in the identification of the substance of interest.

Table 2. Yield of alpha and beta-amyrins mixture according to the type of solvent.

Solvent	Average yield (%)
Hexane	37.91 ± 5.35^{a}
Ethyl acetate	26.50 ± 6.70^{b}
Ethanol	21.59 ± 4.81^{b}

[a,b]For different letters, the treatments differ significantly from one other at the 5% level obtained by the Tukey test.

As the highest yield percentage was obtained by using solvent hexane, a test comparing the means of the maceration and sonication methods with this solvent was conducted, and the yield was obtained in the columns of pure resin. By means of this comparison, no significant difference was verified between the yield obtained in the columns using hexane and that using pure resin, as observed in table 3.

Table 3. Yield of alpha and beta-amyrins according to the type of extraction using hexane.

Extraction method	Yield (%)
Maceration	38.16 ± 2.06^{a}
Sonication	37.67 ± 8.21^{a}
Direct method	32.05 ± 2.40^{a}

[a]Fordifferent letters, treatments differ significantly at the 5% level obtained by the Tukey test.

The statistical analysis of the extract yields showed that the type of solvent, the extraction method and the solvent interaction versus extraction method significantly ($p<0.05$) affected the resin yield in the extracts, allowing the ideal extraction method to be chosen, as well as the solvent.

Ethyl acetate extracts showed higher extraction yields and, when purified by column chromatography, the fractions obtained with hexane as solvent showed a higher content of alpha and beta-amyrins isolated in fractions F3 and F4. The direct method presented a 34% yield; however, the major substance did not have the purity of the fractions from the other extracts, requiring further treatment. It is noteworthy that in previous studies with the *Protium heptaphyllum* resin, the yield of the alpha and beta-amyrins mixture was about 3% [4], while that from 20 g resin obtained a 450 mg of alpha and beta-amyrins mixture [21, 22].

All the chromatographic columns made with the extracts, as well as the direct extraction of the resin *in natura*, were accompanied by TLC, which made it possible to observe the retention factor (R*f*) of alpha and beta-amyrins, compared to the commercial standard in elution with hexane /ethyl acetate (9:1) (R*f* = 0.41) (figure 3).

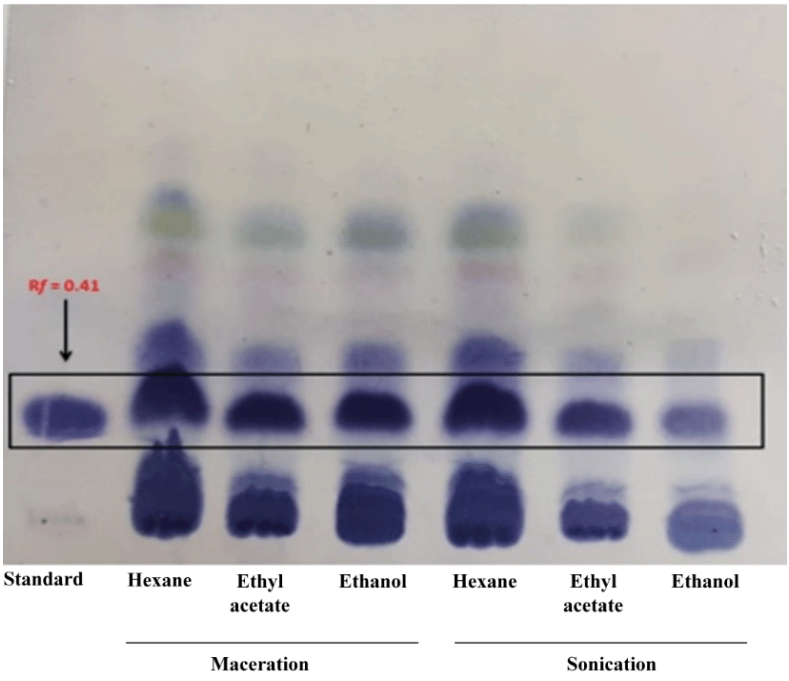

Figure 3. TLC of the extracts obtained by the maceration and sonication processes in comparison to the amyrin standards.

Although the yield of the isolates in maceration and sonication techniques presented higher values (38 and 37% respectively) than direct extraction (32%), it is observed that the use of direct extraction presents greater advantages since it does not need pre-processes with extraction techniques to obtain the enriched extract. Thus, direct extraction becomes an important method of obtaining these substances.

Similar results were also observed from the extraction of amirin from latex of *Calotropis gigantea* using the Soxhlet and batch extraction methods, in which it was observed that the best solvent for extraction using these methods are those of high polarity, methanol and ethanol [23]. However, the yield of the alpha and beta-amyrins mixture obtained in this work was higher.

Analysis by mass spectrometry fingerprint showed ions of m/z 409 corresponding to alpha and beta-amyrins, which are the major ions in the positive mode ESI-MS spectra of all extracts. This ion peak corresponds to a molecular ion of amyrins with the loss of a water molecule (figure 4).

The 425 and 439 m/z ions were identified as being lupenone and lupenone-derived oxime and such substances have already been reported in resins of species of *Protium* sp. There was also the presence of ions 121 and 177 m/z, which are characteristic signals of contaminants known as phthalic acid esters.

The presence of alpha and beta-amirin, as well as lupenone and lupenone-derived oxime have already been reported in literature, both in the resin and in the leaves of *P. heptaphyllum*, corroborating the results of the mass spectrometry analysis of the different resin extracts found in our study [24, 25].

The presence of the mass signals characteristic of phytallic acid derivatives was also observed, however these are considered one of the most known contaminants in spectrometric analysis, derived from the solvent's contact with plastic [26-28]. Thus, they were not considered compounds present in the resin.

The structure of the triterpenic mixture of alpha and beta-amyrins was confirmed by NMR analysis. Although there are some signs of chemical shifts in the NMR of ^{1}H and ^{13}C when compared with the literature data, the structural elucidation presented in this work is unambiguous, since there are many studies in literature discussing the typical shifts presented by these structures, which was clearly detected in our spectra [7, 21, 22, 25, 29].

Analysis of ^{1}H and ^{13}C in nuclear magnetic resonance spectra showed characteristic signals of the oleane skeleton. Doublets corresponding to carbinolic carbons, which are characteristic of triterpenoids of 3-beta-OH type and two triplets in δ 5.16 and 5.21, correspond to the CH bond of olefins. In the ^{13}C NMR spectra, 30 characteristic signals were found: signals of non-hydrogenated sp^2 carbon (C-13) at δ 145.29 and C-12 carbon at δ 121.5 ppm, which corresponded to the double bond between the beta-amyrin carbons, in addition to the displacements at 124.20 and 139.74, referring to the double bond of alpha-amyrin C-12 and C-13 carbons, characteristic of the triterpenic mixture of alpha and beta amyrin (figures A1 and A2 of Appendix) [30].

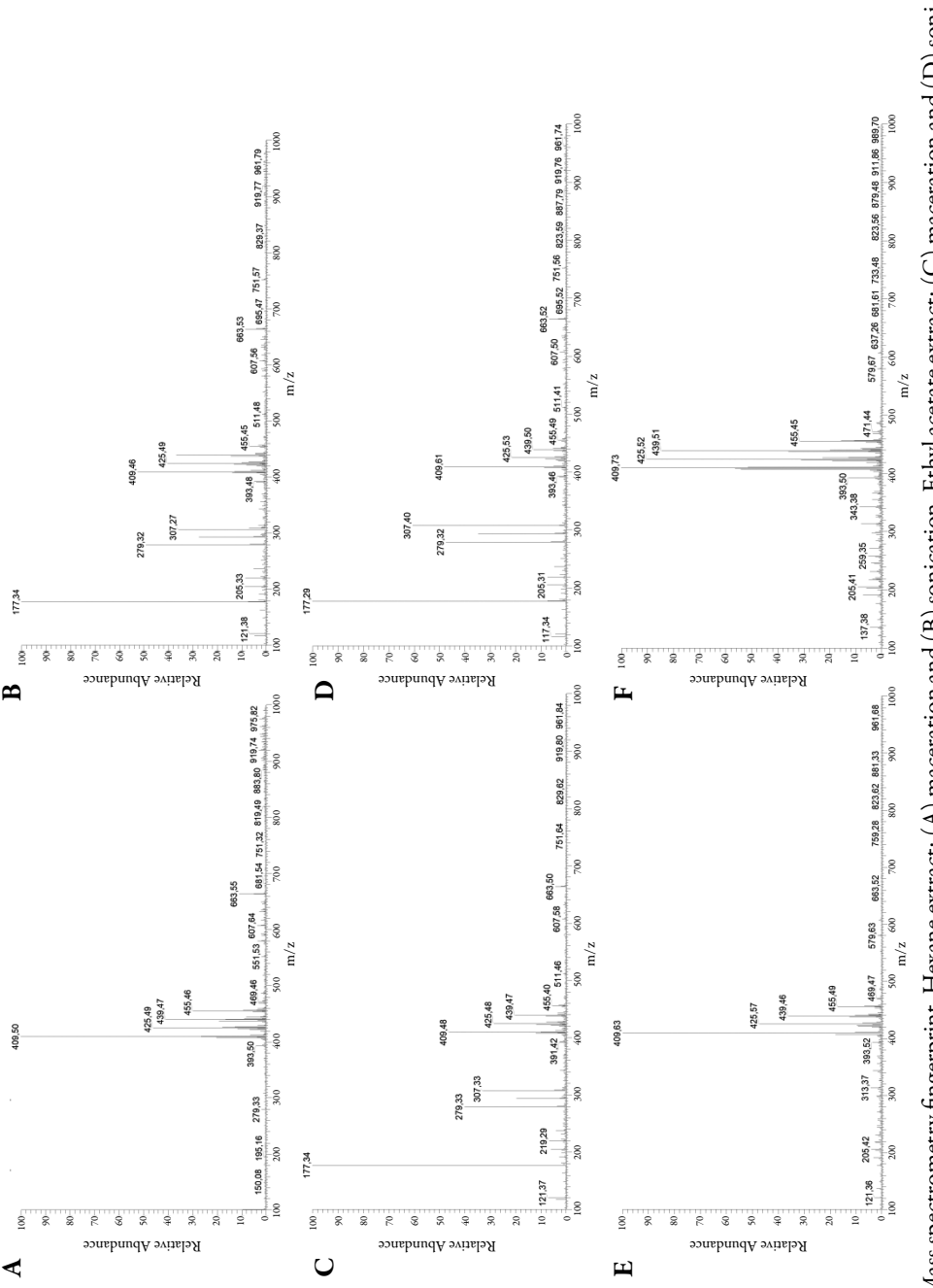

Figure 4. Mass spectrometry fingerprint. Hexane extract: (A) maceration and (B) sonication. Ethyl acetate extract: (C) maceration and (D) sonication. Ethanol extract: (E) maceration and (F) sonication.

Thus, this study was able to optimize the extractive process for obtaining the alpha and beta-amyrins mixture from *Protium* sp oleoresin and opens the perspective for the large-scale isolation of amyrins for future industrial use and pharmacological testing of these substances individually. In addition, using these isolates for chemical synthesis and structural adjustments according to purpose becomes feasible, whether for the cosmetic or pharmaceutical industry.

Acknowledgements

This work was supported by Fundação de Amparo à Pesquisa do Estado do Amazonas (FAPEAM), Manaus, Amazonas, Brazil. The first and second authors were Ph. D. graduate students at Program Rede de Biodiversidade e Biotecnologia da Amazônia Legal (BIONORTE) of the Universidade Federal do Amazonas when this work was carried out.

Disclosure statement

No potential conflict of interest was reported by the authors.

References

1. E.R. da Silva, D.R. Oliveira, P.D. Fernandes, H.R. Bizzo, S.G. Leitão, Ethnopharmacological evaluation of breu essential oils from Protium Species administered by inhalation, *J. Evid. Based. Complementary Altern. Med.*, **2017**, ID 2924171 (2017).

2. E.M. Lima, A.M. Nascimento, D. Lenz, R. Scherer, S.S. Meyrelles, G.A.P. Boëchat, T.U. Andrade, D.C. Endringer, Triterpenes from the *Protium heptaphyllum* resin – chemical composition and cytotoxicity, *Rev. Bras. Farmacogn.*, **24**(4), 399-407 (2014).

3. H. Lorenzi, *Árvores brasileiras: manual de identificação e cultivo de plantas nativas do Brasil*, Plantarum, Nova Odessa, 1992, vol. 1.

4. A.L. Rüdiger, C.C. Silva, V.F. Veiga Júnior, EDXRF Analysis of Amazonian Burseraceae oleoresins, *J. Braz. Chem. Soc.*, **20**(6), 1077-1081 (2009).

5. N.A.J.C. Furtado, L. Pirson, H. Edelberg, L.M. Miranda, C. Loira-Pastoriza, V. Preat, Y. Larondelle, C.M. André, Pentacyclic triterpene bioavailability: an overview of *in vitro* and *in vivo* studies, *Molecules*, **22**(3), 400 (2017).

6. A.L. Rüdiger, A.C. Siani, V.F. Veiga Júnior, The chemistry and pharmacology of the South America genus *Protium* Burm F (Burseraceae), *Pharmacogn. Rev.*, **1**(1), 93-104 (2007).

7. L. Hernández-Vázquez, S. Mangas, J. Palazón, A. Navarro-Ocaña, Valuable medicinal plants and resins: Commercial phytochemicals with bioactive properties, *Ind. Crops Prod.*, **31**(3), 476-480 (2010).

8. E. Biskup, M. Gołębiowski, R. Gniadecki, P. Stepnowski, E. Łojkowska, Triterpenoid α-amyrin stimulates proliferation of human keratinocytes but does not protect them against UVB damage, *Acta Biochim. Pol.*, **59**(2), 255-260 (2012).

9. R.C.P. Lima-Júnior, D.I.M. Sousa, G.A.C. Brito, C.M. Cunha, M.H. Chaves, V.S.N. Rao, F.A. Santos, Modulation of acute visceral nociception and bladder inflammation by plant triterpene, α,β-amyrin in a mouse model of cystitis: role of tachykinin NK1-receptors, and K+ATP channels, *Inflamm. Res.*, **56**, 487-494 (2007).

10. I. Matos, A.F. Bento, R. Marcon, R.F. Claudino, J.B. Calixto, Preventive and therapeutic oral administration of the pentacyclic triterpene α,β-amyrin ameliorates dextran sulfate sodium-induced colitis in mice: the relevance of cannabinoid system, *Mol. Immunol.*, **54**(3-4), 482-492 (2013).

11. R. Medeiros, M.F. Otuki, M.C.W. Avellar, J.B. Calixto, Mechanisms underlying the inhibitory actions of the pentacyclic triterpene α-amyrin in the mouse skin inflammation induced by phorbol ester 12-O-tetradecanoylphorbol-13-acetate, *Eur. J. Pharmacol.*, **559**(2-3), 227-235 (2007).

12. C.M. Melo, T.C. Morais, A.R. Tomé, G.A.C Brito, M.H. Chaves, V.S Rao, F.A. Santos, Anti-inflammatory effect of α,β-amyrin, a triterpene from *Protium heptaphyllum*, on cerulein-induced acute pancreatitis in mice, *Inflamm. Res.*, **60**(7), 673-681 (2011).

13. A.O. Nogueira, Y.I.S. Oliveira, B.L. Adjafre, M.E.A. Moraes, G.F. Aragão, Pharmacological effects of the isomeric mixture of alpha and beta amyrin from *Protium heptaphyllum*: a literature review, *Fundam. Clin. Pharmacol.*, **33**(1), 4-12 (2019).

14. K.K. Okoye, D.L. Ajaghaku, H.N. Okeke, E.E. Ilodigwe, C.S. Nworu, F.B.C. Okoye, Beta-amyrin and alpha-amyrin acetate isolated from the stem bark of Alstonia boonei display profound anti-inflammatory activity, *Pharm. Biol.*, **52**(11), 1478-1486 (2014).

15. M.F. Otuki, F. Vieira-Lima, Â. Malheiros, R.A. Yunes, J.B. Clixto, Topical antiinflammatory effects of the ether extract from *Protium kleinii* and α-amyrin pentacyclic triterpene, *Eur. J. Pharmacol.*, **507**(1-3), 253-259 (2005).

16. F.A. Santos, J.T. Frota, B.R. Arruda, T.S. de Melo, A.A.C.A da Silva, G.A.C. Brito, M.H. Chaves, V.S. Rao, Antihyperglycemic and hypolipidemic effects of α,β-amyrin, a triterpenoid mixture from *Protium heptaphyllum* in mice, *Lipids Health Dis.*, **11**, 98 (2012).

17. M. Shih, J. Cherng, Reduction of adhesion molecule production and alteration of eNOS and endothelin-1 mRNA expression in endothelium by *Euphorbia hirta* L. through its beneficial β-amyrin molecule, *Molecules*, **19**(7), 10534-10545 (2014).

18. B. Gullón, P. Gullón, T.A. Lú-Chau, M.T. Moreira, J.M. Lema, G. Eibes, Optimization of solvent extraction of antioxidants from *Eucalyptus globulus* leaves by response surface methodology: characterization and assessment of their bioactive properties, *Ind. Crops Prod.*, **108**, 649-659 (2017).

19. S. Rodríguez-Rojo, A. Visentin, D. Maestri, M.J., Cocero, Assisted extraction of rosemary antioxidantes qith green solvents, *J. Food Eng.*, **109**(1), 98-103 (2012).

20. C.L. Roriz, L. Barros, M.A. Prieto, M.F. Barreiro, P. Morales, I.C.F.R. Ferreira, Modern extraction techniques optimized to extract betacyanins from *Gomphrena globosa* L., *Ind. Crops Prod.*, **105**, 29-40 (2017).

21. G.F. Aragão, M.C.C. Pinheiro, P.N. Bandeira, T.L.G Lemos, G.S.B. Viana, Analgesic and anti-inflammatory activities of the isomeric mixture of alpha- and beta-amyrin from *Protium heptaphyllum* (Aubl.) March, *J. Herb. Pharmacother.*, **7**(2), 31-47 (2008).

22. P.N. Bandeira, T.L.G. Lemos, S.M.O. Costa, H.S. dos Santos, Obtenção de derivados da mistura triterpenoídica α- e β-amirina, *Rev. Bras. Farmacogn.*, **17**(2), 204-208 (2007).

23. S.J. Wagh, J.G. Gujar, V.G. Gaikar, Experimental and modeling studies on extraction of amyrins from latex of mandar (*Calotropis gigantea*), *Indian J. Chem. Technol.*, **19**, 427-433 (2012).

24. K.M.M.B. Carvalho, J.D.B. Marinho Filho, T.S. de Melo, A.J. Araújo, J.D.S. Quetz, M.D.P.S.S. da Cunha, K.M. de Melo, A.A.D.C.A. da Silva, A.R. Tomé, A. Havt, S.G.D.C. Fonseca, G.A.D.C. Brito, M.H. Chaves, V.S. Rao, F.A. Santos, The resin from *Protium heptaphyllum* prevents high-fat diet-induced obesity in mice: scientific evidence and potential mechanisms, *J. Evid. Based Complementary Altern. Med.*, **2015**, 106157 (2015).

25. G.M. Vieira Júnior, C.M.L. de Souza, M.H. Chaves, Resina de *Protium heptaphyllum*: isolamento, caracterização estrutural e avaliação das propriedades térmicas, *Quim. Nova*, **28**(2), 183-187 (2005).

26. X. Guo, A.P. Bruins, T.R. Covey, Characterization of typical chemical background interferences in atmospheric pressure ionization liquid chromatography-mass spectrometry, *Rapid. Commun. Mass Spectrom.*, **20**(20), 3145-3150 (2006).

27. Y. Hayasaka, Analysis of phthalates in wine using liquid chromatography tandem mass spectrometry combined with a hold-back column: Chromatographic strategy to avoid the influence of pre-existing phthalate contamination in a liquid chromatography system, *J. Chromatogr. A*, **1372**, 120-127 (2014).

28. H. Shen, L. Ying, Y. Cao, G. Pan, L. Zhou, Simultaneous determination of phthalates and parabens in cosmetic products by gas chromatography/mass spectrometry coupled with solid phase extraction (in Chinese), *Se Pu*, **25**(2), 272-275 (2007).

29. M.O. Dias, L. Hamerski, A.C. Pinto, Separação semipreparativa de α e β-amirina por cromatografia líquida de alta eficiência, *Quim. Nova*, **34**(4), 704-706 (2011).

30. F.W.A. Barros, P.N. Bandeira, D.J.B. Lima, A.S. Meira, S.S. de Farias, M.R.J.R. Albuquerque, H.S.D. Santos, T.L.G. Lemos, M.O. de Morais, L.V. Costa-Lotufo, C.D.O. Pessoa, Amyrin esters induce cell death by apoptosis in HL-60 leukemia cells, *Bioorg. Med. Chem.*, **19**(3), 1268-1276 (2011).

How to cite this article

R. Gomes da Silva Ferreira, F. Guilhon-Simplicio, K. Kazumy de Lima Yamaguchi, P. Duarte de Lira, T. Marques Machado, M.A. Couto Ferreira, V.F. da Veiga-Júnior, E. Silva Lima, The selective obtaining of amyrins from Amazonian *Protium* oleoresins, *Rev. Colomb. Cienc. Quím. Farm.*, **49**(2), 482-497 (2020).

Appendix

Nuclear magnetic resonance data

Alpha and beta amyrin: white powder. ^{1}H NMR (300 *MHz*, $CDCl_3$): δ 0.84 (s, 3H, –CH3), 0.88 (d, 3H, -CH_3), 1.07 (d, 3H, –CH_3), 1.14 (3H, –CH_3), 0,96 (s, 3H, –CH_3) 0.73 (3H, –CH_3), 0.91 (3H, -CH_3), 0.78 (3H, -CH_3), 1.84 (2H), 1.91 (m, 1H), 1.69 (d, 2H), 1.90 (m, 2H), 5.16 (d, 6H), 1.55 (2H), 0.71 (s, 1H), 3.23 (s, 1H). ^{13}C NMR (300 *MHz*, $CDCl_3$) δ 38.7,27.2, 79.0, 38.6, 55.1, 18.36, 32.6, 39.6, 47.6, 38.7, 23.6, 121.7, 145.2, 41.7, 26.1, 27.2, 32.5, 47.2, 46.8, 31.1, 34.7, 37.1, 28.1, 15.5, 15.6, 16.8, 26.1, 28.4, 33.3, 23.7.

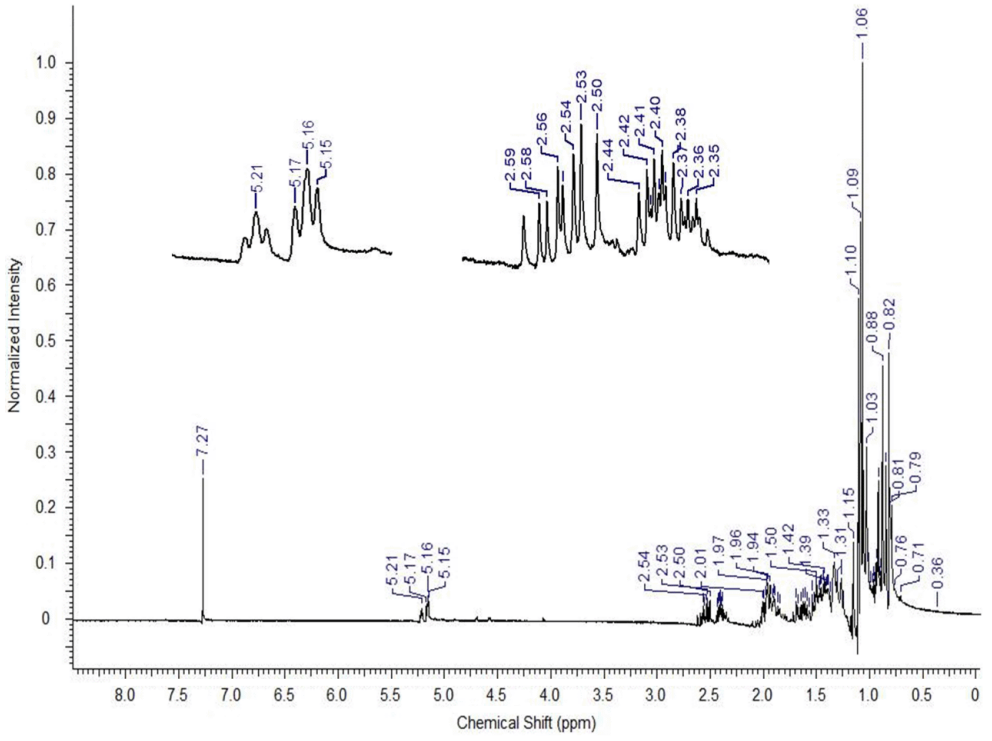

Figure A1. ^{1}H NMR (300 *MHz*, $CDCl_3$) spectra of the alpha and beta amyrin.

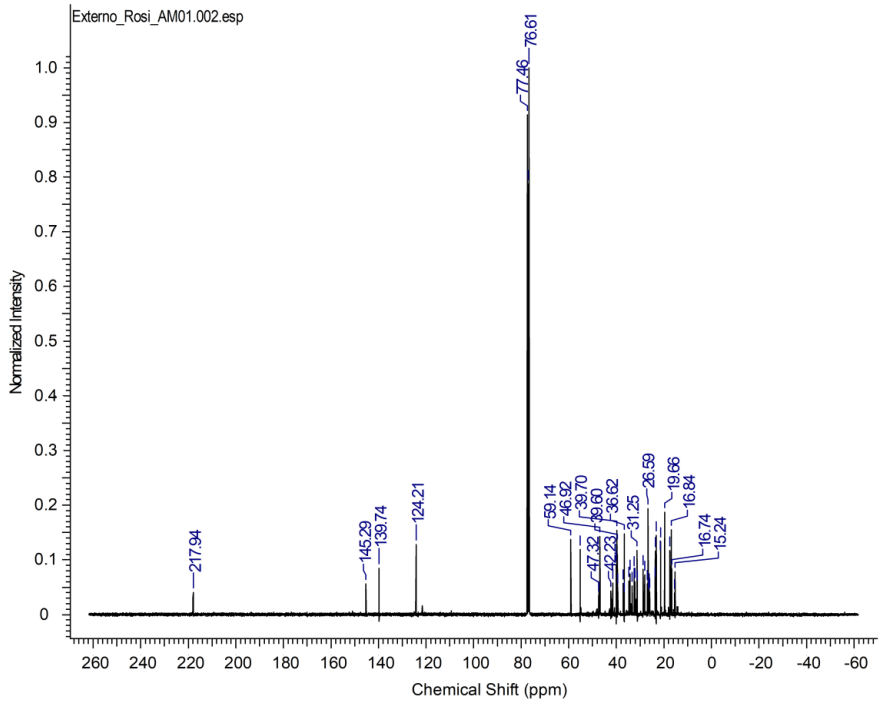

Figure A2. ^{13}C NMR (300 *MHz*, $CDCl_3$) spectra of the alpha and beta amyrin.

Artículo de revisión / *http://dx.doi.org/10.15446/rcciquifa.v49n2.89925*

Régimen jurídico de las recetas médicas en España e Iberoamérica

Francisco Miguel Bombillar Sáenz

Profesor titular de Derecho Administrativo, Facultad de Derecho, Universidad de Granada, Plaza de la Universidad s/n 18071, Granada, España.

*Correo electrónico: bombillar@ugr.es

Recibido: 21 de abril de 2020

Revisado: 24 de mayo de 2020

Aceptado: 24 de mayo 2020

Resumen

Esta contribución se ocupa de uno de los ejes sobre los que se articula la prestación farmacéutica en nuestro sistema sanitario: la receta médica. En este artículo se abordan las notas más relevantes que caracterizan el régimen jurídico de la receta médica en España y en Latinoamérica: concepto, tipos, reconocimiento por otros estados, identificación de fármacos por la denominación común internacional, objeción de conciencia del farmacéutico, receta médica electrónica o atención farmacéutica.

Palabras clave: Receta médica, régimen jurídico, España, Iberoamérica.

Summary

Legal regime of medical prescriptions in Spain and Iberoamerica

This paper deals with one of the axes on which the pharmaceutical provision in our health system is articulated: the medical prescription. Here you will find some of the most relevant notes that characterize the legal regime of the medical prescription in Spain and Latin America: concept, types, recognition by other States, identification of medications by the international common name, conscientious objection of the pharmacist, electronic medical prescription or pharmaceutical care.

Keywords: Medical prescription, legal regime, Spain, Iberoamerica.

Introducción

Régimen jurídico-administrativo del medicamento

Este artículo de revisión se ocupa de uno de los ejes sobre los que se articula la prestación farmacéutica en nuestro sistema sanitario: la receta médica, abordando algunas de las notas más relevantes que caracterizan su régimen jurídico en España y en Iberoamérica: concepto, tipos, reconocimiento por otros estados, identificación de fármacos por su denominación común internacional, objeción de conciencia del farmacéutico, receta médica electrónica o atención farmacéutica.

El medicamento no es un mero producto de consumo sujeto a las leyes del mercado, es un bien sanitario, objeto de una fuerte intervención administrativa (como estudian, entre otros autores, Bombillar Sáenz [1], Doménech Pascual [2], Sarrato Martínez [3], Vida Fernández [4] o González Bueno y Del Castillo Rodríguez [5]) durante todas las fases de su *vida* (invención, fabricación, distribución, prescripción o dispensación). No en vano, el medicamento se desenvuelve dentro de un ámbito de incertidumbre científica, en el marco de lo que se ha dado en llamar la sociedad del riesgo (analizada con detalle por Beck [6] y Esteve Pardo [7]). En consecuencia, bajo la supervisión y control de la administración queda la producción, desarrollo [8] y fabricación de los medicamentos, su distribución y almacenamiento, su prescripción y financiación, en este caso, por el sistema público de salud, y su dispensación por profesionales específicos, con titulación y autorización para ello: los farmacéuticos [9].

En Europa, la amplia intervención administrativa sobre el fármaco es liderada de forma preferente por la normativa y decisiones de las instituciones comunitarias, ejecutadas, en el marco de una red de trabajo colaborativo, por las diferentes autoridades nacionales del medicamento, erigiéndose en uno de los mayores exponentes de las políticas en materia de salud pública [10] emprendidas desde la Unión Europea [11]. En la actualidad, en Europa, los dos textos normativos de referencia en este sector son: la Directiva 2001/83/CE, por la que se establece un código comunitario sobre medicamentos para uso humano, de cuya transposición en España se ocupa el Real Decreto Legislativo 1/2015, de 24 de julio, por el que se aprueba el Texto Refundido de la Ley de garantías y uso racional de los medicamentos y productos sanitarios (TRLGURMPS [12]), y el Reglamento (CE) N.° 726/2004, por el que se establecen procedimientos comunitarios para la autorización y el control de los medicamentos de uso humano y veterinario y se crea la Agencia Europea de Medicamentos.

El TRLGURMPS ha sido objeto de un prolijo desarrollo reglamentario. Sin ánimo de ser exhaustivos podemos citar, entre otros, y por lo que a las recetas se refiere: el Real Decreto 618/2007, de 11 de mayo, por el que se regula el procedimiento para

el establecimiento, mediante visado, de reservas singulares a las condiciones de prescripción y dispensación de los medicamentos; el Real Decreto 1345/2007, de 11 de octubre, por el que se regula el procedimiento de autorización, registro y condiciones de dispensación de los medicamentos de uso humano fabricados industrialmente; el Real Decreto 1718/2010, de 17 de diciembre, sobre receta médica y órdenes de dispensación; el Real Decreto 1675/2012, de 14 de diciembre, por el que se regulan las recetas oficiales y los requisitos especiales de prescripción y dispensación de estupefacientes para uso humano y veterinario; el Real Decreto 954/2015, de 23 de octubre, por el que se regula la indicación, uso y autorización de dispensación de medicamentos y productos sanitarios de uso humano por parte de los enfermeros; y el Real Decreto 1015/2009, de 19 de junio, por el que se regula la disponibilidad de medicamentos en situaciones especiales. A este amplio entramado normativo se acogen las recetas médicas y órdenes de dispensación, sea de la asistencia sanitaria pública o de la privada, y sean extendidas en papel o en soporte informático.

Concepto de receta médica

La receta médica es el documento de carácter sanitario, normalizado y obligatorio mediante el cual los médicos, odontólogos o podólogos (únicos profesionales sanitarios con facultad, en el ámbito de sus competencias respectivas, para recetar medicamentos sujetos a prescripción médica en España, de acuerdo con el artículo 79 del TRLGURMPS) prescriben a los pacientes los medicamentos o productos sanitarios (sujetos a prescripción médica). Estos medicamentos son dispensado por un farmacéutico o bajo su supervisión, en las oficinas de farmacia y botiquines dependientes de las mismas. La receta médica, por tanto, es uno de los ejes sobre los que se articula la prestación farmacéutica en nuestro sistema sanitario.

El farmacéutico dispensará con receta aquellos medicamentos que lo requieran. Dicho requisito deberá especificarse expresamente en el embalaje del medicamento. Los medicamentos estarán sujetos a receta médica cuando puedan presentar un peligro, incluso en condiciones normales de uso, si se utilizan sin control médico; si se utilizan frecuentemente en condiciones anormales y ello puede suponer un peligro para la salud; si contienen sustancias o preparados a base de éstas cuya actividad y reacciones adversas sea necesario estudiar con más detalle; o si se administran por vía parenteral por prescripción médica (art. 19.2 TRLGURMPS).

La orden de dispensación hospitalaria para pacientes no ingresados, por su parte, es el documento de carácter sanitario, normalizado y obligatorio para la prescripción por los médicos, odontólogos y podólogos de los servicios hospitalarios, fuera por tanto del ámbito de la atención primaria, de los medicamentos que exijan una particular vigilancia, supervisión y control, que deban ser dispensados por los servicios de farmacia hospitalaria a dichos pacientes.

Por último, hemos de mencionar la orden de dispensación. Los enfermeros [13] y los fisioterapeutas, de forma autónoma, podrán indicar, usar y autorizar en España la dispensación de todos aquellos medicamentos no sujetos a prescripción médica y los productos sanitarios relacionados con su ejercicio profesional (art. 79.1 *in fine* TRLGURMPS). Esta orden de dispensación es el documento de carácter sanitario, normalizado y obligatorio mediante el cual estos profesionales, en el ámbito de sus competencias, y una vez hayan sido facultados individualmente mediante la correspondiente acreditación, indican o autorizan, en las condiciones y con los requisitos que fija para la Enfermería el Real Decreto 954/2015, de 23 de octubre (modificado por el Real Decreto 1302/2018, de 22 de octubre), la dispensación de medicamentos, sujetos o no a prescripción médica, y productos sanitarios por un farmacéutico o bajo su supervisión.

En otros ordenamientos jurídicos iberoamericanos, como el mexicano, también se disciplina la prescripción enfermera (acuerdo del Secretario de Salud, de 8 de marzo de 2017, en conexión con el artículo 28bis, en la redacción vigente desde 2012, de la Ley General de Salud); así como aquella otra desarrollada por los profesionales de la obstetricia (parteras o matronas), en Perú (Reglamento de la Ley 27853 de Trabajo de la obstetriz, en conexión con el artículo 26 de la Ley General de Salud).

Tipos de receta médica

En España, las autoridades competentes, en el marco de lo previsto por la normativa europea y el TRLGURMPS, clasificarán los medicamentos –con la incidencia que esto tiene en el campo de la prestación farmacéutica y el uso racional del medicamento– del siguiente modo: medicamentos sujetos a receta médica o medicamentos no sujetos a receta médica (art. 19.3 TRLGURMPS). Las autoridades competentes podrán subdividir los primeros en medicamentos con receta médica renovable o no renovable, medicamentos con receta médica especial y medicamentos con receta médica restringida, reservados a determinados medios especializados.

Las recetas médicas renovables son aquellas que prescriben fármacos destinados a tratar ciertas enfermedades crónicas con carácter permanente. Es el caso de los "tarjetones médicos" cubanos, un ejemplo iberoamericano, documentos que, prescritos por certificado médico, autorizan a las farmacias a vender los medicamentos por un período prolongado. Estos tarjetones deberán ser renovados a su expedición, luego de una revisión médica por el facultativo que acredite su necesidad, y emita nuevo certificado médico, donde ha de constar el período y las dosis del tratamiento que se precisa.

Atenderán a la subcategoría de medicamentos sujetos a receta médica especial, aquellos fármacos que contengan una sustancia clasificada como estupefaciente o psicótropo –con arreglo a los convenios de Naciones Unidas–, aquellos que puedan provocar tóxico

dependencia en caso de utilización anormal o ser desviados para usos ilegales, o, finalmente, aquellos cuya novedad o propiedades hagan conveniente la utilización de una receta como medida de precaución. Estas cautelas se pueden apreciar, en prácticamente los mismos términos, en los diferentes Ordenamientos jurídicos del orbe Iberoamericano. Así, en Chile, a modo de muestra, véanse los artículos 24 y siguientes sea del Reglamento de Estupefacientes, Decreto núm. 404 de 1983, que, del Reglamento de Productos Psicotrópicos, Decreto núm. 405 de 1983.

Se acogerán a la subcategoría de *medicamentos sujetos a receta médica restringida* aquellos fármacos que se reserven para tratamientos que sólo puedan seguirse en el medio hospitalario (a causa de sus características farmacológicas, novedad o por motivos de salud pública); aquellos destinados al tratamiento de enfermedades que deban ser diagnosticadas en medio hospitalario u otro adecuado, aunque la administración y seguimiento se pueda realizar fuera; y aquellos que estén destinados a pacientes ambulatorios, pero cuya acción pueda producir reacciones adversas muy graves, requiriendo una receta médica expedida por un especialista y una vigilancia especial durante el tratamiento.

En atención a la adscripción a la sanidad pública o privada del facultativo que prescriba estos medicamentos, podemos distinguir también en España entre recetas oficiales, emitidas en el ámbito del Sistema Nacional de Salud, y recetas *privadas*, para la actividad privada o libre ejercicio profesional. En el marco del corpus normativo aquí someramente esbozado, los consejos generales de médicos, odontólogos, podólogos y enfermeros, y también las propias aseguradoras privadas (aunque esto es una cuestión objeto de debate) serán responsables de la edición, gestión, control e inspección de la impresión, distribución y entrega de sus talonarios e impresos de recetas médicas y órdenes de dispensación; adoptarán cuantas medidas resulten necesarias con el fin de evitar o corregir cualquier fraude, abuso, corrupción o desviación en esta materia; y homologarán los sistemas de prescripción electrónica.

Desarrollo

Reconocimiento de recetas médicas

En los últimos años, gracias a la jurisprudencia del Tribunal de Justicia de la Unión Europea, se ha apostado por la armonización de los derechos de la ciudadanía sanitaria europea (por ejemplo, en el campo de las enfermedades raras [14]). Este acervo comunitario lo ha recogido la Directiva 2011/24/UE del Parlamento Europeo y del Consejo, de 9 de marzo de 2011, relativa a la aplicación de los derechos de los pacientes en la asistencia sanitaria transfronteriza (DAST), de cuya transposición en España se ocupa el Real Decreto 81/2014, de 7 de febrero. Esta dimensión transfronteriza [15]

se extiende también al ámbito de la prescripción y dispensación de fármacos, proclamando el artículo 11 de la DAST el reconocimiento de las recetas extendidas en otro estado miembro [16]. De este modo, en España, la receta médica no sólo será válida en todo el territorio nacional, como marca el artículo 78.3 del TRLGURMPS, también en el resto de estados miembros de la Unión Europea. Todo ello sin perjuicio de la decisión del estado miembro de afiliación relativa a la inclusión, en su caso, del fármaco correspondiente entre las prestaciones cubiertas (esto es, financiadas públicamente) por el sistema de seguridad social de afiliación.

Denominación común internacional (DCI)

La receta médica, válida en todo el territorio nacional, se editará en España en castellano y en las respectivas lenguas cooficiales de las Comunidades Autónomas que dispongan de ella (artículo 79.3 TRLGURMPS), acogiendo los datos básicos de identificación de prescriptor, paciente y medicamentos (artículo 79.4 TRLGURMPS), respetando para ello los postulados que rigen en relación con la protección de datos de carácter personal (Arias Mora y Muñoz Ureña analizan este particular "mercado de datos" en Costa Rica [17]).

Para facilitar la dispensación correcta de medicamentos, en particular, en el marco de la asistencia sanitaria transfronteriza, así como para tratar los asuntos relativos a la seguridad de los pacientes en relación con la sustitución de estos fármacos, cuando la legislación así lo permita, es crucial la utilización de la denominación común internacional (DCI). Esto permite la identificación correcta de los medicamentos que se comercializan con marcas distintas en diferentes estados de la Unión Europea, así como de los que no se encuentran a la venta en todos ellos.

Debe utilizarse la DCI recomendada por la OMS o, en su defecto, la denominación común usual (considerando 4 de la Directiva de Ejecución 2012/52/UE). La OMS, desde principios de los años cincuenta, se ha ocupado de la selección de las denominaciones comunes de los medicamentos, creando un sistema de partículas comunes a cada grupo terapéutico. En esta misma dirección se mueven otros ordenamientos jurídicos iberoamericanos, como el argentino (Ley 25649, de 28 de agosto de 2002) o el brasileño (Ley 9787, de 10 de febrero de 1999), promocionando la utilización de medicamentos por su nombre genérico.

Objeción de conciencia del farmacéutico

Tras la STC 145/2015, parece que el Tribunal Constitucional español ha reconocido la posibilidad de objetar la dispensación de un medicamento, autorizado y comercializado y convenientemente prescrito por un profesional sanitario acreditado para ello. En este pronunciamiento el Tribunal Constitucional estima el recurso de amparo

promovido –por vulneración del derecho a la objeción de conciencia, vinculado al derecho a la libertad ideológica– por un farmacéutico español (sevillano) en relación con las sanciones impuestas a la oficina de farmacia que regentaba por carecer de existencias de medicamentos con el principio activo levonorgestrel (la conocida como píldora del día después). Este derecho a la objeción de conciencia del recurrente se impondría sobre el deber legal del profesional farmacéutico de disponer de las existencias mínimas de medicamentos establecidas por las administraciones competentes (artículo 86.3 del TRLGURMPS).

Receta médica electrónica

Las nuevas tecnologías de la información y comunicación han permitido que hoy contemos con recetas médicas en soporte informático [18], sin que ello suponga una merma de las garantías establecidas en nuestro Ordenamiento jurídico. La receta electrónica se ha demostrado más eficaz y eficiente que la receta convencional (sobre todo en relación con el ahorro de tiempo de trabajo del médico), evitando, además, prácticas fraudulentas (como sucede en relación con el dopaje en el deporte, donde se han falsificado recetas para obtener medicamentos con fines dopantes y revenderlos en el mercado negro). Esta decidida apuesta de la Administración sanitaria por la receta extendida en soporte informático ha arrinconado la tradicional receta en formato papel (en Granada, sólo un 3% de las recetas, unas 15.000 al mes). La aparición y creación de la receta electrónica en España la inició, a nivel estatal, la Ley 62/2003, de 30 de diciembre, pero han sido las Comunidades Autónomas las que han apostado por su implantación, destacando las experiencias de Galicia, Madrid, Valencia o Andalucía (*Receta XXI,* en el marco del Decreto 181/2007, de 19 de junio).

En otros países del orbe iberoamericano, como Costa Rica, aunque se asiste a una paulatina implantación fáctica de la receta en formato digital, sólo se disciplinan jurídicamente aquellas recetas destinadas a la dispensación de medicamentos que contienen psicotrópicos y estupefacientes. Véase el interesante pronunciamiento a este respecto del Colegio de Farmacéuticos de Costa Rica, de 3 de enero de 2019, exhortando a que las exigencias científicas y legales (donde ocupa un rol fundamental la firma por el médico prescriptor) se observen en ambos formatos de receta.

Atención farmacéutica

La receta electrónica afianza la nueva dimensión que ha adquirido el farmacéutico en los últimos años, centrada en proporcionar una atención más personalizada al paciente, en lo que se ha dado en llamar atención farmacéutica [19]. El farmacéutico, en este contexto, ha de adaptarse a los diferentes escenarios que se le presentan, procurando que tanto la dispensación como la posterior farmacovigilancia [2] sean óptimas para

que el paciente pueda tener garantizado un correcto acceso a los fármacos prescritos. De ahí que, en España, el artículo 79.5 del TRLGURMPS prevea que, en las recetas y órdenes hospitalarias de dispensación, el facultativo incluya las pertinentes advertencias para el farmacéutico y para el paciente, así como las instrucciones para un mejor seguimiento del tratamiento.

Así, en España, la regulación de la dispensación farmacéutica en la receta electrónica permite que el farmacéutico pueda suspender cautelarmente la posibilidad de dispensación de un medicamento prescrito, cuando existan dudas sobre posibles errores en la prescripción, adecuación de esta a las condiciones de la persona enferma, medicación concomitante o cualquier otro motivo que pueda suponer un riesgo para la salud del paciente. Esta circunstancia se comunicará al paciente y, de forma telemática, al profesional que realizó la prescripción, quien podrá reactivar la prescripción si lo considera conveniente.

Régimen de responsabilidades

En relación tanto con la responsabilidad profesional, incluso en vía penal, del médico prescriptor (con comportamientos que van desde la prescripción de un medicamento inadecuado para tratar esa enfermedad o que presenta contraindicaciones evidentes para ese paciente, el error en la dosis prescrita o la firma de recetas en blanco) como con la del farmacéutico dispensador (con conductas que engloban desde el despacho de medicamentos sin receta, caducados o deteriorados a la equivocación en la dispensación consecuencia de una lectura precipitada de la receta), me remito, por su claridad, a la voz 'receta médica' en la *Enciclopedia de bioderecho y bioética* elaborada por José Fernández Hierro [20].

Conclusiones

La receta médica –y, especialmente, la electrónica– constituye el cauce principal para la transmisión de información entre los profesionales de la salud, así como para la implantación de las políticas de uso racional del medicamento. A través de este artículo de revisión hemos comprobado que los diversos cambios normativos operados por el legislador sobre la receta médica, con el fin de traer, por ejemplo, las herramientas de la sociedad digital al campo de la prescripción y dispensación de fármacos no suponen ruptura alguna con el modelo de farmacia mediterráneo que impera en España y los países del orbe iberoamericano.

La forma de la receta médica cambia, pero no la esencia. La prescripción sigue quedando en manos del médico y la dispensación del farmacéutico. La receta médica

electrónica no implica menoscabo alguno de las funciones asignadas desde antaño en nuestro ordenamiento jurídico a los farmacéuticos ni ataque al rol de las oficinas de farmacia como establecimientos sanitarios privados de interés público. La prescripción y dispensación de medicamentos sigue moviéndose, pues, dentro del circuito oficinal, el medio que se ha entendido mejor garantiza la protección de la salud de la población, asegurando la calidad y uso racional del medicamento; conjurando, de este modo, el peligro de la automedicación o el abuso: el gran riesgo aquí siempre en presencia.

Es más, la receta médica electrónica potencia las garantías propias de la atención farmacéutica y asegura la correcta información terapéutica, un mejor seguimiento de los tratamientos farmacológicos, así como un coherente y articulado sistema en red de farmacovigilancia; en fin, posibilita un intercambio interactivo, ágil y pertinente entre el paciente y los profesionales sanitarios llamados a prescribir y dispensar estos medicamentos: médicos y farmacéuticos, respectivamente.

No en vano, el fin último que justifica la regulación que aquí ha sido objeto de estudio no es otro que dar amparo a nuestro bien más preciado: el derecho a la protección de la salud [21]. Ojalá este mandato deje de ser una suerte de *papel mojado* en muchos Estados y se erija en una realidad palpable de la que en toda la comunidad iberoamericana por entero podamos sentirnos partícipes y orgullosos.

Conflicto de intereses

El autor declara no tener conflictos de intereses.

Referencias

1. F.M. Bombillar-Sáenz, Intervención administrativa de orden público sanitario y régimen jurídico del medicamento, en: *Tratado de derecho sanitario*, dirs. A. Palomar-Olmeda, J. Cantero-Martínez, Thomson-Aranzadi, Cizur Menor, Navarra, vol. 2, 2013, p. 499-570.

2. G. Doménech-Pascual, *Régimen jurídico de la farmacovigilancia*, Thomson-Aranzadi, Cizur Menor, Navarra, 2009; y G. Doménech, New European legislation on pharmacovigilance, *Pharmaceuticals, Policy and Law*, **13**(1-2), 7-27 (2011).

3. L. Sarrato-Martínez, *Régimen jurídico-administrativo del medicamento*, La Ley, Madrid, 2015.

4. J. Vida-Fernández, *Concepto y régimen jurídico de los medicamentos*, Tirant lo Blanch, Valencia, 2015.

5. A. González-Bueno, C. del Castillo-Rodríguez, *Manual de legislación farmacéutica*, Dykinson, Madrid, 2019.

6. U. Beck, *La sociedad del riesgo global*, Siglo XXI, Madrid, 2002.

7. J. Esteve-Pardo, *El desconcierto del Leviatán. Política y derecho ante las incertidumbres de la ciencia*, Marcial Pons, Madrid, 2009.

8. F. Antúnez-Estévez, Los ensayos clínicos, en: *Derecho y medicina. Cuestiones jurídicas para profesionales de la salud*, Eds. P. Rivas-Vallejo, Mª D. García-Valverde, Thomson-Aranzadi, Cizur Menor, Navarra, 2009, p. 229-287.

9. F.L. Villalba-Pérez, *La profesión farmacéutica*, Marcial Pons, Madrid, 1996; y F. Villalba-Pérez Support of the ECJ for the regulated model of pharmacy in the European Union, *Pharmaceuticals, Policy and Law*, **12**(3-4), 229-239 (2010).

10. C. Cierco-Seira, *Administración pública y salud colectiva. El marco jurídico de la protección frente a las epidemias y otros riesgos sanitarios*, Comares, Granada, 2006. Por lo que se refiere al campo de los medicamentos, véase: C. Cierco-Seira, Emergencias de salud pública y medicamentos, *Revista Española de Derecho Administrativo*, **184**, 148-192 (2017).

11. J.L. Valverde-López, El estatuto jurídico del medicamento, en: *España y Europa, hacia un ideal sanitario común. Recopilación comentada de textos comunitarios y nacionales en materia de Sanidad y Salud Pública*, Ministerio de Sanidad y Consumo, Madrid, 2002, p. 85-176.

12. El TRLGURMPS es objeto de un profundo análisis en la obra colectiva de J. Faus-Santasusana, J. Vida-Fernández (dirs.), *Tratado de derecho farmacéutico*, Thomson Reuters-Aranzadi, Cizur Menor, Navarra, 2017.

13. La prescripción enfermera es analizada por J.F. Pérez-Gálvez (dir.), *Prescripción, indicación, uso y autorización de dispensación de medicamentos y productos sanitarios*, Tirant lo Blanch, Valencia, 2017.

14. Con relación a las enfermedades raras y los medicamentos huérfanos, consúltense los trabajos de N. Garrido-Cuenca, *Derecho, salud pública y prestaciones sanitarias: retos éticos y jurídicos de las enfermedades raras*, Tecnos, Madrid, 2019; y F.M. Bombillar-Sáenz, Acceso al medicamento y derecho a la protección de la salud:

régimen jurídico de los medicamentos huérfanos en la Unión Europea, *Cadernos Ibero-Americanos de Direito Sanitario*, **3**(3), 123-148 (2014).

15. La asistencia sanitaria transfronteriza es objeto de un minucioso análisis en las obras colectivas dirigidas por J. Cantero-Martínez, *La liberalización de la asistencia sanitaria transfronteriza en Europa*, Thomson-Aranzadi, Cizur Menor, Navarra, 2017; y E.M. Álvarez-González, *Sanidad transfronteriza y libertad de circulación. Un desafío para los lugares europeos de retiro*, Tirant lo Blanch, Valencia, 2018.

16. F.M. Bombillar-Sáenz, Cross-border healthcare and recognition of medical prescriptions issued in another Member State, *Pharmaceuticals Policy and Law*, **19** (1-2), 47-61 (2017).

17. F. Arias-Mora, H. Muñoz-Ureña, De pacientes y prescriptores a simples consumidores de medicamentos. Referencia especial al mercado de medicamentos en Costa Rica, en: *Problemas actuales de Derecho y Salud. Perspectivas desde España y Latinoamérica*, coord. A. Pelayo González-Torre, Comares, Granada, 2014, p. 157-185.

18. F.M. Bombillar-Sáenz, Receta médica electrónica y venta de medicamentos online, en: *Salud electrónica. Perspectiva y realidad*, dir. J.F. Pérez-Gálvez, Tirant lo Blanch, Valencia, 2016, p. 221-258.

19. C. del Castillo-Rodríguez, Políticas americanas de salud y de formación farmacéutica, *Revista Colombiana de Ciencias Químico Farmacéuticas*, **40**(1), 47-53 (2011).

20. J. Fernández-Hierro, Receta médica, en: *Enciclopedia de bioderecho y bioética*, dir. C.Mª. Romeo-Casabona, Comares, Granada, 2011, accesible en la URL: https://enciclopedia-bioderecho.com/voces/271. Véase también L. Sarrato-Martínez, *La responsabilidad administrativa, civil y penal en el ámbito del medicamento*, Thomson-Aranzadi, Cizur Menor, Navarra, 2014.

21. F.M. Bombillar-Sáenz, A. Pérez-Miras, El derecho a la protección de la salud desde una perspectiva multinivel y de Derecho comparado, *Revista Europea de Derechos Fundamentales*, **25**, 299-331 (2015).

Cómo citar este artículo

F.M. Bombillar-Sáenz, Régimen jurídico de las recetas médicas en España y en Iberoamérica, *Rev. Colomb. Cienc. Quím. Farm.*, **49**(2), 498-508 (2020).

Technological research article / *http://dx.doi.org/10.15446/rcciquifa.v49n2.89926*

Forced degradation studies and stability-indicating liquid chromatography method for determination of tirofiban hydrochloride and synthetic impurities

Adriane Lettnin Roll Feijó[1], Fernanda Macke Hellwig[2], Clésio Soldateli Paim[1], Marcelo Donadel Malesuik[1]*

[1]Post Graduate Program in Pharmaceutical Sciences, Federal University of Pampa, UNIPAMPA, Uruguaiana, RS, Brazil.

[2]Federal University of Pampa, UNIPAMPA, Itaqui, RS, Brazil.

*Corresponding author E-mail address: marcelodonadel@gmail.com

Received: 26 August 2019

Revised: 9 June 2020

Accepted: 12 June 2020

Summary

This study aimed to develop and validate a stability-indicating liquid chromatography method for the determination of tirofiban hydrochloride and two synthetic impurities (impurity A and impurity C). The method utilizes a RP-18 column (250 mm × 4.6 mm; 5 μm) with the PDA detector for quantitation. A mixture of triethylamine 0.1% (acidified to pH 5.5 with phosphoric acid) and acetonitrile was used as the mobile phase at a flow rate of 1 mL min^{-1} with gradient elution. The method presented satisfactory linearity, precision, accuracy and robustness, as well as low limits of detection and quantification, which demonstrate sensitivity in the determination of tirofiban and impurities A and C. It was selective for the determination of the drug and impurities analysed, without interference of the degradation products generated under forced conditions, demonstrating the stability-indicating capacity of the proposed method. Tirofiban showed to be practically stable to oxidative (30% H_2O_2 for 24 h) and thermal (75 °C for 24 h) conditions, but presented degradation to UVA light and acid hydrolysis, obeying the first order kinetics for both. In this way, it can be used as a stability-indicating method in the quality control of the raw material of tirofiban hydrochloride, as well as of the finished product. The obtained results demonstrate the importance of deepening the studies in this area, to guarantee the quality of commercialized pharmaceutical products.

Key words: Degradation products, HPLC, impurities, tirofiban, stability.

Resumo

Estudo da degradação forçada e método indicativo da estabilidade por cromatografia líquida para determinação de cloridrato de tirofibana e impurezas sintéticas

Este estudo teve como objetivo desenvolver e validar método indicativo da estabilidade por cromatografia líquida para determinação de cloridrato de tirofibana e duas impurezas de síntese (impureza A e impureza C). O método utilizou coluna de fase reversa RP-18 (250 mm x 4,6 mm; 5 μm) e detector PDA para quantificação. A fase móvel foi composta por uma mistura de trietilamina 0,1% (acidificada com ácido fosfórico para pH 5,5) e acetonitrila, à vazão de 1 mL/min, no modo gradiente. O método apresentou linearidade, precisão, exatidão, robustez, bem como baixos limites de detecção e quantificação, demonstrando sensibilidade na determinação da tirofibana e impurezas A e C. O método apresentou seletividade na determinação do fármaco e das impurezas, sem interferência dos produtos de degradação gerados na degradação forçada da tirofibana, demonstrando sua capacidade indicativa de estabilidade. O fármaco apresentou-se estável a oxidação (H_2O_2 30% por 24 h) e a degradação térmica (75 °C por 24 h), mas degradou frente à luz UVA e hidrolise ácida, obedecendo cinética de primeira ordem para ambas. Dessa forma, pode ser utilizado como um método indicativo de estabilidade no controle de qualidade da matéria -prima do cloridrato de tirofibana, bem como no produto acabado. Os resultados obtidos demonstram a importância de aprofundar os estudos na área, com intuito de garantir a qualidade dos produtos farmacêuticos comercializados.

Palabras clave: Produtos de degradação, HPLC, impurezas, tirofibana, estabilidade.

Introduction

Antiplatelets are drugs with property of inhibiting platelet and thrombus aggregation and formation, without significantly interfering with other segments of the coagulation cascade. Although clinically efficacious, they have some limitations, since platelet inhibition is relatively weak and can cause systemic side effects, such as irreversible inhibition of cyclooxygenase, which may lead to peptic ulcer, caused by the administration of aspirin, or the administration of ticlopidine, associated with agranulocytosis [1].

The discovery of the glycoprotein IIb/IIIa receptor (GP IIb/IIIa) as a common final pathway of platelet aggregation generated interest in the investigation of antagonists for this site, aiming for more specific effects and minimizing adverse reactions.

Receptors can be blocked and/or antagonized by various therapeutic agents, such as abciximab (monoclonal antibody), eptifibatide (synthetic heptapeptide), and tirofiban (non-peptidic intravenous mimetic of the sites of the amino acid sequence Arginine-Glycine-Aspartic Acid (RGD)) [2].

Tirofiban (figure 1) is a non-peptidic GP IIb/IIIa receptor antagonist derived from tyrosine. It mimics the geometry, stereoactivity and electrical characteristics of RGD, interfering with platelet aggregation [1, 2]. Due to its specific action, it was quickly adopted as treatment of acute coronary syndrome and became the most widely used drug for intravenous treatment [3]. Currently, the drug (tirofiban hydrochloride - Agrastat®) is marketed in Brazil due to the partnership between the pharmaceutical industries Aspen Pharma and Merck Sharp & Dohme, in the injectable pharmaceutical form (0.25 $mg.mL^{-1}$).

Whereas even small changes in pharmaceutical formulations can lead to significant changes in the safety of the medicinal product, constant updating of analytical methodologies is required to ensure their quality and effectiveness. To ensure consumer safety, the methodologies developed should be stability-indicating and enable the identification and determination of levels of the main pharmaceutical impurities (figure 1) and degradation products in commercial formulations [4-6].

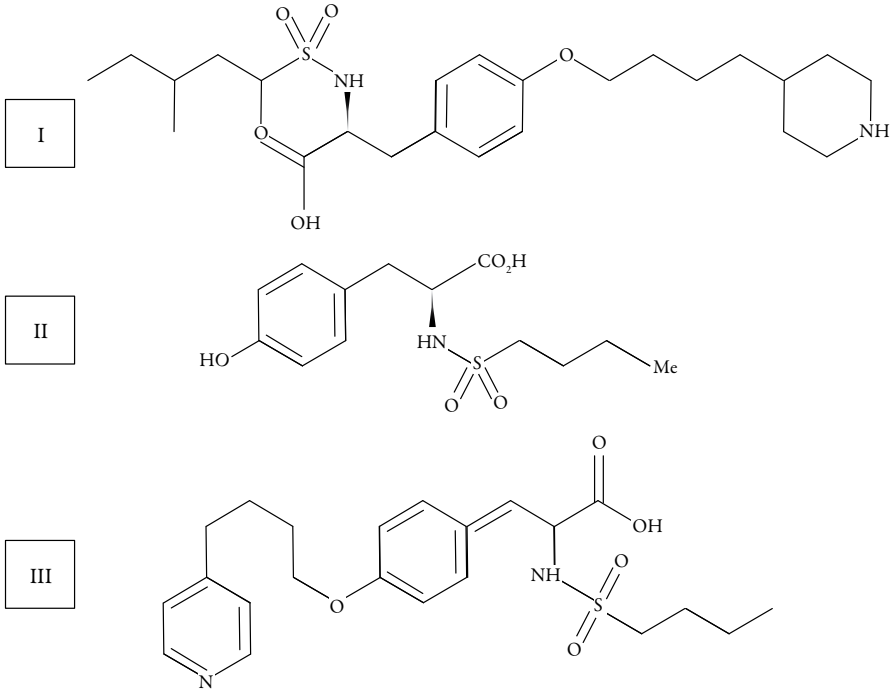

Figure 1. Chemical structures of tirofiban (I), impurity A (II) and impurity C (III).

There are reports in the literature of methods using HPLC for the determination of tirofiban in pharmaceutical form [7-14] and biological matrix [15-21]. However, there is a lack of papers on the determination of tirofiban hydrochloride in the presence of synthetic impurities and degradation products. The drug was evaluated for the presence of tyrosine [14], however, an analytical method is necessary to determine different impurities, since different synthetic routes for the design of the same drug can generate different impurities [22]. In addition, methods that can assess tirofiban hydrochloride in the presence of its degradation products are required, which are also impurities, but obtained from the decomposition of the drug.

In this sense, the present work proposes the development and validation of a stability-indicating HPLC method for the determination of tirofiban and synthetic impurities, as well as to perform a stability preliminary study under forced conditions.

Material and methods

Chemicals

For the method development was used the chemical reference substances (RS) of tirofiban, hydrochloride (Toronto Research Chemicals-TRC, Canada), impurity A (debutilpiperidine tirofiban or LN-butylsulfonyl-p-hydroxyphenylalanine) (TRC Canada) and impurity C (N-butanosulfonyl)-O-[4- (4-pyridinyl)butyl](S)-tyrosine) (TRC, Canada). The following reagents were also used: acetonitrile HPLC grade (Tedia, OH, USA), citric acid (Vetec, RJ, Brazil), hydrochloric acid (Synth, SP, Brazil), phosphoric acid (Vetec, sodium dihydrate (Vetec, RJ, Brazil), sodium chloride (Alphatec, Brazil), sodium hydroxide (Alphatec, Brazil), methanol HPLC grade (Panreac, OH, USA) and triethylamine (CRQ, SP, Brazil).

Chromatographic conditions

For the methodology development was used a high efficiency liquid chromatography Thermo Scientific Ultimate 3000 (Dionex), consisting of quaternary pump (LPG-3400SD), automatic sampler (WPS-3000 TSL), column compartment with temperature controller (TCC-3000RS), column C18 (4.6x250 mm, 5 μm-Agela Technologies, Promosil) and diode arrangement detector (DAD-3000) at 226 nm. Data acquisition and analysis were performed by Chromeleon software version 6.8 (Dionex, Thermo Fisher Scientific Inc.).

The mobile phase was composed of an aqueous phase of triethylamine 0.1%, acidified with phosphoric acid to pH 5.5, and an organic fraction composed of acetonitrile. The mobile phase was filtered with 0.45 μm membrane (Analytica, SP, Brazil).

The gradient system was used for mobile phase elution, with a proportion of 22% acetonitrile in the period between 0.0 and 2.5 min, varying to 25% in the period between 2.6 and 5.9 min, 35% in period between 6.0 and 16.9 min, returning to 22% until the end of the chromatographic run, in 20 minutes. The flow rate was maintained at 1 $mL.min^{-1}$ and the injection volume was 20 μL. All samples were filtered with nylon syringe filter (0.45 μm; 13 mm) prior to chromatographic analysis.

Validation of the method

The validation of the analytical method was performed according to the International Conference on Harmonization of Technical Requirements for Registration of Pharmaceuticals for Human (ICH Q2R1) by analyzing the following analytical parameters: specificity, linearity, precision, accuracy, robustness, limit of detection (LOD) and limit of quantification (LOQ) [23].

The tirofiban hydrochloride RS and the impurities were dissolved in methanol and sonicated for 5 minutes in an ultrasonic bath to obtain the stock solution. Tirofiban is highly soluble in methanol [19]. Subsequent dilution in methanol was performed to obtain the working solutions of 200 $\mu g.mL^{-1}$ for tirofiban and 10 $\mu g.mL^{-1}$ for impurities A and C. The tirofiban commercial form working solution was prepared by diluting it in methanol and sonicated for 5 minutes in an ultrasonic bath to obtain the final concentration of 200 $\mu g.mL^{-1}$.

The method specificity was evaluated against the confirmation of the absence of interferents inherent in the formulation excipients and satisfactory separation of the degradation products formed in the preliminary degradation study with respect to the pharmaceutical and its impurities. The placebo was composed by sodium chloride (8 $mg.mL^{-1}$), sodium citrate dihydrate (2.7 $mg.mL^{-1}$) and citric acid (0.16 $mg.mL^{-1}$), on an aqueous basis, using ultra purified water [24].

The determination of the LOD and LOQ was performed from the signal-noise of the analytical run, verified through the baseline, where the solutions were prepared at the calculated concentrations and evaluated experimentally for the drug and impurities.

The linearity of the method was established with calibration curves of 160, 180, 200, 220 and 240 $\mu g.mL^{-1}$ for tirofiban hydrochloride, and 0.1; 1.5; 5.0; 10.0 and 12.0 $\mu g.mL^{-1}$ for the impurities A and C. The results were plotted in graphs of the areas obtained as a function of the respective concentrations. Linearity was evaluated from the correlation coefficient (r) and analysis of variance by Anova, where the linear regression and linearity deviation of three curves obtained on different days for each analyte were verified.

The precision of the methodology was determined by repeatability (intraday) and intermediate precision (interday) tests. For the evaluation of the repeatability, six

samples (n = 6) of concentration 200 μg.mL^{-1} for tirofiban hydrochloride and 10 μg.mL^{-1} for impurities A and C were prepared under the same conditions by the same analyst, in a short period of time. For the determination of intermediate precision, six samples, at the same concentrations above, were prepared under the same conditions, for three different days, by two different analysts (n = 18). The analysis of the results was performed by calculating the relative standard deviation between the determinations.

Accuracy was determined by the percent recovery of tirofiban hydrochloride and impurities, by adding known concentrations of drug reference chemical (160, 200 and 240 μg.mL^{-1}) and impurities A and C (8, 10 and 12 μg.mL^{-1}) in the placebo, being evaluated the percentage of recovery in each level of concentration.

Robustness was evaluated from the determination of the drug and its impurities by small changes in the nominal chromatographic conditions of the developed method. Six factors were selected and were evaluated by a Plackett-Burman factorial design (n = 12). The effect (E) of each factor and the estimated experimental error (EE) [25] were calculated. Changes in the pH of the mobile phase (± 0.3 units), flow rate (± 0.05 units), acetonitrile in the mobile phase (± 2%), wavelength (± 2 nm), column temperature (± 3 °C) and column mark, were valuated.

From the statistical evaluation, a numerical limit value was obtained, which defines if the modification effected interfered in the quantitative analysis. This value is usually derived from the test analytical method *t*, according to equation 1:

$$t = \frac{|E_x|}{(SE)_e} \qquad \text{(Equation 1)}$$

Here, Ex = effect of each factor, SEe = estimated experimental error. The effect is considered significant if it results in $t > t$ critical.

Forced degradation study

The study of forced degradation of tirofiban hydrochloride was carried out by means of hydrolytic conditions (acidic and basic), oxidative, thermal and photolytic [26]. The acid hydrolysis occurred by addition of hydrochloric acid to the tirofiban hydrochloride solution, with final concentration of 1 mol.L^{-1}, for 2 h. The basic hydrolysis, by addition of NaOH to the solution of tirofiban hydrochloride with final concentration of 1 mol.L^{-1}, during 8 h. After the exposure period, the samples submitted to hydrolytic stresses were neutralized. Oxidative stress was performed by adding hydrogen peroxide 30 volumes to tirofiban hydrochloride at room temperature for 24 h. Thermal degradation occurred through the submission of tirofiban hydrochloride at 75 °C in a forced circulation oven 24 h. Photolytic degradation occurred by exposure of tirofiban hydrochloride to UVA radiation for 1 h. In all stress situations the final working

concentration of tirofiban hydrochloride was 200 μg.mL^{-1}. After the stress periods had ceased, to the determination of the specificity was added to the samples impurities A and C, both in the final concentration of 10 μg.mL^{-1}. All samples were filtered and submitted to chromatographic analyse. The analyses were performed in triplicate in each condition tested.

Results and discussion

The determination of the maximum absorption band of tirofiban hydrochloride was evaluated in the analytical standard and dissolved in three different solvents: ultrapurified water, methanol and acetonitrile, by spectral sweeping, in the visible ultraviolet region using the photodiode arrangement detector. The absorption maxima were 226 and 276 nm, without distinction among the solvents used, even when compared to those reported in the literature in aqueous media [11]. However, it was observed that when acetonitrile was used as the diluent, the absorptivity was lower when compared to the other solvents. Impurities exhibited absorption maxima of 226 and 276 nm for impurity A and 226 and 255 nm for impurity C. Due to the results, 226 nm was used as the detection wavelength for determination of tirofiban hydrochloride and synthetic impurities A and C.

For methodology development, mobile phase proportions between 50:50 and 90:10, consisting of triethylamine 0.1%:acetonitrile were tested, and the pH of the aqueous constituent was analysed between 3.0 and 6.0. Elution in the isocratic mode was not satisfactory for the determination of tirofiban hydrochloride in the presence of impurity C, factor corrected using gradient.

Gradient use provided good resolution between the compounds analysed. The working chromatographic condition was established in the proportion of 78:22 between 0.0 and 2.5 minutes; 75:25 between 2.6 and 5.9 minutes; 65:35 between 6.0 and 16.9 minutes, with the initial proportion returning between 17.0 and 20.0 minutes. The flow remained constant at 1 mL.min^{-1} and the injection volume was 20 μL. Retention times for impurity A, tirofiban and impurity C were 4.72, 8.38 and 12.88 minutes, respectively (figure 2), showing efficiency in the separation of the compounds, as well as specificity to differentiate structurally similar products. The chromatographic system was adequate, with resolution, symmetry and number of theoretical plates, according to the recommended in the literature [27, 28].

The specificity of the method was assessed by absence of excipients interference and degradation products formed under different stress conditions. The tirofiban hydrochloride pharmaceutical form is marketed in Brazil in citrate buffer, in this way an SSE on an aqueous basis, was analysed in triplicate.

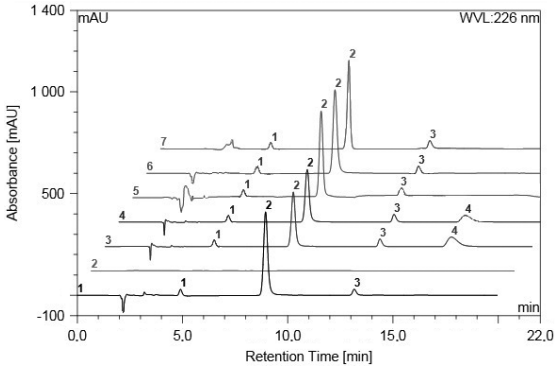

Figure 2. Chromatograms: **1** Impurity A (10 μg.mL^{-1} - peak 1), tirofiban (200 μg.mL^{-1} - peak 2) and impurity C (10 μg.mL^{-1} - peak 3); **2** Placebo; **3** Acidic degradation: tirofiban (peak 2), impurity A (peak 1), impurity C (peak 3) and degradation product (peak 4); **4** Alkaline degradation: tirofiban (peak 2), impurity A (peak 1) and impurity C (peak 3) and degradation product (peak 4); **5** Photolytic degradation: tirofiban (peak 2), impurity A (peak 1), impurity C (peak 3); **6** Oxidative degradation: tirofiban (peak 2), impurity A (peak 1), impurity C (peak 3); **7** Thermal degradation: tirofiban (peak 2), impurity A (peak 1), impurity C (peak 3).

Based on the chromatogram, shown in figure 2, it is possible to verify no interference of the SSE, both with respect to the drug and its impurities. The specificity of the analytical method was also evaluated in relation to the degradation products generated by exposure of tirofiban hydrochloride to stress conditions.

The results showed susceptibility to hydrolytic reactions. Acidic degradation, for example, showed a greater influence, leading to degradation of 19.63% of the initial concentration in 2 h of exposure, whereas in basic media degraded 14.39% in 8 h of exposure (figure 2).

In both hydrolysis reactions, it was possible to detect a degradation product with the same elution time (16.8 minutes) and the same ultraviolet absorption spectra, suggesting that the same PD occurs in acidic and basic hydrolysis.

The tirofiban was also susceptible to photolysis, with a decrease of 11.07% of the concentration when exposed to UVA light for 1 h, however, the developed methodology was not able to detect the products from this degradation.

The drug did not present a decrease of the concentration, nor the appearance of degradation product during the 24 h analysed under drastic conditions of thermal and oxidative stress, being considered practically stable to these conditions [26].

The method was selective, in other words, it was able to determine the drug and impurities A and C in the presence of the degradation product formed (figure 2). The peak purity analysis, evaluated by the equipment software, using the photodiode array detector, suggests that in all cases the peaks analysed were of adequate purity. Consi-

dering the data, it can be confirmed that the developed method presents the stability-indicating capability capacity indicative of the stability.

LOQ and LOD levels were respectively 2.12 and 1.00 $\mu g.mL^{-1}$ for tirofiban, 0.09 and 0.07 $\mu g.mL^{-1}$ for impurity A and 0.08 and 0.06 $\mu g.mL^{-1}$ for impurity C. The value of LOQ found for impurities was lower than the respective threshold of notification established by ICH [29] and, therefore, the methodology developed serves its purpose.

The linearity of the method was established by triplicate assay, individually for tirofiban and its impurities. The correlation coefficients (r) obtained for the analytical curves presented values of 0.9999, 0.9999 and 0.9999 for tirofiban hydrochloride, impurity A and impurity C, respectively. These results demonstrated a high correlation between the analytes concentration analysed and the equipment response, according to the literature [23]. In the ANOVA statistical analysis, the results were significant for linear regression and not significant for linearity deviation, at a significance level of 5%, thus proving a linear correlation between the variables.

The precision of the method was determined by repeatability (intraday) and intermediate precision (interday) tests. The results obtained (table 1) show that the precision of the developed method is within acceptable limits since it presented a relative standard deviation (RSD) of less than 2% in both repeatability and intermediate precision analyses [27, 28].

Table 1. Results obtained for evaluation of precision and accuracy of the analytical methodology for determination of tirofiban and impurities A and C.

Precision									
	Tirofiban			**Impurity A**			**Impurity C**		
	Day 1	Day 2	Day 3[a]	Day 1	Day 2	Day 3[a]	Day 1	Day 2	Day 3[a]
Average (*n*=6)	100.21	99.82	99.80	99.49	97.92	97.67	99.88	98.13	99.28
RSD (%)	0.40	0.49	0.44	0.94	1.54	1.17	1.02	1.77	1.77
Average (*n*=18)	99.94			98.36			99.09		
RSD (%)	0.46			1.44			1.65		

Accuracy									
	Tirofiban			**Impurity A**			**Impurity C**		
	80%	100%	120%	80%	100%	120%	80%	100%	120%
Concentration ($\mu g.mL^{-1}$)	160.0	200.0	240.0	8.0	10.0	12.0	8.0	10.0	12.0
Recovery (%)	100.19	99.55	100.05	102.12	100.42	97.13	99.22	100.91	96.89
Average (*n*=9) (RSD%)	99.93 (0.33)			99.89 (2.54)			99.01 (2.04)		

[a] **Analyst** 2; RSD= relative standard deviation.

Table 2. Parameters evaluated and results obtained in the robustness test.

		pH		Flow rate (mL.min^{-1})		% ACN		λ (nm)		Temperature (°C)		Column	
		(+)	(–)	(+)	(–)	(+)	(–)	(+)	(–)	(+)	(–)	(+)	(–)
Tirofiban	Average (%)[a]	99.35	100.59	99.99	99.95	99.85	100.10	100.13	99.81	100.02	99.92	99.79	100.16
	RSD (%)	0.82	0.50	0.63	1.20	1.09	0.78	0.53	1.22	0.57	1.22	1.08	0.77
	t calc[b]	2.531		0.078		0.514		0.651		0.194		0.759	
	p-value[c]	0.052		0.941		0.629		0.544		0.854		0.482	
Impurity A	Average (%)[a]	100.88	101.90	101.27	101.51	101.35	101.43	101.04	101.74	101.56	101.22	101.33	101.45
	RSD (%)	1.88	2.96	1.85	3.08	1.19	3.39	1.86	3.02	1.82	3.10	1.20	3.39
	t calc[b]	0.509		0.116		0.042		0.351		0.171		0.062	
	p-value[c]	0.632		0.912		0.968		0.740		0.871		0.953	
Impurity C	Average (%)[a]	95.83	99.02	94.04	100.81	95.29	99.57	99.32	95.53	100.16	94.70	96.93	97.92
	RSD (%)	9.83	6.41	4.64	9.34	2.55	10.92	7.09	9.18	10.53	2.61	9.61	7.07
	t calc[b]	0.694		1.471		0.930		0.824		1.185		0.216	
	p-value[c]	0.519		0.201		0.395		0.447		0.289		0.838	

[a] **Average** n=6

[b] Not significant for p=0.05 (p critical = 2.57)

[c] Statistical responses of the Student T test application by comparing the parameters evaluated with the nominal parameter

% ACN= percentage of acetonitrile in the mobile phase composition; %M= average percentage; λ= wavelength; RSD= relative standard deviation; *t* calc= *t*-value calculated from Student's *t*-test.

Accuracy was determined through the recovery test, by the method of addition of standard in the matrix, relating the observed and nominal concentration. The obtained averages are described in table 1. A satisfactory recovery content for tirofiban hydrochloride and its impurities A and C, of 99.93%, 99.88% and 99%, respectively, it was observed, corresponding to works of the literature admitting a variation of 2% for the finished product [27, 28], although some authors allow the expansion of this content by up to 20% for synthetic impurities [27, 28].

The robustness of the method was evaluated from the determination of the drug and its impurities by small changes in the nominal chromatographic conditions of the developed method. Table 2 presents the factorial design and statistical analysis. The results show no statistically significant difference using the Student's t-test for p = 0.05 (critical $t = 2.57$).

Considering the results obtained, the method developed and validity by HPLC-DAD showed to be specific, selective, sensitive, linear, precise, accurate and robust to quantify tirofiban hydrochloride and synthetic impurities A and C, in the presence of the products of degradation. In this way, it can be used as a stability-indicating method in the quality control of the raw material of tirofiban hydrochloride, as well as of the finished product.

Acknowledgments

The authors thank FAPERGS and CNPq (Programa Primeiros Projetos - ARD/PPP/FAPERGS/CNPq, Edital 08/2014) for the support.

Disclosure statement

No potential conflict of interest was reported by the authors.

References

1. M.E.W. Gomes, C. Fabris, J.L.B. Filho, R. Dreher, G.A. Rosito, Antagonistas do receptor plaquetário GPIIb/IIIa, *Revista da Associação Médica Brasileira*, **46**(3), 255-264 (2000).

2. R.M. Rocha, Glicoproteínas IIIb/IIIa, *Revista SOCERJ*, **14**(1), 34-39 (2001).

3. S. King, M. Short, C. Harmon, Glycoprotein IIb/IIIa inhibitors: The resurgence of tirofibana, *Vascular Pharmacology*, **78**, 10-16 (2016).

4. J.Y.L Chung, D. Zhao, S.L. Hughers, E.J.J. Grabowski, A practical synthesis of fibrinogen receptor antagonist MK-383. Selective functionalization of (S)-tyrosine, *Tetrahedron*, **49**(26), 5767-5576 (1993).

5. M. Sitting, *Pharmaceutical Manufacturing Encyclopedia*, 3rd ed., William Andrew Publishing, New York, 2007.

6. C. Barata-Silva, R.A. Hauser-Davis, A.L.O. Silva, J.C. Moreira, Desafios ao controle da qualidade de medicamentos no Brasil, *Cadernos de Saúde Coletiva*, **25**(3), 362-370 (2017).

7. P.A. Bergquist, W.A. Hunke, R.A. Reed, D. Manas, R.R. Forsyth, J. Cook, M. Holahan, Compatibility of tirofiban HCl with dopamine HCl, famotidine, sodium heparin, lidocaine HCl and potassium chloride during simulated Y-site administration, *Journal of Clinical Pharmacy and Therapeutics*, **24**(2), 125-132 (1999).

8. P.A. Bergquist, D. Manas, W.A. Hunke, R.A. Reed, Stability and compatibility of tirofiban hydrochloride during simulated Y-site administration with other drugs, *American Journal of Health-System Pharmacy*, **58**(13), 1218-1223 (2001).

9. M.J. Garabito, L. Jimenez, F.J. Bautista, I. Perez-Rodrigo, Stability of tirofiban hydrochloride in 0.9% sodium chloride injection for 30 days, *American Journal Health-System Pharmacy*, **58**(19), 1850-1852 (2001).

10. M. Gandhimathi, S.T. Athoti, T.K. Ravi, Three newer methods for the estimation of tirofiban hydrochloride from pharmaceutical formulation, *Indo American Journal of Pharmaceutical Research*, **3**, 9310-9315 (2013).

11. T. Henriet, P.H. Secrétan, F. Amrani, H. Sadou-Yayé, M. Bernard, A. Solgadi, N. Yagoubi, B. Do, Phototransformation patterns of the antiplatelet drug in aqueous solution, relevant to drug delivery and storage, *New Journal Chemistry*, **40**(2), 1182-1194 (2016).

12. K.S. Nataraj, S.V.S. Kumar, N.V.V.S. Kalyani, M.B. Duza, Development and validation of a reverse phase high performance liquid chromatographic method for the estimation of tirofiban in pharmaceutical dosage forms, *International Journal of Pharmacy and Pharmaceutical Sciences*, **5**(Suppl. 1), 200-203 (2013).

13. K.S. Ranjitha, A.L. Rao, Development and validation of new RP-HPLC method for the determination of tirofiban in pharmaceutical formulation, *International Journal of Pharmaceutical, Chemical and Biological Sciences*, **1**, 43-47 (2011).

14. R.I. El-Bagary, E.F. Elkady, N.A. Farid, N.F. Youssef, Stability study and validated reversed phase liquid chromatographic method for the determination of tirofiban hydrochloride in presence of tyrosine as a process impurity, *Journal of the Chilean Chemical Society*, **63**(2), 3958-3967 (2018).

15. M. Di Rago, E. Saar, L.N. Rodda, S. Ufus, A. Kotsos, D. Gerostamoulos, O.H. Drummer, Fast targeted analysis of 132 acidic an neutral drugs and poisons in whole blood using LC-MS/MS, *Forensic Science International*, **243**, 35-43, 2014.

16. J.D. Ellis, E.L. Hand, J.D. Gilbert, Use of LC-MS/MS to cross-validate a radioimmunoassay for the fibrinogen receptor antagonist, Aggrastat (tirofiban hydrochloride) in human plasma, *Journal of Pharmaceutical and Biomedical Analysis*, **15**(5), 561-569 (1997).

17. R. Oertel, A. Köhler, A. Koster, W. Kirch, Determination of tirofiban in human serum by liquid chromatography–tandem mass spectrometry, *Journal of Chromatography B*, **805**(1), 181-185 (2004).

18. M. Darkovsaka-Serafimovska, E. Janevik-Ivanovska, Z. Arsova-Sarafinovska, I. Djorgoski, N. Ugresic, Development and validation of reverse phase high performance liquid chromatographic method for determination of tirofiban in serum, *International Journal of Pharmacy*, **4**(4), 115-120 (2014).

19. M. Darkovsaka-Serafimovska, E. Janevik-Ivanovska, T. Balkanov, N. Ugresic, Development of alternative HPLC method for the determination of tirofiban in rat serum, *Macedonian Journal of Chemistry and Chemical Engineering*, **35**(2), 217-223 (2016).

20. S. Vickers, A.D. Theoharides, B. Arison, S.K. Balani, D. Cui, C.A. Duncan, J.D. Ellis, L.M. Gorham, S.L. Polsky, T. Prueksaritanont, H.G. Ramjit, D.E. Slaughter, K.P. Vyas, *Drug Metabolism and Disposition*, **27**(11), 1360-1366 (1999).

21. S. Yang, G. Peiwu, Y. Lin, Z. Zhang, Bioavailability and pharmacokinetic study of tirofibana in rat by liquid chromatography mass spectrometry, *Latin American Journal of Pharmacy*, **35**(1), 44-46 (2016).

22. L. Ng, G. Lunn, P. Faustino, Organic impurities in drug substance: origin, control, and measurement, In: *Analysis of Drug Impurities*, Blackwell Publishing, Oxford, 2007.

23. ICH - International Conference on Harmonization of Technical Requirements for Registration of Pharmaceuticals for Human Use, *Guideline on Validation of Analytical Procedure–Methodology Q2 (R1)*, ICH Steering Committee, Switzerland, 2005.

24. Aggrastat (Tirofiban Hydrochloride Injection) is manufactured for: AGGRASTAT® (Tirofiban Hydrochloride Injection Premixed and Tirofiban Hydrochloride Injection) Baxter Healthcare Corporation, Deerfield, Illinois USA, 1998, URL: https://www.accessdata.fda.gov/drugsatfda_docs/label/1998/20912lbl.pdf, accessed May 10, 2018.

25. H.Y. Vander, A. Nijhuis, J. Smeyers-Verbeke, B. Vandeginste, D. Massart, Guidance for robustness/ruggedness tests in method validation, *Journal Pharmaceutical and Biomedical Analysis*, **24**(5-6), 723-753 (2001).

26. M. Bakshi, S. Sing, Development of validated stability-indicating assay methods – critical review, *Journal of Pharmaceutical and Biomedical Analysis*, **28**(6), 1011-1040 (2002).

27. J. Ermer, J.H.McB. Miller, *Method Validation in Pharmaceutical Analysis. A Guide to Best Practice*, Wiley-VCH, Weinheim, 2005.

28. M. Ribani, C.B.G. Bottoli, C.H. Collins, I.C.S.F. Jardim, L.F.C. Melo, Validação em métodos cromatográficos e eletroforéticos, *Química Nova*, **27**(5), 771-780 (2004).

29. International Conference on Harmonization of Technical Requirements for Registration of Pharmaceuticals for Human Use, *Impurities in New Drug Substances - Q3A (R2)*, ICH Steering Committee, Switzerland, 2006.

How to cite this article

A.L. Roll-Feijó, F. Macke-Hellwig, C. Soldateli-Paim, M.D. Malesuik, Forced degradation studies and stability-indicating liquid chromatography method for determination of tirofiban hydrochloride and synthetic impurities, *Rev. Colomb. Cienc. Quím. Farm.*, **49**(2), 509-522 (2020).

Red Iberoamericana de Farmacometría

Abstracts of 3th Iberoamerican Pharmacometrics Network Congress
Havana, Cuba. November 28th-30th, 2019

Scientific Committee

Name	Affiliation
Ignacio Hernández González, B. Sc.	Development Department, Isotopes Centre, Mayabeque, (CENTIS), Cuba
Leyanis Rodríguez Vera, Ph. D.	Institute of Pharmacy and Food (IFAL), University of Havana, Cuba
Gledys Reynaldo Fernández, Ph. D.	Institute of Pharmacy and Food (IFAL), University of Havana, Cuba
Niurys de Castro Suárez, M. Sc.	Institute of Pharmacy and Food (IFAL), University of Havana, Cuba
Miguel Ángel Cabrera Pérez, Ph. D.	Universidad Central de la Villas ¨Marta Abreu¨, Santa Clara, Cuba
Manuel Ibarra Viñales, Ph. D.	Pharmacokinetics and PK/PD Modeling Laboratory, Faculty of Pharmacy, Federal University of Rio Grande do Sul, Porto Alegre, RS, Brazil
Teresa Dalla Costa, Ph. D.	Pharmacokinetics and PK/PD Modeling Laboratory, Faculty of Pharmacy, Federal
Bibiana Verlindo de Araujo, Ph. D.	Universidade Federal do Rio Grande do Sul, Porto Alegre-RS, Brazil
Maiara Pigatto, Ph. D.	Research and Innovation Deparment, Eurofarma Laboratories S.A., Itapevi, Sao Paulo. Brazil

Organizing Committee

Name	Affiliation
Ignacio Hernández González	Development Department, Isotopes Centre, Mayabeque, (CENTIS), Cuba
Leyanis Rodríguez Vera	Institute of Pharmacy and Food (IFAL), University of Havana, Cuba
Gledys Reynaldo Fernández	Institute of Pharmacy and Food (IFAL), University of Havana, Cuba
Niurys de Castro Suárez	Institute of Pharmacy and Food (IFAL), University of Havana, Cuba
Mariela León Pérez	Development Department, Isotopes Centre, Mayabeque, (CENTIS), Cuba
Nubia Martín Columbié	Development Department, Isotopes Centre, Mayabeque, (CENTIS), Cuba
Adriel Brito Llera	Institute of Pharmacy and Food (IFAL), University of Havana, Cuba

Plenary lectures

Moving from basic PK/PD towards systems models: lessons from corticosteroids

Willian J. Jusko
SUNY Distinguished Professor, University of Buffalo, USA
E-mail: wjjusko@buffalo.edu

Over the past five decades, technological advances in bioanalysis, -omics, and computation have evolved to allow for comprehensive assessments of the molecular to whole-body pharmacology of diverse corticosteroids. Such studies have led to advancements in pharmacokinetic and pharmacodynamic (PK/PD) concepts and models that often generalize across various classes of drugs. These models encompass the 'pillars' of pharmacology, namely PK and target drug exposure, the mass-law interactions of drugs with receptors/targets, and the consequent turnover and homeostatic control of genes, biomarkers, physiological responses, and disease symptoms. Pharmacokinetic theory and methodology has come to appreciate noncompartmental (NCA), compartmental, reversible, physiological (full PBPK and minimal PBPK), and target-mediated drug disposition (TMDD) models with enactments using a growing array of pharmacometric considerations and software. Several basic PK/PD models and components have emerged (simple direct, biophase, slow receptor binding, indirect response, irreversible, turnover with inactivation, and transit models) that place emphasis on parsimony, are mechanistic in nature, and serve as a catalog of highly useful 'top-down' methods of quantitating the actions of diverse drugs. These are often components of more complex quantitative systems pharmacology (QSP) models that help explain the array of therapeutic and adverse effects of various drugs including corticosteroids. A progressively deeper mechanistic appreciation of PBPK, drug-target interactions, and systems physiology from the molecular (genomic, proteomic, metabolomic) to cellular to whole body levels have laid the foundation for building enhanced PK/PD to more comprehensive QSP models. Our research based on various animal, clinical, and theoretical studies with corticosteroids have provided ideas and quantitative methods that have broadly advanced the fields of PK/PD and QSP modeling. These models demonstrate the transition towards a global system understanding of actions of many types of drugs.

Physiologically based pharmacokinetic modeling (pbpk) in drug development and regulatory science: from bench to bedside

Lawrence J. Lesko
University of Florida, USA
E-mail: llesko@cop.ufl.edu

PBPK is an established discipline in drug development and regulatory science in the developed world. There were 253 PBPK submissions in 94 New Drug Applications to the US FDA in 2017. Enzyme-based drug-drug interactions (ddis) accounted for 60% of submissions, pediatrics for 15%, special populations for 10%, and transporter-based ddis for 7% of all submissions. PBPK models for ddis have been re-purposed for multiple uses including virtual bioequivalence (VBE). PBPK models with high impact have predicted PK in untested scenarios, supported dose selection and facilitated PK bridging studies across formulations. PBPK is an emerging discipline in the developing world but substantial progress is being made to foster greater use of PBPK by the efforts of redif across Latin America, Bill and Melinda Gates Foundation across Africa, and WHO globally to promote model-based risk assessments. We have good reason to be optimistic. Pharmaceutical companies are using PBPK models to support the "Quality by Design" pharmaceutical manufacturing processes and to perform VBE studies of mainly generic drugs. The clinical utility of PBPK models has been demonstrated for enzyme-based ddis between combination hormonal contraceptives and HIV, tuberculosis and infectious disease medications especially in developing countries. FDA recently approved a new drug (Pretomanid R) in combination with bedaquiline and linezolid for highly treating treatment-resistant tuberculosis (TB). A PBPK population model of pretomanid was available to simulate PK in pulmonary TB patients with application to pretomanid dose selection in individual patients receiving pretomanid-containing anti-TB regimens. VBE studies have been used to develop generic formulations of nifedipine and levothyroxine that minimize the *in vivo* absorption consequences of interactions between formulations and gastrointestinal tract physiology. PBPK models of VBE have been used post-approval to modify dissolution specifications for formulations used in phase 3 trials. This presentation will highlight selected case studies illustrating these advancements in PBPK modeling.

Pharmacometrics to combat antimicrobial drug resistance

Lena Friberg
Uppsala University, Sweden
E-mail: lena.friberg@farmbio.uu.se

Worldwide, the prevalence of bacterial resistance to antibiotics is rapidly increasing. In spite of the urgency to identify new treatments, the interest from pharmaceutical industry for antibiotic drug development is low due to the small expected return on investment compared to other disease areas. It is also not feasible to cover all plausible bug-indication-patient status combinations in clinical trials. There is therefore a need for streamlined processes to determine antibiotic dosing strategies for new and existing antibiotics, administered in mono- or combination therapies. Through pharmacokinetic and pharmacodynamic modelling and simulation, dosing regimens can be tailored to overcome infections with resistant bacteria while minimizing the risk of developing resistance during treatment. Bacteria can rarely be quantified over time in patients and therefore knowledge on PKPD for antibiotics rely on preclinical systems. The traditional PK/PD index methodology for translation of effects from preclinical models to patients has however several limitations. For example, PK/PD indices ignore resistance dynamics, assume that the PD target is independent of the PK profile, and are not applicable for drug combinations. PKPD-models, developed based on *in vitro* data, can on the other hand describe the time-course of bacterial growth and killing. After adjusting for *in vivo* conditions, such models may provide a more predictive approach to define efficacious doses in patients. There is also a need to connect PKPD to clinical outcomes. The response to antibiotics is typically evaluated on dichotomous endpoints, such as success/failure or alive/dead, at a certain day after treatment initiation. Time-to-event analyses of survival and discharge, bounded integer models of sequential organ failure assessment (SOFA) scores, and multi-state models for microbiological status, can contribute to the pharmacometric toolbox, aiming to better understand disease progress and changes in treatment effects to efficiently slow down the accelerating antibiotic resistance.

Translational pharmacometrics and system pharmacology models in oncology

Donald E. Mager
University at Buffalo, USA
E-mail: dmager@buffalo.edu

Cancer continues to represent a major source of morbidity and mortality around the world despite significant advancements in the development of precision chemotherapy,

biologics, and cell-based therapies. Compounds designed to treat cancer continue to exhibit one of the highest rates of attrition in drug development, primarily owing to a lack of efficacy and unanticipated adverse drug effects in later phase trials. The use of clinically approved drugs is also challenged by tumor heterogeneity and known and unknown factors that result in innate and acquired resistance. Substantial innovations in the computational modeling of cancer therapeutics have been made in pharmacometrics (Pmx) and quantitative systems pharmacology (QSP). Pmx is grounded in the basic principles of pharmacokinetics (PK), statistics, and pharmacodynamics (PD), and can be readily extended to diverse data types. Traditional PK/PD models contain a minimal number of identifiable parameters to describe temporal profiles of therapeutic and adverse drug effects. Coupled with nonlinear mixed effects modeling and relatively large clinical trials, a covariate analysis can be used to identify patient-specific characteristics that explain the variability in model parameters and clinical outcomes. This approach can be limited by study designs and is rarely sufficient for recapitulating multiple, complex genotype-phenotype relationships. A major opportunity for pharmacometrics is the extension of pharmacostatistics to QSP models, which recognize that both drugs and disease processes give rise to complex and dynamic phenotypes by altering natural interconnected biochemical networks. Multi-scale QSP models that combine physiological PK/PD principles and signaling networks can serve as a platform for integrating factors that regulate drug effects and therapeutic outcomes. This presentation will discuss basic principles of translational Pmx and QSP modeling in oncology and highlight approaches to identify or qualify drug targets, design and evaluate combinatorial drug regimens, explore the impact of tumor heterogeneity, and identify factors influencing anti-cancer drug action.

Oral presentations

PBPK/PD & QSP/ Seminar session

Open-systems-pharmacology: a platform for pre-competitive research in translational medicine leveraging a qualified framework for pbpk/pd

Pavel Balazki*, Stephan Schaller
1esqlabs gmbh, Saterland, Germany
*E-mail: pavel.balazki@esqlabs.com

Over the years, there has been an ever growing demand for specialized use-scenarios in PBPK modelling and for analyses of complex mechanism-based treatment effects

through integration of systems-biology concepts within large therapeutic-area- / disease-specific models, which is getting more and more challenging and requires an extension, i.e. An increased flexibility of current simulation software. In addition, the recently issued draft guideline on PBPK modeling by the European Medicines Agency demands the qualification of the intended use related to the PBPK platform for any type of simulation scenario in regulatory submissions. While the database and many models developed within the OSP Suite have been extensively validated over the years, changes in the software platform require continuous requalification of (these) models. OSP has implemented a technical solution for automated requalification of PBPK models. This will allow convenient and quality controlled (re-)qualification of models for their intended use, which is required once changes in the software platform have been made e.g. For a new release. This development is currently extended towards PBPK/PD (QSP) models together with a technical solution for modularization of complex disease platforms built within the software. (The) OSP (Community) is well prepared to solve these two major challenges in PBPK and complex systems modeling & simulation for the OSP Suite, namely, 1) the requirement for continuous (re-)qualification of models throughout their life-cycle and 2) handling the growing complexity of the developed models. This is achieved by 1) implementation of an automated (re-) qualification routine and by 2) improving the methods and tool functionalities for model building.

Use & applications of systems pharmacology models

Iñaki F. Trocóniz[1,2]

[1] Pharmacometrics & Systems Pharmacology, Department of Pharmaceutical Technology and Chemistry, School of Pharmacy and Nutrition, University of Navarra, Pamplona, Spain

[2] idisna, Navarra Institute for Health Research, Pamplona, Navarra, Spain

E-mail: itroconiz@unav.es

The objective of this work is to encourage members of Redif to consider Systems Pharmacology (SP) models in their academic/research plans given (i) its great potential in well-established fields as basic research in pharmacology and patient management beyond therapeutic drug monitoring (TDM), and (ii) the weak presence of research and development in Latin American's pharmaceutical industry.

Different cases studies are presented covering immune-oncology, mrna-based therapeutics for the treatment of rare diseases, and dual neutralizing antibodies. The work gives examples of the application of (contrary to the general perception) not necessarily multi-scale complex models in designing combination therapies, translation approach, early dose selection, and understanding drug disposition in critically ill patients.

Efficient ways to use prior knowledge based either on (i) data published previously in literature or (ii) predefined hypothesis supported by current biological understanding are also shown and discussed.

Virtual bioequivalence / Seminar session

Determination of bioequivalence of locally applied drugs

Hartmut Derendorf
University of Florida, Dept. Of Pharmaceutics, Gainesville, FL 32610, USA
E-mail: harmut@ufl.edu

Determination of bioequivalence of locally applied drugs is challenging since the usual approach of comparing blood levels may not be applicable. For example, there are only few approved generic inhaled corticosteroids available on the US market. This is surprising since this indication represents a lucrative market and the patents of some of the market leaders are already expired. The reason for this situation is the lack of a regulatory guidance that will enable generic manufacturers to submit an ANDA tor approval of a bioequivalent product. The concern, as with any topical product, is that the conventional bioequivalence study based on a comparison of drug exposure in plasma may not be appropriate and not correctly reflect the relative availability at the site of action in the lungs. Hence, the only way that a generic company can get a product approved is to undergo expensive clinical trials, which defeats the purpose of the generic drug product concept. Interestingly, the approach of the EMA in Europe has been exactly the opposite. The EMA has issued a guidance document that may allow generic approval based on in-vitro equivalence alone. However, the detailed criteria are so strict that this scenario seems not very realistic. If *in-vitro* equivalence is not achieved, then a pharmacokinetic study based on drug exposure in plasma can be submitted. Interestingly, even if the pharmacokinetic studies fail to show equivalence, generic approval is still a possibility if clinical equivalence can be shown. It can be shown that of the three different measures (*in-vitro* performance, pharmacokinetics, clinical study) the pharmacokinetic approach is the most sensitive. Hence, it is proposed to harmonize the equivalence criteria world-wide and base the approval on both in-vitro studies and pharmacokinetic studies but not require any clinical studies.

PBPK modelling in the selection of the most sensitive analyte for bioequivalence studies

J. Reig-Lopez[1,2], M. Merino-Sanjuan[1,2], M. Prado-Velasco, V. Mangas-Sanjuan[1,2]

[1] Pharmacy and Pharmaceutical Technology Area, University of Valencia, Spain

[2] Interuniversity Research Institute for Molecular Recognition and Technological Development, Polytechnic University of Valencia, 46100 Valencia, Spain

[3] Multiscale Modeling and Bioengineering Research Group, Faculty of Engineering, University of Seville, Spain

E-mail: victor.mangas@uv.es

The Physiological-based Pharmacokinetic models have recently emerged as a valuable tool during drug development process. The aim of this work is to explore and assess the most sensitive analyte (parent drug or any of the metabolites) to changes in drug product performance using a semi-physiological models in two different softwares and to make recommendations based on the simulations outcome. A semi-physiological one- and two-compartment pharmacokinetic model with two active metabolites (primary (PM) and secondary metabolites (SM)) with saturable and non-saturable pre-systemic efflux transporter, intestinal and hepatic metabolism have been developed. Several scenarios were generated as a factorial combination of Biopharmaceutics Classification System (BCS) drug types, KM Pgp values, intestinal and liver metabolic scenarios, dose levels and quality levels of the drug product. Monte Carlo simulations of all bioequivalence studies were performed in NONMEM 7.3 and physpk Biosimulation Software (PPK). Results showed the parent drug (PD) was the most sensitive analyte for bioequivalence trials in all the studied scenarios. PM and SM revealed less or the same sensitivity to detect differences in pharmaceutical quality as the PD. Mean point estimate of Cmax and AUC methodology from Monte Carlo simulations allows to select more accurately the most sensitive analyte compared to the criterion on the percentage of failed or successful BE studies. The adequacy of PPK as a reliable software was demonstrated based on model predictions based on post-hoc PK estimates derived from NONMEM. Parent drug has been selected as the most sensitive analyte to detect differences in dissolution performance or orally administered formulations. The recommendation of measurement of PM by the FDA guideline when PM is formed substantially through pre-systemic metabolism might not be longer supported based on the results of this study.

Virtual bioequivalence: new perspectives in drug development

Miguel Ángel Cabrera-Pérez

Unidad de Modelación y Experimentación Biofarmacéutica, Centro de Bioactivos Químicos, Universidad Central "Marta Abreu" de Las Villas, Cuba

E-mail: macabreraster@gmail.com

Bioequivalence is an integral part of development and regulations for both generic and new drugs, and it is based on the determination of human bioavailability. In order to reduce the high variability of this type of test as well as the cost for failure in bioequivalence trial, the virtual bioequivalence have arisen as alternative decision-making tool. Physiologically-based pharmacokinetic (PBPK) modeling provides an approach that enables the plasma concentration–time profiles to be predicted from preclinical *in vitro* and *in vivo* data and can be used to predict bioequivalence of controlled release and immediate release oral products. Here, we proposed a new modelling strategy using different machine learning algorithms implemented in KNIME Analytics Platform to predict pharmacokinetic properties and to implement PBPK models.

PK/PD modeling / Seminar session

Individual model averaging for drug effect assessments

M.O. Karlsson[1]*, Estelle Chasseloup[1], Adrien Tessier[2]

[1] Dept. Of Pharmaceutical Biosciences, Uppsala University, Uppsala, Sweden

[2] Dept. Of Clinical Pharmacokinetics and Pharmacometrics, Institut de Recherches Internationales Servier, Suresnes, France

*E-mail: mats.karlsson@fambio.uu.se

Model misspecifications in longitudinal data analysis may affect both the type 1 error and the estimates of drug effects. We used simulated and real data sets to compare these aspects of the standard pharmacometric approach (STD) and a new approach, Individual Model Averaging (IMA). Multiple simulated and three reals (ADAS-Cog composite score, 11-point pain score and daily counts of epileptic seizures), placebo-only, patient data sets were used. To create data sets mimicking trials where the drug would have no effect, repeated randomizations of the subjects to "drug" vs "control" were implemented. Different combinations of models describing the placebo effect and the drug effect were used. STD contrasted nested models without (base) or with (full) the drug effect. IMA assumed two sub-models, the placebo effect with

or without the drug effect. IMA compared nested models (i) equal probability for all patients for the two sub-models (base), and (ii) the probability of each sub-model estimated using the allocation arm as covariate (full). For simulated data sets Type 1 error was better controlled for IMA than STD. IMA showed better performances in type I error control than STD on all three real data sets (nominal 5%): 26.4%, 96.9% and 45.5% (STD) versus 3.5%, 5.0% and 5.0% (IMA). For all three real data sets, STD showed considerable bias in the drug effect estimates in the majority of the scenarios, but no bias was evident for IMA in any scenario. When both STD and IMA estimates were unbiased, IMA in most cases provided more precise estimates. IMA was more robust towards model misspecifications and over-parameterization with better control of the type I error and more accurate effect size estimates. IMA seems promising to evaluate the treatment effect in longitudinal data analysis.

Antimicrobial dose optimization based on microdialysis and PK/PD modeling

F.J. Azeredo
Faculty of Pharmacy, Federal University of Bahia, Salvador-BA, Brazil
E-mail: francinej@gmail.com

The PK/PD indexes used to calculate antimicrobials dosing regimens have important limitations regarding both PK and PD measurements. It is well know that the free drug concentration in the site of action is responsible for the pharmacological effect and that MIC value does not explain fully the antimicrobial effect since it is used as a threshold. Evaluation of free levels of Fluconazole and Amphotericin B in the kidney of healthy, *Candida albicans* infected Wistar rats using microdialysis after intravenous and oral administration of both drugs in different dosages. Plasma and kidney microdialisate were collected up to 24h after the administration of drugs. Levofloxacin microdialysis was performed in tuberculosis cavitary lesions of patients after oral dosing of 750 or 1000mg. Samples were collected up to 8 hours after administration. To evaluate the effect of fluconazole against Candida spp., amb against *C. Albicans* and levofloxacin against *M. Tuberculosis*, an *in vitro* system that exposes the microorganism to the human PK profile was set. Multiple drug concentrations were administered into the system, then the CFU/ml was counted for 7 days. Data was modelled using developed Emax model. Simulations were performed to optimize the dosing of all antimicrobials tested. No statistical difference was found when comparing free serum and cavitary lesions levofloxacin concentrations. Fluconazole showed higher potency against *C. Albicans* than against *C. Parapsilosis* and *C. Tropicalis* and equivalent efficacy against these yeasts, amb showed higher potency than fluconazole against *C. Albicans*.

Regarding levofloxacin dose selection, for the resistant population an increase in the current dose is necessary to eliminate the microorganisms according to the studied IC50 values. Microdialysis is a useful technique to obtain free antimicrobial drugs concentration in the site of action. PK/PD modeling is used to simulate alternative regimens, to compare antimicrobial drugs pharmacological effect and to optimize therapy to treat infections that are a Public Health issue.

Acknowledgments: cnpq – Brazil

Enteric reabsorption of drugs: influence on pharmacokinetics and pharmacodynamics revisited

Manuel Ibarra

Pharmaceutical Sciences Department, Faculty of Chemistry, Bioavailability and Bioequivalence Centre for Medicine Evaluation, Universidad de La Republica, Uruguay

E-mail: mibarra@fq.edu.uy

Enteric reabsorption occurs when a fraction of drug transferred from the systemic circulation to the gastrointestinal tract is subsequently reabsorbed back into the arterial bloodstream. When present as a discontinuous process, it can be observed as secondary or multiple peaks in the plasma-concentration-time profile. The most studied process of this kind is referred to as enterohepatic cycling (EHC), i.e. Through hepatobiliary secretion. However, this is not an exclusive pathway: basic drugs could suffer enterogastric cycling (EGC), i.e. Through gastric secretion. These processes are currently regarded as pure distribution, with no impact neither on drug systemic clearance nor oral bioavailability. It seems settled, however, that drug half-life result increased with higher reabsorption, commonly attributed to a higher volume of distribution. In this presentation, the impact of drug enteric reabsorption on primary pharmacokinetic parameters will be discussed. With this purpose, semi-mechanistic pharmacokinetic models were developed for EHC and EGC to perform simulations and sensitivity analysis using the package mlxr (Lixoft®, France) at the R environment for statistical computing (R-project.org). Under the model established, equations were deducted for systemic clearance, volume of distribution and oral bioavailability. Results and examples will be shown. For EHC, given the interplay between hepatobiliary secretion and hepatic drug metabolism, results show that the reabsorbed fraction correlates negatively with the hepatic clearance and positively with oral bioavailability for drugs with high hepatic extraction. This could be of importance for the assessment of drug-drug interactions. For EGC these correlations are not expected. Valproic Acid and Nevirapine pharmacokinetic data will be used to show both scenarios. Moreover, a theory for the concentration and time dependent hepatobiliary secretion for phenytoin will be discussed as a mechanism for its nonlinear pharmacokinetics. Finally, the impact of drug reabsorption on the effect vs. Time profile will be discussed.

Therapeutic drug monitoring / Seminar session

Alternative dosing guidelines for childhood tuberculosis: applications of model-based approaches

Kendra K. Radtke

University of California at San Francisco, USA

E-mail: .Kendra.Radtke@ucsf.edu

Tuberculosis (TB) kills 234,000 children each year. Malnourished and young children are especially vulnerable to severe forms of TB, poor treatment response, and death. Current WHO guidelines recommend dosing children based on weight alone, with the same mg/kg dose range applied to children of all ages. These guidelines may lead to subtherapeutic exposures and worse outcomes in young and underweight children. We aimed to evaluate the population impact of current guidelines in 20 countries with highest child TB incidence and explore how novel dosing strategies may improve the child TB epidemic. We used a novel, integrated model linking country-specific individual-level demographic data to pharmacokinetic, outcome, and epidemiological models to assess TB treatment outcomes in children under 5 years. Drug exposures and outcomes were predicted under WHO guidelines and a proposed algorithm that utilizes age, weight, and available formulations. We estimated that 57,234 (43%) of 133,302 treated under-5 TB cases would be underdosed with WHO dosing and only 47% of children would reach recommended rifampicin exposure target. Subtherapeutic exposures and unfavorable outcomes were more common in malnourished children. A proposed simple dosing approach, by age and nutritional status, might ensure adequate exposure in 62% of children. This proposed method has the potential to reduce unfavorable treatment outcomes by at least 1/3, saving 2436 children at minimum and up to 7884 children if all cases are diagnosed and treated in these countries annually. This simple change in dosing method to include age and nutritional status could be immediately implemented in clinic and greatly improve child TB treatment outcomes, especially among malnourished children who are at high risk of mortality.

Application of pharmacometrics to therapeutic drug monitoring in Uruguay: paving our way

Cecilia Maldonado

Biopharmacy and Therapeutics, Pharmaceutical Sciences Department, School of Chemistry, Therapeutic Drug Monitoring Service, University Hospital udelar, Montevideo, Uruguay

E-mail: ceciliamaldonadocorbo@gmail.com

Pharmacometrics is a relatively new discipline in Uruguay and so is its application to therapeutic drug monitoring. The presentation focuses on the first steps we have taken

in Uruguay to apply PMX tools as way to build models for own population. The two group of drugs we have worked to date are immunosupressants (IS) and antiepileptics (aeds).

Cyclosporine (csa), an IS, was the first drug we were able to build a preliminary model for Pharmacokinetic parameter estimation was performed using nonlinear mixed effect modelling. A two-compartment model with first order disposition model including lag time was used as a structural model. The covariate analysis identified creatinine clearance (clcrea) as an individual factor influencing the Cl of csa. The model was then externally validated with another set of patients. The model developed reasonably estimates the individual csa clearance for patients. Hence it can be utilized to individualize csa doses for prompt and adequate achievement of target blood concentrations of csa.

Tacrolimus is another IS that has been approached to, however, taking into consideration the nuances with csa metabolism, its model is still under construction and should be improved by the incorporation of other parameters.

In the case of aeds, levetiracetam (LEV) and valproic acid (VPA) were of choice due to safety concern regarding efficacy and adverse drug reactions. For LEV, a preliminary model for terminal patients under palliative care was developed. Though number of patients was low, and the condition fortunately not common LEV Cl and half-life were successfully estimated for the condition and age of the patients.

Regarding VPA our aim was to develop a model for the understanding of the mechanisms behind VPA induced hyperammonemia and the assessment of the benefits related to carnitine supplementation (CS). A mechanistic QSP model describing the VPA-Ammonia pathway was built including CS to reverse this adverse drug reaction.

Methodologies / Seminar session

A brief history of nlmixr & lessons learned

Wenping Wang
Novartis Pharmaceuticals Corporation
E-mail: wenping.wang@novartis.com

Nlmixr is a free and open source R package for fitting nonlinear pharmacokinetic (PK), pharmacodynamic (PD), joint PK/PD and quantitative systems pharmacology (QSP) mixed-effects models. Currently, nlmixr is capable of fitting both traditional compartmental PK models as well as more complex models implemented using ordinary differential equations (odes). It is under intensive development and has succeeded in attracting extensive attention and a willingness to make contributions from the

pharmaceutical modeling community. We believe that, over time, it will become a capable, credible alternative to commercial software tools, such as NONMEM, Monolix, and Phoenix NLME. The fast growth and development of nlmixr is a shining example of the power of open-source software and an inspiration to computational pharmacometrics. In this talk, the development history of nlmixr is briefly reviewed. I then use nlmixr as a case study to promote future open-source tools for pharmacometrics.

Covariate model building

Ana Ruiz-Garcia

Department of Pharmacometrics, Pfizer Inc., 10555 Science Center Dr. CB-10, San Diego, CA, 92121, USA

E-mail: Ana.Ruiz@pfizer.com

Introduction: Population pharmacokinetic (PK), pharmacodynamic (PD) or PKPD analyses aim to summarize the model parameters and its sources of variability among individuals who are the target patient population receiving the drug of interest. Covariates are used to describe predictable sources of variability in model's parameters leading to a decrease in unpredictable variability. A good understanding of the relationships between model parameters, patient characteristics and other intrinsic and extrinsic factors will facilitate dose adjustment decisions. Materials and Methods: Different methodologies could be used to screen and estimate relevant covariates: stepwise covariate modeling (SCM), full fixed effects modeling (FFEM), and full random effects modeling (FREM). Results and Discussion: The most common approach is the incorporation of covariates in a stepwise manner. With SCM p-values are difficult to interpret and difficult to adjust appropriately for multiple comparisons (selection bias), further, correlated covariates lead to difficulties in interpretation and estimation. FFEM has been presented as an alternative to stepwise regression, however, pre-defined covariates have its own limitations. Adding covariate relations to only some of the model parameters can lead to selection bias. Allowing all covariates to affect all parameters mitigates the risk of selection bias. This could be accomplished by using FREM. This methodology proposes the incorporation of covariate relations using random effects. With FREM covariates are treated as observations and all covariate-parameter relations are estimated simultaneously. Conclusions: This presentation will provide an overview of the methodologies. Predictable and robust covariate modeling is key in drug development; thus, a good understanding of the different methodologies will help selecting the appropriate approach for a better covariate characterization.

Statistical tests and model building strategy for mixed effects models

Marc Lavielle
Inria Saclay and CMAP (Ecole Poytechnique), France
E-mail: Marc.Lavielle@inria.fr

Building and validating a mixed effects model are generally difficult and laborious tasks for the modeler. Indeed, it requires to find the "best" covariate model, i.e. To identify which covariates significantly explain the variability of some individual parameters, to identify the "best" correlation model for the random effects, and to find the "best" residual error model for continuous data. I will present an extension of the EM algorithm that allows to build a linear mixed effects model by optimizing a penalized likelihood criterion (AIC, BIC) in an iterative way. I will also present the SAMBA (Stochastic Approximation for Model Building Algorithm) algorithm, an extension of this method for non-linear mixed effects models. Once the model is built, it must be validated, i.e. Each of the hypotheses made on the model must be tested (covariate model, correlation structure of the random effects, distribution of the random effects, distribution of residual errors, etc.). I will show that it is possible to construct unbiased hypothesis tests using test statistics based on observations and random effects sampled from their conditional distributions. These methods for building and validating mixed effects models are implemented in the Rsmlx package (http://rsmlx.webpopix.org). I will illustrate them with applications in population pharmacokinetics.

Internal dosimetry in radiopharmaceutical development / Seminar session

Population approach in non-clinical models for dosimetric evaluation of new radiopharmaceuticals

Ignacio Hernández González
Departamento de Investigaciones no Clínicas, Centro de Isótopos, Mayabeque, San José de las Lajas, Cuba
E-mail: ignacio@ceniai.inf.cu

During the development of new radiopharmaceuticals is necessary to estimate the amount of energy deposited in tissues, as it is directly related with radiation damage to target and non-target tissues. That is the goal of dosimetric evaluations with relevance in the case of radiopharmaceuticals for therapy in order to maximize radiation damage

to target while minimizing it to non-target tissues. All dosimetric evaluation are based on standardized anatomical and kinetic models which make difficult to estimate accurately actual population parameters and its variability. The goal of the present work is to present the use of the population approach to obtain bio-kinetic models during non-clinical evaluation radiopharmaceuticals for therapy. We used a set of data from real pharmacokinetic evaluation of technetium labeled peptide in an animal tumor model following a sparse data design. In sake of simplicity tumor was considered a uniform sphere and accumulated dose (mgy/mbq/h) was estimated for tumor sizes from 0.1 to 4 g using Olinda (version 1, 2003, Vanderbilt University, USA). Tumor retention time, as well as other pharmacokinetic parameters, were estimated by non-linear mixed effect models using Monolix (Suite 2019, Lixoft, France). Then, actual accumulated doses (mgy/mbq/h) were calculated from individual pharmacokinetic parameters and tumor mass. Based on our results we could estimate pharmacokinetic parameters as well as radiation dose in tumor using a non-standardized kinetic model and a modeling option that allow us estimation of corresponding variability, which was 71% for TRT and 65 % for accumulated dose.

Pharmacokinetics and internal radiation dosimetry in the evaluations of new radiopharmaceuticals in humans

Leonel Torres Aroche

Dirección de Investigaciones Clínicas, Centro de Isótopos, Cuba

E-mail: leonel.torres.cuba@gmail.com

The development of new radiopharmaceuticals for diagnosis and therapy demand the use of appropriate formalisms for internal radiation dose estimations. Dosimetry estimations based on good clinical practices are a mandatory requirement to introduce new radioactive compounds in the routine nuclear medicine services. The main objective of this work is to show the available methodologies and formalisms for absorbed dose estimations at organ and voxel levels and to show the available tools for dose calculations in clinical conditions. Principles and mathematical formalism for *in vivo* activity quantification and patient specific dose calculations are presented. Dosimetry formalisms such as the MIRD methodologies, Monte Carlo techniques and "local deposition" approaches are shown enhancing their main features, different steps and their general requirements for practical use; their strengths and limitations are also discussed. The available methods for *in vivo* activity quantification including the description of standardized correction methods to compensate the physical factors

affecting the quantification accuracy are shown. It involves the radiation scatter and attenuation, partial volume effect, background, organ overlapping, count lost dead time, etc. On the other hand, the principal available tools to perform internal radiation dosimetry calculation, developed by vendors independent companies and research groups (dosisoft, mirdcalc, MRT-3dslices, etc., are also evaluated. The main features of these tools, including the implemented methodologies and details of practical use, are presented as well as the scope of their clinical applications. Other requirements, such as inputs/outputs parameters are described and analysis of their strengths and weaknesses are also included. Basic elements of the quality assurance program to warranty the accuracy of dose estimations are finally presented including an integral and detailed evaluation of all its components.

Role and impact of dosimetry in radiopharmaceutical development

Manuel Bardiès
Centre de Recherches en Cancérologie de Toulouse, France
E-mail: manuel.bardies@inserm.fr

Absorbed dose determination in nuclear medicine can be achieved by answering 3 questions:

How many radioactive sources are present in the tissues in space and time?

How much energy is emitted per decay?

How does the emitted energy propagate and is eventually absorbed in the tissues?

These generic steps can be applied to cell, small animal or clinical dosimetry.

The first question is usually related to pharmacometry: how the drug distributes in space and time. Depending on the type of experiment (cell, small animal, humans) the objective is to assess activity distribution, and integrate time-activity-curves to derive the number of radioactive decays that contribute to the irradiation.

The second step is usually the easiest to deal with, as the type of radioactive decay and the number, are usually well known for a given radionuclide.

The third step, which of absorbed dose calculation, may require different methodological approaches depending on the context (scale, but also the level of refinement associated to the determination of the absorbed dose: average absorbed dose, or absorbed dose gradients in a given volume, etc.).

Dosimetry in the context of radiopharmaceutical development can be performed in two different situations:

When the question to address is that of providing an estimate of the irradiation delivered to humans based on preclinical (small animal) experiments, the idea is not to perform small animal dosimetry per se, but rather to obtain pharmacokinetics in animals, to extrapolate from animal to human, and then, based on these estimates, use a human dosimetric model to derive an estimate of the absorbed doses that "could be" delivered to the human.

The only situation where dosimetry is performed in animals is that of experimental molecular radiotherapy, when the objective is to relate the effect (efficacy or toxicity) with an objective index (the absorbed dose or derivate). In that situation, the first steps (assessment of pharmacokinetics and determination of the energy emitted per decay) are the same as in the previous case, but the calculation of the absorbed dose must be performing on the animal itself. There are dosimetric models of small animal that can be used to get a rough estimate of the irradiation delivered. However, specific dosimetry, based on the animal geometry may be needed is some situations, namely when the dimensions of organs and tissues of interest are close to that of radiation range. Dosimetry is an integral part of radiopharmaceutical development. Methodologies have been proposed to allow addressing most of the situations encountered in preclinical experiments. Standardization is needed and guidelines should be written to improve the dissemination of the dosimetric methodology in the world of radiopharmaceutical development.

Posters presentations

Estimation of the cyp2c19 phenotype through the genotype cyp2c19 and cyp3a4

A. Favela-Mendoza[1]*, G. Martínez-Cortés[1], I. Fricke-Galindo[2], E. Romero-Tejeda[2], H. Rangel-Villalobos[1]

[1] cuciénega, Universidad De Guadalajara, Ocotlán, México

[2] CUCEI, Universidad De Guadalajara, Guadalajara, México

*E-mail: alma.fabela@academicos.udg.mx

The CYP2C19 genotypes presumably allow predicting the metabolizer phenotypes: poor (pms), extensive (ems) and ultra-rapid (ums). This is important because of the expected benefits by health care institutions and patients are supported on this premise. However, evidence from previous studies regarding this predictive power combining CYP2C19 and CYP3A4 genotypes Chas been ruled out in Mexican children. Because of the reported metabolism differences between children and adults, we evaluated the association of CYP2C19 and CYP3A4 genotypes and metabolizer phenotypes

established by omeprazole administration in 74 adults from Jalisco (West, Mexico). The genotypes for CYP3A4*1B and CYP2C19*2, *3, *4, *5 and *17 alleles were determined. The CYP2C19 and CYP3A4 phenotypes were obtained after 20 mg omeprazole administration and HPLC quantification in plasma to estimate the Hydroxylation index (HI= OME/HOME) and Sulfonation index (SI= OME/SOME), respectively. Differences in the HI and SI distribution were observed between CYP2C19 and CYP3A4 genotypes ($p<0.05$), respectively. The CYP2C19 and CYP3A4 genotypes and IH and IS distribution (phenotypes) were different to previous studies in Mexico and Latin America ($p<0.05$), respectively. High correspondence was observed between CYP3A4 phenotype and genotype (91.94 %), but for CYP2C19 was less (70.27%) and showed weak concordance ($k=0.0355$). The CYP2C19 phenotype showed high sensitivity (98.077%) with 70.27% of accuracy to predict the phenotype from the genotype. These results are contrary to the previously null diagnostic ability reported in Mexican healthy children (Favela-Mendoza et al., 2018). We demonstrated a poor -but significant- genotype-phenotype association in Mexican adults between CYP2C19 and CYP3A4 genotypes for CYP2C19 phenotyping, which is a valuable alternative to dose individualization for CYP2C19 substrate drugs.

Quantification of polyglutamates of methotrexate in patients with rheumatoid arthritis to evaluate two dosing regimens

A. Rodríguez Báez[1]*, A. Huerta García[1], S. Medellín Garibay[1], C. Abud Mendoza[2], M. Martinez Martinez[2], C. Rodríguez-Pinal[1], S. Romano Moreno[1], R. Milán Segovia[1]

[1] Facultad de Ciencias Químicas, Universidad Autónoma de San Luis Potosí, Mexico

[2] Unidad Regional de Reumatología y Osteoporosis del Hospital Central "Dr. Ignacio Morones Prieto", Mexico

E-mail: coco_baezrdz@hotmail.com

Methotrexate (MTX) is the first-line drug to treat rheumatoid arthritis (RA) due to its sustained effect. Intracellularly, the drug is converted to polyglutamates of MTX (MTX-pgn). MTX-PG3 has been associated with the efficacy of treatment, while MTX-PG5 is associated with adverse events. The suggested initial dose of MTX is 12.5 mg/week; however, although it is common to divide the total dose in daily doses, there is no information of the effectiveness of this dosing schedule. Ninety-two MTX-naïve patients with RA were enrolled in this cross-sectional, observational and analytical study approved by local ethics committee (register 70-18). Each patient was randomly assigned into two groups: 1) Daily dose (n=45) and 2) Weekly dose (n=47) of MTX.

Patients were evaluated by a rheumatologist at baseline and after 6, 12, 24 weeks; one blood sample was taken 24 h post-dose of MTX. Red blood cells MTX-PG concentrations were analyzed by UPLC-MS/MS. Most of patients included were female (97%); the mean age was 45 years and total body weight was 68.51 kg. No significant differences in baseline clinical and anthropometric characteristics were observed between groups ($p>0.05$). Twenty-eight patients receiving daily dose and eighteen patients with weekly dose of MTX were able to complete this study; there were no significant differences in MTX-PG3 concentrations between groups ($p>0.05$). There was a significant difference between the time in treatment and the intragroup MTX-PG3 levels ($p<0.05$); in the steady state the geometric mean concentration of MTX-PG3 was 159.9 (95%CI of 109, 233) nm. Patients with BMI less than 25 kg/m^2 had higher levels of MTX-PG3. The MTX-PG5 levels was not detected throughout this study. This study shows that there are not differences in red blood cells levels of MTX-PG3 between the weekly and daily dosing schedule; the last one may adequate to ensure adherence to treatment in patients with RA.

Pharmacometric approach to support dosing strategy of nimotuzumab in patients with autosomal dominant polycystic kidney disease

N. De Castro-Suárez[1]*, M.N. Trame[2], M. Ramos Suzarte[3], J.M. Davalos[4], R. Bacallao[4], L. Rodríguez-Vera[1]

[1] Pharmacy Department, Institute of Food and Pharmacy, University of Havana, Cuba

[2] Novartis Institutes for biomedical Research, Inc., Cambridge, USA

[3] Center of Molecular Immunology, Havana, Cuba

[4] National Institute of Nephrology, Havana, Cuba

*E-mail: niurys@ifal.uh.cu

Autosomal dominant polycystic kidney disease (ADPKD) is a genetic disease characterized by an overexpression and mislocalization of epidermal growth factor receptor (EGFR) to the apical membranes of cystic epithelial cells. Nimotuzumab is a humanized monoclonal antibody targeted to the extracellular domain of human EGFR. To develop a population pharmacokinetic (poppk) model for nimotuzumab as well as to identify demographic, biochemical and clinical predictive factors of the pharmacokinetic variability. A Phase I, single center, and non-controlled open clinical study was carried out in patients with ADPKD. Five patients were enrolled at each of the following fixed dose levels: 50, 100, 200 and 400 mg. Blood samples were drawn during 28 days for pharmacokinetic assessments. Poppk analysis of 409 concentration-time data from 20 patients was performed using the nonlinear mixed-effect model approach with

NONMEM 7.3. The first-order conditional estimation method with interaction was used throughout the modeling process. The unexplained residual variability was best described with an additive residual error model. Impact of patient demographics and clinical indices on pharmacokinetic parameters were explored using automated stepwise covariate model-building technique in psn. Quasi Steady State approximation of the full TMDD model with constant target concentration best described the concentration-time profiles. The final model estimates (res%) were 0.0102 L/h (5%) for linear clearance, 2.32 L (8%) for central volume (Vc), 0.0126 L/h (21%) for inter-compartimental clearance (Q), 4.27 L (21%) for peripheral volume (Vp), 7.27 mg/L (15%) for steady-state constant, 0.299 h-1 (4%) for internalization rate, and 0.432 mg/L (6%) for total target concentration. Interindividual variability was associated with Vc, Q, Vp. In addition, serum creatinine was identified as significant covariate for Vp. This is the first poppk study of nimotuzumab in non-oncological disease. The model was able to describe the effect of the mab–target binding, and target and mab–target complex turnovers on nimotuzumab pharmacokinetics.

Population pharmacokinetics of levetiracetam in Mexican adult patients with epilepsy

M.P. Hernández-Mitre[1]*, S.E. Medellín-Garibay[1], Rodríguez-Leyva[1], H. Castillo-Ibarra[2], C.J. Rodríguez-Pinal[2], S. Zarazúa-Guzmán[2], H.H. Jung-Cook[3], S. Romano-Moreno[3], R.C. Milán-Segovia[3]

[1] Facultad de Ciencias Químicas de la Universidad Autónoma de San Luis Potosí, S.L.P, México.

[2] Hospital Central "Dr. Ignacio Morones Prieto", San Luis Potosí, S.L.P., México.

[3] Facultad de Ciencias Químicas de la Universidad Nacional Autónoma de México, CDMX, México.

*E-mail: patomitre@live.com

Levetiracetam (LEV) is an antiepileptic drug (AED) used to treat all types of seizures in patients from all ages. Objective: The aim of this study was to develop and validate a population pharmacokinetics (poppk) model of LEV in Mexican adults with epilepsy to design individualized dosage regimens. The study was approved by the Hospital's Research Ethics Committee (No. 86-16). A total of 109 adult patients under treatment with oral LEV in monotherapy or polytherapy with other aeds were enrolled, 375 plasma samples between 15 minutes and 12 hours post-dose were obtained, and covariate information as sex, age, bodyweight, height, body surface area (BSA), serum creatinine, creatinine clearance (crcl), concomitant diseases, polypharmacy and the administered innovative or generic product of LEV were collected. Samples

were analyzed by a validated HPLC-UV method. Poppk modelling was executed with NONMEM v.7.4.1. Software. Pharmacokinetics of LEV was best described by a one-compartment open model with first order absorption and linear elimination. The final model equations were: Ka(h-1)=3.64, V/F(L)=29.9*(BSA/1.7)2.44 and CL/F(L/h)=2.79*(crcl/99.4)0.59. Interindividual variability (IIV) of V/F and CL/F decreased from 44.7% and 51.6% in the base model to 33.2% and 43%, respectively in the final model. Results are in accordance with other published poppk models of LEV. Significant influence of the LEV products over bioavailability (F) was noticed but didn't remain in the final model. Internal validation was performed by bootstrap and Visual Predictive Check. A priori estimation allowed proposing dosing recommendations to reach target trough concentrations (12–46 μg/ml) and maximum a posteriori estimation showed the developed poppk model is useful to optimize dosage regimens using Bayesian approach. In this model, LEV CL/F was related to crcl and V/F to BSA. The developed model will allow optimizing dosage regimens to achieve better control of epilepsy, avoiding risks of under or over dosage.

Circadian variation of the urinary 6β-hydroxycortisol to cortisol ratio in HIV-infected women during third trimester of pregnancy and postpartum

J.R.L. Benzi[1]*, F.L. Moreira[1], M.P. Marques[1], G. Duarte[2], G. Suarez-Kurtz[2], V.L. Lanchote[3]

[1] Faculdade de Ciências Farmacêuticas de Ribeirão Preto da Universidade de São Paulo, Ribeirão Preto, São Paulo, Brazil

[2] Faculdade de Medicina de Ribeirão Preto da Universidade de São Paulo, Ribeirão Preto, São Paulo, Brazil

[3] Coordenação de Pesquisa, Instituto Nacional de Câncer, Rio de Janeiro, Brazil

*E-mail: jbenzi@usp.br

Chronopharmacological studies have demonstrated the impact of the time of day on pharmacokinetics and pharmacodynamics. Even though the evidence that pregnancy alters the CYP3A activity, little is known about the impact of HIV, antiretroviral treatment and biological rhythms. The aim of this study was to evaluate the circadian variation of the 6β-hydroxycortisol to cortisol ratio (6β:C), a known endogenous biomarker for CYP3A phenotyping, in HIV-infected women during third trimester of pregnancy (3T) and postpartum (PP). After ethics committee approval, HIV-infected pregnant women taking oral raltegravir in combination with tenofovir/lamivudine during 3T (n = 9) and 4-5 weeks PP (n = 7) were enrolled in this study. The 6β:C ratios evaluated each 2 h for 24 h were compared intra (among the urine collection times; Kruskal-Wallis, $p < 0.05$) and inter period (3T and PP; Wilcoxon test,

p < 0.05). There was no significant difference in 6β:C ratios between 3T and PP periods or among urine collection times. In the 3T period, the 6β:C ratios ranged from 2.57 to 51.69 with median of 12.73. Similar values were obtained in the PP period, ranging from 3.48 to 44.54, with median of 10.66. The data show that CYP3A activity was not upregulated in the 3T period when compared to PP in HIV-infected pregnant women taking raltegravir and tenofovir/lamivudine. However, the observed high variability in the 6β:C ratios and the small sample size remain as a study limitation. Additionally, the lack of difference between 6β:C ratios during the urine collection times in both periods demonstrate that this biomarker can be sampled in any time, with no circadian variation. Urine collection for CYP3A phenotyping using 6β:C ratios can be sampled at any time due no circadian variation in HIV-infected women during third trimester of pregnancy and postpartum.

Population PK of nimotuzumab in patients with colorectal metastatic cancer

José Miguel Calderín-Miranda[1]*, Niurys de Castro Suárez[1], Gledys Reynaldo Fernández[1], Anabel Lavastida[2], Betsy Fernández[3], Mayté Lima Pérez[4], Jorge Luis Soriano García[4], Ivis Mendoza Hernández[5], Evelyn Galano Frutos[5], Carmen E. Viada González[2], Patricia Hernández Casaña[2], Leyanis Rodríguez Vera[1]

[1] Pharmacy Department, Institute of Food and Pharmacy, University of Havana, Cuba

[2] Center of Molecular Immunology, Havana, Cuba

[3] Center for Genetic Engineering and Biotechnology, Havana, Cuba

[4] "Hermanos Ameijeras" Hospital, Havana, Cuba

[5] National Coordinating Center for Clinical Trials, Havana, Cuba

*E-mail: jm.calderin5@gmail.com

Nimotuzumab is a humanized monoclonal antibody targeted to the extracellular domain of human epidermal growth factor receptor.

To develop a population pharmacokinetic (poppk) model for nimotuzumab as well as to identify demographic, biochemical and clinical predictive factors of the pharmacokinetic (PK) variability.

A Phase I, single center, and non-controlled open clinical study was carried out in patients with colorectal metastatic cancer. Five patients were enrolled at each of the following fixed dose levels: 200, 400, 800 and 1200 mg. Blood samples were drawn during 14 days for PK assessments. Poppk analysis of 179 concentration-time data from 19 patients was performed using the nonlinear mixed-effect model approach with NONMEM 7.3. The first-order conditional estimation method with interaction was used throughout the modeling process. Interindividual variability (IIV) was modeled assuming a lognormal distribution and was associated with clearance (CL), central

volume of distribution (Vc), volume of tissue distribution (Vt) and steady-state rate constant (Kss). The unexplained residual variability was best described with an additive residual error model.

Quasi Steady State approximation of the full Target Mediated Drug Disposition model best described the concentration-time profiles. The model was able to describe the effect of the mab–target binding, and target and mab–target complex turnovers on nimotuzumab PK. The final model parameters (IIV) were CL 0.0304 L/h (49.5%), Vc 6.36 L (44.9%), Q 0.057 L/h, Vt 2.52 L (138.9%), Kss 0.0717 mg/L (1.2%), Kint 0.0089 h^{-1}, Ksyn 17.3 (mg/L)/h, Kdeg 703 h^{-1}. Exploratory covariate analysis indicated dose and weight as potential covariates on Vt and Kss. Therefore, as a final step, correlation between several covariates and model parameters will be examined using the automated stepwise covariate model-building technique in psn.

The developed poppk model can be used to guide the dose selection for nimotuzumab during routine clinical practice in patients with colorectal metastatic cancer.

Development and validation of a bioanalytical method for simultaneous quantification of four antimalaric drugs using dried blood spot by LC-MS/MS for surveillance of antimalarial drug efficacy

C. Silva[1], A. Silva[1]*, D. Pinto[1], E. Coelho[1], H. Pereira[2], G. Silveira[2], L. Vilhena[2], A. Daher[2], L. Fonseca[2]

[1] Equivalence and Pharmacokinetics Service, Vice Presidency of Research and Innovation in Health - Oswaldo Cruz Foundation, Rio de Janeiro, Brazil

[2] Institute of Drug Technology (Farmanguinhos), Oswaldo Cruz Foundation (Fiocruz), Rio de Janeiro, RJ, Brazil

*E-mail: aline.azevedo@fiocruz.br

Malaria is still a neglected disease and a major public health concern worldwide. Objectives: The aim of this work was to develop and validate a bioanalytical method for the simultaneous determination of four antimalarial drugs (chloroquine, mefloquine, primaquine and lumefantrine) in dried blood spot (DBS) using carbamazepine as an internal standard (IS) by LC-MS/MS to evaluate safety and efficacy of the schizonticidal drugs with concomitant use of primaquine in a clinical trial in Brazil. The method was based on the liquid-liquid extraction (LLE) using tert-butyl methyl ether (TBME). The chromatography separation was achieved on ACE® C8 column (100mm×4.6mm×3.0μm) using a mixture (25:75, v/v) of 40mm ammonium acetate buffer ph 3.5 and methanol/ acetonitrile (80:20, v/v), using a flow gradient. The chromatographic run time was 5.5min. The ion transitions monitored were m/z 320.0<247.0 for chloroquine, m/z 379.0<321.0 for mefloquine, m/z 260.0<86.0 for

primaquine, m/z 530.2<512.1 for lumefantrine and m/z 237.0<194.1 for IS. In this study, the blood samples patients were collected on days 3, 7, 14, 21, 28, 42 and 63. The parameters pharmacokinetics Area Under the Curve (AUC) and the terminal elimination half-life (t1/2β) were determined. The assay exhibited a linear dynamic range of 5-500ng/ml for chloroquine, 10-2500ng/ml for mefloquine, 1-50ng/ml for primaquine, and 1-500ng/ml for lumefantrine in DBS. The values for inter- and intra-day precision and accuracy were within the generally accepted criteria for analytical methods (<15%). Selectivity, linearity (correlation coefficients were >0.99 for all four analytes), lower limit of quantification (LLOQ), precision, accuracy, stability, matrix effect and carry-over effect were evaluated for all four analytes. The overall AUC (μg/ml.h) for mefloquine, chloroquine and lumefantrine were 338.6, 103.8 and 6.7, respectively. The t1/2β (days) for mefloquine was 17.8 and chloroquine was 18.7. The developed and validated method was successfully applied for surveillance of antimalarial drug efficacy in accordance with WHO guidelines.

Simultaneous quantification of sofosbuvir and its major metabolite gs-331007 in three different biological matrices by lc-ms/ms and its application to a pharmacokinetic study

L. Vilhena[1], D. Pinto[1], A. Silva[1], G. Silveira[1], E. Coelho[1], L. Silva[1], H. Pereira[1], *T.* Souza[2], L. Fonseca[1]*

[1]Equivalence and Pharmacokinetics Service, Vice Presidency of Research and Innovation in Health - Oswaldo Cruz Foundation, Rio de Janeiro, Brazil.

[2]Center for Technological Development in Health (CDTS), Oswaldo Cruz Foundation (Fiocruz). Brazil.

*E-mail: lais.fonseca@fiocruz.br

Sofosbuvir, an approved drug against Hepatitis C virus, has demonstrated activity against Zika virus (ZIKV). This pathogen causes severe neurological disorders such as microcephaly and Guillain-Barré Syndrome. Moreover, it may be transmitted through sexual contact. Objectives: The aim of this survey was to develop and validate bioanalytical methods to quantify sofosbuvir and its metabolite GS-331007 in plasma, cerebrospinal fluid (CSF) and semen by LC-MS/MS. The methods were applied in a pharmacokinetic study in healthy research participants. They took a 400 mg tablet (Sovaldi®) and samples of CSF, semen and blood were collected at 0.00h, 1.50 h (Cmax) and 5.00h and analyzed. The validation showed that the methods had selectivity, linearity, precision and accuracy. The LOQ for sofosbuvir in the three matrices was 0.50 ng/ml, for the metabolite it was 2.0, 5.0 and 10.0 ng/ml for plasma, CSF and semen respectively. The results of the research participants are in the tables below. Table 1. Concentrations in plasma and CSF Time (h) [Sofosbuvir] ng/ml [GS-331007] ng/ml

Plasma CSF Plasma CSF 1.50 88.45±78.12 Undetected 575.68±348.88 2.04±3.78 5.00 3.27±4.38 Undetected 809.95±233.66, 36.80±26.83, Table 2. Concentrations in plasma and semen Time(h) [SFB] ng/ml [GS-331007] ng/ml Plasma Semen Plasma Semen 1.50 48.29±32.0, 983.46±111.00, 435.95±204.09 78.71±115.76, 5.00, 4.92±8.26, 10.57±4.51, 830.38±536.46, 1285.63±1218.42 Sofosbuvir was undetected in CSF, while low concentrations of GS-331007 were found in this matrix. However, an infected person may have a higher permeability to sofosbuvir due to an inflammatory process that occurs in the case of meningitis. In semen, the penetration rate of sofosbuvir were (127.5±92.6) % and (145.6±97.4) % at 1.50h and 5.00h, respectively and the penetration of GS-331007 were (18.5±21.4) % and (158.5±201.5) %. As sofosbuvir was found in semen, the data suggested that the drug may have a clinical relevance such as preventing sexual transmission of ZIKV. This work demonstrates that the methods were adequate to the objective and provide new opportunities in the clinical area.

Assessment of the impact of S2 results (on pharmacopeial dissolution tests) on multisource pharmaceutical products on the list of medications of the social insurance of Costa Rica priority drugs and which must demonstrate therapeutic equivalence in vitro

E. Castiglioni[1], N. Ramírez[2]*, O. Moya[3], M. Alvarado[3]

[1] Laboratorio de Normas y Calidad de Medicamentos (LNCM), Caja Costarricense de Seguro Social (CCSS), Costa Rica

[2] Laboratorio de Biofarmacia y Farmacocinética (LABIOFAR®), Instituto de Investigaciones Farmacéuticas (Inifar), Facultad de Farmacia, Universidad de Costa Rica.

[3] Escuela de Ingeniería en Producción Industrial, Instituto Tecnológico de Costa Rica

*E-mail: nilsramirez@yahoo.com

An evaluation of the variability of the results of the pharmacopoeia dissolution test for Irbesartan, developed by Laboratory C and distributed by the Social Security of Costa Rica, was carried out. To evaluate its possible impact on the similarity of the comparative dissolution profiles of Irbesartan, a USP II dissolution assay was developed at 75 rpm, using a dissolution medium at ph 6.8 and 900 ml of the dissolution volume. In addition, a criterion was established to select the best available drug, together with a protocol for the implementation of the comparative dissolution profile, its respective validation of the system and method, as well as the statistical correlations established between the results of the pharmacopoeia (Q: 87.7, 83.5 and 90.9 %) tests and the

values obtained from f 1 (3.63, 7.48 and 4.53) and f 2 (74.2, 64.6 and 72.7) respectively. It was concluded that the higher the Q value obtained when evaluating a production batch for the dissolution test, the lower its difference factor (f 1) and the higher its similarity factor (f 2) in a comparative dissolution profile. However, with the data obtained for the production batches it cannot be demonstrated that this product is or is not an *in vitro* therapeutic equivalent compared to the reference product.

Development and application of a workflow to process high-throughput combinatorial data using the general pharmacodynamic interaction model

R. Michelet[1]*, A.R. Brochado[2], A. Typas[3], S.G. Wicha[4], C. Kloft[1]

[1] Freie Universitaet Berlin, Institute of Pharmacy, Dept. Of Clinical Pharmacy & Biochemistry, Berlin, Germany

[2] European Molecular Biology Laboratory, Genome Biology Unit, Heidelberg, Germany

[3] Wuerzburg University, Chair of Microbiology, Wuerzburg, Germany. European Molecular Biology Laboratory, Structural & Computational Biology Unit, Heidelberg, Germany

[4] University of Hamburg, Institute of Pharmacy, Dept. Of Clinical Pharmacy, Hamburg, Germany

E-mail: robin.michelet@fu-berlin.de

Antimicrobial resistance is one of the key challenges in the current healthcare system. As new antibiotics are lacking, combinations of existing drugs can help to treat multi-drug-resistant (MDR) infections. These combinations can be investigated using high-throughput methods. Here, a dataset of ~3000 compounds in Gram-negative species was analysed using a robust workflow based on the General pharmacodynamic Interaction (GPDI) model. Using this approach, the magnitude and directionality of an interaction can be quantitatively elucidated. A model selection & evaluation workflow was developed using R (v.3.4.4) and rstudio (v.1.1.447). First, linear, power and EMAX-type models were fitted to single compound concentration-effect data, after which their parameters were fixed and all combinations of interactions and model structures were estimated by ELS regression and precision was assessed using the Fisher Information Matrix. Model selection was based on precision and the Akaike Information Criterion. The parameters of the best GPDI model were then used to assess the magnitude and direction of each interaction. A validation dataset consisting of extended-dose data was first analysed using the developed workflow. The selected models described the experimental data well and identified similar interactions as conventional response-surface analyses suggested. As opposed to convention, using the estimated interaction parameters, the nature and directionality of the interactions could be identified. The workflow was then applied to the entire dataset of ~3000 combinations leading to quantification of synergistic combinations such as vanillin and

spectinomycin, and colistin and macrolide antibiotics. A GPDI-based robust workflow was set up and applied to high-throughput data. Promising combination candidates could be identified, and their interaction quantified. These combinations can now be further investigated and pushed towards pre-clinical and clinical testing. Furthermore, clustering approaches will be applied to the model repository to group interactions according to their intensity and directionality to inform mechanistic hypotheses.

Therapeutic drug monitoring of isoniazid and rifampicin and genotyping analysis in patients with tuberculosis

L. Espiricueta-Zavala[1]*, A. Huerta-García[1], R. Urbina Rodriguez[1], A. Rodríguez-Báez[1], S. Medellín-Garibay[1], C. Rodríguez-Pinal[1], A. Ortiz-Álvarez[2], S. Romano Moreno[1], R. Milán-Segovia[1]

[1] Facultad de Ciencias Químicas, Universidad Autónoma de San Luís Potosí, Mexico

[2] Hospital Central "Dr. Ignacio Morones Prieto", SLP, Mexico

*E-mail: luxzavala@icloud.com

Directly observed treatment, short-course (DOTS) for tuberculosis (TB) includes isoniazid (INH), rifampicin (RMP), pyrazinamide and ethambutol. One strategy to improve the response to treatment is the individualization of doses with Bayesian estimation of individual pharmacokinetic parameters using the monitoring of INH and RMP plasma concentrations (Cp). A prospective, analytical, observational and cross-sectional study was approved by ethics committee (register 66.18). Venous blood samples were taken at 2- and 4-hours post-dose. Genotyping analysis was carried out for NAT2 gen (codes for the enzyme NAT2 involved in the metabolism of INH) and MDR1gene (codes for the P-Gp efflux protein, which participates in the absorption process of RMP). Anthropometric and clinical data were collected from medical records. The RMP and INH Cp quantification was made using an UPLC-MS/MS validated method. NONMEM® software was used to estimate the individual pharmacokinetics parameters on each patient; a posteriori dose adjustment was proposed to reach therapeutic Cp of INH (38 mg/L) and RMP (8-24 mg/L). A total of 77 TB patients from 18 to 80 years old and 29 to 117 kg of total body weight were included; 57% presented CT genotype for the MDR1gene and 60% were slow acetylators for the NAT2 enzyme. Subtherapeutic Cp for both drugs were found in 16 patients, while 3 patients only for INH. For example, a male patient with meningeal TB (37 years old and 75 kg of total body weight; slow acetylator and CC genotype of MDR1gene) was receiving a standard dose of 600 mg (RMP) and 300 mg (INH). He remained with symptoms and drug monitoring was performed; Cp was subtherapeutic for both drugs. After Bayesian estimation of the pharmacokinetic parameters, it was required

an increase to 750 mg of RMP and 375 mg of INH. Dose adjustment resulted in clinical improvement and therapeutic concentrations of both drugs.

Analysis of substrates and metabolites of NAT's enzymes by HPLC from cell culture for pharmacometrics and toxicology studies

M.J. Alonso-Cerda[1]*, O. Hernández-González[2], C.J. Rodríguez-Pinal[2], D.P. Portales-Pérez[2], R.C. Milán-Segovia[2]

[1] Estudiante de Maestría en Ciencias Farmacobiológicas, Facultad de Ciencias Químicas, UASLP, Mexico

[2] Facultad de Ciencias Químicas de la Universidad Autónoma de San Luis Potosí, S.L.P., Mexico

*E-mail: acmarijo@gmail.com

Acute Lymphoblastic Leukemia (ALL) is an oncology disease very frequent in children. The decrease of the efficiency of the detoxification process by enzymes N-acetyltransferases (NAT's) can be associated with the probability of presenting neoplasms. The objective was implement and validate two methods by High Performance Liquid Chromatography (HPLC) for quantify substrates and metabolites of NAT's enzymes, from peripheral blood mononuclear cell (PMBC) culture as base for study its enzymatic activity in drugs metabolism and ALL research. The PMBC were obtained from blood samples and were cultured RPMI® medium with the corresponding substrate and metabolite. We used one equipment HPLC Waters System, mixtures of INH (substrate) y Ac-INH (metabolite) (NAT2); and PABA (substrate) y Ac-PABA (metabolite) (NAT1). The column and pre-column used were X-Terra RP18. The mobile phase was formed by acetic acid and acetonitrile for NAT1 activity; sodium 1-heptanesulfonate combined with phosphates buffer and acetonitrile for NAT2 activity. Detection was at 270 and 266 nm in UV, respectively. The retention times for substrate and metabolite of NAT1 activity were 4.5 and 5.5 minutes for PABA and Ac-PABA; for NAT2 were of 6.6 and 8 minutes for Ac-INH and INH, respectively. Each method was validated according NOM-177-SSA1-2013. The linear interval of each method was established: 0.56–18 μg/ml (NAT1, r=0.999) and 1.35–18 μg/ml (NAT2, r=0.998). Both methods were precise and accurate in terms of intra- and inter-day (CV<15%). The analytes were stable up to 30 days at -80°C. The limit of quantification was 0.56 μg/ml for NAT1 and 1.35 μg/ml for NAT2. The limit of detection was 0.082 μg/ml for NAT1 and 0.366 μg/ml for NAT2. These methods will be applied for evaluate the activity of NAT's enzymes in PMBC and their mechanism of participation in pharmacometrics and toxicology studies such as ALL, other hematological neoplasm, and the pharmacokinetics of drugs substrates of the NAT's.

Model-based characterization of neutrophil dynamics in children receiving busulfan or treosulfan for haematopoietic stem cell transplant conditioning P

B. Perez-Solans[1,2]*, R. Chiesa[3], Z.P. Parra-Guillen[1,2], P. Veys[3,4], I.F. Trocóniz[1,2], J.F. Standing[4,5,6]

[1] Pharmacometrics and Systems Pharmacology, Department of Pharmaceutical Technology and Chemistry, School of Pharmacy and Nutrition, University of Navarra, Pamplona, Spain

[2] idisna; Navarra Institute for Health Research, Pamplona, Spain

[3] Bone Marrow Transplantation Department, Great Ormond Street Hospital for Children, London, UK

[4] Infection, Immunity, Inflammation Programme, UCL Great Ormond Street Institute of Child Health, London, UK

[5] Department of Pharmacy, Great Ormond Street Hospital for Children, London, UK

[6] Paediatric Infectious Diseases Group, St George's, University of London, UK

*E-mail: bperez.8@alumni.unav.es

Busulfan and treosulfan are used in the conditioning prior to paediatric haematopoietic stem cell transplantation (HSCT). To establish: (i) a PKPD model for the treatment effects on neutrophil counts, (ii) optimised dosing schedules, and (iii) optimised PK sampling for Bu TDM. Records from 72 children receiving Bu (7 m-18 y, 5.1–47.0 kg) and 54 Treo (4 m–17 y, 3.8–35.8 kg), were collected. 8,935 neutrophil counts were recorded for 3 months. The Friberg model was extended to account for HSCT effects. The model was used to evaluate dosing schedules through simulations. The optimal Bu PK sampling collection times were determined using the R package poped. A 2-compartment model best described Bu and Treo profiles. A maturation function was included affecting clearance - PM50 was 45.7 and 42.2 weeks for Bu and Treo, and Hill was 2.3 for both drugs. The final model included separate steady-state neutrophil count (CIRC0) before and after transplant ($p<0.01$). The HSCT enhanced cell proliferation and maturation increasing by 2-fold the parameters ($p<0.01$). HSCT increased proliferation and γ in a 5%. System parameters were consistent across drugs (CIRC0, MTT and γ), estimated as 0.79·109 cells/L, 8.02 days and 0.10. The neutrophil decline was modelled with a linear model for Bu (KKILL=0.7) and an EMAX model for Treo (EMAX=1.2). The presence of alemtuzumab enhanced the HSCT effect, with a 2.9-fold increase in proliferation. A 2-day delay in Treo administration would leave the patient less time immunocompromised without damaging the HSCT. The optimal design exercise suggested a reduced sampling schedule (5 vs 6 samples), obtaining similar parameter precision (maximum bias <10%) The semi-mechanistic PKPD model developed predicts neutrophil reconstitution trajectories from children after HSCT, being a useful tool to improve their clinical management. New dosing and sampling schedules are proposed.

A quantitative systems pharmacology model characterizing the main immune components involved in Crohn's disease to test new therapeutic scenarios

V. Balbas-Martinez[1]*, E. Asin-Prieto[2], Z. Parra-Guillen[2], I.F. Troconiz[1]

[1] Pharmacometrics & Systems Pharmacology, Department of Pharmacy and Pharmaceutical Technology, School of Pharmacy and Nutrition, University of Navarra, Pamplona, Spain

[2] idisna, Navarra Institute for Health Research, Pamplona, Spain

*E-mail: vbalbas@alumni.unav.es

Crohn's disease (CD) is a complex inflammatory bowel disease, which causes a functional impairment of the gut wall. The reported lack of effectiveness in the standard of care require the application of techniques aiming to find new targets and therapeutic strategies. We aimed to develop a quantitative SP (QSP) model in humans characterizing the dynamics of the main immune system components involved in CD. We followed a workflow for robust application of SP model: (i) identify main project goals; (ii) selection of species and literature search for blood levels in healthy subjects (HS) and CD patients; (iii) representation of model topology and parametrization of the interactions using data extraction and curation. Model components kinetics were characterized by zero or first-order synthesis and first-order degradation constants. Constant levels for ils and cells at the steady state (SS) of HS and CD were assumed for synthesis rate constant derivation. To parametrize the IL interactions, different sub-models were tested using nonlinear regression in Rv3.5.0. Ordinary differential equations (odes) were implemented in simbiology® (MATLAB®vr2018b). Afterwards, (iv) deterministic simulations for CD were run and model evaluation was performed. A total of 21 species representative of the innate and adaptive immune response in CD were included. Graphical representations were generated providing a big picture of model structure. The developed QSP model included 21 odes. A quantitative reproduction of CD was obtained. We present a QSP model for the main ils and cells involved in CD. Not only is supported by a comprehensive repository summarizing the most relevant literature in the field, but also by a standardized methodology for QSP model building. This model proved to be promising for the in silico evaluation of potential therapeutic targets and the search for specific biomarkers. Finally, it can be expanded or reduced as demanded, leading to different quantitative model/s to address research gaps regarding CD.

Population pharmacokinetics of variants of Cuban pegilated recombinant human erythropoietins

K.E. Rodríguez-Fernández[1*], D. Amaro, J. Solozábal[2], V. Mangas-Sanjuan[3,4], I.F. Troconiz[5], M.N. Trame[6], E.M. Fernández-Sánchez[7], L. Rodríguez-Vera[7], G. Reynaldo-Fernández[7]

[1] Drug Research and Development Center, Cuba

[2] Center of Molecular Immunology, Cuba

[3] Pharmacy and Pharmaceutical Technology Area, University of Valencia, Spain

[4] Interuniversity Research Institute for Molecular Recognition and Technological Development, Polytechnic University of Valencia, 46100 Valencia, Spain

[5] Pharmacometrics & Systems Pharmacology, Department of Pharmacy and Pharmaceutical Technology, School of Pharmacy and Nutrition, University of Navarra, Pamplona, Spain

[6] Novartis Institutes for biomedical Research, Cambridge, Massachusetts, USA

[7] Department of Pharmacy. Institute of Pharmacy & Foods, University of Havana, Havana, Cuba

*E-mail: karinerguez.1219@gmail.com

Recombinant human erythropoietin stimulates the formation of erythrocytes in the bone marrow. This therapeutic glycoprotein has a short half-life (4-11h), so it is rapidly eliminated from the body. One of the technological strategies used to solve this problem is pegylation. The aim of this study was to develop a population pharmacokinetic of two newly pegylated-EPO analogues (PEG-EPO 32 and 40 kda) formulations compared with the reference products ior®EPOCIM and MIRCERA®. For each product, a single dose of 10 μg/kg was administered via intravenous bolus in 19 New Zealand rabbits and serum concentrations were determined at different times. Initial population pharmacokinetic modeling was conducted using NONMEM version 7.3., via FOCEI method. Standard goodness-of-fit plots, individual predicted/experimental versus time profiles, eta histograms and normalized prediction distribution error plots were generated to evaluate the model performance. The final model obtained was translated into rxode and executed using nlmixr, with SAEM method, in order to allow for performance comparison between NONMEM and the open-source R based software nlmixr. A two-compartment population pharmacokinetic model with linear elimination was obtained. The interindividual variability was associated with CL and V1. The PEG-EPO 32 and 40 kda had lower clearance than with ior®EPOCIM and MIRCERA® ($CL_{EPO-\ PEG-32}$: 5.77×10^{-3} L/h, $CL_{EPO-PEG\ 40}$: 4.34×10^{-3} L/h, $cl_{ior®EPOCIM}$: 1.02×10^{-1} L/h, $CL_{MIRCERA®}$: 1.06×10^{-2} L/h); which allowed a decrease in the frequency of administrations. Model output comparison between NONMEM and nlmixr resulted in very similar results when comparing the final parameter estimates and goodness-of-fit plots of model performance. The results of this investigation contributed to establish the potential of PEG-EPO 32 and 40 kda formulations obtained in Cuba as promising candidates for the use in the clinic. Additionally, this work demonstrated the availability of nlmixr as a reliable tool for the use of pharmacometric analyses.

Antiretroviral blood monitoring and effectiveness analyses of Cuban HIV-AIDS patients treated with generics AZT3TC-NVP

L. Gil del Valle*, C. Fonseca Gómez, A. Tarinas Reyes, R. Gravier Hernández, Y. Bemúdez Alfonso, D. Hernández Requejo, R. León Canga, J. Pérez Avila

Institute of Tropical Medicine Pedro Kourí, La Habana, Cuba.

*E-mail: lgil@ipk.sld.cu

Quantification of the blood concentration of antiretroviral drugs (BCAD) allows individuals evaluation to guarantee an appropriate suppression of the viral load. This monitoring activity in HIV-aids patients don't include in clinical practice in Cuba. It was carried out a cross sectional and analytic study including 100 Cuban patients assisted at IPK Hospital and treated with AZT/3TC/NVP combination. For the evaluation of the BCAD (AZT, 3TC, NVP) was used chromatographic conditions of previous analytical validated methods in a liquid chromatograph Knauer. It was evaluated the number of T lymphocytes CD4+, the viral load and the behavior of hematological and hemochemistry indexes previous and two months after of the determinations. The age median was 40 ± 10 years, with prevalence of the masculine sex (81/100) and white skin color (92/100). Most of the BCAD for the studied group were in the effective therapeutic interval (NVP: 3.94 ± 2.99, AZT: 0.39 ± 0.46, 3TC:0.27 ± 0.28 x 10^{-3} μg/ml). The progression markers (number of lymphocytes TCD4+ and the viral load) evidenced a simultaneous modification with effectiveness of 23% for the group, as well as alterations of some hematologic and hemochemistry indexes without pathological or toxic significance. Different number of patients with drug concentrations in effective therapeutic range were detected through the individual analysis (NVP: 49/100, AZT:88/100, 3TC:61/100). Analysis allowed to the identification of sub optimal concentrations in 75% of the evaluated patients. The effectiveness analysis of patients considering BCAD in the therapeutic range for the three drugs was 86.3%. The findings corroborate relationship between the BCAD and the drug effectiveness. Similar analysis can contribute to prolong the useful period of each combination, to prevent both the resistance and the associate toxicity and to consider the treatment accomplishment objectively.

Systematic review of the most reliable analytical methods for monitoring fluconazole, itraconazole and amphotericin b, in routine clinical practice

S.S. Tarragó*, D. García, R. Gravier, D. Ortega, M.T. Illnait, L. Gil

Institute of Tropical Medicine "Pedro Kourí", Cuba

*E-mail suryt@ipk.sld.cu

To identify the most reliable analytical methods for the therapeutic monitoring of fluconazole, itraconazole and amphotericin B in routine clinical practice. A literature search was conducted in the databases of electronic data LILACS, pubmed, Medline, Cochrane and scielo. The search was conducted from January 2018 to June 10, 2019. "Analytical methods", "Antifungals", "Fluconazole", "Itraconazole" and "Amphotericin B" and their equivalents in English and Portuguese. Studies that describe the methodology of antifungal therapeutic monitoring and study that evaluates the different analytical methods for the quantification of antifungal agents were established as inclusion criteria. Review studies of pharmacokinetic and pharmacodynamics properties of antifungals and studies on antifungal resistance. Of 132 records identified, only 5 were included. In the selected articles, it is recommended to monitor high resolution liquid chromatography according to the pharmacokinetic properties of fluconazole and itraconazole in clinical practice. For amphotericin B there are still no studies to support its monitoring. This procedure allows adjusting the dose of treatments for each patient and minimizing the risks associated with their use. The most reliable methods for the therapeutic monitoring of antifungals in clinical practice are liquid chromatography with high efficacy, ultraviolet-visible and coupled to mass spectrometry, which is a high specificity and rapidity of response.

Characterization of the pharmacokinetics and pharmacodynamics of three Cuban recombinant interferon alpha formulations

I. García-García[1]*, I. Hernández-González[2], C. González-Delgado[3], P. López-Saura[4], I. Bello-Rivero[4]

[1] University of Medical Sciences of Habana, "Manuel Fajardo" Faculty of Medical Sciences, Havana, Cuba.

[2] Isotope Center, Cuba.

[3] National Center for Toxicology, "Carlos J. Finlay" University Hospital, Cuba

[4] Center for Genetic Engineering and Biotechnology, Playa, Cuba

*E-mail: idriangg@infomed.sld.cu

Pharmacokinetics (PK) and pharmacodynamics (PD) are critical for the evaluation of biopharmaceutical products. The aim of the entire work was to characterize these

properties in the Cuban recombinant interferon (IFN) alpha present in its different formulations, establishing in each case comparisons with similar reference products. Three clinical studies were carried out in healthy male volunteers, to evaluate PK, PD, and biological safety of three respective formulations containing IFN alpha, developed at the Center for Genetic Engineering and Biotechnology (CIGB) in Havana. These were a liquid formulation without albumin, a second formulation with the molecule conjugated to polyethylene glycol ("pegylated") and another combined with IFN gamma in synergistic proportions. Clinical studies were randomized, double-blind and crossover, with a 3-week washout period between the administration of test and reference formulations. Serum IFN concentrations and serum classic IFN-inducible markers were measured by commercial enzyme immunoassays. Non-compartmental and compartmental methods were applied. An integrated PK/PD model was written using the build-in MLXTRAN code in MONOLIX, based on the best-fit PK model and a classical indirect response model with response stimulation. PK and PD parameters, as well as the observed adverse events, demonstrated the similarity between Cuban IFN alpha formulations and their commercial referents. Pegylated IFN demonstrated slow absorption and elimination. The combination of IFN alpha and gamma produced pharmacodynamic potentiation. Neopterin levels were nine-fold higher than initial, 48 hours post-injection, beta2-microglobulin was approximately the double, while 2'-5' oligoadenylate synthetase concentrations were four-fold higher than baseline on the eighth day and the moment to return to normality could not be predicted. Formulations were safe; flu-like symptoms and hematological count reductions were the most common adverse events. The formulations of the Cuban recombinant IFN alpha have favorable pharmacological properties, being the same comparable to their respective commercial similar.

Genotype-driven pharmacokinetic simulations of warfarin levels in Puerto Ricans

R.E. Jiménez-Ramos[1], J. Rivera-Robles[1], G. Reynaldo-Fernández[2], L. Rodríguez-Vera[2], B. Jiménez-Vélez[3], J. Ducongé-Soler[1]*

[1] University of Puerto Rico Medical Sciences Campus, Department of Pharmaceutical Sciences, School of Pharmacy, San Juan, PR, USA

[2] Department of Pharmacy, Institute of Pharmacy & Foods, University of Havana, Havana, Cuba

[3] University of Puerto Rico Medical Sciences Campus, Department of Biochemistry, School of Medicine, San Juan, PR, USA

*E-mail: jorge.duconge@upr.edu

The variability in response to warfarin among individuals has been linked to genetic polymorphisms. This study was aimed at performing genotype-driven pharmacokinetic

(PK) simulations to predict warfarin level differences among Puerto Rican subjects with CYP2C9 genetic polymorphisms. A PK simulation analysis of each individual dataset was performed by one-compartmental analysis using winnonlin® software (v6.4, Certara, USA). The elimination rate constants (Ke) of warfarin given a CYP2C9 genotype were: *1/*1=0.0189 hr^{-1} (wild-type); *1/*2=0.0158 hr^{-1}; *1/*n=0.0132 hr^{-1}; *2/*2=0.0130 hr^{-1}; *2/*n=0.009 hr^{-1}; *n/*n=0.0075 hr^{-1}, being n=*3, *5, *6 or *8. Data from 128 male subjects, mostly elderly of Caribbean Hispanic origin, were used to perform secondary analyses in this study. Subjects were divided into wild-types and carriers and statistical analysis by two-sample unpaired t-tests were performed to compare their corresponding PK parameters. In the carrier group (n=64), 53 subjects were single carriers (i.e., 30 with *1/*2 and 23 with *1/*3, *1/*5 or *1/*8 genotypes) and 11 double carriers of CYP2C9 polymorphisms (i.e., two *2/*2, seven *2/*3 or *2/*5 and the other two with *3/*5 and *3/*8 genotypes, respectively). The mean peak concentration (Cmax) was higher for wild-types (0.36 ±0.12 mg/L vs. 0.32 ±0.14 mg/L). Likewise, the average clearance (CL) was faster among non-carriers (0.22 ±0.03 L/h vs. 0.17 ±0.05 L/h; p=0.0001), with lower area under the curve (AUC) when compared to carriers (20.43 ±6.97 h·mg/L vs. 24.78 ±11.26 h·mg/L; p=0.025). Statistical analysis revealed a significant difference between carriers and wild-types with regard to AUC and CL, but not for Cmax and Vd. The latter parameter being on average higher in carriers, due probably to larger body weights in this group versus non-carriers. These pharmacogenomic-driven PK simulations provided useful information for further development of warfarin dosing prediction models that account for individual pharmacokinetics and genotyping. Further assessments are needed to validate our findings.

Cyclosporine pharmacokinetic model for kidney transplant hosts and autoimmune disease patients

C. Maldonado[1,2]*, M. Umpierrez[1,2], N. Guevara[1,2], M. Ibarra[2], P. Fagiolino[1,2], M. Vázquez[1,2]

[1] Therapeutic Drug Monitoring Service, Hospital de Clínicas Dr. Manuel Quintela, Uruguay

[2] Pharmaceutical Sciences Department, Facultad de Química, Universidad de la República, Montevideo, Uruguay

*E-mail: cmaldonado@fq.edu.uy

Calcineurin inhibitor, Cyclosporine (CYA) is widely used in the hospital setting, either to prevent graft rejection or to control autoimmune diseases. CYA nephrotoxic effects has led to a reduction in its use in kidney transplantation, whereas it has grown considerably in autoimmune diseases. TDM of CYA is a common practice to avoid adverse drug effects or inefficacy. For many years now, predose (C0) and concentration 2 hours post administration (C2) have been adopted as the most common samples in practice, though it is known that a complete profile of concentration (C0, C1, C2, C3, C4) is

the most accurate way to follow treatments due to CYA high interindividual variability. As a consequence, model building is a useful tool to take into consideration population characteristics and formulations available in the country to optimize dose regimen. For model building we analyzed curves of concentration vs time and we also included C0 and C2 when possible. Blood samples were analyzed using an immunoassay chemiluminescent microparticle immunoassay (CMIA, Architect® analyzer, Abbott Laboratories). To validate our pharmacokinetic model new patients' blood samples were analyzed and their results compared with the predicted concentrations using root mean square error. Data modeling were performed using Monolix® 2019R1, meanwhile the R package mlxr developed by Lixoft. A bicompartimental model with lag time is the one that best fits CYA pharmacokinetic model. Only Creatinine CL is a significant covariable in the model. During the validation of the model, C2 concentrations were the ones that were predicted with less error, and C0 predictions highly improved from one occasion to another. Creatinine Clearance proved to be the most important parameter to explain CYA CL changes in patients. In case only one sample could be drawn, C2 determination appears to be the one that is best predicted by our model.

Pharmacokinetics of xylazine in horses

Cristian Valiante[1], Silvana Alvariza[1]*, Nadia Crosignani[1], P. L. Stelio Luna[2], Miguel Marcilla[2], Pablo Magalhaes[2], Paula Barreto[2], Manuel Ibarra[3]

[1] Pharmacology Department, Facultad de Veterinaria, Universidad de la Republica, Uruguay

[2] Surgery and Anesthesiology Department, Facultade de Veterinaria e Zootecnia, Universidade Estadual Paulista, Brasil

[3] Department of Pharmaceutical Science, Chemistry School, Universidad de la República, Uruguay

*E-mail: silvana.alvariza@gmail.com

Xylazine is widely used drug in veterinary practice for its potent sedative, analgesic and myorelaxant properties. Nevertheless, despite its extensive use, no pharmacokinetics population models have been published for this drug in horses. In this prospective study, six horses (three males and three females) were selected and randomly assigned in two groups according to two periods, crossover compensated design, comparing two doses, 0.5 and 1 mg/kg of Xylazine via iv bolus. Two jugular catheters were implanted for injection (right) and blood sample collection (left). Blood samples were collected at 2, 5, minutes and 0.25, 0.5, 0.75, 1.0, 1.5, 2- and 3 hours post dose. Pharmacokinetic analysis was performed for Xylazine using Monolix® software (Monolix Suite 2019R1, Lixoft S.A.S). Structural and statistical models were evaluated with basic goodness of fit plots and metrics and visual predictive checks. The final model described Xylazine disposition in horse appropriately, consisting in a two-compartment structure with first order elimination kinetics. Typical parameter estimates were: CL = 2268 L/h,

V1=984 L, Q=2454 L/h and V2=450 L. Interoccasion variability was included for CL and V1, with estimates of 5.36% and 14.2% respectively. A combined residual model was implemented. Weight was included as covariate in all disposition parameters according to an allometric model with an exponent of 0.75 and 1.0 for clearance and volume terms respectively. Reported estimates are the typical parameters for a 400 kg bodyweight animal.

Pharmacokinetics of methadone in horses

Silvana Alvariza[1]*, Nadia Crosignani[1], Manuel Ibarra[2], Maiara Pigato[3], P. L. Stelio Luna[3], Eutalio Pimenta[3], Teresa Dalla Costa[4], Bruna Torres[4]

[1] Pharmacology Department, Faculty of Veterinary, Universidad de la República, Uruguay

[2] Department of Pharmaceutical Science, Chemistry School, Universidad de la República, Uruguay

[3] Surgery and Anesthesiology Department, Facultade de Veterinaria e Zootecnia, Universidade Estadual Paulista, Brazil

[4] Faculdade de Farmácia, Universidade Federal do Rio Grande do Sul, Porto Alegre, RS, Brazil

*E-mail: silvana.alvariza@gmail.com

Methadone is a synthetic μ-opioid agonist with potent analgesic properties useful in the treatment of both, acute and chronic pain. This work describes the pharmacokinetic of methadone in horses. In this prospective study, six female horses were selected and randomly assigned in four groups according to four periods, crossover compensated design, comparing three doses, 0.1 and 0.2 mg/kg via iv bolus and 0.5 mg/kg via iv bolus or intramuscular of Methadone. Two jugular catheters were implanted for injection (right) and blood sample collection (left). Blood samples were collected at 2, 5, 10 minutes and 0.25, 0.33, 0.75, 1.0, 1.33, 1.67, 2.0, 2.33, 2.66- and 3.0 hours post dose. Pharmacokinetic analysis was performed for Xylazine using Monolix® software (Suite 2019R1, Lixoft S.A.S). Structural and statistical models were evaluated with basic goodness of fit plots and metrics and visual predictive checks. The final model described Methadone disposition in horse appropriately, consisting in a two-compartment structure with first order elimination kinetics. Typical parameter estimates were: CL = 208.8 L/h, V1=66.7 L, Q=774 L/h and V2=59.3 L. Absorption parameters for intramuscular administration were F= 0.82 and ka=20.76 h-1. Interindividual variability was included for CL with an estimate of 27.0% and interoccasion variability was included for CL and V1, with estimates of 25.8% and 29.0% respectively. A combined residual model was implemented. Weight and administered dose were included as covariate for V1.

Naïve-pooled pharmacokinetic analysis of betulinic acid in mice plasma after oral administration as nano-emulsion type formulations

S. Chinas, O. Núñez, J. Serrano, C. Cortez, A. Cavazos, E. Romero*

Departamento de Farmacobiología, Centro Universitario de Ciencias Exactas e Ingenierías, Universidad de Guadalajara, Mexico

*E-mail: elba.romero@academicos.udg.mx

Betulinic Acid (abet) arouse special interest in the scientific community as substances with beneficial health effects, and is evidenced by studies involving effects, actions and risk prevention in certain diseases. Information related to bioavailability and pharmacokinetics process is required to development of abet as a functional food alternative. A murine model was applied to describe the pharmacokinetics of a single oral dose of abet (50 mg/kg) as a conventional emulsion (EMC) and nano-emulsions with original phosphatidylcholine (NEM-PC1) and enzyme-modified phosphatidylcholine (NEM-PC2), under fasting conditions. Pharmacokinetics profiles were obtained by chromatographic analysis of plasma samples. Pooled naïve and NCA analysis was performed by Monolix-Lixotf (v2019r1) to obtain pharmacokinetics parameters and evaluate bioavailability between formulations. The plasma sampling times from experimental animals were as follows: 0.5, 1.0, 2.0, 3.0, 4.0, 8.0 and 12.0 h. 3 experimental animals were used for each sampling time, giving a total of 21 mice per formulation. Data from all formulations were adjusted to a monocompartmental pharmacokinetic model with a first order process of absorption and elimination. Population parameters values and random standard error (%) obtained as follows: ka=0.185 h^{-1} (17.5), V/F= 0.850 L (38.0), CL=1.1 L/h (7.02). Inclusion of formulation as covariate increased the performance of the model. Non compartmental analysis between formulations demonstrated the average and standard deviation of ABC0-inf (mcg.h/L) and Cmax (mcg/L) of EMC, NEM-PC1 and NEM-PC2 (1059.14±105.61 / 195.104±56.93), (3059.28±601.4 / 515.05±115.24), (4308.10±875.27 / 536.66±69.06) respectively, indicated significant differences (P<0.0001) between EMC and nanoemulsions. Half-life between formulations reveal an important increase of permanence of abet in NEM-PC2. The bioavailability of nano-emulsions is superior compared to EMC as reported in previous studies, where the enzymatic modification of phosphatidylcholine is a starting point for the control of bioavailability.

Effect of ^{177}Lu-ipsma on viability and dna damage of human glioblastoma cells under hypoxia-mimetic conditions

L. Aranda Lara[1*], E. Azorín Vega[2], E. Torres García[1], K. Isaac Olivé[1]

[1] Facultad de Medicina, Universidad Autónoma del Estado de México, Toluca, 50180, Estado de México, Mexico

[2] Laboratorio Nacional de Investigación y Desarrollo de Radiofármacos, Instituto Nacional de Investigaciones Nucleares, Ocoyoacac 52750, Estado de México, Mexico

*E-mail: larandal@uaemex.mx

Glioblastoma is a human neoplasm characterized by a high degree of hypoxia. Hypoxic condition improves therapy resistance of cancer cells. Lutetium-177 has been used in targeted radiotherapy, due to its physical properties allow beta particles to deposit their energy in small volumes and deliver high doses to targeted cells. PSMA is a transmembrane protease that is considered a target for different therapeutic strategies because of its overexpression in the neovasculature of several solid tumors, including glioblastoma. The aim of this work was to evaluate the effect of ^{177}Lu-ipsma on cell viability and DNA damage in U87MG human glioma cells under hypoxia mimetic conditions.U87MG cells treated with ^{177}Lu-ipsma were incubated with $cocl_2$ in order to induce hypoxia-mimetic conditions. The cytotoxic and genotoxic effect was evaluated with an *in vitro* viability test and a neutral comet assay. ^{177}Lu-ipsma exposure time significantly reduced the percentage of viable cells both with and without $cocl_2$ (72 and 78%, respectively). Percentage of DNA in U87MG cell comet tails indicate that 177Lu-ipsma treatment had a genotoxic effect after 4 h. Even though $cocl_2$ exposed cells acquired important radioresistance, the continuous emissions from Lu-177 produced an increase in DNA damage at 24 and induced irreparable DNA double strand breaks in U87MG human glioma cells under hypoxia-mimetic conditions. ^{177}Lu-ipsma produced the maximum effect at 48 h, suggesting that this radiopharmaceutical could be used as a strategy for the treatment of human glioma hypoxic cells.

Pharmacokinetics and pharmacogenetics of valproic acid in Chilean patients with epilepsy

Jaime Sasso[1, 2]

[1] Escuela de Química y Farmacia, Facultad de Medicina y Ciencia, Universidad San Sebastián, Chile

[2] Departamento de Biología, Facultad de Química y Biología, Universidad de Santiago de Chile

E-mail: jaime.sasso@uss.cl

The use of valproic acid (VPA) is licensed for the monotherapy or the adjunctive treatment of any form of epilepsy in patients of any age, however, it is estimated that

approximately 30% of patients are refractory. There are many factors that could affect drug response, such as drug-drug interactions and the presence of some allelic variants, which result in large differences between individuals in the dose-to-plasma concentration relationship. The aim of this study was analyzing the effect of the associations of allelic variants CYP2C9*2, *3 and UGT2B7*2 plus coadministration of inducers drugs on pharmacokinetic of valproic in patients with epilepsy. A total of 52 adult patients on stable treatment with VPA as mono or adjunctive therapy attended at "Complejo Asistencial Dr. Sótero del Río" and "Centro de Referencia de Salud Dr. Salvador Allende Gossens" were included. The Cl/F were calculated by non-compartmental analysis using one plasma sample per patient and the genotype of epileptic patients was obtained by PCR-RFLP technique. The allelic frequencies of UGT2B7*2, CYP2C9*2 and CYP2C9*3 were 0.302, 0.080 and 0.058, respectively. The presence of one or more copies of the T allele for the UGT2B7(T<C) polymorphism results in an increase in valproic acid clearance, particularly, significant differences were observed when the drug is administered together with an antiepileptic drug that induce its metabolism and when the patients are extensive metabolizers for the CYP2C9 genotype classification.

Population pharmacokinetic modeling of clozapine-loaded nanocapsules in male Wistar rats

A.C.R. Funghetto, F.B. Carvalho, S.E. Haas*
College of Pharmacy, Federal University of Pampa, UNIPAMPA, Uruguaiana-RS, Brazil
*E-mail: sandra.haas@gmail.com

Clozapine is an atypical antipsychotic of first choice in refractory schizophrenia. Its therapeutic use is limited due to agranulocytosis and cardiotoxicity. Our research group developed polysorbate 80 (NC1), PEG (NC2) or chitosan (NC3) coated clozapine-nanocapsules and published data from non-compartmental and compartmental pharmacokinetic analysis, demonstrating the relevance of nanoencapsulation. In this context, our aim was to develop the populational approach (poppk) of nanoencapsulated Clozapine. 384 observations from 25 individuals (male Wistar rats, IV administration, 25 mg/kg clozapine dose) were used to poppk via Monolix (Lixoft®, 2018R2). We consider the formulations as covariate. Visual predictive assessment (VPC), relative standard deviation (R.S.E. %), *P* value, Akaike Information Criteria (AIC) and -2xlog likelihood were considered for model selection. A 3-compartment open model with intravenous bolus administration and linear elimination process was selected as the best model, corroborating previously published data. Clearance population was 1.89 L/h, NC1 and NC2 showed negative beta. V1 was reduced with NC3 acted as covariate, while V2 decreased by NC2. V3 was significantly altered by NC2

(beta = 3.81). Important changes in pharmacokinetic parameters were observed from nanoencapsulation, suggesting Clozapine-loaded nanocapsules are promising in the treatment of schizophrenia.

Therapeutic peptides quantitation in human plasma using mass spectrometry: our experience applied to pharmacokinetic studies during clinical trials

A. Cabrales Rico[1]*, L.J. González[1], J. Gil[1], Y. Ramos[1], V. Besada[1], X.L. Sobrino[1], Y. Támbara[1], G. Lemus[1], A. Vazquez[1], A. Berlanga[1], S.E. Perea[1], M.C. Dominguez[1], M. Guerra[1], F. Hernández Bernal[1], L. Méndez[1], M.A. Miragaya[2]

[1] Center for Genetic Engineering and Biotechnology (CIGB), Cuba

[2] Center for the State Control of Drugs, Equipment and Medical Devices (CECMED), Cuba

E-mail: ania.cabrales@cigb.edu.cu

Mass Spectrometry (MS) has impressive capabilities in terms of sensitivity, resolving power, mass accuracy and different scan-modes versatility. Either alone or in combination with liquid chromatography it is the analytical tool of choice for synthetic therapeutic peptide characterization. Nevertheless, for peptide quantitation in human plasma or other biological sample, the design of the Internal Standard (IS) and the optimization of the sample processing and LC-MS analysis are also key elements for a successful outcome. In consequence, all strategies involving the peptide quantitation in biological fluids are still a challenge and need to be tailored. We present here our recent experiences in the development and validation of customized bioanalytical methods applied to pharmacokinetic studies included in phase I clinical trials. For the absolute quantitation of these three therapeutic peptides, alternatives to the AQUA® methodology were used. However, the design of the IS, sample processing and mass spectrometry techniques were optimized case by case for CIGB-500, CIGB-300 and CIGB-814 candidates. IS for CIGB-500 and CIGB-814 were synthetic peptides labeled with stable isotopes (^{13}C and/or ^{15}N) in specific residues within the amino acids sequence, instead of IS for CIGB-300 that was a N-terminus acetylated peptide. Sample processing mainly based on plasma proteins organic or acid precipitation was adapted according to the peptide recovery. In the particular case of CIGB-300, no liquid chromatography separation was needed before MS analysis by MALDI-TOF MS. For CIGB-500 it was applied LC-MS analysis with Simultaneous Ion Monitoring (SIM) in full scan mode. For CIGB-814 it was used LC-MS analysis in Single Reaction Monitoring Mode (SRM). The three bioanalytical methods were fully validated and applied to Pharmacokinetic (PK) analysis in a phase I clinical trials. It was possible to obtain PK profiles and main PK parameters for all of the assessed candidates.

Pharmacokinetics characterization of cyclosporine A after oral administration of nanoparticles Gantrez® and using nonlinear mixed effects models (nlme)

M. Pecchio[1,2*], E. Romero[3], J. Irache[1], M. Renedo[1], M. Dios-Viéitez[1]

[1] Facultad de Farmacia, Universidad de Navarra, España

[2] INDICASAT AIP, República de Panamá

[3] Universidad de Guadalajara, México

*E-mail: mpecchio@indicasat.org.pa

Cyclosporine A (csa) has been used as a potent immunosuppressive agent despite its low oral bioavailability and formulation problems. In our work we develop 4 new formulations of PVM/MA nanoparticles loading Cyclosporine including cyclodextrin derivatives or poly (ethylene glycol) 2000 (PEG2000) in order to increase their bioavailability. The content of Cyclosporine A in the nanoparticles was quantified by HPLC in order to determine stability, encapsulation efficiency and *in vitro* release; we also determine the particle size and surface charge of nanoparticles. The bioavailability of nanoparticles loaded Cyclosporine was evaluated in rats, compared to the currently available cya microemulsion (Neoral®) and csa pharmacokinetic was characterized using nonlinear mixed effect models. Formulations A, C and D showed the best results in the characterization of nanoparticles and were evaluated in order to describe their *in vivo* behavior. When Formulation A is administered orally in rats, the bioavailability of the drug has been found to increase in magnitude by 21.43% than when administered in sandimmunneoral® oral. The results of pharmacokinetic characterization suggest that the type of formulation that is administered to rats has influence on the pharmacokinetic parameters obtained and two-compartment model fits to our data. Our results suggest that new formulations A, C and D may be an alternative to commercial csa formulations and formulation A increases the bioavailability of the drug.

Population pharmacokinetic approach of 400 mg ibuprofen oral dose soft gelatin capsules in healthy volunteers. Covariates matters

O. Herrera[1], G. Amor[2], L. Ureña[3], M. Pecchio[4], E. Romero[5*]

[1] Universidad Nacional de San Marcos, Perú

[2] Centro Regional Universitario de Veraguas, Universidad de Panamá, Panamá

[3] Universidad Autónoma de Chiriquí, Panamá

[4] INDICASAT AIP, República de Panamá, Panamá

[5] Centro Universitario de Ciencias Exactas e Ingenierías, Universidad de Guadalajara, México

*E-mail: elba.romero@academicos.udg.mx

Ibuprofen (ibpf) has largely been administered as an anti-inflammatory non-steroidal drug by oral administration. Usually noncompartmental analysis (NCA) has been considered to describe pharmacokinetics, however, the inclusion of covariates as age, weight, gender, Body Mass Index (BMI), has not been clearly explored. This type of analysis requires the development of mixed effects models to incorporate covariates to the analysis. Data were obtained from previous 2x2x2 crossover bioequivalence study where 24 healthy volunteers (9F/15M) participated. All received an oral administration of reference and test soft gelatin capsule containing 400 mg ibpf solubilized in a polymeric semi-liquid matrix after a wash period of 7 days. 17 sampling times (basal included) of plasma were analyzed by UPLC-Mass assay. Five covariates were recorded: age, gender, BMI, type of formulation (Reference or Test) and occasion (OCC). We focused our study to the estimation of the parameters and the selection of the covariate model. A maximum likelihood expectation maximization approach was used to fit the data. Ibuprofen pharmacokinetics was best described by one-compartment (volume V) and a linear elimination clearance (Cl). Type of administration was extravascular with a first order absorption (rate constant k_a) and a lag time (T_{lag}). Typical values and SD for ibpft$_{lag}$, k_a, V/F, Cl/F were 0.314 ± 0.017 h, 2.26 ± 0.645 h^{-1}, 7.4 ± 0.293 L/kg, 0.802 ± 0.376 L/h respectively. Type of formulation was found to be a statistically significant covariate of T_{lag} and k_a, meanwhile BMI was found to be a covariate of Cl. Our results support the need to evaluate in this study covariates to develop pharmacokinetics models to enhance predictions of plasmatic concentrations of drugs. This evidence is relevant to development of new pharmaceutical formulations and the design of clinical studies taking in to account such information.

Pharmacometric study of ^{125}I-neuroepo after intranasal and intravenous administration in Sprague Dawley rats

A. Brito Llera[1]*, I. Hernández González[2], T. D. J. Rodríguez Obaya[3], M. León Pérez[2], N. Martín Columbié[2]

[1] Institute of Pharmacy and Foods, University of Havana, Cuba

[2] Center of Isotopes, Cuba

[3] Center of Molecular Inmunology, Cuba

*E-mail: adriel@ifal.uh.cu

Neuroepo is a nasal formulation of recombinant Human Eritropoietin (rhuepo) whit low content of sialic acid and proved neuroprotector effect in non-clinical and clinical

assays. Its distribution in the central nervous system is rapid but the pharmacokinetics of the product have not been previously characterized. A pharmacokinetic study of sparse data in Sprague Dawley rats was designed for intranasal and intravenous administration of 50 μg of [125I]-neuroepo. The amount of [125I]-neuroepo in blood and tissue of different organs of interest was determined at different times for 24 hours. The population pharmacokinetic parameters were modeled using MONOLIX (Suite 2018, Lixoft S.A.S, Francia). The formulation is weakly captured in the central nervous system, approximately 0.1% of the dose administered per gram of tissue according to a previous study in Mongolian gerbils and macaques. The preliminary analysis of the data showed a better adequacy of the plasma concentration profile to the model represented by the tri-exponential equation. Population pharmacokinetic parameters were determined. For the estimation of the areas under the curve, together with the rest of the non-parameterized parameters, an enriched data set was simulated using the resampling bootstraping. The adjustment to a tri-exponential model implies a very rapid plasma elimination of the molecule at an initial stage after administration. Part of the dose administered intranasally passes into the digestive and respiratory system influencing the variability observed. The uptake of 125 I-neuroepo in the central nervous system is quantitatively very low and has a high dispersion, which makes mathematical modeling difficult following a sparse data design. The exploration of other statistical methods should be continued to achieve a model that adequately describes the process studied.

Labelling and pharmacological study of ^{188}Re-nimotuzumab

A. Perera[1]*, L.A. Torres[1], G. López[2], A. Casaco[3], J.F. Batista[1], Y. Peña[1], M.A. Coca[1], I. García[2], J. Figueredo[2], R. Leyva[1], R. Gamboa[1], A. Hernández[1], A. Prats[1], Y. Sánchez[1], S. Romero[1], R. Quesada[1], L. Alberdi[1]

[1] Centre of Isotopes, Mayabeque, Cuba

[2] International Centre for Neurological Restoration, Havana, Cuba

[3] Centre for Molecular Immunology, Havana, Cuba

*E-mail: alejandro.perera@infomed.sld.cu

The aim of the present work was to label monoclonal antibody nimotuzumab with ^{188}Re, to assess its biodistribution in an animal model and to evaluate its internal dosimetry and toxicity in patients with grade III-IV gliomas through a phase I clinical trial. Labelling efficiency of ^{188}Re-nimotuzumab was 98.0±0.4%. Animal biodistribution was assessed at 3 and 24 h after IV administration of ^{188}Re-nimotuzumab through tale vein of male Wistar rats, showing a similar pattern as ^{99m}tc-nimotuzumab (control). A phase I clinical trial was performed by administering into the post-surgery

cavity through an indwelling catheter a single dose of 3 mg of ^{188}Re-nimotuzumab (370 mbq - group I and 555 mbq - group II). Biodistribution and dosimetric studies were performed. ^{188}Re-nimotuzumab showed a high retention in the tumoral cavity with an effective $T_{1/2}$=9.4±1.6 h. The mean absorbed doses in the tumor was 24.1±2.9 Gy for group I and 31.1±6.4 Gyfor group II. Highest doses were received by kidneys, liver, and urinary bladder: 0.754, 0.223 and 0.604 mgy/mbq, respectively. The maximal tolerated dose was considered 3 mg of the antibody labelled with 370 mbq of ^{188}Re. One patient with has a partial response for more than 1 year and 2 patients showed complete response after 3 years of treatment. No patient developed a HAMA response. Proposed procedure allowed the stable efficient labelling of nimotuzumab with ^{188}Re. Preliminary results of this study strongly suggest that loco-regional radioimmunotherapy of high-grade glioma using ^{188}Re-nimotuzumab may be safe and constitute a promising therapeutic approach for these patients.

Development and preclinical assessment of ^{18}F-Amylovis as a potential PET radiopharmaceutical for b-amyloid plaque

A. Perera Pintado[1*], S. Rivera Marrero[2], S. León Chaviano[2], M. Sablón Carrazana[2], A. Bencomo Martínez[2], R. Pérez Perera[2], O. Díaz García[2], D. Merceron Martinez[2], A. Prats Capote[1], F. Zoppolo[3], I. Kreimerman[3], L. Fernández-Maza[4], M. Balcerzyk[4], T. Pardo[3], L. Reyes[3], A. Paulino[3], A. Corral[4], D. Orta-Castello[4], A. Parrado-Gallego[4], I. Fernández-Gómez[4], H. Garay-Pérez[5], H. Engler[3], E. Savio[3], C. Rodríguez Tanty[2]

[1] Centro de Isótopos, Mayabeque, Cuba

[2] Centro de Neurociencias de Cuba, La Habana, Cuba

[3] Centro Uruguayo de Imagen Molecular, Montevideo, Uruguay

[4] Centro Nacional de Aceleradores, Sevilla, España

[5] Centro de Ingeniería Genética y Biotecnología, La Habana, Cuba

*E-mail: alejandro.perera@infomed.sld.cu

Alzheimer's disease (AD) is the most common form of dementia. Neuroimaging methods have widened the horizons for the AD diagnosis and therapy. Herein, the synthesis of 2(3-fluoropropyl)-6-methoxynaphthalene and its ^{18}F-radiolabeled analogue (^{18}F-Amylovis) were described. ^{18}F-Amylovis was obtained with satisfactory yield, high radiochemical purity and specific activity. A comparative *in silico* studies with Amylovis and PIB and the Aβ peptide were carried out. All studies predict that Amylovis should have affinity to the peptide and the ligand-Aβ peptide complexes is stable. Determinate log P value point out its potential ability of crossing the blood brain barrier (BBB). *In vitro* stability (ethanol, HAS, PBS and plasma protein binding) were assayed and it was found stable for 12 h and had low plasma protein binding.

Higher affinity to Aβ plaques were found for Amylovis than PIB. Biodistribution and PET imaging studies in healthy and transgenic appswe/PS1dE9 mice, showed that ^{18}F-Amylovis crosses BBB, and has different behaviour in healthy animals and transgenic mice, the plasma half-life was 37±10 min. Radiopharmaceutical was *in vivo* metabolised in 60 min. Preclinical assessment of ^{18}F-Amylovis showed that it could be a new potential radiopharmaceutical for the imaging of β-amyloid plaque.

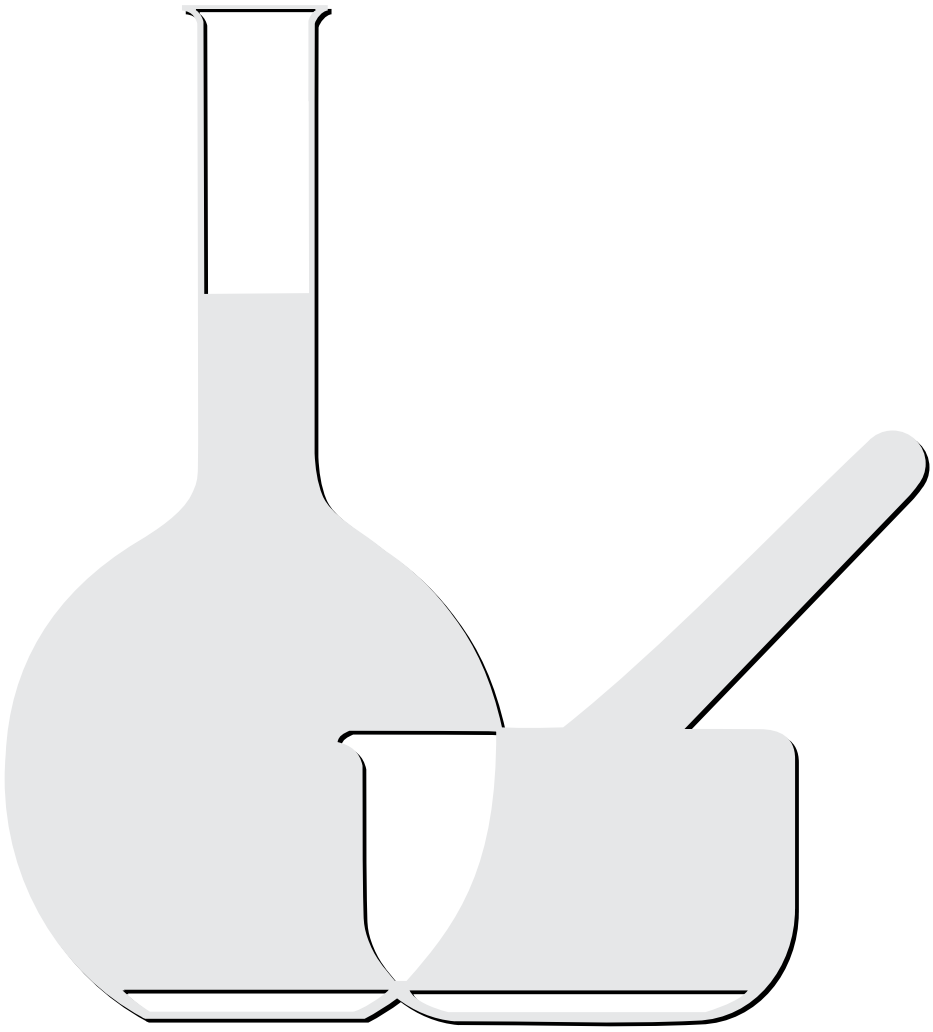

NORMAS PARA PUBLICACIÓN

La Revista Colombiana de Ciencias Químico Farmacéuticas es editada por el Departamento de Farmacia de la Universidad Nacional de Colombia (Sede Bogotá), con una periodicidad cuatrimestral y tiene como objetivo publicar artículos originales de diversos tópicos relacionados con las ciencias farmacéuticas como recursos naturales, atención farmacéutica, evaluación clínica y preclínica, y los relacionados con la industria farmacéutica, la salud y los medicamentos.

Además de artículos completos, la revista acepta revisiones, comunicaciones breves y cartas al Editor. Las contribuciones pueden enviarse en español, portugués o inglés, en letra Times New Roman, tamaño 12, al correo electrónico rccquifa_fcbog@.unal.edu.co o a través del sistema OJS en el sitio web: https://revistas.unal.edu.co/index.php/rccquifa.

Todo el material propuesto para publicación será revisado por el Comité Editorial, y luego de su aceptación para evaluación, será sometido a revisión por pares académicos. Las evaluaciones recibidas por el Comité Editorial serán remitidas al autor para que se realicen los ajustes sugeridos. Los autores tendrán un lapso de tres semanas para responder cada una de las observaciones, introducir en el texto las modificaciones del caso y retornar el documento corregido al Comité Editorial. Después de que los evaluadores o el Comité Editorial lleven a cabo una segunda revisión del manuscrito, la revista comunicará a los autores la decisión sobre la publicación o no del mismo. Los manuscritos deberán acompañarse de una carta firmada por todos los autores en la cual se declare que el trabajo es inédito; es decir, que el artículo ni parte de este ha sido publicado o está en vía de publicación en otra revista, y en la que se responsabilizan por la información publicada. Se entiende claramente que los trabajos enviados no están siendo considerados para su publicación en otros medios.

Criterios para la presentación de manuscritos

- La fuente de los manuscritos debe ser Times New Roman tamaño 12.
- No se admiten notas a pie de página.
- Título, centrado y en minúscula.
- Autor(es) con su respectiva filiación institucional y correo electrónico del autor principal.
- Resumen, *Summary* o Resumo. Incluye la justificación del estudio y los principales hallazgos y conclusiones, debe tener entre 50 y 200 palabras. Se debe incluir el título del artículo y el resumen en inglés (*Summary*) independiente del idioma del manuscrito.
- *Key words* (debajo de *Summary*) y Palabras clave (debajo del Resumen) o Palavras chave (debajo de Resumo). De tres a seis palabras en minúscula, excepto la primera, y separadas por coma y espacio. Preferiblemente tomadas del Index

Medicus (http://www.nlm.nih.gov/mesh/meshhome.htm).

- En los manuscritos en español y portugués se empleará la coma (,) como separador decimal, en inglés se utilizará el punto (.).

- Los artículos se dividirán en las siguientes secciones: Introducción, Metodología, Resultados y Discusión, Conclusiones (si las hay), Agradecimientos, Conflicto de intereses y Referencias. Los títulos deben estar separados por dos espacios en sus partes superior e inferior, centrados y en negrilla. Los detalles acerca de la metodología experimental utilizada deberán ser lo suficientemente claros como para repetir la experimentación.

- Las tablas deben llevar numeración arábiga de acuerdo con el orden de aparición en el texto. El título debe ir en su parte superior y las notas en la parte inferior. En los encabezamientos de las columnas se deben anotar los símbolos de las unidades utilizadas.

- Las fotografías, gráficas, dibujos y esquemas se denominan 'figuras' y deben llevar numeración arábiga de acuerdo con el orden de aparición en el texto. El título debe ir debajo de las figuras.

De otro lado, los artículos relacionados con experimentación con animales deben ajustarse plenamente a los lineamientos éticos trazados por la Organización Mundial de la Salud. Los extractos o fracciones evaluados *in vitro* o *in vivo* deben definirse químicamente, cuando menos en cuanto a la clase de constituyente. El material vegetal deberá estar clasificado botánicamente.

Las abreviaturas de pesos y medidas serán las indicadas por la Farmacopea de los Estados Unidos en su edición oficial o unidades SI. Los datos espectroscópicos se deben presentar de la siguiente manera:

UV λ max (solvente ε) nm (log ε). Ej.: UV λ max (MeOH) 275 (log ε 2,94).

IR ν max (medio) cm^{-1}. Ej.: IR ν max (KBr) 1740, 1720 cm^{-1}.

EM *m/z* (% intensidad relativa). Ej.: em *m/z* (%): 340 (M^+, 100), 295 (10), 134 (26) ...

RMN ^1H (solvente, frecuencia de registro) δ ppm (integración, multiplicidad, J en Hz, asignación). Ej.: RMN ^1H ($CDCl_3$, 400 MHz) 3,84 (1H, *d*, J = 10,3 Hz, H-30).

RMN ^{13}C (solvente, frecuencia de registro) δ ppm (multiplicidad, asignación). Ej.: RMN ^{13}C ($CDCl_3$, 600 MHz) 16,60 (t, C-12).

Las abreviaturas usadas para describir la multiplicidad de las señales en RMN son: *s* = singlete, *d* = doblete, *t* = triplete, *m* = multiplete, *dd* = doble de dobletes, *ddd* = doble de doble de dobletes.

Las abreviaturas para los solventes y reactivos más comúnmente usados son: EtOH= etanol, MeOH = metanol, $CHCl_3$ = cloroformo, C_6H_6 = benceno, AcOEt = acetato de etilo, EP = éter de petróleo, Me_2CO = acetona, DMSO = dimetilsulfóxido, AcOH = ácido acético.

Se evitará el uso excesivo de tablas y figuras que estarán numeradas y que se anexarán en hojas separadas con su respectiva descripción

Referencias de los manuscritos

Las referencias se citarán en el texto con su respectiva numeración. Solo se pueden citar tesis y libros o artículos que hayan sido publicados. Deben incluir: autor(es), título de la publicación, año, volumen y páginas, así:

Revistas: Iniciales del nombre y apellido completo de todos los autores, título completo del artículo, nombre abreviado o nombre completo de la revista dependiendo si aparece en el Chemical Abstract o en índices equivalentes. El nombre de la *revista debe ir en letra itálica*, **volumen en negrilla**, páginas inicial y final, y año entre paréntesis. Ej.:

1. H.P. Baden, L.A. Goldsmith, B. Fleming, A comparative study of the physicochemical properties of human keratinized tissues, *Bioch. Biophys. Acta*, **322**, 269-278 (1973).

Comunicaciones personales: Iniciales del nombre, apellido completo e institución, seguido por las palabras comunicación personal y el año. Ej.:

2. A.J.M. Leeuwenberg, Agricultural University, Wageningen, Holanda, comunicación personal, 1984.

Libros: Iniciales del nombre y apellido completo de los autores, título del libro entre comillas, editorial, ciudad, año, volumen y página. Ej.:

3. D.R. Morris, "The Biochemistry of Disease", Morris et Marton Eds., London, 1981, Vol. 8, p. 223.

Capítulos de libros escritos por varios autores: Iniciales del nombre y apellido completo del autor, título del capítulo, seguido de: En: título del libro entre comillas, editores, editorial, ciudad, año, volumen, páginas. Ej.:

4. A.D. Elbein, R.J. Molyneux, The chemistry and biochemistry of simple indolizidine and related polyhydroxy alkaloids. En: "Alkaloids: Chemical and Biological Perspectives", Ed. por S.W. Pelletier, Wiley, New York, 1987, Vol. 5, pp. 1-54.

Tesis: Iniciales del nombre y apellido completo de los autores, *título en cursiva*, Tesis de..., institución, ciudad, año, páginas. Ej.:

5. F. Salcedo, *Contribución al estudio de las Cinchonas colombianas*, Tesis de Grado, Universidad del Valle, Cali, 1983, pp. 14-16.

Referencias de Internet: Iniciales del nombre y apellido completo del autor, título del documento, dirección URL y fecha de revisión. Ej.:

6. Lipidat, Lipid thermotropic phase transition database, Ohio State University, URL: http://www.lipidat.chemistry.ohio-state.edu, consultado en septiembre de 2001.

La correspondencia puede enviarse a la siguiente dirección o al correo de la revista *rcciquifa_fcbog@unal.edu.co*

Comité Editorial

Revista Colombiana de Ciencias Químico-Farmacéuticas
Departamento de Farmacia
Facultad de Ciencias
Universidad Nacional de Colombia

Cra. 30 N.° 45-03
Fax: 57-1-3165060

Bogotá - Colombia
Correo electrónico:
rcciquifa_fcbog@unal.edu.co

Dirección WEB:
http://www.revistas.unal.edu.co/index.php/rccquifa

Revista Colombiana
de Ciencias Químico-Farmacéuticas, 49(2)
se terminó de editar, imprimir y encuadernar
en Proceditor, sobre papel bond de 90 gramos
Bogotá, D. C., Colombia.